

# **Wavelength Agnostic WDM Strategies for Avionic Telecommunications**

by

**Eoin Murphy**

A thesis submitted for the Degree of  
Doctor of Engineering

Department of Electronic and Electrical Engineering  
University of Strathclyde  
Glasgow G1 1XW  
United Kingdom

October 2014

# Declaration

This thesis is the result of the author's original research. It has been composed by the author and has not been previously submitted for examination which has led to the award of a degree.

The copyright of this thesis belongs to the author under the terms of the United Kingdom Copyright Acts as qualified by University of Strathclyde Regulation 3.50. Due acknowledgement must always be made of the use of any material contained in, or derived from, this thesis.

Signed:

Date:

# Abstract

This thesis investigates the possibility of deploying a fibre optic network on aircraft; the network should provide 1.25 Gbps links between various end nodes throughout the aircraft. Particular attention has been paid to Wavelength Division Multiplexing (WDM) in Passive Optical Networks (PONs) and how the network is affected by the harsh environment found on aircraft. The harsh environment presents a particular challenge with respect to the operational temperature range. Over this range it is desirable to minimise any additional weight and power consumption associated with cooling network components.

One technique assessed to implement WDM with minimised cooling is to use spectrum slicing to seed reflective semiconductor optical amplifiers which will be positioned at each end node. In theory these 'colourless' nodes will be temperature insensitive and capable of uncooled operation. This has been thoroughly studied and temperature ranges for uncooled operation identified with different end node components. Different cooling techniques have also been studied; one technique using a phase change material for passive cooling with no direct power consumption and the other using a thermo-electric cooler. The efficiencies of these techniques have been compared by analysing their impact on fuel burn.

The use of distributed feedback lasers in a WDM PON has also been investigated and a novel method for reducing power consumption has been proposed. It has been predicted that this could reduce the power consumption of the optical transmitters in a realistic avionic environment by up to 20 %. This network has been compared to the network using the spectrum slicing technique with particular attention paid to the relative power consumptions. The merits of both networks in the avionic context have been discussed and different scenarios where each network is suitable have been identified.

# Acknowledgements

First of all I would like to thank my industrial supervisor Henry White at BAE Systems Advanced Technology Centre where the majority of the work in this thesis was carried out. I would also like to thank all in the photonics group at BAE Systems in Filton for all the guidance they gave me over the course of my four years there and all they taught me about the benefits of strong black coffee.

I would like to thank my academic supervisors, Craig Michie and Walter Johnstone. Craig for the expertise and advice offered from the beginning my research to finally writing up. And Walter for ironing out any difficulties associated with being enrolled at a university 300 miles from where you are working.

# Table of Contents

Declaration.....	i
Abstract.....	ii
List of Figures .....	vii
List of Tables .....	x
List of Abbreviations.....	xi
1. Introduction .....	1
1.1 Next Generation Network for Military Avionics .....	2
1.2 Thesis Layout .....	3
1.3 Findings and Contributions .....	5
1.4 Publication List .....	6
2. Literature Review .....	7
2.1 Multiplexing .....	7
2.1.1 Time Division Multiplexing, TDM .....	7
2.1.2 Space Division Multiplexing, SDM.....	7
2.1.3 Wavelength Division Multiplexing, WDM .....	8
2.2 Networks .....	10
2.2.1 Advantages of Optical Networks .....	11
2.2.2 Network Architectures .....	12
2.2.3 Passive Optical Networks.....	15
2.2.4 Avionic WDM Local Area Network, LAN.....	17
2.2.5 Protocols.....	18
2.3. Components .....	19
2.3.1 Transmitters .....	21
2.3.2 Receivers .....	24
2.3.3 Multiplexers / De-multiplexers .....	26
2.3.4 Amplifiers and Modulators.....	28
2.4. Requirements .....	31
2.4.1 Environmental Requirements .....	31
2.4.2 Functional Requirements .....	34
2.5. Current Research .....	36
2.5.1 Access Networks.....	36
2.5.2 Avionics .....	41

2.6 Conclusions.....	42
3. Compatibility with Avionic Requirements.....	46
3.1 Introduction.....	46
3.1.1 Test Matrix .....	47
3.2 Circulator.....	48
3.2.1 Thermal testing .....	49
3.3 Red/Blue C-band Coupler.....	53
3.3.1 Thermal Testing.....	53
3.4 Multiplexer.....	65
3.4.1 AWG .....	65
3.4.2 Thin Film Filter .....	75
3.5 Network Demonstrator.....	83
3.6 Conclusions.....	87
4. Reflective Semiconductor Optical Amplifiers in a Spectrum Sliced Wavelength Division Multiplexed Passive Optical Network .....	91
4.1 Introduction.....	91
4.2 Network Architecture .....	92
4.2.1 DWDM PON.....	92
4.3 Modelling.....	94
4.3.1 Bit Error Rate .....	94
4.3.2 Noise Terms.....	95
4.3.3 Point to Point Link Model.....	97
4.3.4 Results of Model .....	100
4.4 RSOA Thermal Measurements.....	104
4.4.1 Elevated Temperature Operation .....	104
4.4.2 Performance Comparison .....	107
4.4.3 Low Temperature Operation .....	109
4.5 Conclusions.....	113
5. Thermoelectric Cooler Power Consumption and Passive Phase Change Cooling.....	114
5.1 Introduction.....	114
5.2 Thermo-Electric Cooling .....	115
5.2.1 Theory.....	115
5.2.2 Power Consumption.....	116
5.3 Passive Cooling using Phase Change Materials.....	118
5.3.1 Theory.....	118
5.3.2 Package Design and Modelling.....	119

5.3.3 Cooling Performance of PCM.....	123
5.4 TEC PCM Comparison .....	126
5.4.1 Impact on Fuel Burn.....	126
5.5 Conclusions.....	128
6. Energy Savings in DWDM-PON.....	130
6.1 Introduction.....	130
6.2 Amplified WDM-PON.....	131
6.2.1 Problem Formulation.....	132
6.3 Power Consumption of Cooling .....	132
6.3.1 TEC Measurements .....	133
6.4 Modelling the Amplified Link .....	136
6.4.1 Model Results .....	137
6.5 Power Savings.....	141
6.5.1 Idealized Environment.....	141
6.5.2 LRU Cooling.....	144
6.5.3 Full Temperature Specification.....	147
6.6 Comparison with RSOA Modulators .....	149
6.6.1 SS-WDM-PON .....	149
6.6.2 LRU Case .....	150
6.6.3 Full Temperature Specification.....	152
6.7 Conclusions.....	154
7. Conclusions .....	157
7.1 Future Work.....	163
References .....	165

# List of Figures

Figure 1: Section of the spectrum split into CWDM bands and overlaid with the curve representing fibre attenuation as a function of wavelength and potential channels. [].....	9
Figure 2: Schematic of the main network layouts .....	12
Figure 3: A ROBUS network before any faults and with a damaged node to show how the re-routing could occur [21].....	15
Figure 4: An example of a passive optical tree network. One central node may transmit data which is broadcast to all nodes via a splitter, at each node a wavelength selective splitter routes data to each user who can have their own wavelength channel. ....	16
Figure 5: Energy band diagram of p-n junction at equilibrium.....	20
Figure 6: Cross section of a segment of Distributed feedback laser .....	21
Figure 7: Cross section of a VCSEL.....	22
Figure 8: Drawing of PIN photodiode showing extended depletion region .....	25
Figure 9: Drawing of an Arrayed Waveguide Grating, the input fibre carries broadband light which is split into its spectral components. The coloured triangles show the path of two separate interfering wavelengths [].....	27
Figure 10: Cross section of a RSOA showing the bend in the active region to achieve low reflection from the output facet [] .....	29
Figure 11: Configuration of a PON with RSOAs in ONU using wavelength remodulation. The blue and red arrows indicate the direction of data and are not indicative of wavelength which is the same up and down stream [54,].....	38
Figure 12: WDM PON based on self-seeded RSOA .....	40
Figure 13: Working of a 3-port optical circulator .....	48
Figure 14: Experimental set-up for thermal testing of circulator .....	49
Figure 15: Insertion loss in circulator, measured from port 1 to port 2 and from port 2 to port 3 respectively .....	50
Figure 16: Isolation in circulator, measured from port 1 to port 3 and port 2 to port 1 respectively.....	52
Figure 17: Experimental set-up for testing the coupler .....	54
Figure 18: Insertion loss in both pass and reflect arms in red/blue coupler as a function of temperature .....	55
Figure 19: Insertion loss of red/blue coupler pass arm, measured over range of temperatures at 1547 nm and 1563 nm respectively.....	56
Figure 20: Insertion loss of red/blue coupler reflect arm, measured over range of temperatures at 1541 nm and 1528 nm respectively .....	58
Figure 21: 3 dB loss point at edges of pass and reflect band of red/blue coupler as a function of temperature.....	59
Figure 22: 0.5 dB loss points at edges of pass and reflect bands of red/blue coupler as a function of temperature .....	60
Figure 23: Isolation in the pass band of red/blue coupler at the specified storage range for temperature taken at 1541 nm and 1528 nm respectively .....	62
Figure 24: Isolation in the reflect band of red/blue coupler at the specified storage range for temperature taken at 1547 nm and 1563 nm respectively .....	64
Figure 25: Sketch of the internal structure of an arrayed waveguide grating .....	66



Figure 26: Central wavelength as a function of temperature for channels of an AWG on ITU grid 1550.334 nm, 1550.116 nm and 1561.419 nm .....	68
Figure 27: Schematic of the experimental set-up to measure the crosstalk and insertion loss of a multiplexer when spectrum slicing or with a laser transmitter .....	70
Figure 28: Insertion loss and adjacent channel crosstalk for the channels of an AWG centred on ITU wavelengths as a function of wavelength difference between mux and demux. ....	72
Figure 29: Insertion loss of three channels on the AWG over the storage temperature range. ....	73
Figure 30: Adjacent channel crosstalk over the AWG operational temperature range .....	75
Figure 31: Centre wavelength of thin film multiplexer channels 31, 29 and 33 respectively, as a function of temperature. ....	77
Figure 32: Insertion loss and adjacent channel crosstalk as a function of the difference between the centre wavelengths of mux and demux of TFF multiplexer.....	78
Figure 33: Passband shape of the thin film multiplexer and the AWG respectively.....	80
Figure 34: Insertion loss and crosstalk of TFF multiplexer as a function of demultiplexer temperature .....	81
Figure 35: Crosstalk and insertion loss measured for channel 31 on TFF multiplexer with a laser transmitter .....	82
Figure 36: Schematic of the proposed RSOA network .....	83
Figure 37: Lab layout of network demonstrator, red lines indicate electrical connections and blue lines indicate optical connections .....	85
Figure 38: Photograph of working demonstrator in laboratory environment.....	86
Figure 39: An example of SS WDM-PON using RSOA transmitters.....	93
Figure 41: An example of how the network is reduced to a point to point link.....	98
Figure 42: Parametric Performance of Commercial RSOA.....	99
Figure 43: Example of results produced by model.....	100
Figure 44: Experimental set up used to validate model .....	102
Figure 45: Comparison of predicted path loss capability and experimentally measured path loss capability using both laser seed and ASE seed.....	103
Figure 46: Experimental layout of system used for measurements of Gain and $P_{SAT}$ .....	105
Figure 47: Gain and $P_{SAT}$ of standard RSOA as a function of Peltier temperature for all tested wavelengths.....	106
Figure 48: Gain and $P_{SAT}$ of standard RSOA as a function of Peltier temperature for all tested wavelengths.....	106
Figure 49: Plot of the maximum loss allowed in the link in order to keep a BER of $10^{-9}$ as a function of RSOA chip temperature. The thin dashed lines are the standard bulk active region device and the thicker solid lines are the MQW RWG-RSOA. ....	108
Figure 50: Schematic of experimental set-up to measure RSOA parameters at low temperature .....	110
Figure 51: Plots of Gain and $P_{SAT}$ at low temperatures .....	111
Figure 52: Maximum acceptable loss in link while maintaining a BER of $10^{-9}$ as a function of temperature .....	112
Figure 53: Schematic of a thermoelectric cooler.....	115
Figure 54: Power consumption of a TEC in a butterfly package cooling an SOA with a 100 mA drive current over a range of set points as a function of ambient temperature [81].....	117
Figure 55: Schematic of passive cooling package including heat flows .....	120
Figure 56: Graph showing the temperature as a function of time for an RSOA with an active load of 0.3 W.....	122

Figure 57: Melt time (effective cooling duration) as a function of PCM mass for a range of active loads with an ambient temperature of 85 °C .....	123
Figure 58: Size and weight of cooling package required to cool RSOA with 0.3 W active load in a 85 °C ambient temperature .....	124
Figure 59: Size and weight of cooling package in a 125 °C ambient temperature .....	125
Figure 60: Size and weight for a PCM cooling package with a 125 °C ambient temperature cooling to 70 °C with an active load representative of 20 RSOAs.....	127
Figure 61: Schematic of amplified WDM-PON.....	131
Figure 62: Schematic of the experimental set up to measure the TEC power consumption as a function of temperature over a range of SOA drive currents.....	134
Figure 63: Plot of TEC power consumption with 25 °C set point with a different SOA drive current for each curve .....	135
Figure 64: Functional schematic of WDM-PON .....	136
Figure 65: Dynamic range of an amplified WDM-PON link showing reach extension .....	138
Figure 66: Dynamic ranges of 32 channel link both with and without amplification and a plot of the enhancement delivered with the use of an amplifier. ....	140
Figure 67: Relative power consumption of amplified WDM-PON to unamplified WDM-PON as a function of channel count for three amplifier technologies .....	142
Figure 68: Measured temperatures in an LRU on a commercial jet .....	145
Figure 69: Relative power consumption of amplified network to unamplified network in an environment found on a commercial jet.....	146
Figure 70: Relative power consumption of amplified WDM-PON with respect to an unamplified network in a temperature range specified for operation throughout aircraft ....	148
Figure 71: Schematic of WDM-PON network using RSOA modulators seeded with a spectrum sliced broadband lightsource. ....	149
Figure 72: Ratio of the power consumptions of the DFB network to the RSOA network in a temperature range found on a civil aircraft. ....	151
Figure 73: Ratio of the power consumptions of the DFB network to the RSOA network in the full temperature range specified for aircraft. ....	153

# List of Tables

Table 1: Conditions in which an avionic network must operate [52].....	33
Table 2 : Parameters of insulation.....	121
Table 3: Amplifier parameters .....	143
Table 4: Breakdown of power consumptions for both networks .....	152
Table 5: Power requirements of each network .....	153

# List of Abbreviations

AFDX	Avionic Full Duplex Switched Ethernet
APD	Avalanche Photodiode
ASE	Amplified Spontaneous Emission
AWG	Arrayed Waveguide Grating
BER	Bit Error Rate
BERT	Bit Error Rate Test equipment
BLS	Broadband Lightsource
CFC	Chlorofluorocarbon
COTS	Commercial Off The Shelf
CSA	Communications Signal Analyser
CWDM	Coarse Wavelength Division Multiplexing
DEMUX	De-multiplexer
DFB	Distributed Feedback Laser
DWDM	Dense Wavelength Division Multiplexing
EAM	Electro-Absorption Modulator
EDFA	Erbium Doped Fibre Amplifier
EMI	Electro-Magnetic Interference
EMP	Electro-Magnetic Pulse
ER	Extinction Ratio
EUR	Euro
FBG	Fibre Bragg Grating
FEC	Forward Error Correction
FRM	Faraday Rotating Mirror
FSAN	Full Service Access Network
G	Gain
Gbps	Gigabit per second
G-PON	Gigabit Passive Optical Network
GPS	Global Positioning Systems
IEEE	Institute of Electrical and Electronics Engineers
IFE	In Flight Entertainment
ISI	Inter Symbol Interference
ITU	International Telecommunication Union
LAN	Local Area Network
LRU	Line Replaceable Unit
Mbps	Mega bit per second
MUX	Multiplexer
MQW	Multiple Quantum Well
NASA	National Aeronautics and Space Administration
NF	Noise Figure
NG-PON2	Next Generation Passive Optical Network 2
OLT	Optical Line Terminal
ONU	Optical Network Unit

PCM	Phase Change Material
PDG	Polarisation Dependant Gain
PIN	Positive-Intrinsic-Negative
PLC	Path Loss Capability
PON	Passive Optical Network
PRBS	Pseudo Random Binary Sequence
PSAT	Saturation Output Power
REAM	Reflective Electro-absorption Modulator
RN	Remote Node
ROBUS	Robust Bus
RSOA	Reflective Semiconductor Optical Amplifier
RWG	Ridge Waveguide
RWG-	
RSOA	Ridge Waveguide Reflective Semiconductor Optical Amplifier
RX	Receiver
SDM	Space Division Multiplexing
SFP	Small Form-factor Pluggable
SLD	Super-luminescent Diode
SMA	Sub-miniature version A
SMF	Single Mode Fibre
SNR	Signal to Noise Ratio
SOA	Semiconductor Optical Amplifier
SS-WDM-	Spectrum Sliced Wavelength Division Multiplexed Passive Optical
PON	Network
TDM	Time Division Multiplexing
TE	Transverse Electric
TEC	Thermo Electric Cooler
TFF	Thin Film Filter
TM	Transverse Magnetic
TO-CAN	Transistor Outline Can
TX	Transmitter
UAV	Unmanned Aerial Vehicle
VCSEL	Vertical Cavity Surface Emitting Laser
WDM	Wavelength Division Multiplexing
WDM-	
PON	Wavelength Division Multiplexed Passive Optical Network
XGM	Cross Gain Modulation
XG-PON	10 Gigabit capable Passive Optical Network
XPM	Cross Phase Modulation
XT	Crosstalk

# 1. Introduction

Avionics are the electronics systems on an aircraft; the word avionics is a combination of 'aviation' and 'electronics'. Avionics can range from Global Positioning Systems, GPS, to radar or control systems. They are necessary to control the aircraft and ensure that it can fulfil its role whilst maintaining flight safety. As technology has progressed so has the sophistication of avionics, to the point now where proposed future military aircraft can be considered a platform of high bandwidth sensors. Information generated by these sensors must be relayed to other areas throughout the aircraft such as flight computers and hardware in the cockpit. Similarly, on commercial aircraft, there is a trend towards ever increasing bandwidth demands with airlines keen to offer high definition video on demand to each seat as part of advanced in-flight entertainment, IFE, systems. Projected data rates are now at the point where copper links will not be able to deliver the bandwidth required on future aircraft, both civil and military, whilst maintaining feasible weight and costs. Future aircraft will have to use fibre optic links to practically meet bandwidth demand. In addition to increased bandwidth there are further advantages associated with the introduction of fibre optic cable over copper such as significant weight savings leading to lower running costs per flight.

Optical links have been used on aircraft before with the Boeing 777 being the first commercial aircraft to install these links; the AVLAN system was launched in 1995 and could operate up to 100 M bits per second (Mbps) [1]. This idea was built on by Airbus who introduced a full fibre optic backbone network for IFE on the Airbus A380; this provides entertainment and information on demand to 550 passengers but eventually will be in the region of 750 to 800 passengers. Each of these passengers will be connected to the main fibre backbone via a wired connection and the main backbone capacity is 1 Gbps. These networks are designed for civil aviation and the vast majority of the network and its components will be within pressurised, conditioned areas of the aircraft. The aircraft of interest to BAE Systems and the subject of this thesis are future military aircraft. This may be a fast jet, a transport aircraft or an unmanned aerial vehicle, UAV. There will be differences between the requirements of the networks in the civil and military domains ranging from the power available to components in each network and the environment that the network and its associated components must operate in. There are also differences in what each network is designed to do, the civil network is used for IFE so the data flow is predominantly in one direction, from a central computer to each seat headset with a low data rate link back to the central computer. The data rates in each direction in the network in a military aircraft will be

more symmetrical with high data rates required in either direction. Even with these differences the evolution of fibre optic networks in the military sector has been broadly similar to that of the civil sector. The Eurofighter Typhoon for example is equipped with a star fibre optic network albeit operating at low data rates of 100 Mbps [2], this must be increased in future systems.

## **1.1 Next Generation Network for Military Avionics**

Technologies which are currently being proposed for next generation military jets have the potential to generate large amounts of data, wide area motion imaging, for example, may produce up to 40 Gbps. Although this may be supported with a copper network it will be expensive and will add considerable weight to the aircraft, it is also far beyond the capabilities of the currently deployed optical avionic links and networks. The optical networks required for next generation military aircraft must make significant improvements on those currently in use. It is no longer the case that point to point links and low bandwidth networks can be deployed throughout the aircraft, many end nodes must be connected either to points throughout the aircraft or to a central flight computer and at higher bandwidths than are currently in operation. BAE Systems have indicated that it would be desirable for many channels in future networks to use the gigabit Ethernet standard; this means the data rate from each node would be 1.25 Gbps. It would also be beneficial for BAE Systems if the signal from many channels could be combined and carried down a single fibre, this would make efficient use of the fibre bandwidth but having multiple signals carried down a single fibre will also minimise any penetrations which may be needed throughout the airframe and allow use of optical rotary joints so one end of the network can rotate with respect to the other. The obvious solution to combining signals is to use wavelength division multiplexing (WDM). WDM is explained in detail in subsequent chapters but involves operating each channel at a different wavelength. These channels can then be combined and carried by a single fibre over a large distance, they can then be separated with very little mixing of the signals before decoding the signal at the receivers. This is a widely used technique in the telecoms industry and is a very mature technology, as such there is a large marketplace for sourcing WDM components and if possible, the proposed network should take advantage of economies of scale associated with the telecoms market as opposed to using bespoke components.

The major problem with using both WDM and commercial off the shelf, COTS, components is the operational temperature range on aircraft, this can vary depending on what area of the aircraft the components are situated but the standard for use throughout the

aircraft, excluding the engines, is  $-55\text{ }^{\circ}\text{C}$  to  $+125\text{ }^{\circ}\text{C}$ . This presents a problem with respect to WDM systems because many optical transmitters suitable for use in a WDM network are temperature sensitive and use over a wide temperature range would cause network failure. In addition COTS components tend to be specified for use in a more benign temperature range suitable for telecoms of  $0\text{ }^{\circ}\text{C}$  to  $+70\text{ }^{\circ}\text{C}$ . For both these reasons it is reasonable to expect that many components throughout the network, particularly optical transmitters, must be thermally regulated to prevent network failure. Ideally, this is to be avoided, as cooling and heating individual components over such a wide temperature range will have a large power consumption and adding additional equipment to thermally regulate the network will also add to the weight of the aircraft. For a smaller platform such as a UAV, where power consumption is limited and any increase in weight has a significant impact on the aircraft's ability to carry out missions this could lead to building such an aircraft being unfeasible. This thesis will aim to identify methods for using WDM networks on aircraft while attempting to minimise the power requirements and weight of additional cooling.

## **1.2 Thesis Layout**

In order to design a WDM network which can realistically be deployed on a future aircraft the design must be kept as generic as possible so as not to rule itself out when aircraft designs are finalised. This thesis is aimed towards developing such a novel, generic network suitable for WDM with each channel operating at 1.25 Gbps with minimal cooling used throughout the network and using COTS components where possible. The thesis is structured as follows.

Chapter 2 presents the background areas of interest to the thesis and provides a review of the current state of the art. It begins with a basic overview of multiplexing using time, space and wavelength then going into WDM in more detail.

The advantages of optical networks over copper networks for use on aircraft are discussed in more detail and different network architectures are introduced. The suitability of these architectures for use as a generic network on an aircraft is considered. Particular attention is paid to the passive optical network and how effective it may be, when used in conjunction with WDM, for the problem in hand.

The basic concepts of semiconductor optics are introduced and the application of this to building network components is discussed. A number of these semiconductor components are discussed and the most suitable for use on the proposed network pointed out with



particular attention paid to semiconductor optical amplifiers. Passive fibre optic components are also introduced and multiplexing technologies for combining and separating WDM signals examined in detail.

There are particular requirements of an avionic network which are unique from other networks in differing sectors. These are broadly divided into two sets, environmental requirements and functional requirements. Both these sets of requirements are discussed in detail along with how they affect the network design and performance.

The final section of chapter 2 reviews the current relevant research, focussing on work on both access networks and avionic networks and how this research may or may not be used with the proposed network.

Chapter 3 details thermal testing undertaken on the passive components to assess their compatibility with the environmental requirements. Other environmental requirements, such as tolerance to vibration, may also cause the network to fail but this is assumed to be an issue with packaging. While this is also true in the case of temperature cycling, wavelength selective devices in particular can display strong temperature variations in their operational characteristics and this needs to be understood. A selection of passive fibre optic components have been selected which allow a flexible network to be built in multiple possible architectures are tested and their performance discussed bearing in mind the roles they must fulfil in the network

Chapter 4 builds on research from the literature review at the end of chapter 2 on using a spectrum sliced broadband source to seed a reflective semiconductor optical amplifier (RSOA) and create a temperature tolerant end node for WDM. Two different RSOAs are investigated for use in this configuration and with a combination of experimental measurements and modelling the performance of these devices and their effect on the performance of the network as a whole is characterised.

Chapter 5 introduces thermal management and investigates the power consumption of different thermal management techniques give the limits on network performance discovered in chapter 4. The idea of passive thermal management, cooling with no direct power consumption, is introduced and this is compared to cooling using a thermo-electric cooler through mathematical modelling work.

Chapter 6 moves away from the idea of spectrum slicing and details a novel power saving technique when using a WDM passive optical network, PON, with laser transmitters and optical amplification. This is presented as an alternative to using the network detailed in

chapter 4 and as such there will be cases where each network will perform better than the other. The power savings using the novel technique are calculated and the reduced power consumption compared to the power consumption of the RSOA network in a number of realistic avionic conditions. The applicability of each solution to these situations is discussed in detail.

Chapter 7 provides a summary of the thesis and draws conclusions from the work presented.

## **1.3 Findings and Contributions**

1. Identification of the operational temperature ranges of standard telecoms fibre optic components. In particular multiplexing components, a 100 GHz spaced athermal arrayed waveguide grating (AWG) can be used from 0 °C to 60 °C when spectrum slicing and a 200 GHz spaced, thin film filter multiplexer from -40 °C to +85 °C.
2. A spectrum sliced wavelength division multiplexing passive optical network (SS WDM-PON) demonstrating bi-directional 1.25 Gbps traffic using RSOAs as amplifiers and modulators has been demonstrated.
3. A numerical model has been made to predict the path loss capability of a WDM-PON using RSOAs has been made and its output has been validated experimentally
4. RSOA parameters taken from experimental work have been used in the model to predict that use of a novel RSOA can operate in a SS WDM-PON as a modulator, uncooled, from -55 °C to +70 °C. This is an improvement on standard devices which are predicted to operate up to +50 °C before the signal quality becomes unsatisfactory.
5. Passive cooling in the form of phase change materials have been investigated and shown to be less efficient than thermo-electric cooling when deployed on a Boeing 737-800.
6. A novel power saving technique for WDM-PON networks on aircraft has been proposed and is predicted to offer savings of 20% in power consumption of the optical transmitters in a realistic environment.
7. Power consumptions of the RSOA network and distributed feedback (DFB) laser based networks have been compared. In conditioned areas of the aircraft the

DFB is more efficient whereas operating over the full avionic temperature range the RSOA network is more efficient.

## **1.4 Publication List**

- [1] C. Michie, W. Johnstone, I. Andonovic, E. Murphy, H. White, A. E. Kelly, "Semiconductor Optical Amplifiers in Avionics", AVFOP 2011, pp 73-74
- [2] E. Murphy, C. Michie, H. White, W. Johnstone, "Phase Change Materials for Passive Cooling of Active Optical Components", AVFOP 2012, pp 11-12
- [3] E. Murphy, C. Michie, H. White, W. Johnstone, A. E. Kelly, I. Andonovic, "High Temperature Wavelength Division Network for Avionic Applications", Journal of Lightwave Technology, Vol. 31, pp 3006-3013, 2013
- [4] E. Murphy, C. Michie, H. White, W. Johnstone, "Power Saving Technique Suitable for DWDM-PON on Aircraft", AVFOP 2013, pp 21-22
- [5] E. Murphy, C. Michie, H. White, W. Johnstone, A. E. Kelly, I. Andonovic, "Energy Savings in WDM Networks using Reflective Semiconductor Optical Amplifiers [Invited]", ICTON 2014, Tu.C4.3
- [6] E. Murphy, C. Michie, H. White, I. Andonovic, W. Johnstone, "Power Savings for DWDM-PON for Aircraft", Optical Engineering, Accepted for publication

## **2. Literature Review**

### **2.1 Multiplexing**

In order to take full advantage of the fibre bandwidth it is necessary to carry multiple channels down a single fibre simultaneously. This is known as multiplexing. Multiplexing is usually carried out in the time or frequency (referred to as wavelength in optical communications) domains.

#### **2.1.1 Time Division Multiplexing, TDM**

Communications bandwidth can be increased by using one of three well established multiplexing techniques. The simplest multiplexing technique is time division multiplexing (TDM); this involves multiple users transmitting data along the same fibre. The fibre bandwidth greatly exceeds the data which each individual user wishes to transmit, therefore each user can be assigned a time slot in which the user can utilise the entire bandwidth to transmit their data. TDM does not increase the fibre bandwidth but does increase functionality and efficiency with multiple users and multiple signals using the same fibre [3]. If the users require high bandwidths then TDM is not a desirable solution and it is also more prone to obsolescence than other forms of multiplexing.

TDM is commonly used in the telecommunications sector in access networks. Due to fast growing bandwidth demands in the home and workplace copper based access networks are being replaced with fibre optic networks. These networks use TDM to increase the number of potential users. TDM coupled with wavelength division multiplexing is a topic which is currently being widely researched for this application [4,5]. Although research on access networks can sometimes be adapted to the topic of avionic networks due to similarities in both this work is not as applicable. The bandwidth requirements per 'user' on an aircraft are likely to be much higher than that of a user in an access setting. For this reason TDM will not be considered for use in this thesis.

#### **2.1.2 Space Division Multiplexing, SDM**

An alternative which may not use a single fibre but can be considered as multiplexing is space division multiplexing. This entails using multiple fibres for multiple signals with each channel having its own dedicated fibre. Clearly this can lead to large bit rates but at the price

of multiple components adding increased weight and cost. This technology is currently used in avionic platforms using 850 nm over multimode fibre [6]. This wavelength has been chosen as light sources such as a Vertical Cavity Surface Emitting Laser (VCSEL, see section 2.3.1.2 Vertical Cavity Surface Emitting Laser) and detectors are less expensive at this wavelength, although the telecommunications industry has now driven down the cost of 1550 nm sources.

SDM is progressing to studies of multicore fibres and modal multiplexing [7], where a multimode fibre is used and each mode is used as an individual channel. Both these techniques are being investigated as the spectral efficiency of long haul links are approaching a fundamental limit, known as the non-linear Shannon limit, and high data rates are being reported [8]. The data rates required on an aircraft are in the order of tens of Gbps, when compared to hundreds of Tbps required in the telecoms links it is clear that the non-linear Shannon limit will not be a problem for the foreseeable future. As a result SDM will not be considered in this thesis although it is reasonable to assume that multicore fibres may have uses on aircraft in the future.

### **2.1.3 Wavelength Division Multiplexing, WDM**

Wavelength division multiplexing is a technique to increase fibre bandwidth by transmitting multiple channels down the same fibre. To stop interference between these channels each is carried by a different wavelength.

#### **2.1.3.1 Coarse Wavelength Division Multiplexing, CWDM**

CWDM stands for coarse wavelength division multiplexing and is sometimes used in access networks. It is possible to achieve data rates of 10 Gbps on each channel using laser transmitters at the end nodes [9].

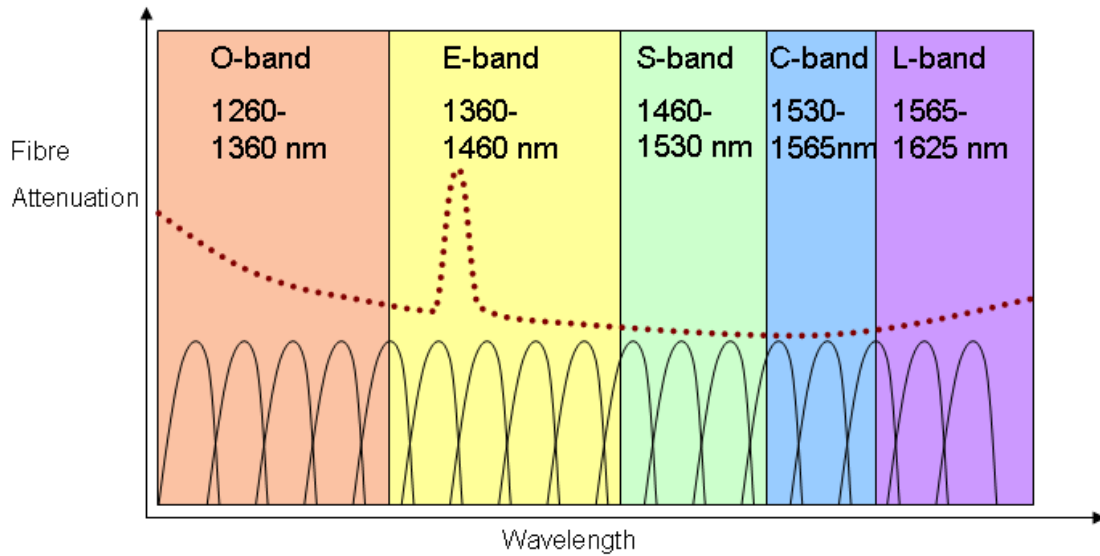


Figure 1: Section of the spectrum split into CWDM bands and overlaid with the curve representing fibre attenuation as a function of wavelength and potential channels. [10]

The basis for CWDM is to transmit a number of 13 nm wide channels separated by 20 nm as specified by ITU G694.2. The signals for each channel are individually generated by a dedicated laser and coupled together by a multiplexer (sometimes called MUX). The signal can be guided by a multimode fibre but link range is limited to around 300 m due to problems introduced by intermodal dispersion [9] and higher losses at multiplexers and de-multiplexers therefore single mode fibre is preferred for longer links. To decouple the signals and send them to the receiver the channels need to pass through a de-multiplexer (DEMUX). The spectral region used for CWDM is shown in Figure 1; this region has been selected as it has the lowest attenuation when propagating light through glass fibre. Figure 1 clearly shows the water peak, in the E-band, where water molecules in the glass increase the absorption; operation at this wavelength is usually to be avoided but fibre manufacturers have eliminated this peak and opened up this entire section of the spectrum [11]. Due to the short lengths of aircraft links fibre attenuation is not a pressing issue.

As the various components needed for CWDM are exposed to changing conditions such as temperature, their performance changes. This change in performance is most notable as a shift in the wavelength used for each channel; the linewidth of the signal is usually small relative to the spacing between channels meaning that CWDM can be forgiving in harsh environments as the signal wavelength has a buffer on either side which it can wander into without interference or crosstalk. This relaxes cooling requirements on the

lightsource and allows for greater tolerance in the fabricated centre wavelength which reduces overall system cost relative to dense wavelength division multiplexing.

### **2.1.3.2 Dense Wavelength Division Multiplexing, DWDM**

Dense wavelength division multiplexing (DWDM) is a technique which is similar to CWDM but uses narrower channels with less spacing. This results in many more channels and gives much higher bandwidth, 25.6 Tbps using 160 WDM channels has been reported [12]. ITU-T Recommendation G.694.1 specifies the channel spacing and wavelengths to be used for DWDM worldwide so different systems can be integrated. Channel spacing of 50 GHz, or approximately 0.4 nm, is possible for telecommunications in the region 1528.77 nm to 1563.86 nm but more commonly channels are spaced at 100 GHz, or 0.8 nm, intervals; in this spectral region fibre optic attenuation is at a minimum and it is also the region where an erbium doped fibre amplifier (EDFA) can be used. Clearly this narrow channel width allows many more channels than CWDM and it is possible to use channels outside the ITU specified range which opens up hundreds of potential channels.

Because these channels are narrow there is a much smaller margin for error than in a CWDM system. The lightsource must have a very narrow and stable linewidth so DFB lasers are used. The emitted wavelength of these lasers is temperature sensitive so in order to ensure that each signal stays within its channel they must be temperature stabilised with a thermo-electric cooler. DWDM has the advantages over CWDM of significantly larger bandwidth but at the expense of systems complexity. For use on an avionic platform with temperatures ranging from -55 °C to +125 °C DWDM poses some significant problems to integration. The cooling requirements over this range would lead to a large heavy system with high power requirements unsuitable for aircraft. A new approach must be taken with reduced cooling requirements if possible.

Regardless of whether coarse or dense WDM is used an additional advantage over other single wavelength systems is the increased options in switching and routing around the network with the use of wavelength selective components. As each channel is assigned an individual wavelength it is possible to add and drop these channels individually or route groups of channels based on wavelength.

## **2.2 Networks**

## 2.2.1 Advantages of Optical Networks

The main driver behind the integration of fibre optics into avionic networks is capacity. Fibre optic systems offer a future proofed solution to bandwidth needs which can be achieved at a reduced cost over the systems operating lifetime when compared to copper alternatives. A copper cable has significantly higher attenuation than a fibre optic cable, for example the typical attenuation for Corning SMF 28 is 0.17 dB/km whereas the minimum attenuation in 0.9 mm copper cable from UM is 4.4 dB/km. Over very short distances a copper cable may be able to carry up to 1 Gbps but once the link range is over 100 m fibre optic cable is the only realistic option for high data rate connections on aircraft. Due to the high potential bandwidth of the fibre an optical network is less susceptible to obsolescence than a copper network as any breakthrough leading to higher bit rates can still be carried by the fibre.

Another advantage of fibre optics is the smaller size and weight. An optical fibre is essentially a thin glass fibre with a protective covering. Copper cables are thicker and consist of pure copper so are considerably heavier. It has been estimated that replacing copper based sensor systems with a fully fibre optic based sensor system on the landing gear of a commercial passenger jet would remove over 100 kg [13]. In any aircraft, be it commercial or military, space and weight are at a premium and can cost large sums of money over the operating lifetime; so any loss of weight is a huge advantage.

Modern aircraft are filled with potential sources of electromagnetic interference (EMI); these sources are shielded to prevent any interference or crosstalk with the copper network. Any damage to this shielding or a faulty connection will lead to EMI in a copper based network. As the carriers in fibre optic networks are photons as opposed to electrons it is immune to any adverse effects arising from EMI although electrical components such as transceivers are still vulnerable. This reduces potential problems associated with EMI and allows some of the shielding to be removed and weight of the overall aircraft to decrease further.

In some military applications it is desirable for the system to withstand an electromagnetic pulse (EMP). Copper cabling acts as an antenna for the EMP and is easily damaged. A fibre optic cable is less susceptible to damage although there may be some change in fibre attenuation. However, while the fibre may withstand EMI levels that would be damaging to copper cables the electronics, such as transceivers, would be vulnerable.

In communications systems fibre optic cables carry light of up to several milliwatts, so there is no spark hazard and the cable can be placed in locations where it would be



potentially dangerous to deploy any copper cables. In addition to this many optical components are passive, i.e. they do not require any power or electronics to function. This further reduces any spark hazard as well as lowering power consumption of the overall system.

There are some drawbacks concerning the use of fibre optic cable, for example it is significantly more difficult to repair a broken cable with both ends of the fibre needing to be cut, cleaned and spliced accurately together. However, at high data rates a copper cable is also difficult to repair so the maintenance problems are beginning to look like less of an issue.

### 2.2.2 Network Architectures

The potential architectures for an avionic network are very similar to those used for a local access network (LAN) and as such are well defined [14].

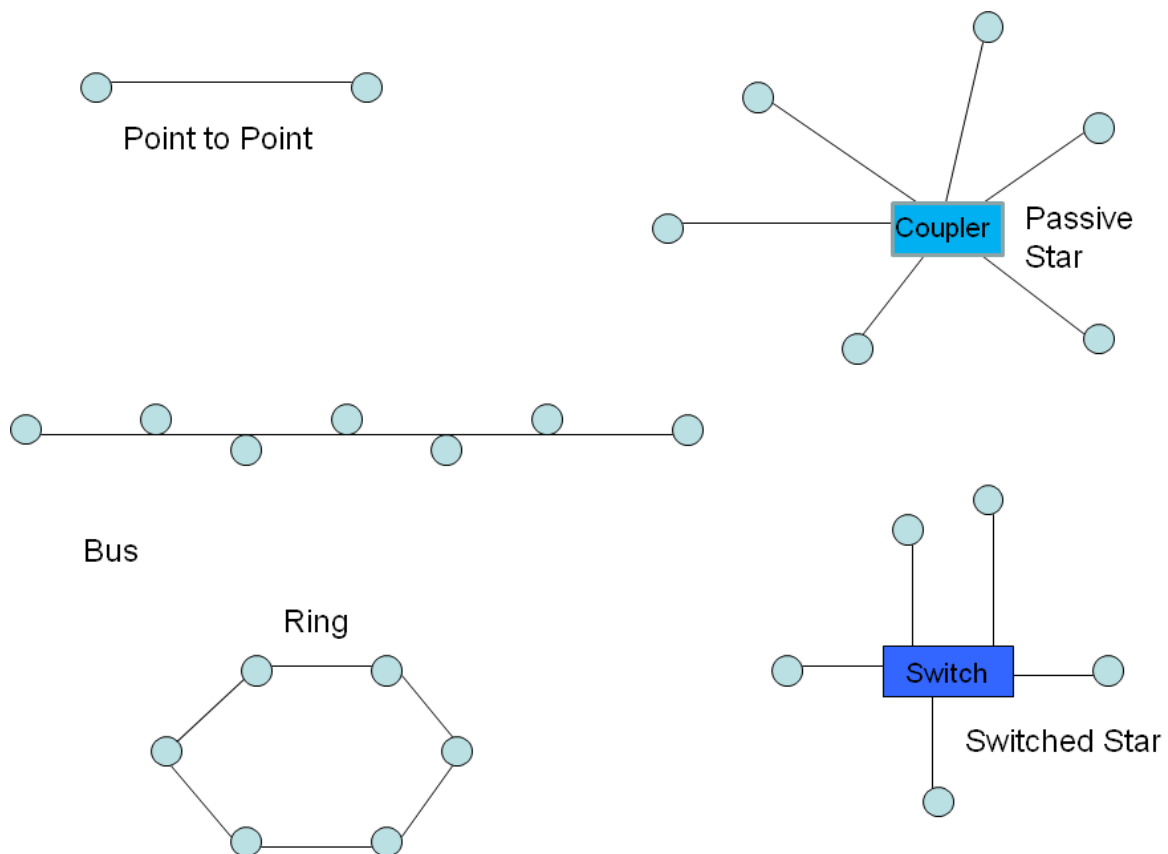


Figure 2: Schematic of the main network layouts

The simplest design is the point to point link, as shown in Figure 2; this has one link between two users. A point to point link can be used in an avionics environment to provide a dedicated link between two devices, for example, a sensor and a processor.

A passive star network has some similarities to a point to multi-point link in that any central node has a physical link to all other nodes in the network via a star coupler. A node can transfer data to all nodes through the coupler and can receive data from any other node. The main advantages of the star are the durability with respect to faulty nodes. Any fault in a node or cable will only affect one node and the rest of the network can carry on as designed. It is also possible to introduce new nodes into the system, although there is usually a limited need to add nodes on aircraft networks. More important is the ability to increase the data rate, due to the inherent high fibre bandwidth the network is scalable and less prone to obsolescence. The main drawback is that the coupler is a single point of failure; if it fails the entire network will fail. It also uses more fibre than other networks which increases the system cost, although due to relatively short fibre lengths in aircraft this is not as much of a concern as it is with telecoms networks. Passive star networks use routing components which consume no power, the central node may route the signal depending on its wavelength or sometimes power splitters can be used. Wavelength selective passive star networks suitable for aircraft have been suggested [15,16]; this would reduce the power consumption of the overall network. However, the transmitters would need to be tuneable if the nodes were to select which other nodes to communicate with; this leads to increased complexity and cost. The use of tuneable sources also slows the network down as it takes time to tune the transmitter between the relevant wavelengths, during this time no data can be sent, however, if TDM is being used the source can be tuned in time allocated to other channels.

A switched star network employs a switch at the central node, the switch will determine which node each packet of data has to be sent to and send it to this node only; this leads to less network traffic but does have additional power consumption than the passive star. A switched star type network has been proposed for use on aircraft [17]. The proposed network operates at 1.25 Gbps using commercial off the shelf components although no considerations have been made regarding the extreme operating temperatures on aircraft so a switched star of this type may have to be used in selected locations throughout the aircraft. The fact that the switched star is selective means it could suffer from a data bottleneck and it may be prone to overloading and failure. Currently 10 Gbps optical Ethernet switches are commercially available which should be sufficient for avionic networks for the foreseeable future. Nevertheless this must be considered when assessing the scalability of the network for future capacity demands.

A ring network consists of a series of nodes connected by consecutive point to point links; each node is connected until the loop is closed by connecting the first and last nodes. The flow of data may occur in one direction around the loop or bi-directionally depending on the design. The ring topology has been used on the Boeing 777 optical network [18] and recently WDM ring networks, where each node is designed to operate at one wavelength, have been proposed for use on aircraft [19]. The network can also be designed with multiple fibres to give bi-directional data transfer around the loop and increased survivability should any fault occur. A key advantage of this approach is that the network is easy to install due to the simple layout, however any changes will affect all nodes down the fibre which could alter link power budgets and achievable data rates.

The bus network usually consists of one main fibre 'backbone' which carries the multichannel signal with all nodes along the fibre having access. Each node has access to the main backbone by tapping off a wavelength or by dropping a small amount of optical power. The bus has advantages that it is relatively straightforward to install and add new nodes due to the simple layout but is vulnerable to failure if no back up is installed. A development of the bus is used on the Airbus A380 to provide an Ethernet connection over fibre [20]. In order for a network to be adopted in an aircraft it must fulfil rigorous safety specifications as any fault could have disastrous consequences. One of the advantages of the bus is how it can be configured to ensure survivability of the network. A method to increase the survivability of the network is to use the robust bus (ROBUS) as shown in Figure 3 [21] which takes elements of both the ring and bus network. This design consists of a number of fibres looped through nodes; these nodes can lead off to the network device. The governor dictates data transfer and can be connected to another ROBUS ring or to further networks. The survivability is shown in Figure 3, if one node is faulty or becomes damaged the two nodes on either side can form connections between the primary and secondary cables to reroute the data avoiding the fault. The system can be made with more back up fibres and a back-up governor should it fail. Another similar method to create a fault tolerant method is to use torus based architecture [22]. This is a set of interlocking ring networks; there are multiple paths to each node so the network can survive multiple faults and each node will still have a connection. Although these two examples are by no means the only design of fault tolerant for use in aircraft it displays the principle used in all designs of multiple fibre paths and redundancy to allow for faults.

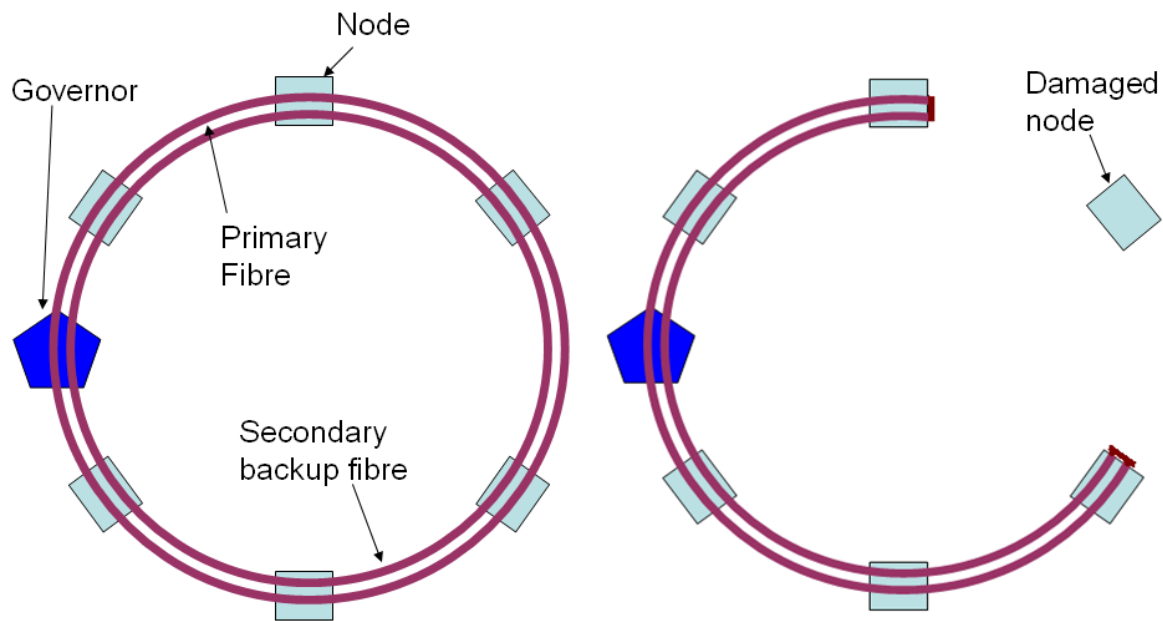


Figure 3: A ROBUS network before any faults and with a damaged node to show how the re-routing could occur [21]

This brief overview of basic network topologies illustrates the range of examples that have been deployed in telecommunications systems and that are appropriate for consideration, either on their own or as a hybridised solution to fit the needs of the avionic application. The challenges of avionic systems are different and care must be taken not to assume all solutions are appropriate. For example modern day telecommunications networks use a mesh network where a wide variety of network components are connected by multiple paths through components or links. This means any faults in the network can be avoided by taking an alternative route. Although this system is excellent for telecommunications it has not been studied in detail for avionic platforms. The highly complex system would be very challenging to integrate onto an aircraft and as of yet no need for this topology has been seen. All the networks described above will have points of failure and for use on aircraft will be deployed with multiple paths and no single point of failure as demonstrated by the ROBUS network.

### 2.2.3 Passive Optical Networks

Passive Optical Networks, PONs, can be considered as a method of implementing certain network architectures. There are many different ways of implementing a PON which give different network performances but the defining characteristic of a PON is that it utilises passive components between the transmitter and receiver, usually a passive component

would be a component with no power consumption but in a PON it is considered to be a non-terminal component. For example, an amplifier has a power consumption but can be treated as a passive component in this case. PON development is being driven by the telecommunications industry which sees a need to deliver fibre to the home in order to supply high bandwidths to customers. PONs are also of interest on avionic platforms, the passive elements reduce the power consumption of the network. To use the terminology of an access network an optical line terminal (OLT) provides information to many optical network units (ONUs) using passive optical splitters i.e. splitters that require no power. The ONUs can send smaller amounts of data back to the OLT. This is called upstream transmission; data transfer from OLT to ONU is referred to as downstream. On an aircraft this is analogous to a flight computer or a central node (OLT) communicating with a network of sensors or end nodes (ONU) throughout the aircraft.

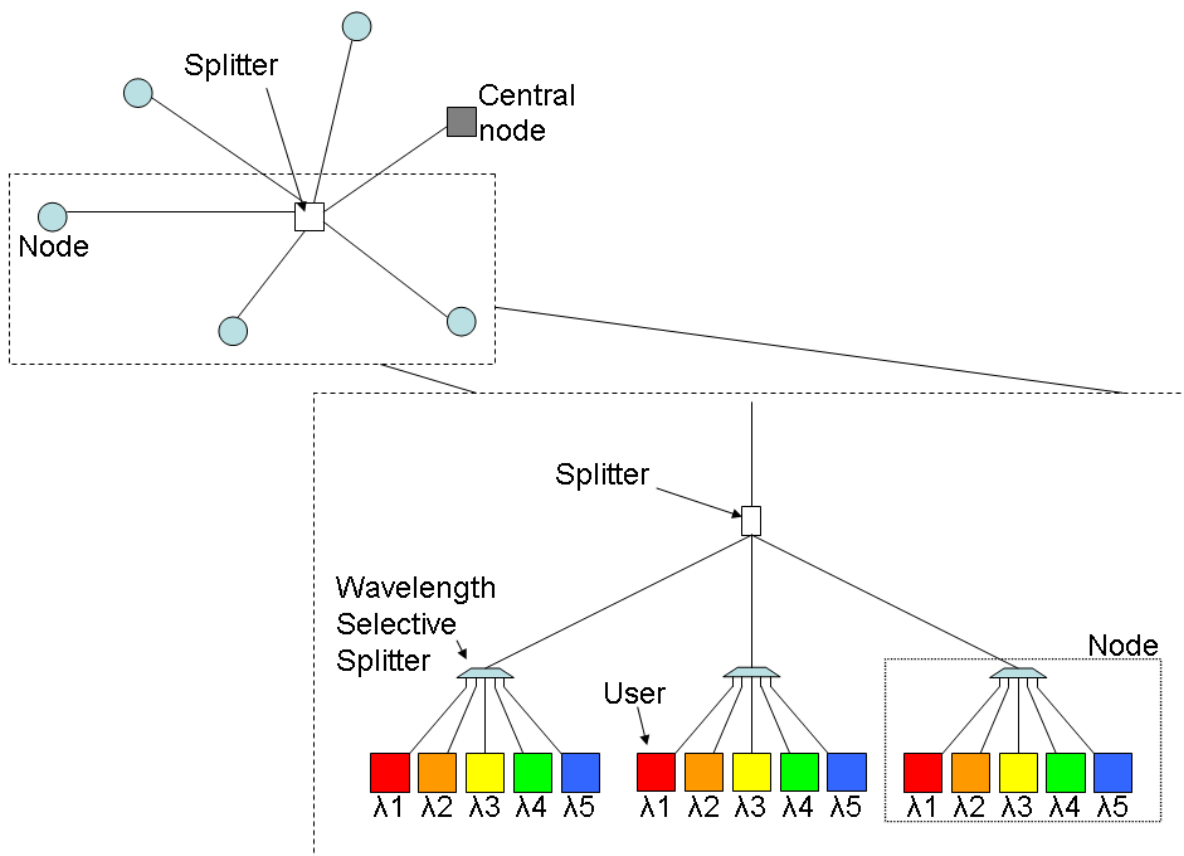


Figure 4: An example of a passive optical tree network. One central node may transmit data which is broadcast to all nodes via a splitter, at each node a wavelength selective splitter routes data to each user who can have their own wavelength channel.

In a tree type network one splitter is needed in a PON to divide the signal between all nodes, in a bus or ring network successive splitters are used to reroute a small portion of the signal to each node with a decreasing signal available for each node.

When transmitting in both downstream and upstream directions measures need to be taken to ensure there is no crosstalk between channels. There are two established methods for doing this, either TDM or WDM. If TDM is used the passive splitter will split the signal regardless of wavelength so there is equal power in each output port, as with the splitter in Figure 4. A timing system must be set up at the ONU so each user receives the correct signal. For upstream transmission from ONU to OLT each ONU has a specified time slot at which it can use the fibres entire bandwidth. In order to specify the start time and length of the transmission a bandwidth allocation scheme is needed, if this scheme must adapt to different levels of traffic flow a dynamic bandwidth allocation scheme is necessary which increases system complexity. In addition to this TDM PONs have limited bandwidth, the layout dictates the central node will transmit large amounts of data and the end nodes will transmit a relatively small amount meaning PONs are more suited to broadcast of data. This is more suited to an in-flight entertainment system than the network on a military aircraft. The telecommunications industry has moved away from the single wavelength TDM PON to introduce WDM working alongside TDM in PON for access networks.

WDM PON technologies are described in detail by Banerjee et al. [23]. WDM PONs typically use different bands for upstream and downstream transmission and both upstream and downstream signals can be sent at the same time. For example 1550 nm can be used in the downstream direction and 1300 nm upstream. At its most basic level a WDM PON can be implemented with a bank of transceivers at the OLT, the signal from these lasers can be coupled into a single fibre backbone by a multiplexer and sent to the ONUs where the signals are separated using a match demultiplexer. In this case the WDM PON is essentially a collection of point to point links carried by a single fibre, this can be used for bi-directional traffic with data rates the same in both directions. Often in telecoms the downstream data rate must be greater than the upstream data rate and a TDM overlay is used to increase the number of end users. In an avionic network the data rates in both upstream and downstream directions are likely to be very similar so no TDM overlay is required.

#### **2.2.4 Avionic WDM Local Area Network, LAN**

In order to develop a suitable PON style network for avionics while taking advantage of the components and some techniques from the telecoms sector, standards for a WDM LAN are

being developed by SAE International (originally the Society of Automobile Engineers) [24], final definition of these standards are still ongoing [25,26]. The standards are designed to create framework to use optical WDM networks that will support a number of protocols and accommodate large channel counts with high bandwidths that are expected on future aircraft. Currently aircraft information reports AIR6004, AIR6005 and AIR6006 define a glossary of terms, general requirements and the current and required states of simulation and modelling of avionic WDM LAN respectively.

These standards are an important part of the development of WDM networks for aircraft although at the current time they are currently geared towards definitions at a higher level of operation than this thesis is concerned with.

## **2.2.5 Protocols**

Every network needs to implement a protocol to govern the communications between each network node. The protocol is essentially a set of rules which describe message formats which include signalling, authentication and error detection. There are many network protocols currently in use but by far the most commonly used is the Ethernet protocol, although this is not the case on aircraft. Although there are numerous protocols being used currently and considered for future avionic networks, such as CAN protocols or FlexRay to name a few [27], an assessment of each one is beyond the scope of this report.

### **2.2.5.1 Ethernet**

In the first realisation of Ethernet each user's computer on the network monitored the traffic; if the network was clear then data could be sent. This is designed with the knowledge that collisions can and will happen when two users try to transmit data simultaneously, both users wait a random length of time and try again. The collisions occur infrequently enough that they do not greatly affect the bit rate supported by the network. However, it is theoretically possible for a message to be involved in a collision every time it is sent meaning it could be delayed for an infinite interval. For certain safety critical applications on aircraft this is not acceptable and we must be certain that the message has been received.

The Ethernet protocol, standardised as IEEE 802.3 [28], requires the data to be sent in frames, the first few sections of the frame synchronise the clocks of transmitter and receiver then carry the address of the recipient and the sender of the data. The data is then sent followed by another section used for error detection in the event of a collision. In an

attempt to limit collisions switched Ethernet was developed, the data is routed through a hub which allows multiple signals to be carried from different transmitters for different users. A major problem with regards to using Ethernet on avionics is that it is non deterministic because collisions are expected. A deterministic network is one in which a message will take a known maximum length of time to reach the recipient. As a message in an Ethernet network can be significantly delayed this means it is unsuitable for safety critical applications in its normal use.

#### **2.2.5.2 Avionic Full Duplex Switched Ethernet (AFDX)**

AFDX was developed by Airbus for use on the A380 with Ethernet type media over multiple point to point links where determinism is essential and research is being carried out into the suitability of AFDX for safety critical applications [29]. The main features of AFDX are determinism through imposed limitations, the bandwidth is limited so the same bandwidth is guaranteed at all times and the maximum length of time between transmission and receipt of a signal is known. All signals are routed through a switch which has the ability to store and transmit signals. This switch has multiple receivers and transmitters so collisions are avoided; the only limitation is delays due to congestion at the switch. In theory a switch could overflow due to severe congestion but in practice components which would lead to overflow would not be selected for high data rate networks.

Although the protocol used in the final design may not be AFDX it is likely to be based on Ethernet in some capacity. Due to the widespread use of Ethernet it has many advantages in terms of compatibility with components and other systems. There are also many working groups developing new technologies for Ethernet, it would be possible to take advantages of any advances in technology if using an Ethernet based system.

### **2.3. Components**

No matter which network architecture has been chosen many of the optical components required will be the same as those in other architectures and protocols. All optical networks need a lightsource, either a lightsource which can be directly modulated to provide encoded data or a continuous wave source with an external modulator. A receiver will be needed to detect the optical signal and convert it into an electrical signal from which the data can be recovered. Between the transmitter and receiver fibre is obviously required in addition to switches, connectors and multiplexers to name but a few components. In order to build an



effective network for an avionic platform each component must be able to withstand the harsh environment they will be exposed to over much of the systems working life.

Most transmitters and receivers used in fibre optics communications are semiconductor p-n junctions with either a forward bias or reverse bias. A p-n junction is simply formed at the interface of p doped and n doped semiconductor as shown in Figure 5, it is described in detail in the literature [30]. The Fermi Level represents the level at which the probability of a site being occupied by an electron is 0.5, it is constant throughout the junction in equilibrium. The bands bend at the junction to accommodate the constant Fermi level and this forms a depletion region where there is a non-zero electric field. The difference between the energies of the same band on either side of the depletion is known as the built in potential and forms a barrier to current flow.

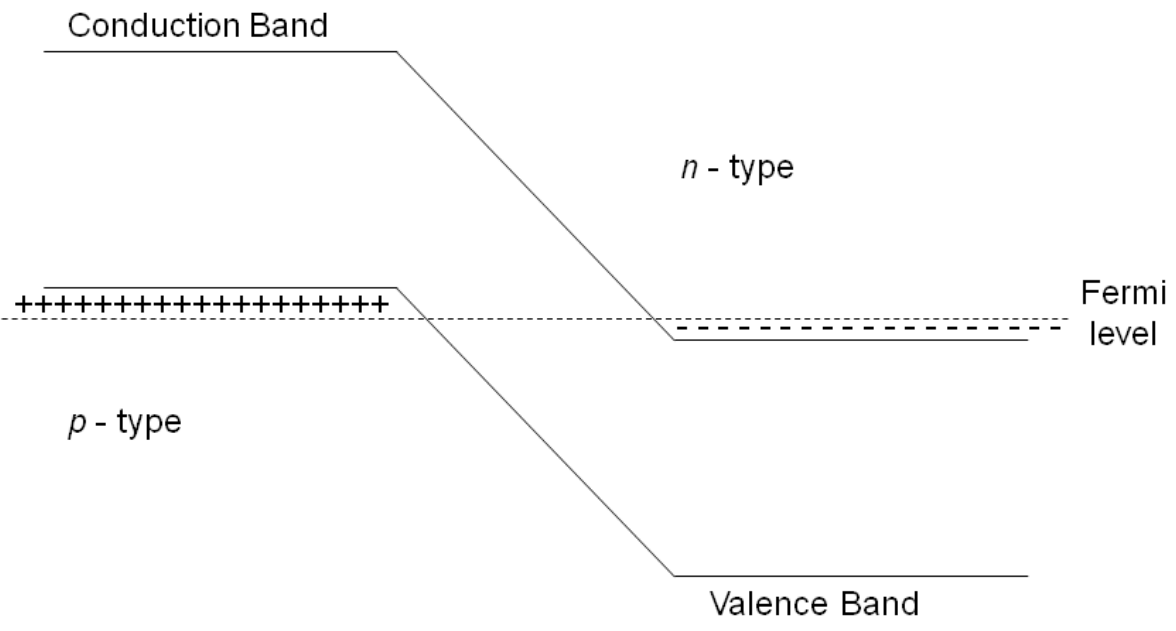


Figure 5: Energy band diagram of p-n junction at equilibrium

When a positive voltage is applied across a p-n junction, i.e. a positive voltage applied to the p doped side of the junction, it is said to be forward biased, this will reduce the potential barrier and cause electrons and holes to be injected into the junction. Excess charges can recombine across the junction and emit a photon. Alternatively when the junction is reverse biased a negative voltage is placed across the junction and the potential barrier increases. A photon with energy greater than that of the bandgap can form an electron hole pair; these

will be swept in opposite directions if formed within the depletion region resulting in a detectable current.

### 2.3.1 Transmitters

For use in a DWDM system it is necessary for a source to have a narrow linewidth and be stable over the operating conditions. It is also desirable to have a fast recovery rate so the output can be modulated at high speeds for high data rates.

#### 2.3.1.1 Distributed Feedback Laser

A DFB laser shows a very narrow linewidth and is commonly used for DWDM [31]. The laser has a grating written into the device as shown in Figure 6 which provides a periodic variation in refractive index. This acts as a Bragg grating which provides feedback to a specific wavelength and its harmonics which can be chosen by changing the period of the variation. Only one of the wavelengths in this set of harmonics should be within the gain profile so this laser exhibits a very narrow linewidth. Each cleaved end of the laser is antireflection coated to prevent feedback which would lead to a Fabry Perot type laser. As this laser relies on the grating for feedback it is temperature sensitive, any change in temperature will change the refractive indices in the grating which changes the wavelength for which feedback is provided. The wavelength drift is usually of the order  $0.1\text{nm}/^\circ\text{C}$  so the device temperature must be regulated (generally cooled) to use in a DWDM system. Uncooled operation of DFB lasers on an avionic platform for WDM is not feasible and the thermo electric coolers which would be needed for each laser make this too costly to use on aircraft.

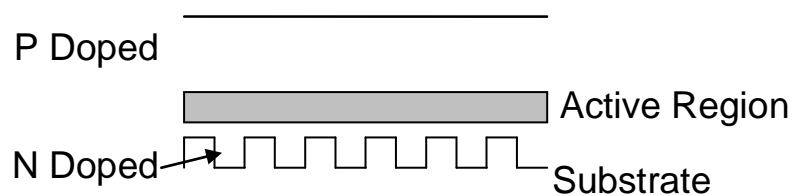


Figure 6: Cross section of a segment of Distributed feedback laser

#### 2.3.1.2 Vertical Cavity Surface Emitting Laser

The VCSEL differs from standard edge emitting semiconductor lasers in that light travels across the active region as opposed to being guided along it in the direction of the epitaxial

layers [32]. This means the output beam does not have the same divergence and astigmatism that is often present in edge emitters. A diagram of the cross section of a VCSEL is shown in Figure 7. The Bragg layers are grown epitaxially in quarter wavelength slices to act as highly reflective mirrors, these mirrors are necessary since the light only propagates through a thin gain region the gain is considerably less than that in an edge emitter. Because of this small active region the modes which will oscillate in cavity are spectrally far apart, this combined with the Bragg reflectors means VCSELs normally operate with a single longitudinal mode. VCSELs are being investigated to provide gigabit Ethernet on avionic platforms [33], so far only proof of principle work has been done and the system has not been proven in the extreme temperatures at which it would operate although VCSELs are currently used in low data rate avionic systems [6]. Since these devices are grown en masse there is the possibility for low cost mass-production, currently VCSELs are available at 850 nm and 1310 nm, 1550 nm devices are in early development and are beginning to become commercially available although, like the DFBs, these will be thermally sensitive.

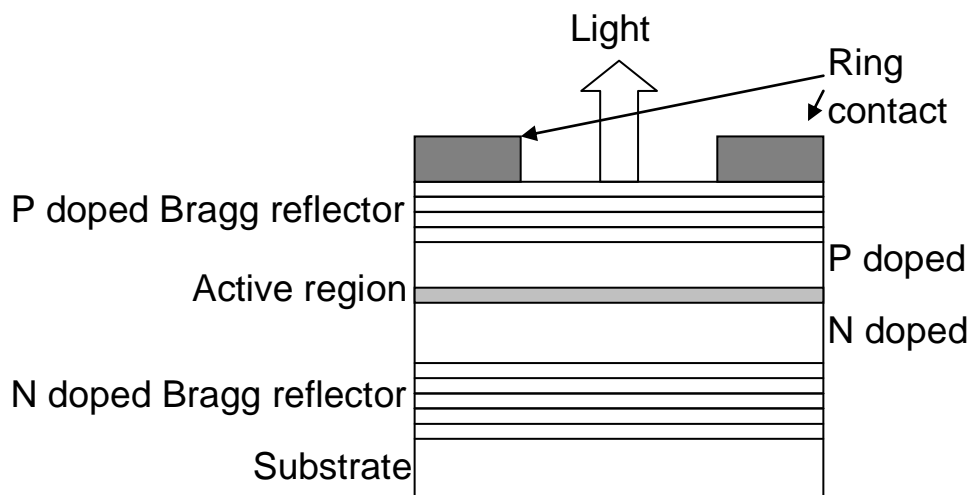


Figure 7: Cross section of a VCSEL

### 2.3.1.3 Tuneable Laser

If it is desirable for one node to be able to communicate using all channels in a WDM system it is not feasible to have multiple lasers at the node. One possible solution is to use a tuneable laser to cover all possible wavelength channels. A tuneable DFB laser has been designed which is suitable for use in DWDM [34] and recently tuneable lasers have been proposed as part of a TDM/WDM PON for next generation access networks [35]. As temperature changes the refractive index in the grating it shifts the emitted wavelength due to the feedback condition, this means that by controlling the temperature in the laser the

emitted wavelength can be fine-tuned. By monitoring the emitted light from one facet it is possible to measure the wavelength of the output while using light from the opposite facet as the source. This technique can take up to a few micro-seconds to tune between wavelengths so is unsuitable for applications where fast switching between wavelengths is needed but could be used as part of a TDM based network. The amount of extra cooling and wavelength monitoring systems make this technique unfeasible in avionic environments. However, in conditioned parts of the aircraft, these devices may offer an attractive option for a high speed 'colourless' transmitter where colourless refers to the fact that the same transmitter can operate at any wavelength over a ~40 nm range.

#### **2.3.1.4 Broadband Sources and Spectrum Slicing**

A major problem with using a source with a narrow linewidth for WDM, particularly for DWDM, is that if the wavelength drifts, some of the signal may leak into an adjacent channel causing crosstalk and errors. As a precaution each source is individually cooled to regulate its wavelength. This leads to a more complex, heavier system which costs more money to build and maintain. An alternative to this is to use a broadband source which can be split into its spectral components to get a number of narrow linewidth channels. One such source is an EDFA which is 'spectrum sliced' by an AWG (more in section 2.3.3.1 Arrayed Waveguide Grating) [36]. An EDFA can be used as a light source as opposed to an amplifier if no light is injected to be amplified, spontaneous emission will occur which will in turn be amplified and lead to a broad emitted spectrum. The EDFA will amplify signals at 1550 nm for telecommunications, the Amplified Spontaneous Emission (ASE) is also in the same wavelength range which sits in the C band (roughly 1520 nm to 1570 nm but many variants have been made) and is useful for WDM. As the spectrum is being split up into a number of channels a high power source is required so each channel can maintain high power in a narrow spectral width after amplification. High power Superluminescent Diodes (SLD) have been developed which are essentially the same as an edge emitting semiconductor laser but with no feedback at the cleaved facets so the output is ASE.

To use the spectrum slicing technique in military aircraft the broadband source must run continuous wave and an external modulation be provided, this can either be done by modulating an amplifier such as a RSOA or using a dedicated modulator such as a Mach-Zehnder modulator with added amplification. The wavelength emitted by the amplifier will be the same as the wavelength input to the amplifier. The wavelength of operation is therefore not specified by the amplifier but by the multiplexer. If an RSOA is used as the modulator, data rates of up to 1.25 Gbps can be readily achieved, with a colourless transmitter, as the

wavelength is now set by the multiplexer. The spectral width of the slice must also be considered carefully [37]. Beat noise between different sections of the spectrum add an extra noise term not present with narrow linewidth lasers which is dependent on the ratio of the spectral slice bandwidth to the bit rate. This noise term increases with decreasing slice width introducing a power penalty to maintain the same bit error ratio. However, a slice with a large spectral width will suffer from dispersion as it propagates down the fibre, this will not be a problem over short avionic links, but it will also not allow as many WDM channels per lightsource.

## **2.3.2 Receivers**

The receiver is the device at the opposite end of the fibre which detects the optical signal and associated circuitry which recovers the signal. The two most common detectors used in optical communications are the positive-intrinsic-negative (PIN) photodiode and the avalanche photodiode (APD), these are both discussed in the literature [38, 39]. The choice of photodiode is dependent on the required bit rate and the rest of the system design which dictates the incident power.

### **2.3.2.1 PIN Photodiode**

The PIN photodiode has the same operating principle as the p-n junction photodiode discussed previously and is sketched in Figure 8. The junction is reverse biased which increases the potential barrier. Light with a wavelength greater than the bandgap energy incident upon the depletion region is absorbed and charge carriers generated. The introduction of an intrinsic undoped layer of semiconductor between the heavily doped positive and negative layers extends the region of the device with a non-zero electric field; this means there is a larger region where absorption of a photon will lead to generation of charge carriers which will be swept away to generate a current. Therefore we see a device with increased sensitivity over a p-n junction photodiode. These devices are fast and give response over a range of wavelengths meaning they are suited to WDM, the simplicity of the device when compared to other detectors means it is a relatively inexpensive detector; the applicability of a PIN photodiode to an avionic platform depends on the overall system design.

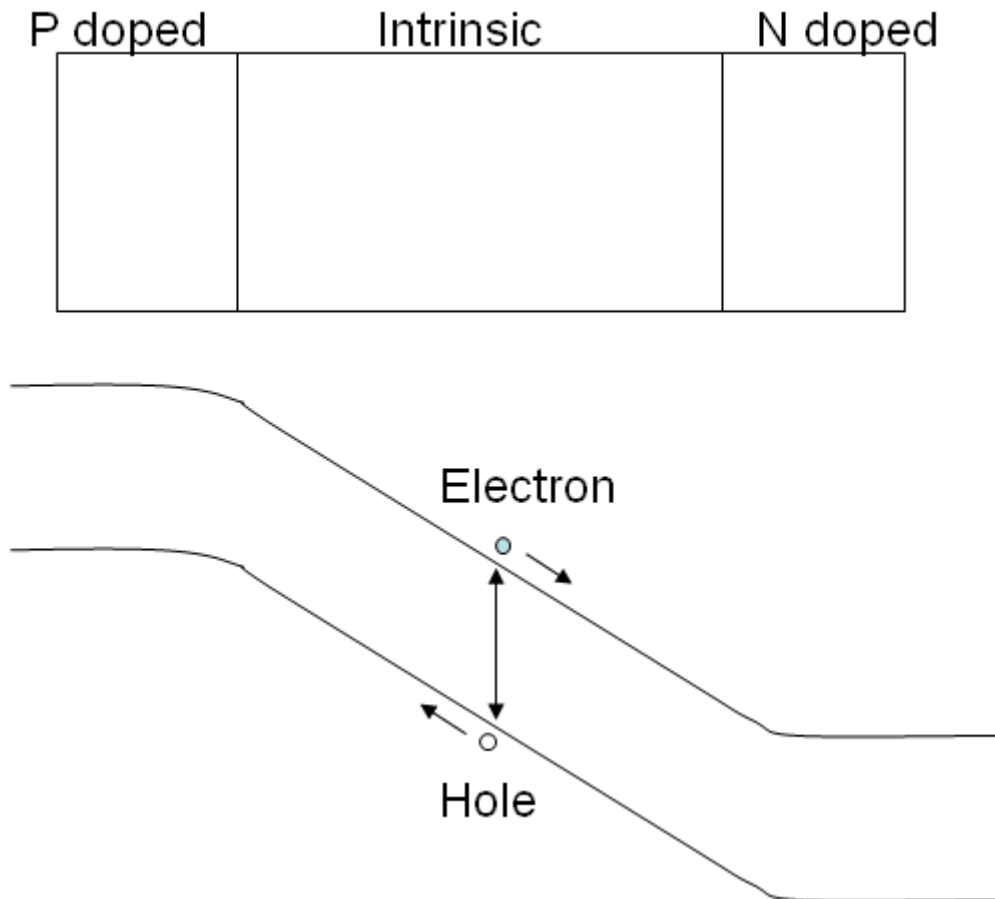


Figure 8: Drawing of PIN photodiode showing extended depletion region

### 2.3.2.2 Avalanche Photodiode

An Avalanche Photodiode, or APD, is a photodiode with internal gain for any current in the depletion region. This gain is derived from impact ionisation. A carrier in the electric field acquires kinetic energy, if this energy is sufficient the carrier can remove an electron from the valence band moving it into the conduction band and creating a hole. This process can continue as carriers move in the field offering high gain. APDs offer much higher sensitivity than PIN photodiodes but do cost more, usually need higher currents and can be severely affected by noise. If we need a high gain device many impact ionisations must take place which clearly occurs over a period of time, because of this high gain APDs can be slow detectors.

Both types of detectors could have a role in an avionic platform but the choice would depend on the rest of the system.

### 2.3.3 Multiplexers / De-multiplexers

An essential part of a WDM system is the multiplexer; this takes the individual channels of different wavelength and combines them so they can propagate as one down the same fibre. The de-multiplexer carries out the reverse operation and splits the broadband light into the individual channels so the signal can be recovered.

#### 2.3.3.1 Arrayed Waveguide Grating

The AWG is a widely used passive multiplexer or de-multiplexer and is shown in Figure 9. The light is launched into the first slab via a fibre. It spreads out by diffraction as it effectively propagates in free space in the slab waveguide and is coupled into the arrayed waveguides. The arrayed waveguides are of differing optical path lengths so the light emerges from them at different phases. Each beam of light interferes as it is guided through the second slab. The system can be carefully designed so the point at which constructive interference occurs at different wavelengths coincides with a fibre to guide the de-multiplexed light. The coloured triangles in Figure 9 represent the path of the interfering light of different wavelengths. AWGs suit applications such as DWDM or spectrum slicing where a small channel width is desirable.

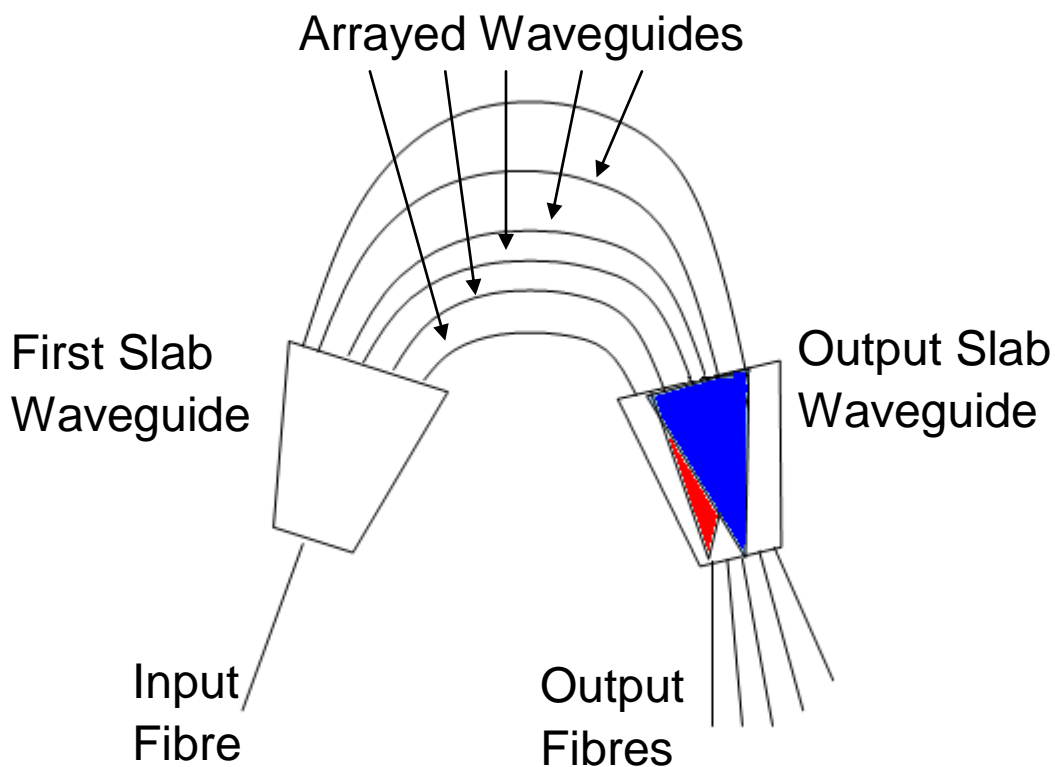


Figure 9: Drawing of an Arrayed Waveguide Grating, the input fibre carries broadband light which is split into its spectral components. The coloured triangles show the path of two separate interfering wavelengths [40]

Since the refractive index of materials is often affected by changes in temperature the AWG is a temperature sensitive device. This is a problem, even in an access network, where the temperature could vary between 0 °C to 60 °C meaning the change in the guided wavelengths could lead to crosstalk. This problem can be solved with the use of a thermo electric cooler but again this leads to increased cost so work has been done in building an athermal AWG [41]. The AWG waveguides are usually made from silica which has a positive thermo optic coefficient so as the temperature increases so does the optical path length. A series of triangular trenches are etched into a slab waveguide and filled with silicone which has a large negative thermo optic coefficient, the trench is shaped so the two changes in path length cancel each other out in each waveguide in the array.

An important property of an AWG is cyclicity; there are multiple wavelengths where the interference conditions will lead to maximums in intensity at the output waveguides. If we have an AWG with N output waveguides the device can be built so the wavelength that would be expected at port N+1 will be output at port 1, this can be repeated over multiple wavelengths. This property is particularly useful in PON type applications where two different wavelength bands can be used for upstream and downstream communication with the use of a single multiplexer.

Another method to get narrow spectral slices or to couple a selection of spectral slices into one fibre is to use a bulk grating. This will split the light into its spectral components but a well-placed lens or lens array is needed to couple the light back into a fibre. This gives athermal operation and channel widths comparable to those of an AWG [42] but does require additional components and free space propagation of the beams. The free space propagation is not suited to avionic platforms where vibrations are commonplace and any misalignment of the grating or lens will lead to a change in the channel width or a loss of power.

Thin film filters (TFF) can be used or fibre Bragg gratings (FBG) can be cascaded to reflect one wavelength at a time and used as multiplexers but high channel counts are not feasible as an additional TFF or FBG is needed for each channel. As well as this problem



FBGs are temperature sensitive due to the refractive index changing as a function of temperature so are not suited for multiplexers on aircraft. The cyclic property is not as easy to create as with the AWG, therefore the network design will be complicated if using different wavelengths for upstream and downstream communications.

## **2.3.4 Amplifiers and Modulators**

### **2.3.4.1 Reflective Semiconductor Optical Amplifier**

The RSOA was developed as an amplifier to be used for telecommunications. It is very similar to an edge emitting laser diode or a SLD in its structure. Simply put a RSOA is like a laser diode with one side cleaved and coated to form a highly reflective surface and the other side engineered to ensure no feedback is set up. This means that when a forward bias is applied to the junction in a RSOA light emission takes place, like a SLD there is spontaneous emission which is amplified, due to the lack of feedback no lasing mode is set up. If the RSOA is seeded with a signal this will cause stimulated emission, the signal will be amplified but some extra noise will be added in the form of ASE. In this respect the RSOA is very similar to another amplifier technology, the EDFA. However the RSOA does have some significant advantages over the EDFA. Firstly the range of wavelengths the EDFA can amplify is specified by the energy of atomic transitions whereas a RSOA can be engineered to provide amplification over a wide range of wavelengths. EDFAs need to be optically pumped, usually by a laser diode, whereas RSOAs can be directly electrically driven meaning they are less costly and more efficient. Perhaps most importantly the upper state lifetime in a RSOA of  $\sim 1$  ns is much shorter than that of an EDFA of  $\sim 10$  ms [43,44]; this means the RSOA can be used as a modulator at higher data rates, 1.25 Gbps being readily achievable.

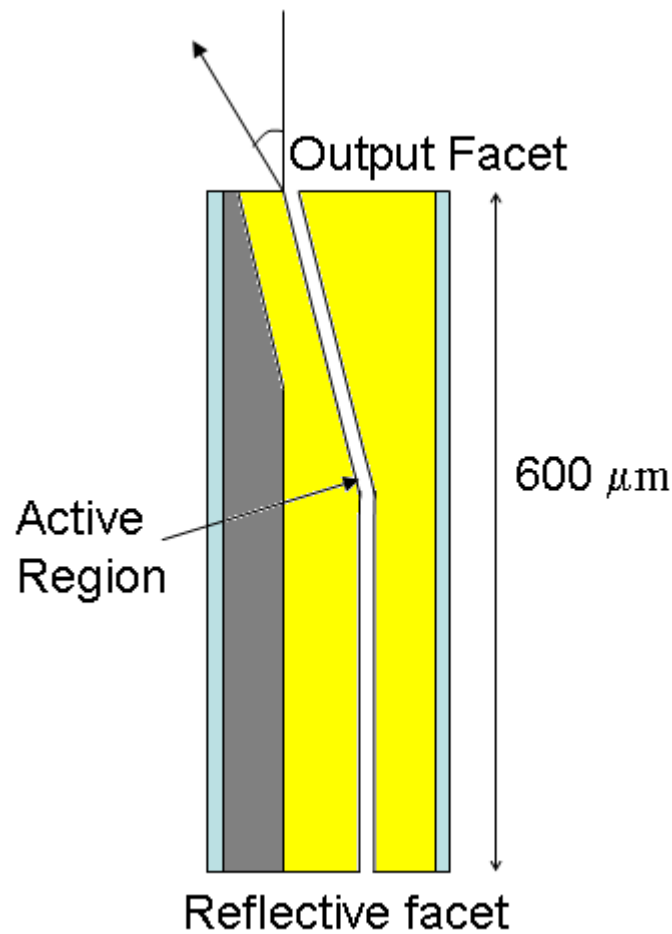


Figure 10: Cross section of a RSOA showing the bend in the active region to achieve low reflection from the output facet [45]

One of the problems presenting RSOAs is the need for a very low reflectivity at the output facet to prevent lasing; the gain of an RSOA can be up to 25 dB so even a very low reflectivity would provide enough feedback to set up laser action. Figure 10 shows a schematic of a recently produced RSOA and a method for overcoming this problem, the light is guided in the active region so by introducing a slight curve into the active region the light will no longer be at normal incidence with the semiconductor/air interface at the output facet meaning any reflections will not be guided back through the active gain region.

Another problem which is found with RSOA is that of polarisation dependant gain. Because the device is grown epitaxially the refractive index is different for light in each plane, with one direction being parallel to the growth layers and the other across the growth layers. This leads to different fractions of the mode being contained in the active region in different planes, different confinement factors. The gain in each plane is the same but the mode fraction is less in one plane so it sees less amplification. To minimise the polarisation

dependency of the gain RSOAs have been made with strained active regions [45,46], this can be achieved by using materials with slightly different lattice constants. The introduction of strain into the active region allows control of the gain in each plane so it is possible to balance the gain and confinement factor in each plane to remove the polarisation dependency.

There are two operating regimes with an RSOA, linear amplification and nonlinear amplification. If a RSOA is to be used as a booster or pre-amplifier it must be used in the linear regime, this means the optical power in the amplifier must not reach the point where it saturates the gain. In this regime a RSOA can provide an improvement in received power and therefore bit error rate (see section 4.3.1 Bit Error Rate) although care must be taken when introducing the amplifier, if the signal input is too low ASE will be significant and high levels of noise will be introduced which could reduce the system performance. ASE noise will always be added with a RSOA, the additional level of degradation from this noise is quantified by the amplifiers noise figure (NF) which is the ratio of the signal to noise ratio before amplification to that after amplification. In the linear operating regime the RSOA can be used in WDM systems with little or no crosstalk between the channels.

Operation in the non-linear regime presents problems with the introduction of crosstalk, patterning and frequency chirp but can also be useful in select circumstances. One of the non-linear effects that acts as a drawback for a linear amplifier is cross-gain modulation (XGM). If an intense signal in one channel is being amplified it uses the gain available to other channels, the power in one beam will affect the power in the other. XGM has been used for wavelength conversion in optical signal processing [47,48] which is a useful technology for WDM. If we input two wavelength channels, the data at  $\lambda_1$  as and a CW signal at the desired wavelength  $\lambda_2$ , XGM between the two signals will impart the opposite pattern on  $\lambda_2$  i.e. 0's will be 1's and vice versa. This inversion of the data is a major shortcoming of the XGM method but good results have been demonstrated. Alternatively the nonlinear effect of cross phase modulation (XPM) can also be used [47]. A signal of sufficient power in the amplifier can alter the refractive index in addition to the gain; other signals will also see this refractive index change hence we see a phase shift in the emitted signals. When the amplifiers are integrated into a Mach-Zehnder type interferometer the phase change will lead to interference when the light is recombined so the inverted signal can be rectified. Other processes which involve nonlinear effects include 2R regeneration (re-amplification and re-shaping) and dispersion compensation. In an avionic network the fibre lengths are relatively short so dispersion is not an issue and it remains to be seen if mid span or pre amplification is needed.

#### **2.3.4.2 Electro-Absorption Modulators**

An electro-absorption modulator (EAM) is a semiconductor device which can be used to modulate the optical intensity of light of a certain wavelength. It works on the basis of the Franz-Keldysh effect where there is a change in the absorption spectrum caused by applying an electric field. The application of an electric field changes the bandgap energy and as such the photon energies which will be absorbed. It has been suggested that EAMs could be used as a modulator in the end node of a PON [49], although the insertion loss of the EAM can be prohibitively high. In order to counteract the high loss of the EAM devices consisting of both an EAM and semiconductor amplifier have been suggested [50,51]. These are constructed with a reflective EAM (REAM) and an SOA, with the signal passing through the SOA before and after modulation by the EAM. The REAM is much faster than the RSOA, discussed above with 11.3 Gbps reported, although in this case 1.3 Gbps is used for forward error correction so 10 Gbps is available to carry data. The REAM devices are more expensive and have greater power consumption in comparison to the RSOAs. The spectral range of the device is also reduced over large temperature ranges.

### **2.4. Requirements**

The environment on an avionic platform needs to be fully investigated and conditions quantified before attempting to integrate a WDM network. It is desirable to have components which can withstand these conditions with minimal support such as cooling, in order to keep the weight and cost to a minimum. As the environment on an aircraft is typically much harsher than that found in commercial telecommunications networks some of the existing components cannot operate within needed specifications, for example the emitted wavelength of a VCSEL or DFB will drift with changing temperature so additional cooling components would be required and they would have to operate throughout the full avionic temperature range. In addition to these environmental requirements there are other functional requirements of the network relating to network performance, an example would be the need for determinism to ensure flight safety.

#### **2.4.1 Environmental Requirements**

A list of some important environmental requirements is included in Table 1 although it is worth note that this list is not definitive. One of the main challenges in avionic systems is the

operational temperature range of  $-55\text{ }^{\circ}\text{C}$  to  $+125\text{ }^{\circ}\text{C}$  which widely exceeds the range that standard telecommunications products are designed to meet. As previously discussed many components such as lasers and some multiplexers are temperature sensitive and will lead to crosstalk and network failure if used for WDM in this environment. The temperature range is split into different regimes. The operating range is the temperature range in which the network is expected to operate for prolonged periods without failure and little or no degradation. The short term operation is the range at which long term operation will lead to degradation but operation over a short period is acceptable and will not lead to immediate degradation. The survival range is the temperature range over which the components are expected to be unharmed but the network is not expected to be operational. Although not stated in Table 1 the operating range of an avionic network in unconditioned areas of the aircraft is generally  $-55\text{ }^{\circ}\text{C}$  to  $+125\text{ }^{\circ}\text{C}$ . The lower range can feasibly be realised on the ground in rare circumstances but is common at altitude whereas the higher temperature can be realised when network components are placed near to areas that become hot due to air friction such as the leading edges of the wings. Even higher temperatures can be realised with equipment mounted near the engines, these areas would be avoided when deciding on network routing and layout so these higher temperatures will not be considered.

The mechanical shock is a measure of impacts and accelerations that can be experienced in normal aircraft operation, these can include a bumpy landing or turbulence experienced mid-flight. The crash safety shock is the maximum shock which can be experienced on a crash landing, it is designed to determine the ruggedness of the network and to ensure no sections of the network will come apart on crash landing. The vibration specifications ensure the system can deal with vibrations present throughout operation whether they are constant like those from the engines or random vibrations associated with turbulence. These conditions, although arguably not as problematic as the temperature range, still present significant problems. Fibres must be well aligned to minimise losses and shock or vibration can lead to misalignment or damage of components which will cause the network to fail. Most of these problems can be solved with ruggedized packaging of components so this thesis will concentrate on the temperature range and how it affects the network performance.

<b>Condition.</b>	<b>Civil Aircraft, Flight deck and passenger cabin.</b>	<b>Civil Aircraft, Flight control surfaces and landing gear.</b>	<b>Military Aircraft, Conditioned avionics bay.</b>
Temperature			
Operating	-15 to +55 °C	-55 to +70 °C	-40 to +70 °C
Short term operation	+70 °C	+70 °C	+90 °C
Survival	-55 to +85 °C	-55 to +85 °C	-55 to +90 °C
Temperature Shock	2 °C / min	10 °C / min	5 °C / min
Steady State Pressure	57.2 to 107 kPa	4.4 to 107 kPa	3.6 to 115 kPa
Pressure Variation	226 kPa / min decreasing	Unpressurised zone	318 kPa / min decreasing 400 kPa / min increasing
Acceleration	Not specified	Not specified	Linear 9.6g Rotational 17 rad / s <sup>2</sup>
Mechanical Vibration	0.003 g <sup>2</sup> / Hz	0.16 g <sup>2</sup> / Hz	0.04 g <sup>2</sup> / Hz
Acoustic Vibration	Not specified	Not specified	140 dB
Mechanical shock			
Operational	6 g half sine wave in 11ms	6g	20g sawtooth in 11ms
Crash Safety	15g half sine wave in 11ms	15g	20g sawtooth in 11ms
Humidity	85% at 38 °C	95% at 55 °C	27 g/kg water/air mix

Table 1: Conditions in which an avionic network must operate [52]

Other factors not included in this discussion are levels and fineness of dust which could be introduced landing in a desert, corrosion and erosion of components and ability to operate with salt mist or mould growth on the platform.

## **2.4.2 Functional Requirements**

The functionality of the network describes another set of requirements which are independent of the environment. As the network may be responsible for carrying safety critical data the robustness of the network with respect to faults must be as high as possible. Typically this can be achieved with the use of back-up fibres although this is at the expense of extra weight. The network must be able to operate with a faulty node and automatically bypass this fault; ideally the network will survive multiple faults. The robustness can also consider how easy the network is to maintain when reconfiguring for different flights. Connectors in particular are delicate and susceptible to contamination, any damage or contaminants on the end faces will result in considerable losses to the signal when the network is in use and will ultimately lead to network failure.

The scalability and capacity of the network is also very important. With required data rates on aircraft continuing to rise, systems are being designed with more bandwidth than currently necessary. In a bid to 'future proof' the network and protect it from obsolescence 1.25 gigabits per second per transmitter is currently the data rate many are working towards [53], this has the advantage of being compatible with gigabit Ethernet standards. In addition to having high bandwidth the network must be flexible. As the aircraft is a multifunctional tool the nodes on the network will see different levels of usage and need different amounts of data for each flight, as a result bandwidth must be reallocated. Different protocols may still be used on aircraft and some degree of flexibility is needed to accommodate these. A highly flexible network will also facilitate the integration of new and removal of old components further protecting the network from obsolescence.

As the number of nodes on the network increases and the network becomes more complex it is likely that the time taken for data to be transferred from one node to another also increases. This transfer time is known as the latency and can compromise the safety if the data takes too long to travel from transmitter to receiver. The latency is highly dependent on the network design and bit rate so an acceptable value will depend upon each individual situation. The concept of latency is linked to determinism, the state of the network must be determined at all times so data can be ensured to get to its destination within a known time.

It must be possible to know if data has successfully been received or if it must be sent again. The introduction of AFDX and an Ethernet switch [17,29] can fulfil this need.

Overall the reliability and functionality of the network is defined almost exclusively by the components making up the network. Each component must be able to operate within the requirements without failure, even with this some faults are inevitable and the network must be able to cope with this with minimal detrimental effects. It is also of importance that the components are compatible and can work together otherwise the reliability of each individual component is irrelevant. In this thesis it is assumed that since the operational data rates will be 1.25 Gbps that gigabit Ethernet can be used. The aircraft that the proposed networks will be used on has not yet been designed so the networks will be kept generic in order to have as wide a range of potential uses as possible, it is assumed that this will allow for the use of Ethernet switches and protocols such as AFDX should the final specifications call for this. The functional requirements which define the bounds of the design space are described in Table 2.

<b>Design Parameter</b>	<b>Requirement</b>
Bandwidth per channel	1.25 GHz
Number of channels	In the near term 8 channels up and downstream would be acceptable but this must scaleable to 32 channels
Power Consumption	This network is to designed for a generic next generation aircraft, as such there are not yet any hard specifications for power consumption. It has been indicated that the power consumption of an SS-WDM-PON network would be acceptable but any reductions in power requirements would be beneficial. A reduction in power consumption of 10% would be seen as worthwhile and a reduction of 20% would be seen as highly beneficial.
Additional Cooling	Where possible additional cooling is to be avoided due to its high power requirements. If additional cooling is to be used its power requirements must be minimised. A relative power requirement of over 20% of the



	network power requirement would be unacceptable.
--	--

Table 2: Functional requirements of avionic network

An important factor in the design is the need for multiple channels, this drives the design towards WDM and away from single channels of high bandwidth which would be the design of choice were multiple channels not required. It is necessary for channels to be separated both for ease of routing to different areas throughout the aircraft but also to separate critical data from non-critical data. In a WDM system these sets of data will be separated by wavelength.

## 2.5. Current Research

Most current work applicable to upgrading optical avionic networks is carried out in two separate fields. The first field is focussed on avionic networks and all work is aimed at avionic applications. Another larger area of research is PON type access networks where some ideas can potentially be carried straight across and applied to avionic networks with little adjustment.

### 2.5.1 Access Networks

An access network forms part of the telecommunications infrastructure. It connects subscribers to their service providers, this could be a home or an office connected to a central local provider. Recently PON type networks have been deployed for access networks; these are similar to the type of networks that may be of use on aircraft, albeit with shorter fibre links given that an aircraft is approximately 100 m long.

#### 2.5.1.1 RSOAs for Access Network

In March 2009 the first Gigabit access network using RSOAs as the modulator at the ONU started commercial use [54]. This technology was built upon years of research, some of which can be applied to the problems faced with optical avionic networks. The transmitter for the downstream data was a RSOA seeded with spectrum sliced incoherent light, the transmitters in each ONU was also a seeded RSOA. While not placed in as harsh an environment as expected on aircraft an access network is still expected to work over a range

of temperatures from -20 °C to +70 °C. This network is an example of a number of recent technologies and work continues to improve these technologies.

#### 2.5.1.1.1 Increasing Modulation Bandwidth

A current commercial PON using modulated RSOAs operates at 1.25 Gbps, due to carrier dynamics the maximum modulation rate of a RSOA is 2.2 Gbps but with the use of external electronics the modulation bandwidth can be extended to 10 Gbps [55,56]. When modulating at bit rates above 2.2 Gbps, intersymbol interference (ISI) can become problematic. ISI occurs when a bit is affected by the other bits on either side of its transmission; this has the same effect as noise and decreases the signal BER. ISI will be worse for the higher frequency components of the transmission (when the signal switches quickly, 0101, as opposed to a series of 0's or 1's) so a process known as equalisation can be used to remove the ISI at the receiver or compensate at the transmitter. Equalisation can be applied at the transmitter to boost the rising edges of the data and the high frequency components, this is known as pre-emphasis. Pre-emphasis has been used alongside forward error correction (FEC) to extend the modulation bandwidth of a RSOA to 10 Gbps [55]. Using FEC redundant bits are transmitted with the signal and upon receiving them are decoded with the original data to increase signal quality.

Increasing the data rates on an aircraft beyond those compliant with gigabit Ethernet may not have use yet but with increasing data rates this capability will be used at some point in the future. This work is reassuring when looking at future proofing the network.

#### 2.5.1.1.2 Re-modulation

If using a RSOA as a modulator in any WDM system it must be seeded with light of the wavelength to be assigned to that data channel. At the OLT, or a central avionics bay, the seed can be easily provided by spectrum slicing a broadband source. There may be a high path loss between the ONU, which can be thought of as equivalent to end nodes throughout the aircraft, and the OLT. This will mean that using spectrum slices which are generated at the OLT will be difficult without the use of any amplification because the signal strength at the RSOA may not be sufficient to clamp it at the assigned wavelength. Mid span amplification will add to the cost of the network as well as introducing noise into the spectral slices before they have been encoded, it would also be easier to just use another broadband source as opposed to an amplifier. If it is not possible to use another BLS one method to seed the RSOA is to use the remodulation technique as illustrated in Figure 11.

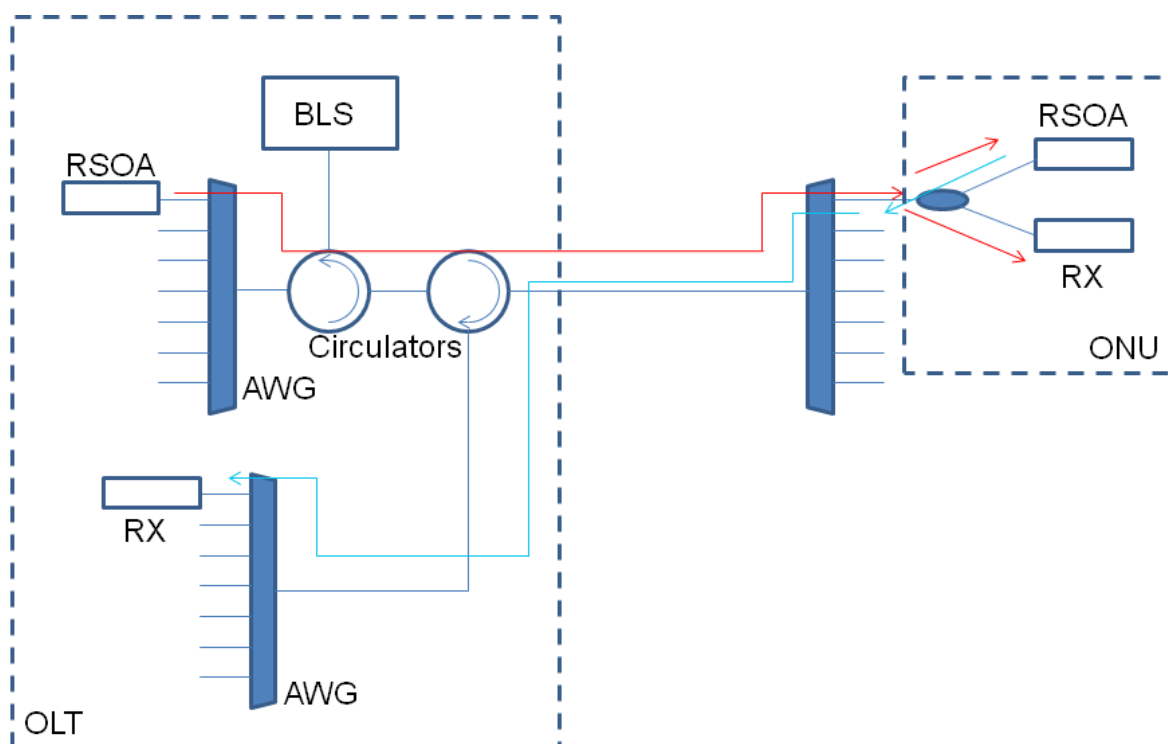


Figure 11: Configuration of a PON with RSOAs in ONU using wavelength remodulation. The blue and red arrows indicate the direction of data and are not indicative of wavelength which is the same up and down stream [54,57].

The re-modulation technique involves using the same wavelength for the upstream traffic as that used downstream. This has the advantage that the downstream signal can be used as the seed light and no additional light sources are needed as the combined output power from the seeded RSOAs is greater than that of the broadband source. Drawbacks arise from the fact that the seed light for the RSOAs at the ONU is modulated and the upstream data can be degraded by 're-modulation noise' leading to a large bit error rate (BER, the ratio of incorrect bits to correct bits). The noise can be reduced if the extinction ratio on the downstream signal is decreased but this will introduce a power penalty, more power will be needed at the receiver to maintain the same BER. Another method to reduce re-modulation noise is to use a gain-saturated RSOA; if the input seed is sufficiently powerful to saturate the gain the amplifier will be effective in suppressing the noise. Detrimental effects previously discussed in the gain saturated non-linear regime, such as cross gain modulation, do not apply here as the RSOA is being used as a modulator so only one wavelength

channel is being amplified. The output power will remain constant for both levels of modulated input; this again requires high powers at the ONU.

Rayleigh back scattering or back reflections of the upstream or downstream signal at connectors add beat noise to the signal and have serious effects on the system performance. As a result reflections in the network must be seriously considered and minimised at any opportunity. An aircraft network may have up to ten connectors throughout one optical path which could lead to serious problems with back reflections. It is unlikely that, in the occasion of the path loss being too high to use a broadband lightsource at a central location, analogous to an OLT, it will not be possible to use a second broadband lightsource closer to the end nodes. It is therefore assumed that remodulation will not be necessary on an aircraft although it offers a potential solution should the use of a secondary broadband lightsource in a high loss network not be possible.

#### 2.5.1.1.3 Self-seeded RSOA

Another method of using a RSOA modulator in a WDM system without spectrum slicing a broadband source is to use the technique of self-seeding [58,59]. A possible access network using self-seeded RSOAs is sketched in Figure 12 [59], the transmitters function in the same way at both the OLT and ONU ends of the network although in this particular system are operating over different bands. The RSOA generates ASE which is filtered by the AWG and directed onto a power splitter; a portion of the light is then reflected at a Faraday Rotating Mirror (FRM in Figure 12) and routed back onto the same AWG. A FRM is required to counteract effects from polarisation dependant gain in the RSOA and to stop the set-up of a lasing mode. The rotation in polarisation provided by the Faraday rotator mean that no standing wave is set up so no resonance can be set up and there will be no lasing mode. Both polarisation dependant gain, and lasing modes would lead to an unstable laser with large power fluctuations. The light is filtered and the RSOAs are seeded with the ASE that they have generated, this seed light has been filtered by the AWG so only the assigned wavelength of each channel is used to seed the RSOAs. Again the wavelength at each channel is set by the AWG so the transmitters are colourless. The RSOAs at the OLT may operate in the C-band and at the ONUs the RSOAs may operate in the L-band so upstream and downstream data are carried by different wavelengths as in some of the PONs previously discussed.

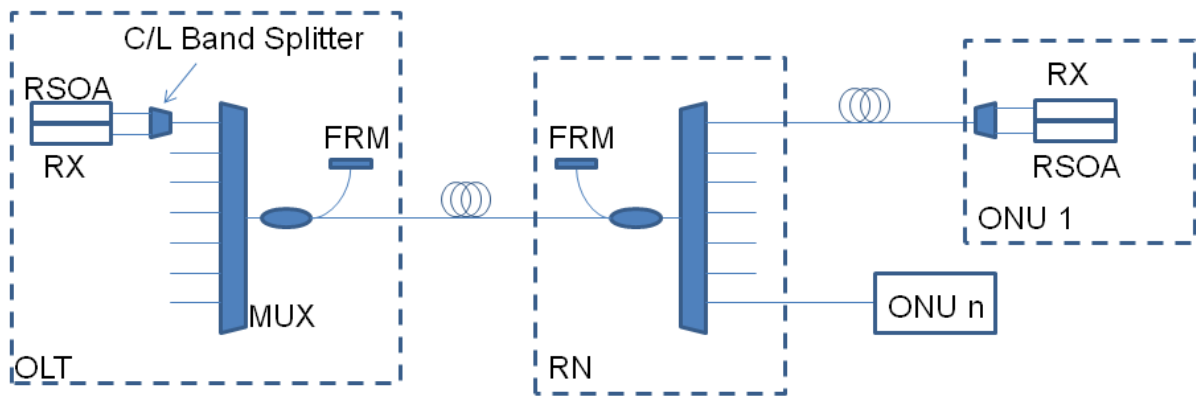


Figure 12: WDM PON based on self-seeded RSOA

The round trip loss over the optical path is an important issue when designing a self-seeded network as this loss, as well as the RSOA gain and the splitting ratio of the splitter will define the output power of the RSOA and the power budget of the network. In the telecoms sector these parameters are likely to stay constant, the splitting ratio will remain constant as will the round trip loss whereas the RSOA gain is a function of temperature. The RSOA may be cooled if the temperature is liable to fluctuate or it may be kept in a cooled cabinet. In the avionic environment the cavity loss may be higher, there may be additional connectors inside the cavity and the cable and component insertion losses can be affected by the extreme temperatures. The gain of the RSOA will be reduced at elevated temperatures and cooling throughout the avionic temperature range is not feasible. As a result this technique is not considered to be as attractive an option as spectrum slicing for use on aircraft.

### 2.5.1.2 Tuneable Lasers

The Full Service Access Network Group (FSAN), which is a group of leading telecommunications providers, test labs and equipment suppliers, are currently researching next generation access networks (NG-PON 2) with the aim of further increasing the bandwidth of access networks. A hybrid, high speed, WDM/TDM PON has been identified as the flexible solution to the next generation access network. One requirement of the proposed network is that it needs tuneable transmitters, these are currently being investigated by many groups with solutions such as tuning DFB lasers using heaters [60] or packaging multiple lasers inside a single package and switching between each laser which will effectively work as a tuneable transmitter [61].

Strictly speaking these transmitters cannot be considered as colourless sources but if deployed carefully colourless style operation is possible. The transmitter in the literature [60]

has a tuning range of approximately 12 nm, the device is tuned using a platinum heater electrode to change the refractive index of the internal grating in the DFB which will change the emitted wavelength. In an avionic network the main attraction of using a tuneable laser transmitter would be that the same device could be used in multiple end nodes which would reduce the inventory and the complexity of network maintenance. The main drawback with these transmitters is the power consumption, the heater power ranges from 0 to 1 W depending on how much heating the device requires. With an additional power consumption of 1 W per transmitter over 50% of the total power consumption of the network would be derived from the heaters, this is an unacceptable increase in power requirement. The reported results have been obtained in a laboratory environment, in the wide temperature range expected on aircraft the power consumption of the heater would be higher and in some cases could be unachievable. If these devices are used in next generation access networks they will be widely available and inexpensive due to economies of scale in the telecoms market, in this case it may be worth investigating their use in a reconfigurable network in conditioned parts of the airframe for higher speed links with 10 Gbps transmitters. For the network in this thesis, which will be throughout the aircraft and requires 1.25 Gbps per transmitter, tuneable lasers will not be useful.

## **2.5.2 Avionics**

Many of the ideas and technologies used in telecoms networks are being investigated for use on aircraft. A main driver for the implementation of telecom techniques and protocols is to benefit from reduced cost from economies of scale leading to inexpensive components and to take advantage of the wealth of research already carried out for telecoms. One such protocol which is being researched to use in avionics, which has been previously mentioned in this chapter, is Ethernet [62]. This protocol has become ubiquitous and is almost the de facto for future applications; this means that there is already work on pushing Ethernet beyond 100G to 1T.

Other research in the avionic domain is based around rugged components which can operate in the harsh environment found on aircraft; most research focuses on the optical transmitters. One proposed method for implementing DWDM on aircraft is to use an 'octal transmitter' [63], this is a device containing 8 transmitters which can be thermally tuned to cover 4 different ITU wavelengths; this allows one package to be tuned across 32 ITU channels. This particular device is designed to operate between -40 °C and +100 °C whilst holding the transmitters at a temperature between 20 °C and 35 °C depending on the required wavelength. This idea of a tuneable transmitter is similar to that pursued in NG-

PON2 albeit with slower switching, nevertheless problems with power consumption remain and it is unlikely that the temperature of operation could be extended to +125 °C due to limitation of the cooler.

Other proposed networks involve broadcasting data to multiple nodes using a star coupler [64], this will not be a wavelength selective device and will act as a power splitter. Each node can transmit at 32 wavelengths on the ITU grid, this will be sent to all nodes where the required data can be extracted given knowledge of the wavelengths used. This network will have limited functionality due to the large splitting loss of a 32 channel star coupler, 32 dB. This high splitting loss also means it is unlikely that the network can be larger than 32 nodes. In addition to the high splitting loss there may also be issues with security, it would not be desirable for flight critical data to be transmitted to every node throughout the network. The proposed network may still find use on aircraft for in flight entertainment (IFE) where one central node transmitting many high data rate channels to many separate nodes is required.

The most promising direction for current research on avionic WDM-LAN is to use spectrum slicing as with the access networks in telecoms. The concept of spectrum slicing to achieve a CWDM network operating at 10 Gbps has been reported [65] and prototype optical sub-assemblies have been built to withstand the harsh environment. Although the reported work uses a channel separation of 20 nm it should be possible to move to narrower channel separations at the DWDM standard of 0.8 nm or 100 GHz by using an AWG as opposed to a CWDM multiplexer. This solution is inherently rugged especially with respect to temperature tolerance which will allow implementation of DWDM over an extended temperature range. It also has the potential to be low cost with many if not all components commercially available in the telecoms marketplace.

## **2.6 Conclusions**

An overview of the state of the art of fibre optic communications links on aircraft has been given. Different multiplexing techniques have been introduced and discussed, including TDM, SDM and WDM. The flexibility of WDM in terms of switching and routing, and the efficient use of fibre bandwidth make this technique the most attractive for use on aircraft. DWDM offers higher data rates than CWDM because of increased spectral efficiency so it will be researched in this thesis, DWDM does however have smaller tolerances with respect to wavelength allocation and use in each channel than CWDM meaning it will be more difficult to implement on aircraft.

The advantages of optical networks over conventional copper have been discussed paying particular attention to advantages which are useful in the avionic context. The advantages of fibre networks are clear, with the most compelling advantages being increased bandwidths at much reduced size and weight. A number of different network designs have been introduced and their potential applications on aircraft discussed. Particular attention has been paid to the PON, this network utilises passive components throughout the link, apart from the transmitters, receivers and any amplification. It is anticipated that PON type networks will be the most suited to avionic applications due to low power consumption and their flexibility. Suitable protocols have also been briefly discussed and it is likely that future aircraft networks will use the Ethernet protocol. This protocol is widespread in its use which will mean it is easy to buy compatible components and that many others worldwide are researching improvements to Ethernet, some of which may be exploited by the proposed network in the future.

A review of components which could potentially be used in aircraft has been presented. As many devices are based on semiconductor p-n junctions a brief explanation of the p-n junction begins this section. By forward biasing the junction an optical transmitter can be created. Different types of semiconductor transmitters such as the DFB and the VCSEL have been discussed and their relative advantages and disadvantages for use on aircraft considered, as these devices are thermally sensitive it may not be feasible to use them in the extreme temperature ranges found throughout aircraft. Similarly tuneable lasers can be manufactured from a semiconductor p-n junction and again these are thermally sensitive devices so may not be useful on aircraft. Another technique which also uses semiconductor transmitters is that of spectrum slicing, although the modulators in this technique are thermally sensitive it is the output power which is affected and not the emitted wavelength. This increases the devices tolerance to changing temperature and makes use on aircraft more feasible than the previous transmitter concepts. When a p-n junction is reverse biased it can be used to make an optical receiver, two different optical receivers have been presented in this chapter, a pin photodiode and an APD. Both these devices may be used on aircraft networks, the choice of receiver would depend on the network design. As previously mentioned it is highly desirable for future aircraft networks to implement WDM, in order to achieve this a multiplexer must be used. One such multiplexer is an AWG, this is a passive multiplexer based on diffraction. How the device is made and various methods to reduce thermal sensitivity in the device have been discussed. The main advantage that this has over other multiplexer technologies, notably thin film filter based multiplexer is that the AWG can be designed to be cyclic. This means that it will work as a multiplexer for various wavelength bands, different bands can then be used for carrying data in different directions



increasing the flexibility of the final network. As the final part of this section amplifiers and modulators were discussed, these will be particularly useful in spectrum slicing. A RSOA is another device based on the forward biased p-n junction, when used as an amplifier it will amplify an input signal within its gain spectrum. As it has a relatively large gain spectrum one device may be used to amplify many different wavelengths, if only one channel is input to the amplifier it can be used as a modulator. The RSOA can be modulated at a speed of 1.25 Gbps and appears to be a promising technology for use on aircraft networks using spectrum slicing. Another device which may be used is an EAM this device can be operated at higher speeds than the RSOA but does have a high insertion loss so signal must be recovered using amplification.

The following section of this chapter focused on the requirements of an optical avionic network. The first set of requirements are environmental requirements, these are very harsh in comparison to standard telecoms environmental requirements. A particularly challenging requirement for a WDM-PON is that of the operational temperature range, this is the range that all components must be able to operate over and maintain high levels of performance so the network quality is not degraded at extreme temperatures and ranges from -55 to +125 °C. The second set of requirements are functional, these relate to the performance of the network and are unconcerned with the environment. Some examples would be the data rate, the maximum latency or whether or not the network is deterministic. Many of these requirements will be fulfilled by using Ethernet; if the data rate used at each channel is 1.25 Gbps this will be compatible with gigabit Ethernet standards.

The final section is a review of current research applicable to WDM-PON on aircraft. Two distinct areas of research are of interest. The first is research on access networks for telecoms, although the ideas from this research may not translate directly to aircraft the research carried out to increase bandwidth of local area networks can be altered slightly and be of use on aircraft. Looking at the research on using spectrum slicing with RSOAs in access networks relevant advances are being made in increasing the modulation bandwidth, although this may be difficult to achieve with the constraints of operating on aircraft it is beneficial to maintain awareness of the work. There is also potentially interesting work on re-modulation of data to increase spectral efficiency and self-seeding. At the moment neither of these concepts are feasible on aircraft but further advances may mean they become more attractive propositions. Another area of research is focussing on tuneable laser transmitters for next generation access networks, these devices must operate at high data rates and be capable of fast tuning. If research in these devices is successful and they become commercially available they may be of interest for use in areas of aircraft with reduced temperature ranges but their use throughout the entire aircraft will not be feasible due to

cooling issues. The second distinct area of research is on optical networks in avionics, there is not as much work being published in this area currently as in the previous access area. Main areas of research include work on moving towards high speed Ethernet whilst still being compliant with legacy issues on aircraft. There is other work on ruggedising components so they can withstand the environment found on aircraft and some prototype devices have been demonstrated which can operate at high speeds up to 100 °C and may be limited by power consumption at higher temperatures. Other published research proposes using spectrum slicing with an RSOA to implement CWDM and this appears to be a promising area for research.

# 3. Compatibility with Avionic Requirements

## 3.1 Introduction

In order to take advantage of the economies of scale associated with the telecommunications marketplace it is desirable to use COTS components. These components could be exposed to the full avionics environment with no additional support. The avionic temperature range is specified in the literature [52] and discussed in detail in section 2.4.1 Environmental Requirements. The most challenging specification with respect to optical components is that for temperature, ranging from  $-55\text{ }^{\circ}\text{C}$  to  $+125\text{ }^{\circ}\text{C}$ . The low extreme could feasibly be reached while on the ground in exceptional circumstances but is more likely to be reached during flight at high altitude. The high temperature extreme can be reached if components are on leading edges of the air frame and are exposed to heating due to air resistance during high speed flight. Areas of the aircraft with high densities of electronic components can get hot due to heat generated by the components but are unlikely to reach  $+125\text{ }^{\circ}\text{C}$  as they tend to be thermally regulated to protect the electronics.

Other conditions described in the literature include pressure, mechanical and acoustic vibrations, and mechanical shock. Although these all may pose problem to components used in the network this work will focus on the temperature. This is because the temperature is likely to have the greatest effect on the optical properties of the components. If a VCSEL or DFB laser, for example, is tested over a large temperature range, both the emitted wavelength and the output power will vary as a function of temperature [31,32]. When passive components are considered a change in temperature could drastically alter their performance. Depending on the materials used in the passive components, the thermo-optic co-efficient of the material and how the device is designed, the effects of temperature can lead to network failure. For example, an AWG is built with internal waveguides of precise differing path lengths; a change in temperature will change these path lengths due to a change in the refractive index of the waveguide. This will mean that the AWG will no longer work as intended and cannot effectively multiplex and demultiplex signals, the network will fail. Although the optical properties of these components can be altered by the other conditions, for example vibration could lead to a change in path length by straining fibres or components, the change will not be as serious and counteracting the effects through ruggedized packaging should be possible. Packaging is beyond the scope of this thesis so

this chapter will focus on the compatibility of components to the avionic requirements with respect to temperature.

It is necessary that these components can withstand the conditions in which they are expected to operate with minimal support, such as additional cooling, to keep weight, power consumption and cost to a minimum. These components, however, are designed to meet specifications for use in telecommunications and may not necessarily operate in the harsher, avionic environment specified in the literature [52]. If the components are tested beyond their specified storage range they will be damaged, this is purely a packaging issue and gives no information on how they will perform at avionic temperatures. Components will be tested throughout their storage temperature range and performance over the larger avionic range inferred from these results.

The effects of temperature on active components such as laser transmitters and amplifiers can also be catastrophic to network operation. There are, however, a number of techniques to avoid catastrophic failure of transmitters and reduce size and power consumption of support provided in the form of cooling. These will be investigated in more detail in later chapters; this chapter will focus on the performance of passive fibre optic components.

### 3.1.1 Test Matrix

A Test matrix to introducing the components under test and describing relevant test parameters is shown in

Component	Test parameter	Evaluation criteria
Circulator	Insertion loss	Measured as the difference between the power input to the device and the power at the desired output.
	Isolation	Measured as the ratio between the power in the desired output port and the non-input port, for example if signal is input to port 1 the desired port is port 2 and port 3 is non-input.
Red/blue Coupler	Insertion loss	This device is wavelength selective so insertion loss is wavelength dependant. Measured as the input signal power and output signal power at relevant port at different wavelengths.
	Isolation	Similar measurement to that in the case of the circulator. Certain wavelength used as an input and the ratio of output power in the port specified for use at input wavelength to other port measured.
AWG (spectrum sliced and laser cases)	Insertion loss	AWG separates multiplexed signal into separate channels, insertion is measured over a sample of wavelengths (channels). Evaluated by measuring the input power at one wavelength and measuring the power at the relevant output port.
	Crosstalk	Again measured over a number of sample

		wavelengths. Measured as the ratio of power in the relevant output port and the two ports of nearest operational wavelength. Each channel has two associated crosstalk measurements.
Thin Film Filter	Insertion loss	As AWG
	Crosstalk	As AWG

### 3.2 Circulator

A circulator is a widely available commercial fibre optic component. The basic function of a circulator is shown in Figure 13, light entering at port 1 travels through the circulator and exits at port 2. Light input to port 2 will be output at port 3 and so on. The circulators tested in this thesis are asymmetric, that is the last port (port 3) does not circulate to the first port (port 1).

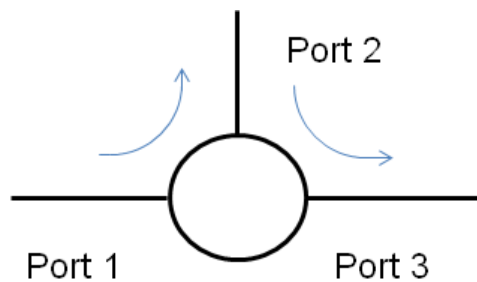


Figure 13: Working of a 3-port optical circulator

The precise design of the circulator tested in this work is not known although the workings will be similar to those described in the IBM white paper ‘Understanding Optical Communications’ [66]. This explains that, although there is no single principle design for a circulator, the underlying principle can be explained using a Faraday rotator. A Faraday rotator will rotate the polarization of light passed through it, although it will not undo this rotation if the light is passed back through the Faraday rotator. This is known as non-reciprocal optical propagation and allows the construction of devices such as isolators and circulators. In the circumstances this thesis is concerned the light may be randomly polarized, in this case the device can be built from various micro components including birefringent filters which will separate the ray into two orthogonally polarized beams and allow construction of a polarization insensitive circulator. These processes should not be adversely affected by the avionic temperature range but the devices will be tested over their specified storage range to validate this assumption.

### 3.2.1 Thermal testing

The device was thermally tested using the set-up shown in Figure 14, a Photonetics Tunics 1550 tuneable laser was used to generate the input signal which was routed through the circulator and detected by an EXFO IQS-1600 power meter. The circulator was placed in a TAS LTCL 600 thermal chamber; the connectors were external to the chamber and not subject to the thermal testing.

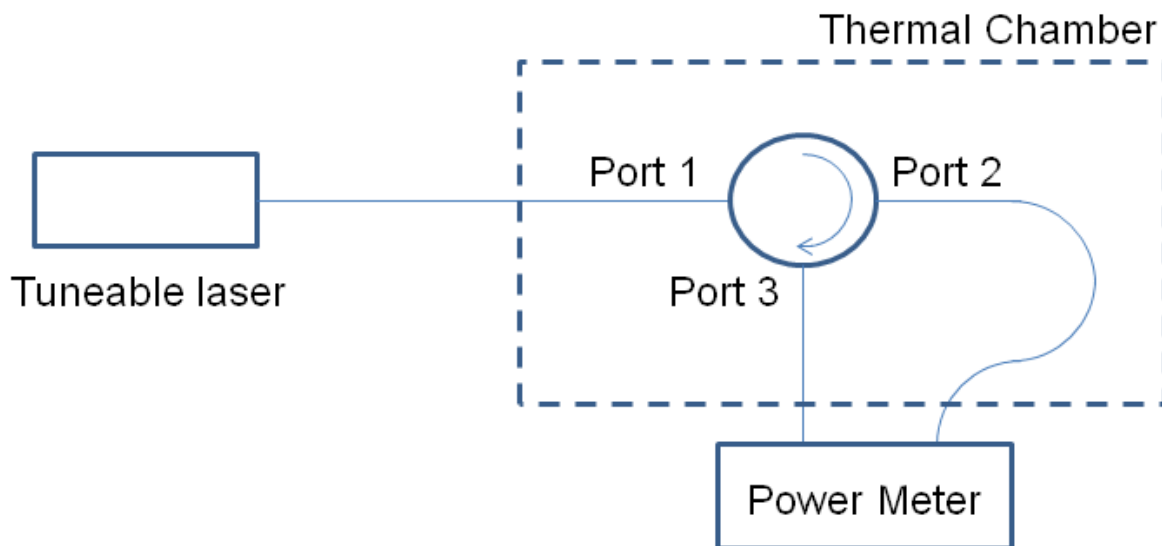


Figure 14: Experimental set-up for thermal testing of circulator

#### 3.2.1.1 Insertion Loss

The insertion loss of the circulator is defined as the loss in the signal on being routed through the circulator from port 1 to port 2 or from port 2 to port 3, there will be two different values for the insertion loss for this component. Both insertion losses over the storage temperature range of the circulator are shown in Figure 15.

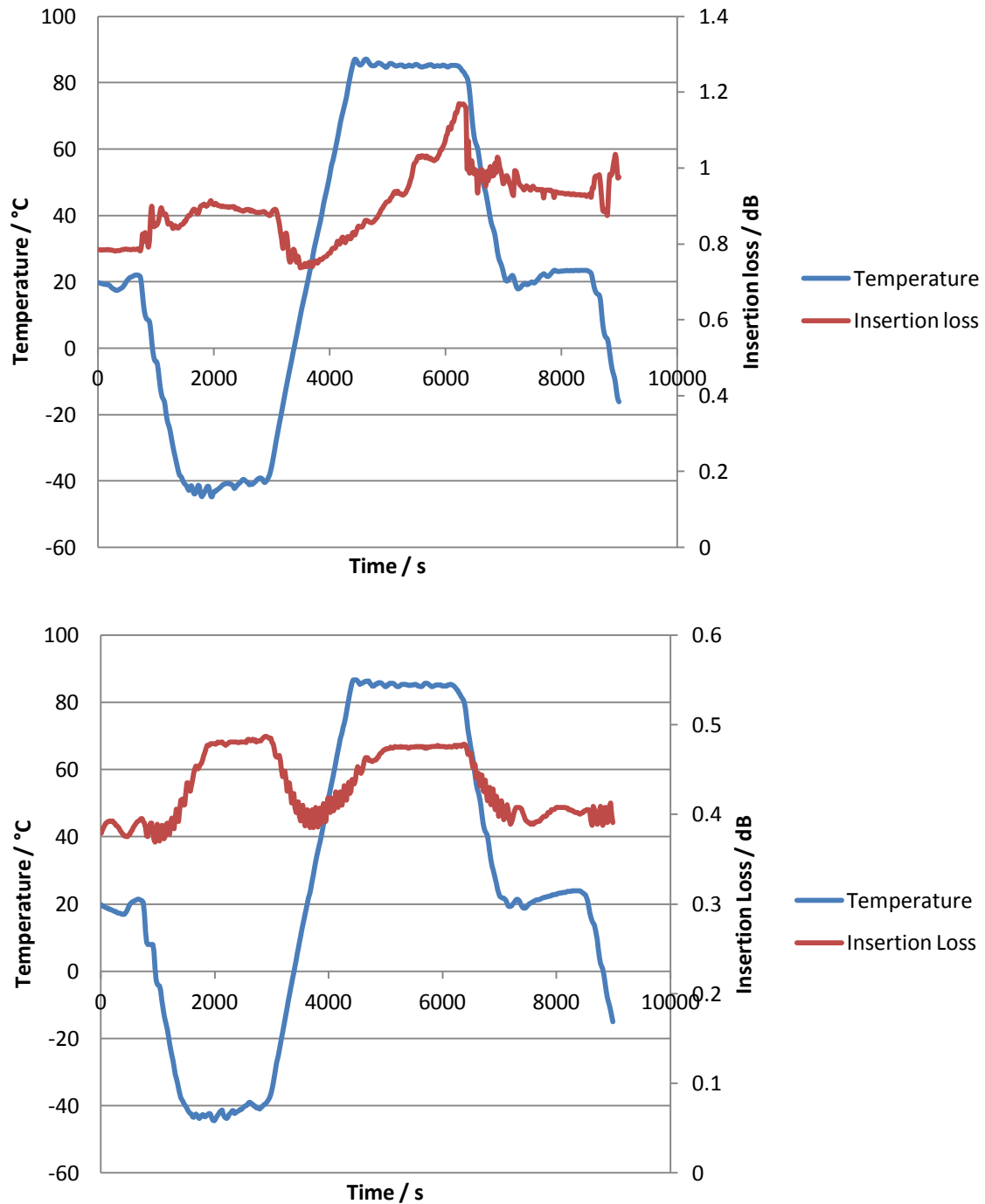


Figure 15: Insertion loss in circulator, measured from port 1 to port 2 and from port 2 to port 3 respectively

In the manufacturers specifications the insertion loss is given as <math>< 1.2 \text{ dB}</math> in both channels over an operational temperature range of

the maximum and minimum temperature in this range. In both channels the insertion loss remains within acceptable levels with a loss of 0.8 to 1.2 dB from port 1 to port 2 and 0.4 to 0.5 dB from port 2 to port 3. While the details of the loss mechanism is not wholly understood, it is likely that mechanical misalignment, resulting when glues used to secure the fibres soften at temperatures may have an influence. It is also possible that glues in the optical path will have a refractive index change with temperature leading to beam walk off. Both these problems can be addressed when designing rugged packaging.

The insertion loss from port one to port 2 shown in Figure 15 increases while the temperature is constant and only begins to decrease when the temperature decreases. This highlights the limitations in these experiments, this work is not aiming to provide definitive parameters for each device over the avionic temperature range. It is attempting to gauge the parameter changes without packing new devices, which would be prohibitively expensive. The increasing loss from port 1 to port 2 may be a material effect and results taken over a longer period would not yield useful information on how a circulator designed for avionic use would perform. It does suggest however, that to operate up to 85 °C the circulator does not require any alterations to its internal structure.

### **3.2.1.2 Isolation**

The isolation in each channel of the circulator is a measure of how much of the signal is leaking into the other channel. For example, if the signal is input into port 1 the isolation will be the ratio of the measured power in port 3 to the measured power in port 2. The isolation for both channels as a function of temperature is plotted in Figure 16.



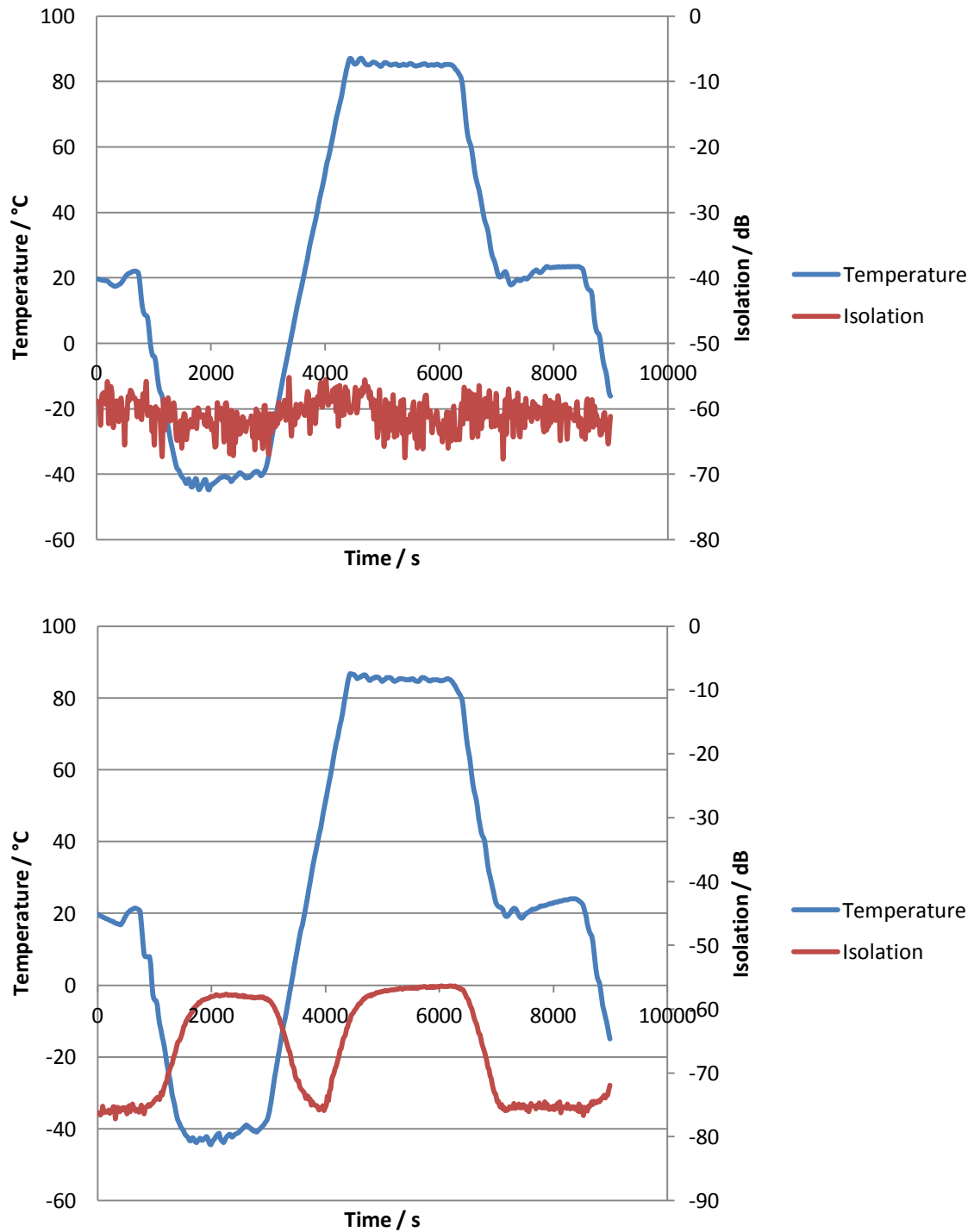


Figure 16: Isolation in circulator, measured from port 1 to port 3 and port 2 to port 1 respectively

The measurements have been taken over the same -40 °C to + 85 °C temperature range and the circulator exposed to the harshest thermal shock over this range as well as spending 30 minutes at the maximum and minimum temperatures. The isolation in both ports of the circulator is very high at around -60 dB, this exceeds the value quoted by the manufacturers

of -40 dB. Although this is affected by the temperature the isolation remains at a level where no problems are predicted over an avionic temperature range.

The insertion loss in the circulator is low and the change in the loss relatively small in comparison to the link budget, the link budget will be analysed in later chapters. The isolation is very low throughout the temperature range so the only problem predicted with using a circulator over the avionic temperature range is packaging related.

### **3.3 Red/Blue C-band Coupler**

Another very commonly used fibre optic component is the coupler. A coupler can be designed to work in different ways. A power splitter will take an input signal and split it into multiple signals, these splits can be of equal or different powers. In this section a wavelength selective coupler will be tested. This will split an input signal into two different wavelength bands, a 'common' input fibre will carry the signal which is then split into the 'pass' and 'reflect' fibres. The coupler in this section will pass the blue section of the C-band, 1525 nm to 1542.54 nm, and reflect the red section of the C-band, 1547.3 nm to 1565 nm.

Wavelength selective couplers are based on thin film filter technology. Like the circulators there could be many different techniques used to create the component and the manufacturer does not reveal the precise design of the component but the working is based around one main concept. Using thin film filters, mirrors that reflect certain wavelengths and pass others can be built in a similar way to Bragg reflectors. The effects of temperature on these devices will depend on the precise structure.

#### **3.3.1 Thermal Testing**

The thermal testing was carried out using the set-up in Figure 17. This is very similar to that used to test the circulator, all the apparatus is the same with the addition of a Kamelain SOA, used unseeded to provide broadband light that the tuneable laser cannot provide.

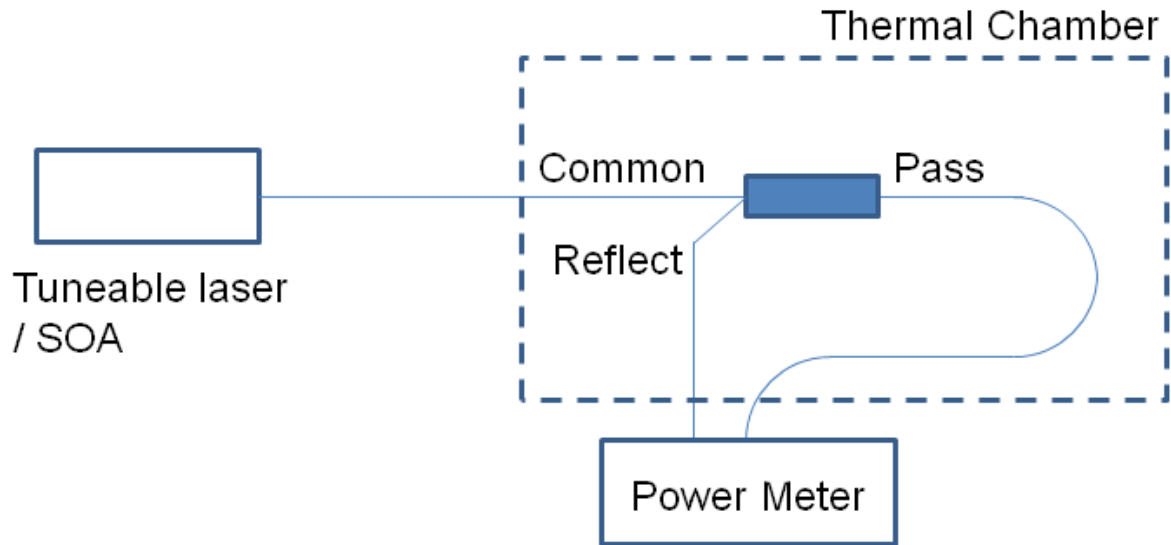


Figure 17: Experimental set-up for testing the coupler

### 3.3.1.1 Insertion Loss

The insertion loss of the coupler has different values for the pass and reflect arms of the device, as this is a wavelength selective device the insertion loss at different wavelengths within both the pass and reflect bands has been investigated. Initially the insertion loss was measured using broadband light from the SOA; the SOA was thermally controlled using an integrated TEC to ensure a constant output power. The insertion loss in each arm as a function of temperature is shown in Figure 18.

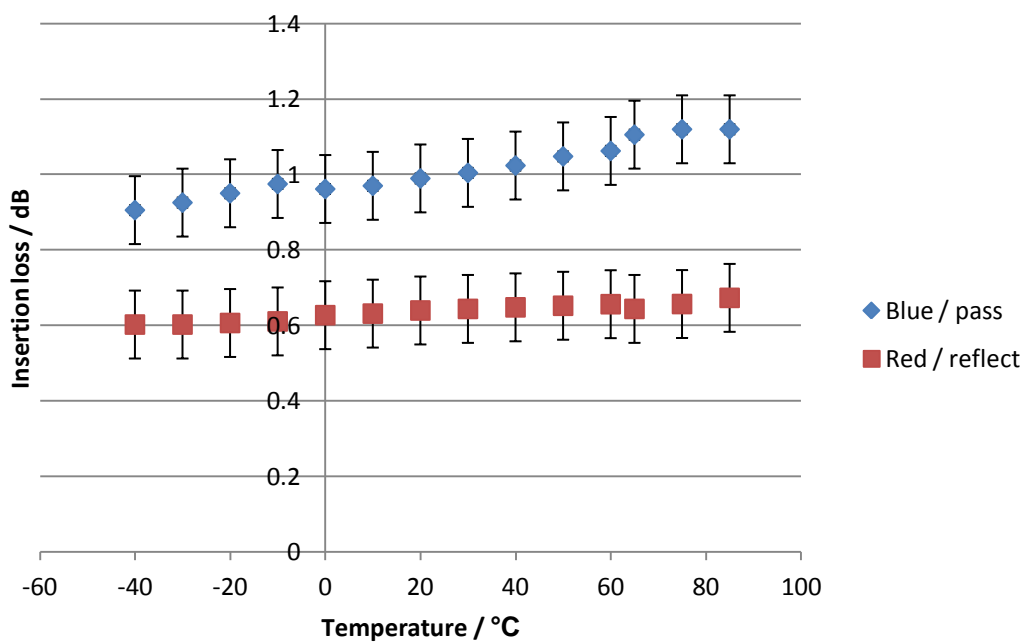


Figure 18: Insertion loss in both pass and reflect arms in red/blue coupler as a function of temperature

Again the device is not being tested beyond its specified storage temperatures as it is likely the device would be permanently damaged and no useful results would be taken. The manufacturers specifications show an insertion loss of 0.99 dB for the pass band and 0.64 dB for the reflect band at a temperature of 23 °C. These readings are an average, taken at each temperature over a period of 5 minutes. The pass arm shows a clear increase in insertion loss with increasing temperature with an increase of 0.2 dB from -40 °C to +85 °C, if this increases at the same rate throughout the avionic temperature range the maximum loss will be realised at 125 °C and is predicted to be less than 1.3 dB. This is not a problematic level of loss. The loss in the reflect arm is not as high and does not increase with temperature as quickly as the pass arm. This also should not present a problematic level of loss over the avionic temperature range. The increase in loss in the pass arm could be due to a shift in the passband to longer wavelengths; this could be a problem as it would mean some central channels could not be used for data to allow for this shift. This can be investigated by interrogating the coupler with the tuneable laser at wavelengths near the transition from pass to reflect and monitoring the 3 dB loss point at the transition.

The insertion loss was measured with light from the tuneable laser at wavelengths of 1547 nm and 1563 nm, these represent the shortest and longest wavelengths that are can be used in the reflect arm of the coupler according to the manufacturers specifications. The temperature was cycled through the specified storage range of the components exposing the components to thermal shock as well as the maximum and minimum specified temperatures. The insertion loss at each wavelength over the specified storage temperature range is shown in Figure 19.

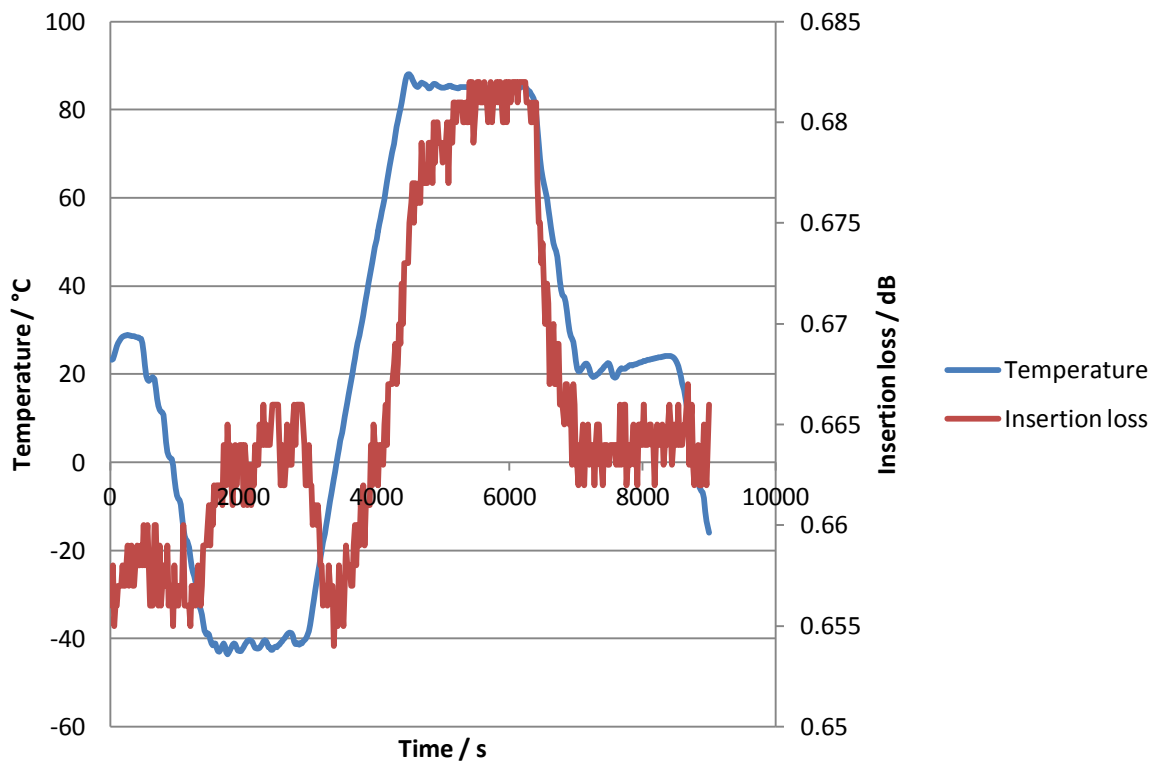
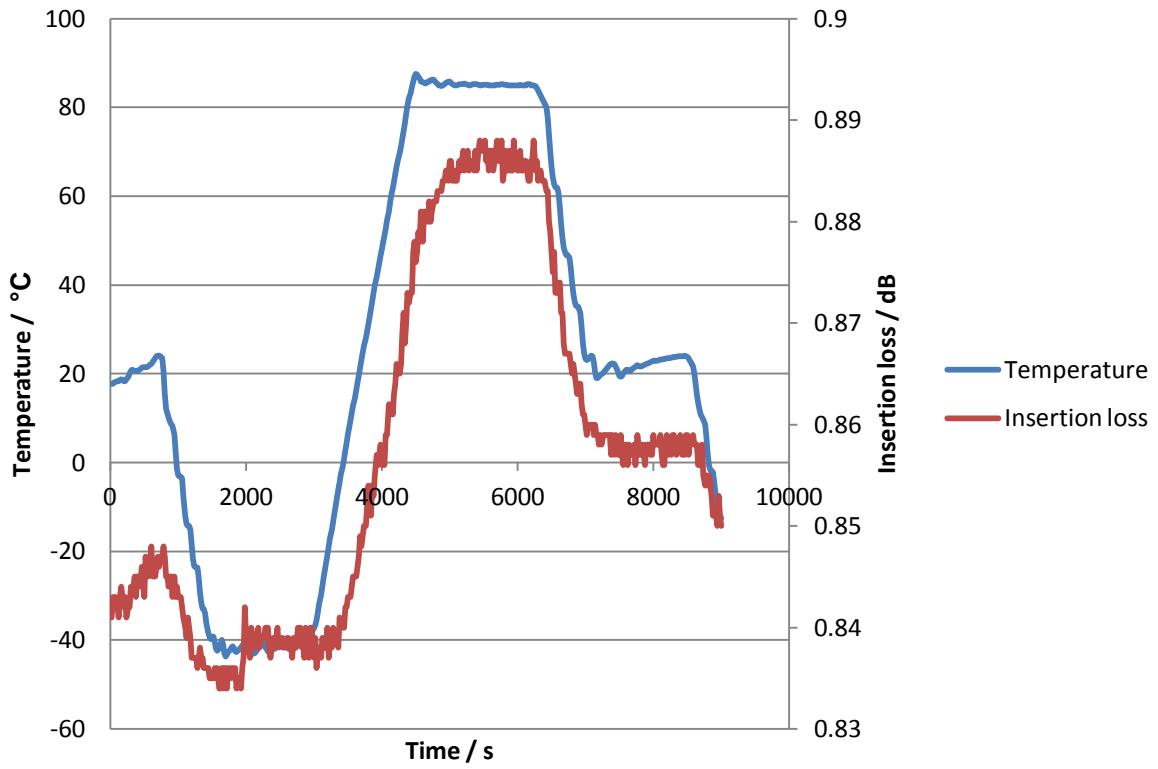


Figure 19: Insertion loss of red/blue coupler pass arm, measured over range of temperatures at 1547 nm and 1563 nm respectively

The loss at each wavelength is slightly different, a loss of between 0.83 dB and 0.89 dB is measured at 1547 nm and a loss of between 0.65 dB and 0.68 dB is measured at 1563 nm. At 1547 nm the loss increases and decreases with temperature, at 1563 nm the loss increases with temperature but decreasing loss does not correlate to decreasing temperature as strongly. Nevertheless, given the rate of change of the insertion loss with changing temperature, this still suggests that the changes in loss across the useful section of the reflect band will not be problematic.

These measurements were then repeated on the pass arm and the results plotted in Figure 20.

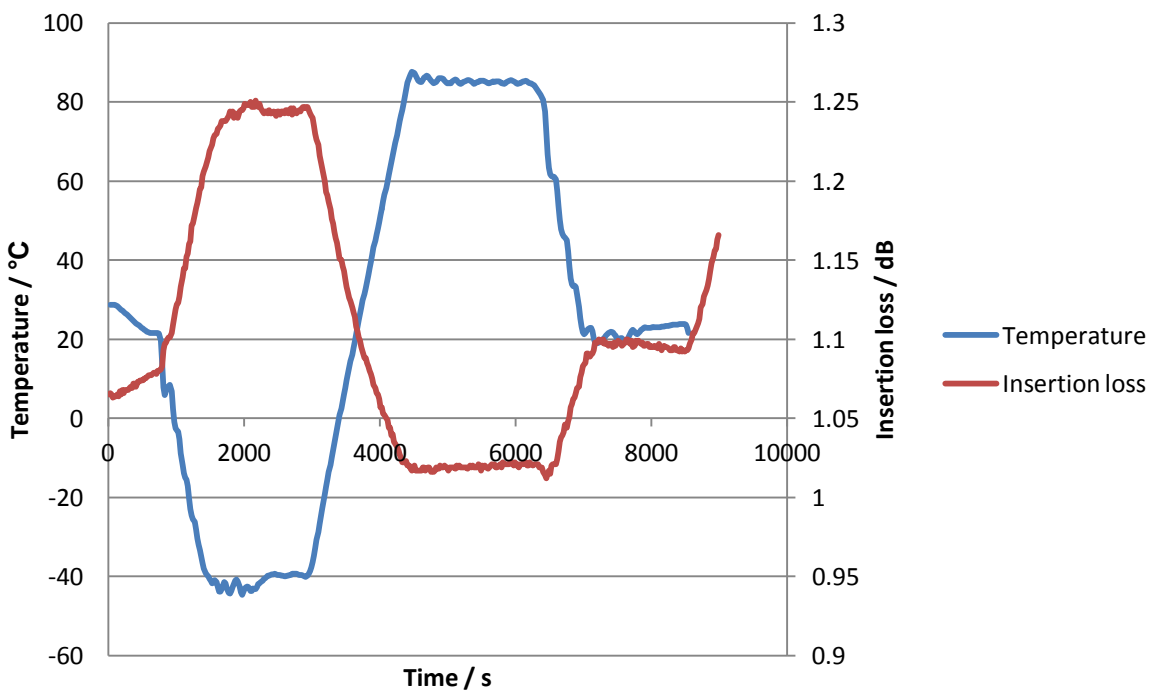
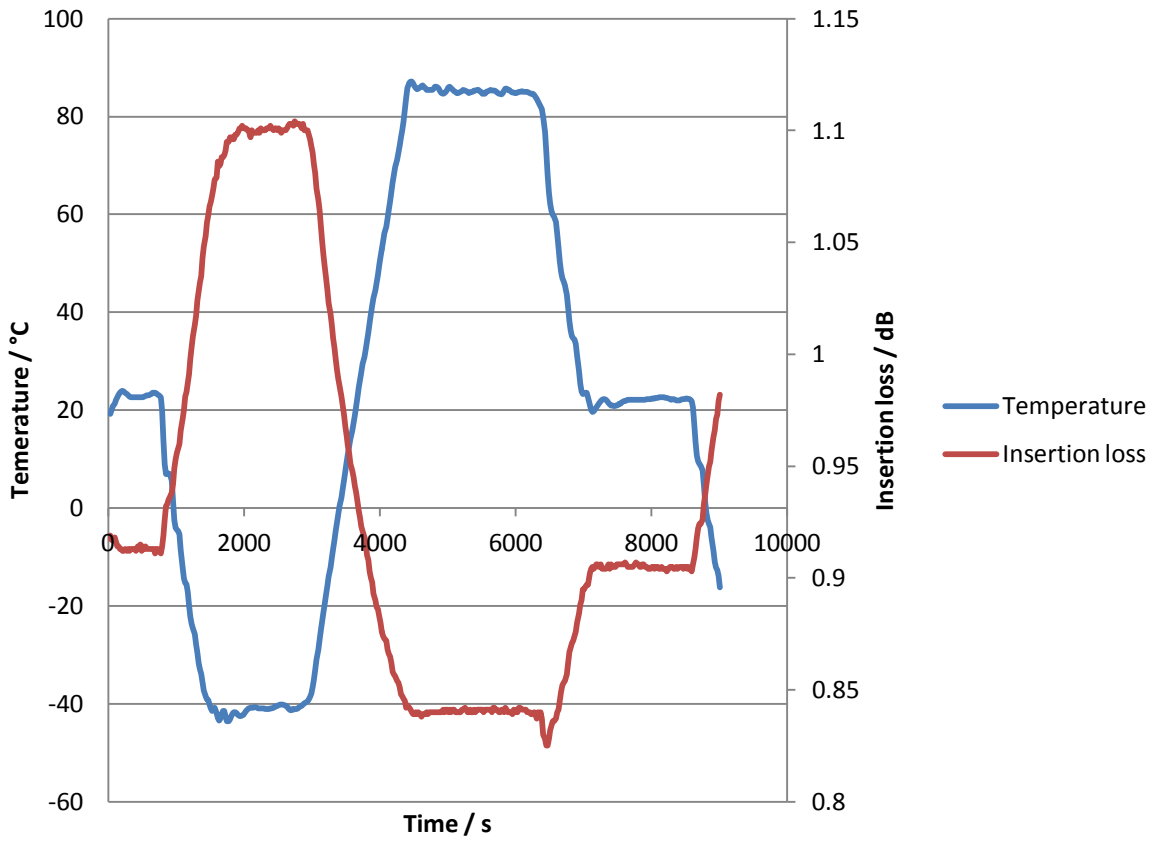


Figure 20: Insertion loss of red/blue coupler reflect arm, measured over range of temperatures at 1541 nm and 1528 nm respectively

The loss at 1541 nm has been measured between 0.84 and 1.1 dB in the specified storage range. The relationship between the insertion loss and temperature is the opposite of that in the reflect arm with the loss decreasing at higher temperatures. This relationship is also visible at 1528 nm suggesting that it will occur across the useful section of the pass band. Although the loss in one arm increases with temperature as the loss in the other arm decreases this does not mean that the transition is drifting but does suggest that the isolation will be affected by temperature. More experimental work must be done to confirm this and is included later in this chapter.

### 3.3.1.2 Transition from Pass to Reflect

In order to measure the wavelengths that mark the transitions from pass to reflect it is necessary to first define the transition. A common way to define this transition is to measure the 3 dB loss point; this is pre-programmed into the optical spectrum analyser so is straightforward to measure whilst avoiding human error. The 3 dB loss points are shown, for both pass and reflect bands, as a function of temperature in Figure 21.

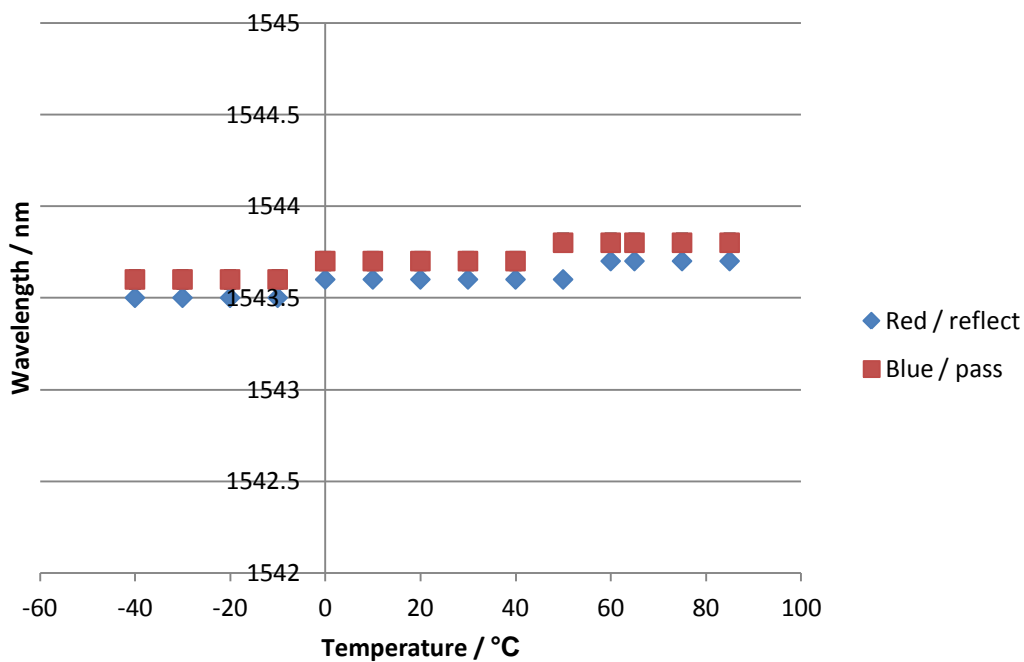


Figure 21: 3 dB loss point at edges of pass and reflect band of red/blue coupler as a function of temperature

An additional insertion loss of 3 dB in the couplers could be lumped with architectural losses of the network in following analyses so the loss level here may not be prohibitive. The edges of the bands are very close however, while this will ensure good spectral efficiency it means that any changes in the pass/reflect transition will lead to failure at certain channels. The 3



dB point of the reflect band ranges from 1543.6 nm and 1543.8 nm over the storage temperature range. The 3 dB point of the pass band over the same temperature range varies between 1543.5 nm and 1543.8 nm. A channel at 1543.7 nm will be passed or reflected by the coupler depending on the temperature, this channel could not be used over this temperature range. As well as the transition drifting with temperature, the isolation at the 3 dB loss point will not be sufficient and a guard band of unused wavelengths must be identified for this device.

To identify the possible wavelength range to define as the guard band for the transition between pass and reflect a lower loss point than 3 dB can be used. As previously mentioned, 3 dB can be included in the lumped losses of all components in the network. However, the analysis will be improved if a smaller loss is included, this will also alleviate the problems with crosstalk between the pass and reflect band. The optical spectrum analyser can be programmed to read the 0.5 dB loss point in the same way as the 3 dB point previously. A plot with the edge of the pass and reflect bands as a function of temperature is shown in Figure 22.

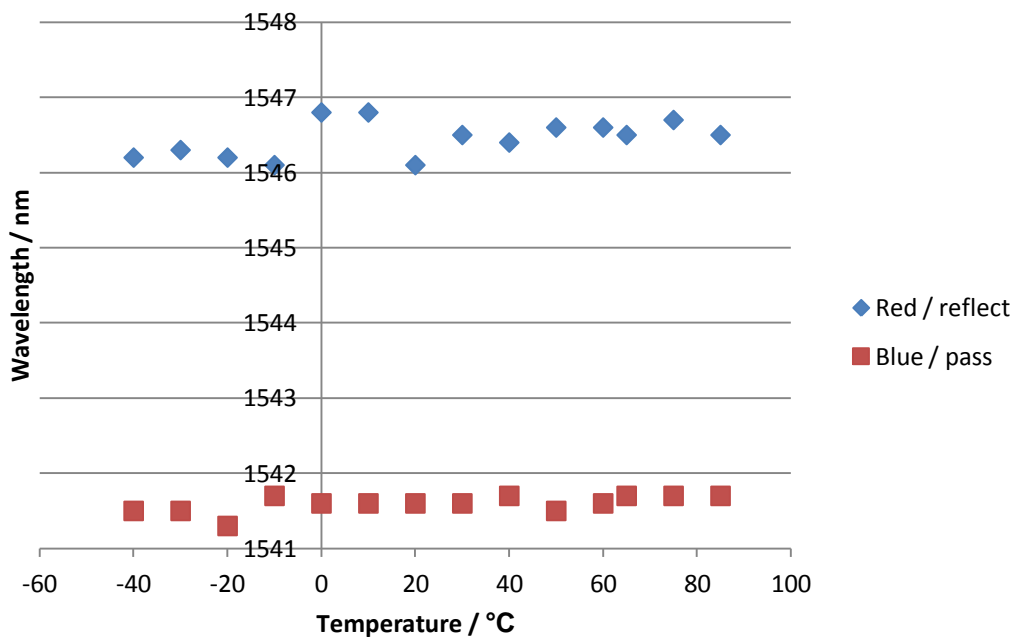


Figure 22: 0.5 dB loss points at edges of pass and reflect bands of red/blue coupler as a function of temperature

The edges of the pass and reflect bands as defined by the 0.5 dB loss point follow the same trend as the 3 dB loss point, both drift to slightly longer wavelengths with increasing temperature. In this case this is not as problematic as there is a gap on the ITU grid from 1541.39 nm to 1546.917 nm which would relate to a gap of 8 channels if using a multiplexer

with 100 GHz spacing, this gap agrees with the information given in the manufacturers specifications. Although this means that there should not be any wavelengths which may be passed and reflected depending on temperature it provides no information on the isolation at these wavelengths.

### **3.3.1.3 Isolation**

The isolation of the pass or reflect band is the ratio of the optical power in the pass or reflect band compared to the other for a wavelength that should have been passed or reflected respectively. The isolation measured for wavelengths in the pass band is shown over the storage temperature range in Figure 23.

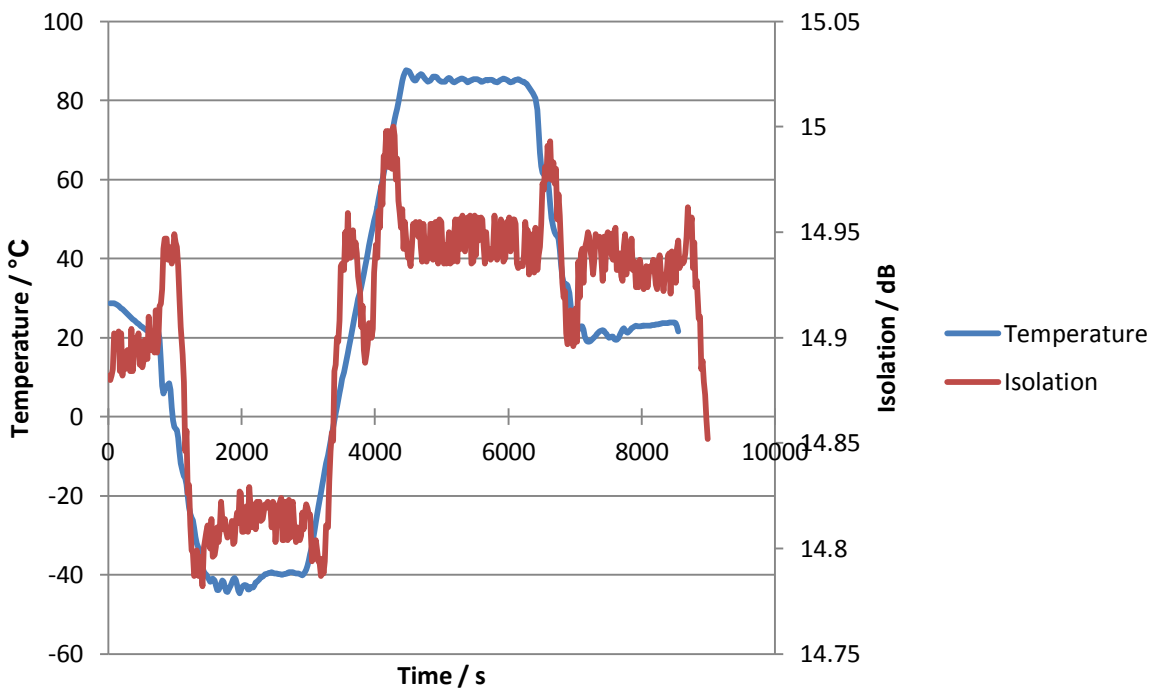
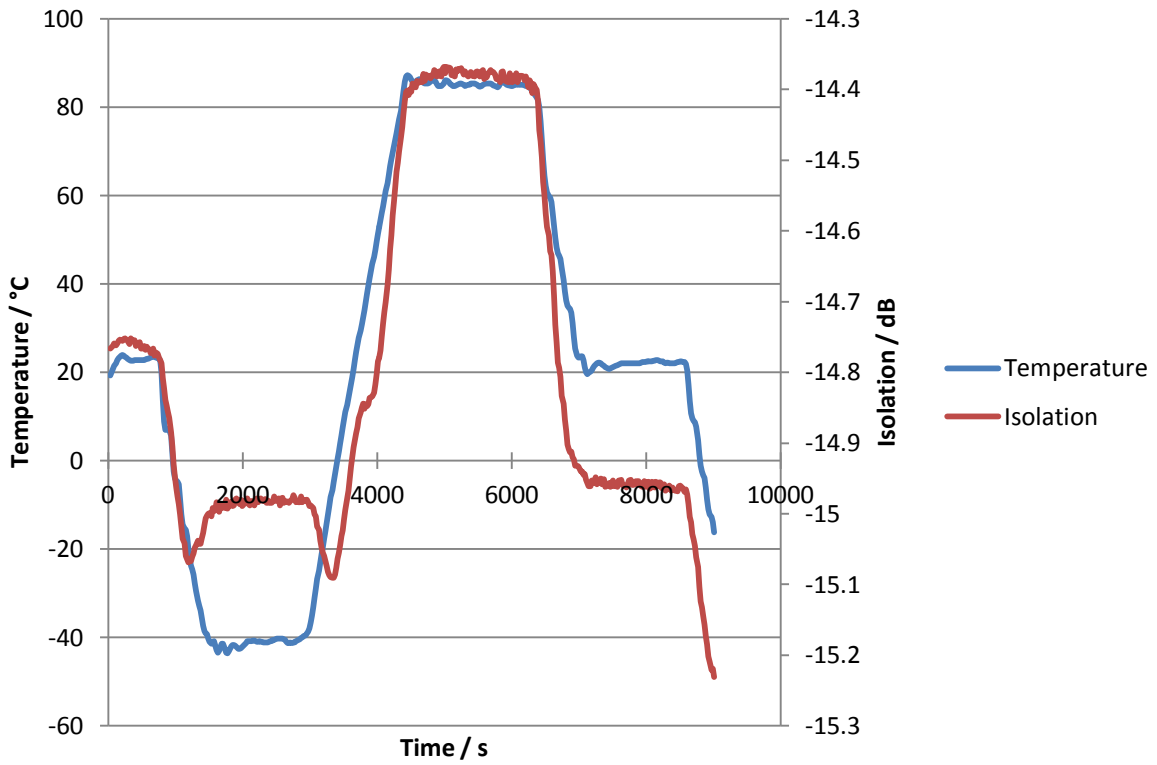


Figure 23: Isolation in the pass band of red/blue coupler at the specified storage range for temperature taken at 1541 nm and 1528 nm respectively

The isolation has been measured at 1541 nm, the longest wavelength in the passband, and at 1528 nm, which is the shortest wavelength that the proposed network will use. At both these wavelengths the isolation varies with 1541 nm having slightly worse performance at

high temperatures with the isolation reaching -14.4 dB as opposed to -14.8 dB at 1528 nm. The isolation in the pass band is quoted as less than -12 dB in the manufacturers specifications and this is maintained across the storage range. The isolation value at 1541 nm is significant as it shows that the edge of the passband has been well defined and that in setting the passband edge at 1541 nm no performance penalties are being incurred.

The isolation in the reflected path has also been measured at the shortest and longest wavelengths that would be used over this band, the results are shown in Figure 24.

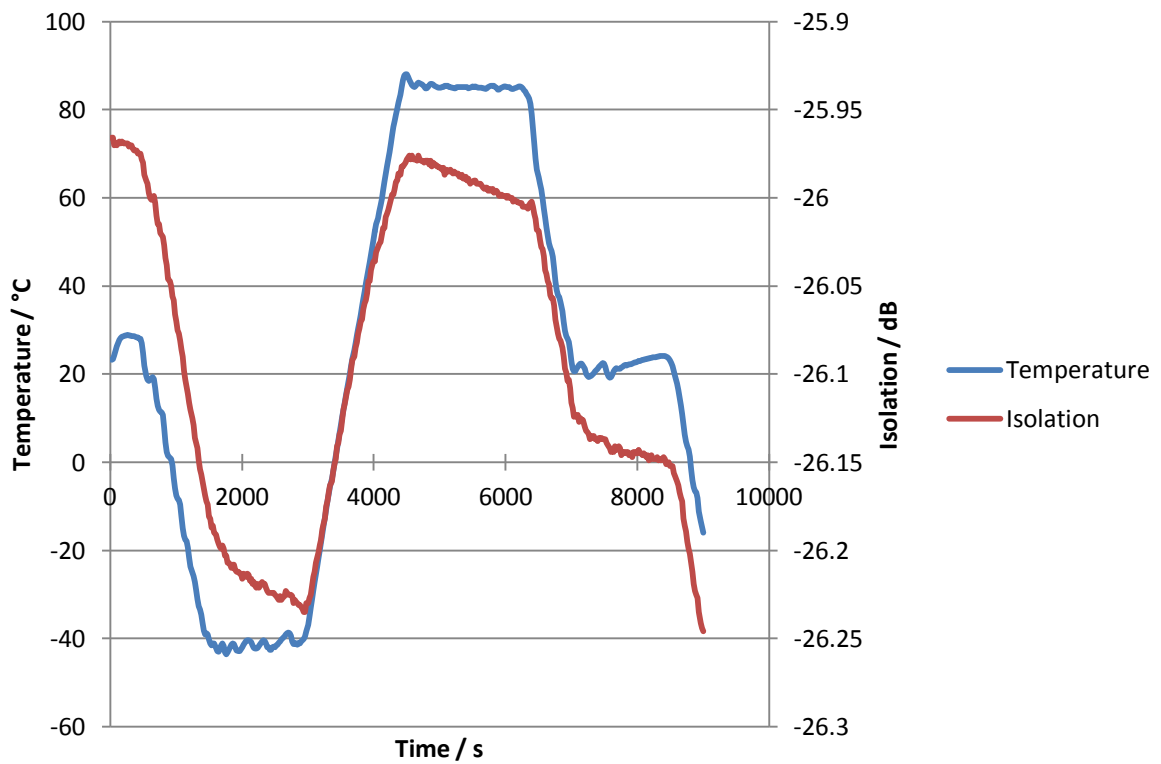
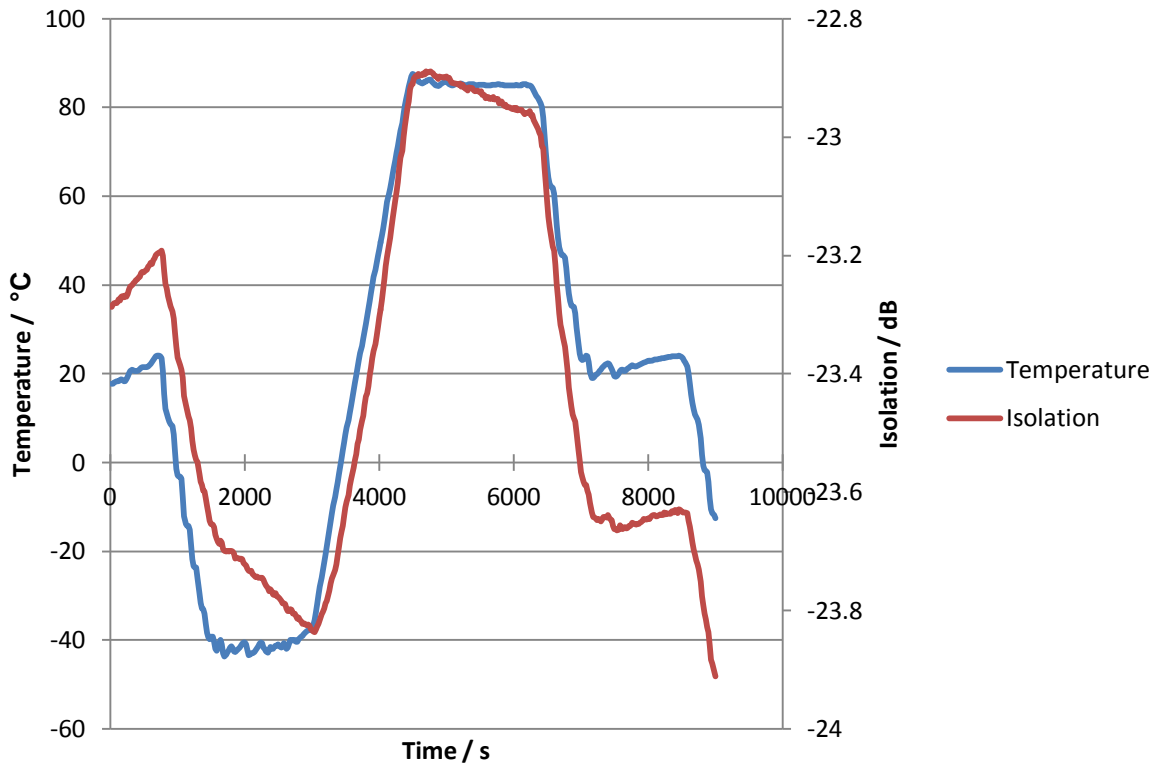


Figure 24: Isolation in the reflect band of red/blue coupler at the specified storage range for temperature taken at 1547 nm and 1563 nm respectively

The isolation specified by the manufacturers is less than -24 dB. The isolation measured at 1563 nm, is in accordance with the manufacturers specification, ranging from -26.25 dB to -26.95 dB. The isolation at the band edge wavelength of 1547 nm is slightly out of the specification ranging from -23.9 dB to -22.9 dB. Although this is not in accordance with the specifications the level of isolation is acceptable and the band edge is well defined at 1547 nm.

In both pass and reflect bands this level of isolation could be problematic depending on the network design. In the proposed network the measured levels of isolation should not be problematic but will be considered throughout future work.

## **3.4 Multiplexer**

The proposed network will use wavelength division multiplexing. A component is needed to combine signals of different wavelengths so they can be carried down a single fibre backbone, a multiplexer, and so they can be separated out from the single fibre at the opposite end of the link, a demultiplexer. Usually multiplexing and demultiplexing is carried out by the same component with the different functions dependant on the direction of propagation of the signal.

In the following work two types of multiplexer will be tested, firstly an arrayed waveguide grating and then a multiplexer based on thin film filters.

### **3.4.1 AWG**

An arrayed waveguide grating is a passive multiplexer which is widely available and is specified meeting telecommunications standards. The workings of an AWG are explained in detail in section 2.3.3.1 Arrayed Waveguide Grating and in the literature [40], the structure is sketched in Figure 25.

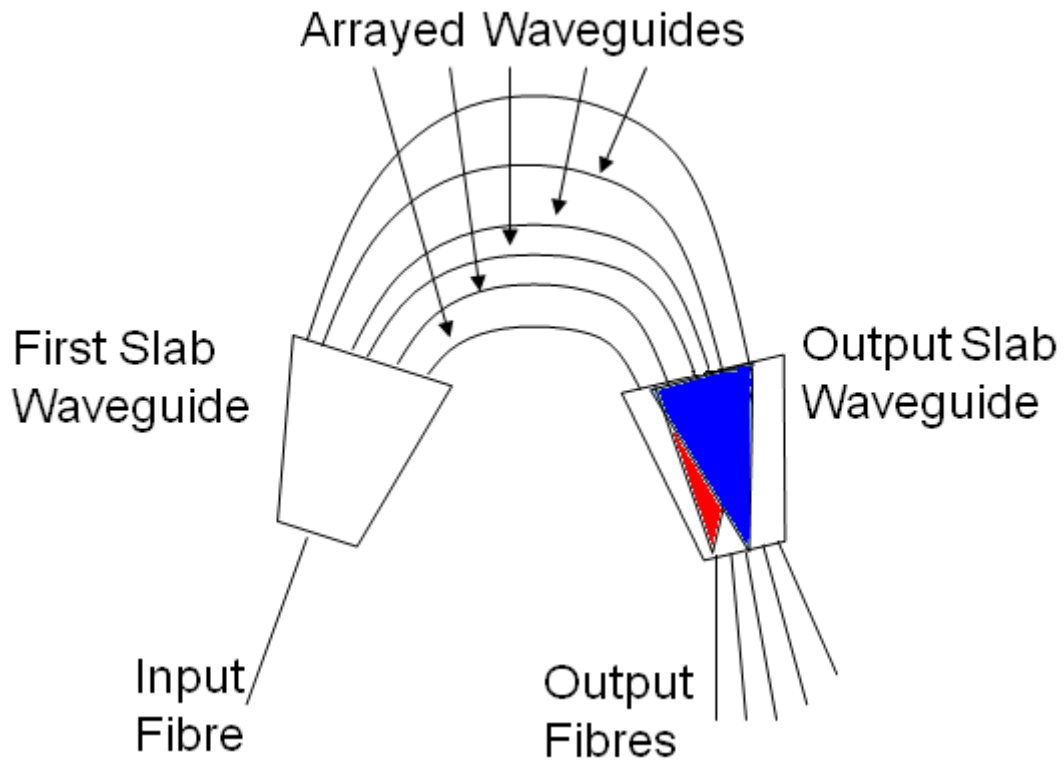


Figure 25: Sketch of the internal structure of an arrayed waveguide grating

Light from the input fibre propagates through the slab waveguide and is coupled into an array of waveguides. On exiting the waveguides each beam interferes according to its phase. The output fibres are positioned to capture light that is focussed by constructive interference; this position will be different for different wavelengths. The two slabs can be thought of as lenses with the arrayed waveguide acting as a grating.

The position of the output fibres is dependent on the constructive interference which is in turn dependant on the difference in optical path length of the arrayed waveguides. The path length will change with as a function of temperature meaning that the AWG is temperature sensitive. It is possible to manufacture an athermal AWG by including materials with differing thermo-optic coefficients which will cancel the changes in refractive index with changing temperature in each material. Although this device is marketed as 'athermal' the performance is affected by temperature, albeit to a lesser extent than the 'thermal' AWG. The effects of temperature on an athermal AWG will be therefore be investigated in the remainder of this section. The athermal AWG tested was a 40 channel 100 GHz athermal AWG supplied by Kaiam Corporation.

### **3.4.1.1 Centre Wavelength**

The central wavelength of each channel, for a multiplexer with channel spacing of 100 GHz, is specified by ITU for use in telecommunications. On an aircraft it is not necessary to meet the ITU specifications. However, in order to take advantage of economies of scale in the telecoms marketplace it is desirable to meet the specifications so inexpensive components are compatible with the network.

In order to measure the centre wavelength in selected channels of the AWG it was interrogated using a broadband source, in this case an unseeded SOA which was thermally regulated using a thermo-electric cooler. The spectral slice at each channel can be measured using an optical spectrum analyser in order to measure the characteristics of the passband of each channel. Although the spectral power distribution is not constant across the C-band it can be assumed to be constant across the narrow passband, of approximately 0.6 nm, of each channel. With this assumption the optical spectrum analyser will analyse the spectral slice from any channel and provide the central wavelength automatically, this will ensure continuity in measuring the central wavelength as a function of temperature.

The central wavelength as a function of temperature was measured at the shortest and longest wavelength channels in the AWG and at the channel corresponding to ITU 1550.116 nm. Again the device was only tested over its specified storage range and not the avionic operating range with respect to temperature. The results of this test are shown in Figure 26.



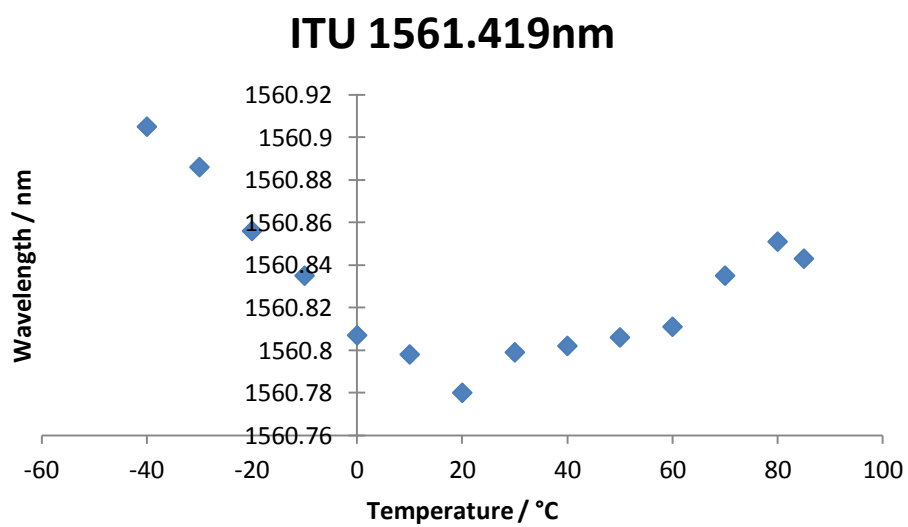
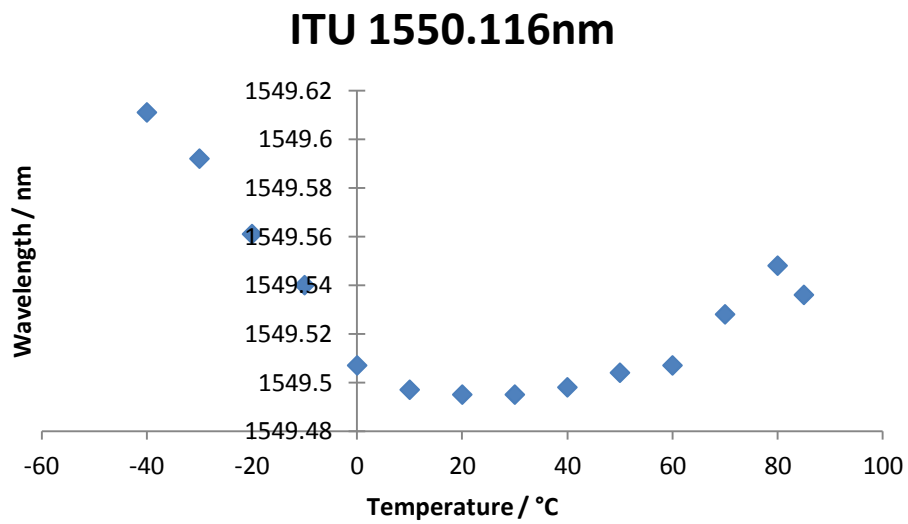
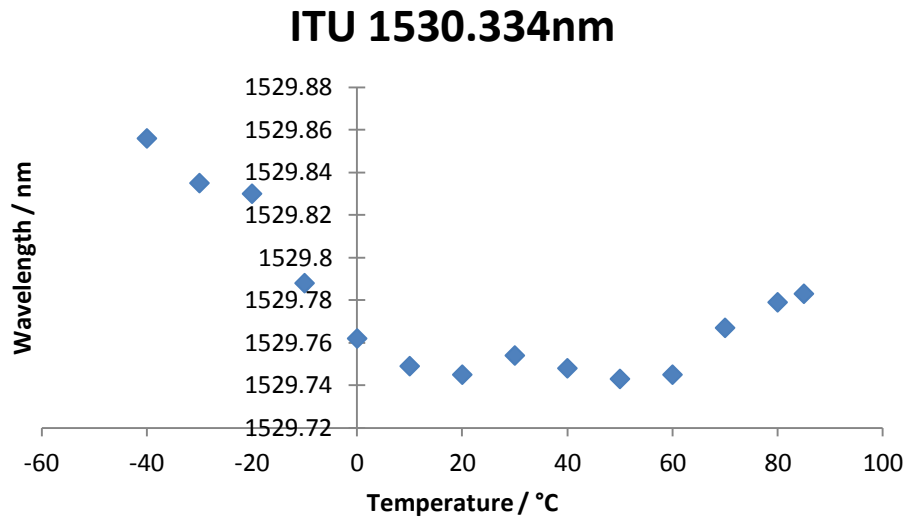


Figure 26: Central wavelength as a function of temperature for channels of an AWG on ITU grid 1550.334 nm, 1550.116 nm and 1561.419 nm

The centre wavelength of each channel does not sit on the wavelength specified by the ITU; this is not a problem for this test. This AWG was supplied by Kaiam free of charge to carry out these tests under the agreement that an old component or one with slight faults would be suitable. If this component were to be ordered for use on a commercial network the component would be of commercial quality. The fact that the wavelengths do not match those specified by the ITU does not affect the validity any conclusions drawn from this work.

The operating range of the AWG is from 0 °C to 60 °C, outside this range athermal performance of the AWG is not guaranteed by the manufacturer. In the operational range the central wavelength drifts by approximately 0.02 nm in each channel. Outside the operational range the drift is more severe, from 0 °C to -40 °C the wavelength drifts by at least 0.1 nm in each channel, from 60 °C to 85 °C the wavelength drifts by approximately 0.05 nm in each channel. When viewed purely as a difference in centre wavelength it is not possible to say whether or not the performance of the AWG is acceptable for use in the proposed network.

The additional loss and crosstalk between adjacent channels will both be dependent on the shift in central wavelength and must be defined as a function of the difference between the central wavelength of MUX and DEMUX. This will represent two AWGs at opposite ends of a link at different temperatures and allows limits to be placed on the total temperature difference acceptable between the two AWGs, this ultimately establishes the limit over which the AWG can be treated as athermal. Proposed networks use both RSOA modulators with spectrum slicing and laser transmitters. This means there will either be amplified ASE which will fill the passband spectrum or narrowband laser light from a DFB which will not fill the passband. The effect of a change in the central wavelength on the loss and crosstalk in both these cases may be very different and both must be investigated.

#### 3.4.1.1.1 Spectral Slicing Case

In a network employing the spectral slicing technique a broadband light source, such as a superluminescent diode, is sliced into its spectral components by a multiplexer. The output from each channel is input to a reflective semiconductor optical amplifier, RSOA, where it is amplified and modulated. The output from the RSOA is the data encoded onto an optical signal of narrow spectral width matching the passband of the multiplexer. The spectral power distribution of the optical signal matches that of the multiplexer. Any change in the centre wavelength of either multiplexer or demultiplexer will have a significant effect on the network performance as some signal will be lost for even very slight changes, although the AWG passband shape is Gaussian so initially the loss will be very small. Potentially more problematic is the crosstalk in adjacent channels which could rise to problematic levels with very little movement in wavelength.

The experimental set up used to investigate the insertion loss and crosstalk, when spectrum slicing, is sketched in Figure 27.

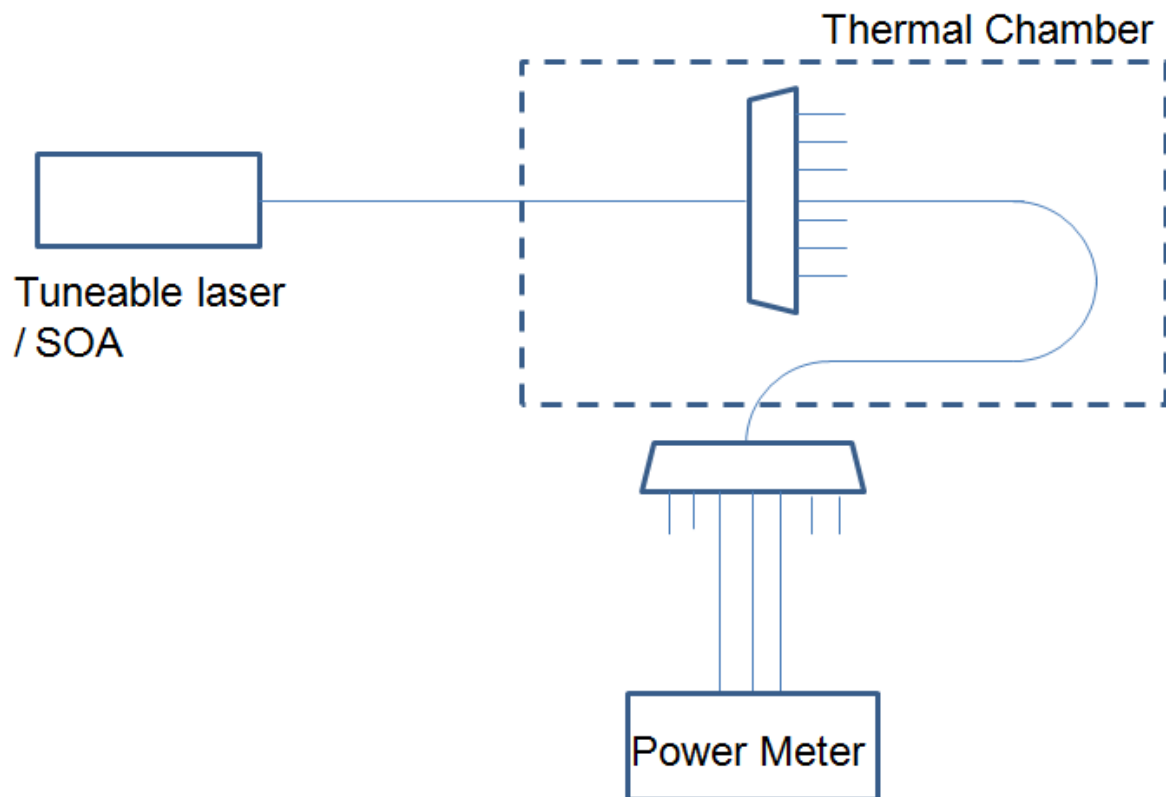


Figure 27: Schematic of the experimental set-up to measure the crosstalk and insertion loss of a multiplexer when spectrum slicing or with a laser transmitter

Broadband light from the SOA, which is thermally regulated using a TEC, is sliced by an AWG which is in the thermal chamber. This means the central wavelength of each channel can be tuned by changing the temperature in the thermal chamber. Measuring the power in the corresponding channel, and its neighbouring channels, on the second AWG allows measurement of the insertion loss and adjacent channel crosstalk at various differences in central wavelength for the two AWGs.

The insertion loss of a demultiplexer, as well as the adjacent channel crosstalk, is plotted in Figure 28 as a function of the difference in centre wavelength,  $\Delta\lambda$ , between the multiplexer and demultiplexer. This has been plotted for the channels centred on the wavelengths, 1531.116 nm, 1550.116 nm and 1560.618 nm.

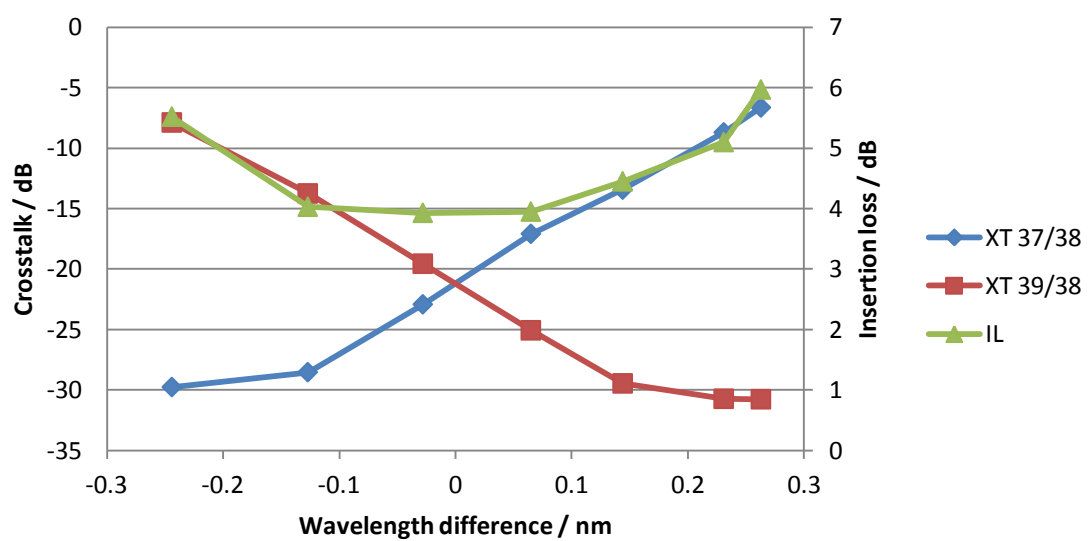
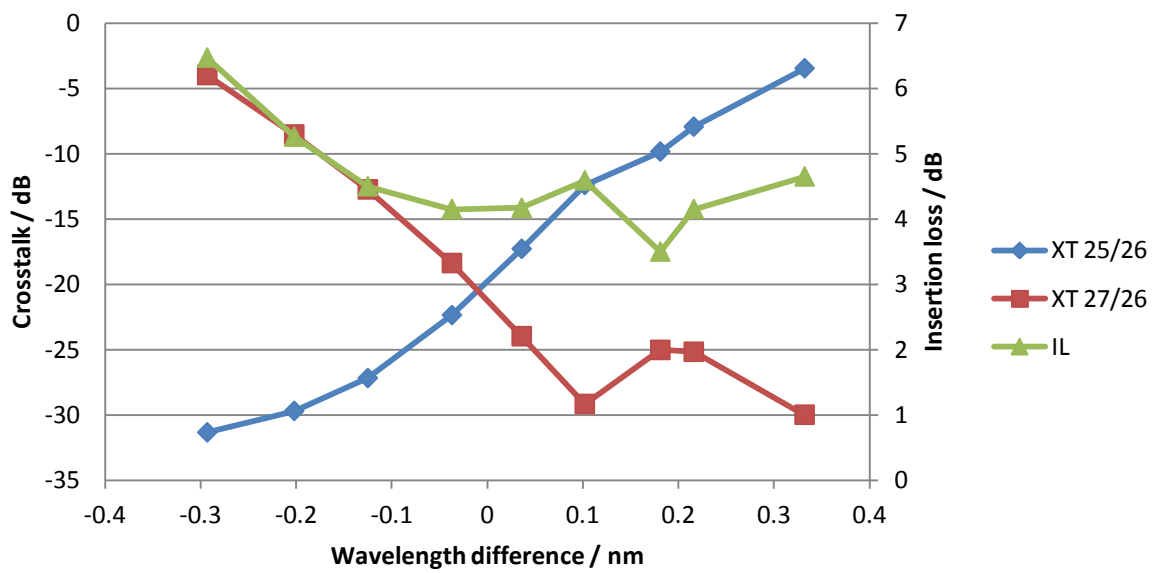
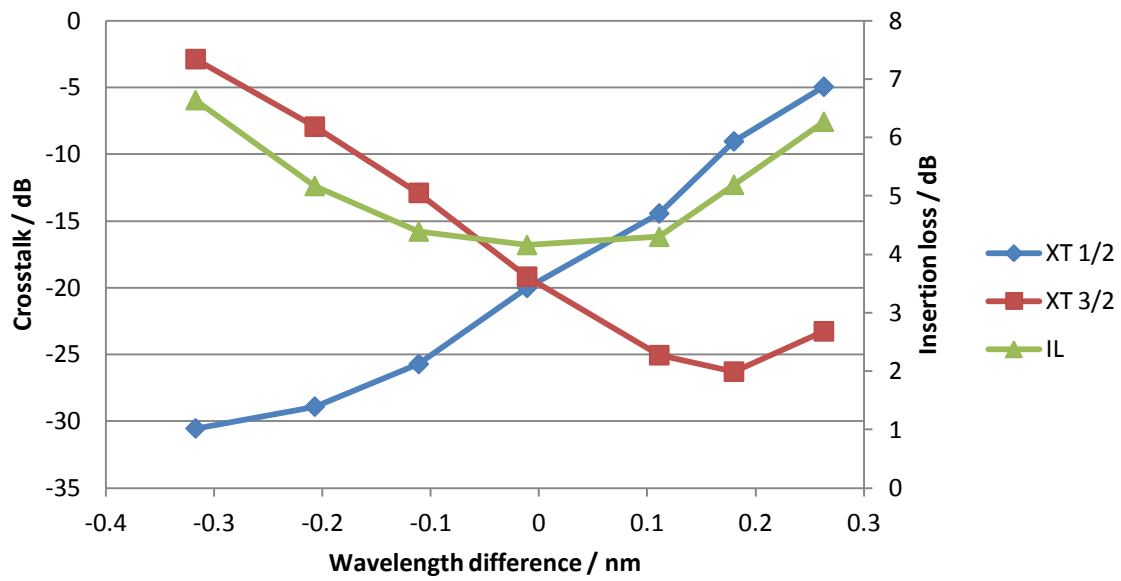


Figure 28: Insertion loss and adjacent channel crosstalk for the channels of an AWG centred on ITU wavelengths as a function of wavelength difference between mux and demux.

If the acceptable insertion loss of the demultiplexer is defined as 5 dB the maximum tolerable  $\Delta\lambda$  is around 0.2 nm in each of the three channels tested. The insertion loss will not be problematic and will not be the limiting factor with respect to the operational temperature. The limiting factor will be the crosstalk between adjacent channels. The crosstalk between channels will lead to some of the signal from one channel being detected at the photodiode of the neighbouring channels, this will erode the extinction ratio of the digital signal and increase the noise at the photodiode, therefore a power penalty will be incurred. There has been much work done on calculating the power penalties in fibre optic communication systems due to crosstalk [67,68] and a full analysis of the power penalties at this point is beyond the scope of the thesis. There are many variables which will affect the power penalty incurred by crosstalk and as the test data from this multiplexer is not definitive and this is not the device which will be used in the final design an accurate estimation of the power penalty will not be made. From calculations in reference [67] an acceptable estimate of the power penalty can be made, for two, incoherent, sources of crosstalk, in a link limited by thermal noise in the receiver, the power penalty for -20 dB crosstalk is approximately 4 dB. If the crosstalk can be reduced to -25 dB this power penalty will fall to approximately 1 dB.

The insertion loss and adjacent channel crosstalk have been plotted as function of the difference in central wavelength of the two multiplexers, what is of more concern is the temperatures corresponding to these differences. Over the region where the device is 'athermal' between 0 °C and 60 °C the maximum difference in two matched multiplexers is 0.02 nm, using the AWG for spectrum slicing over this range presents no problem with insertion loss but may be problematic when crosstalk is considered. If this is the case it is possible to skip channels and operate with channel spacing of 200 GHz thus reducing crosstalk at the expense of reducing the number of channels.

#### 3.4.1.1.2 Laser Case

Typically a DFB laser is used as a transmitter in WDM. This has a narrow linewidth in comparison to the passband of the AWG. Unlike the RSOA scenario, the entire wavelength range of the passband is not used to carry the signal. This should, in theory, mean that the crosstalk between neighbouring channels is much reduced.

As the transmission wavelength is set by the laser and not the multiplexer the centre wavelength of the optical signal will not be affected by the temperature of the multiplexer. The insertion loss and isolation have therefore been measured directly as functions of the

AWG temperature. The insertion loss of three AWG channels when using a DFB transmitter centred on the AWG wavelength at room temperature is plotted in Figure 29.

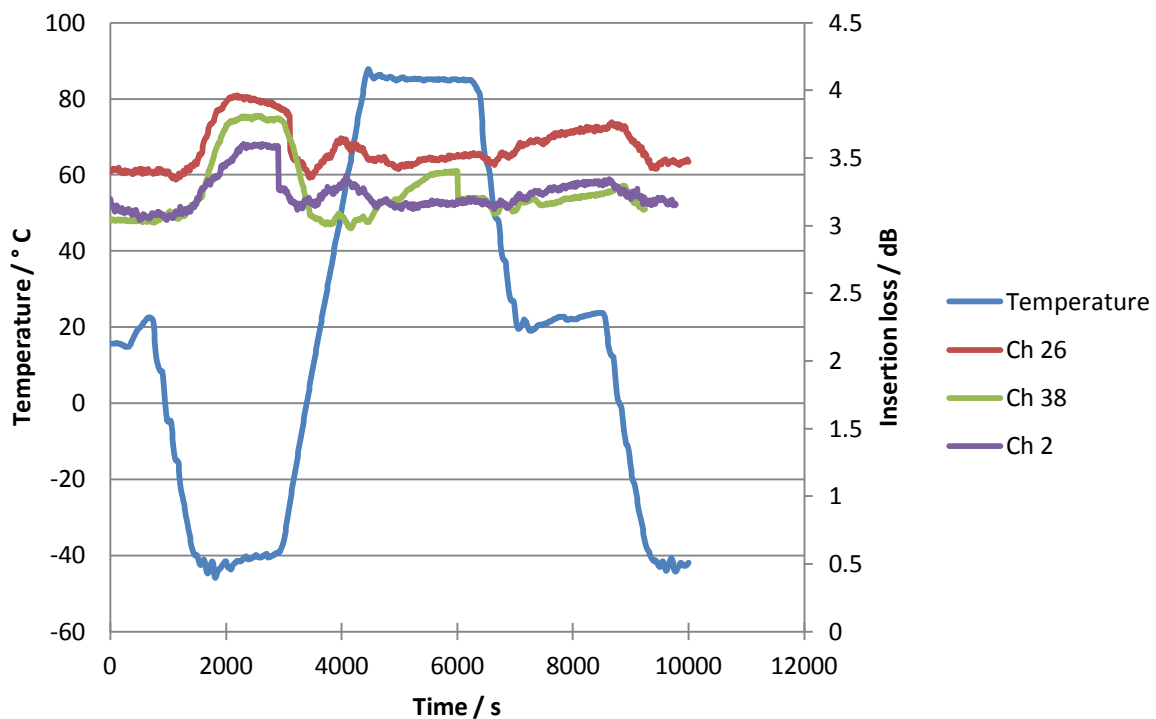


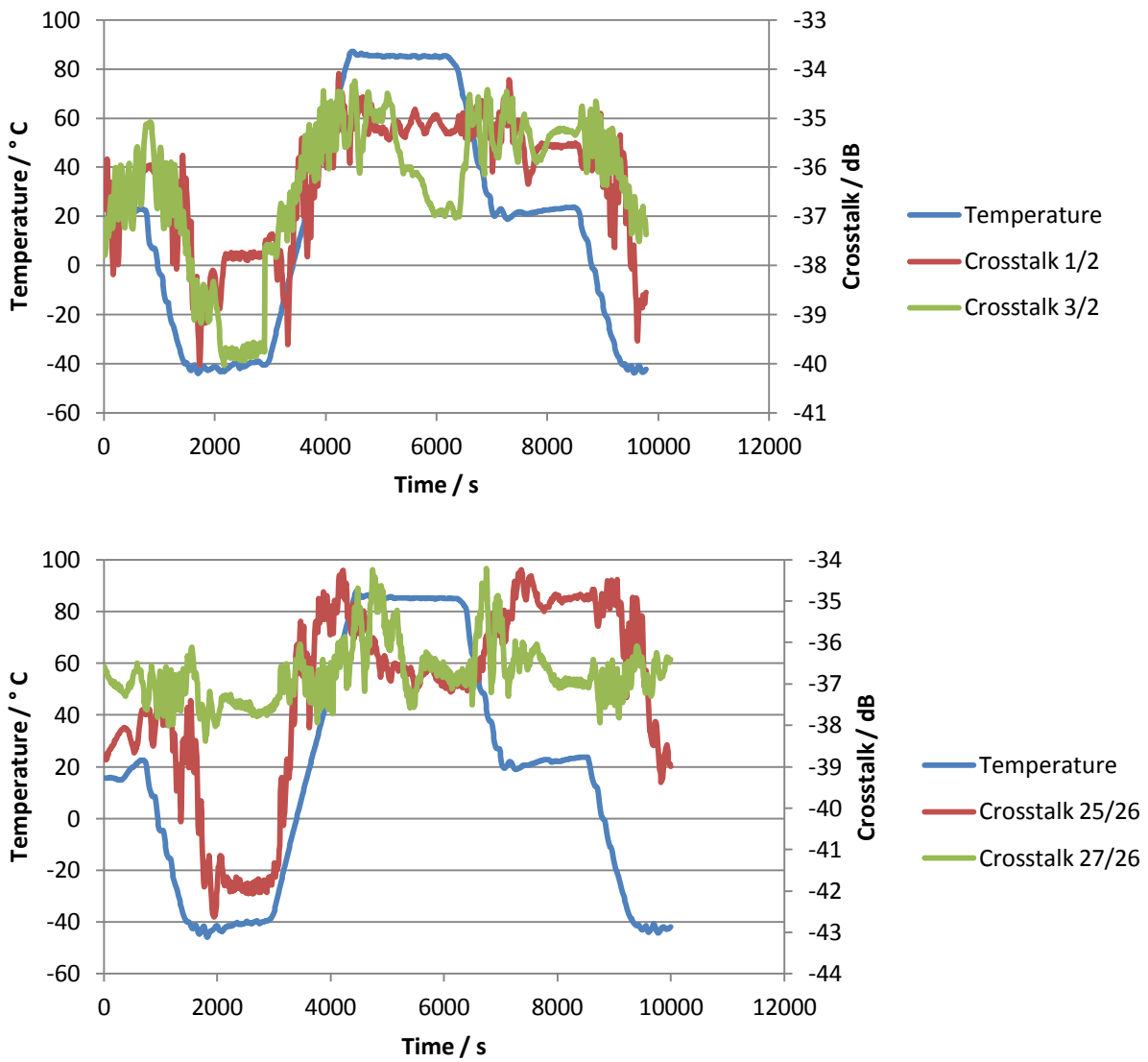
Figure 29: Insertion loss of three channels on the AWG over the storage temperature range.

Channels 2, 26 and 38 are centred on the wavelengths 1531.116 nm, 1550.116 nm and 1559.794 respectively. The specified insertion loss for the AWG across all channels is 3 dB at the specified ITU wavelength and 4.5 dB over the clear passband between 0 °C and 60 °C. The laser is set to the centre wavelength which applies at the operational range of 0 °C to 60 °C, at temperatures outside this range the centre wavelength will drift to a longer wavelength value. The insertion loss of each channel is therefore less than the specified loss value of 4.5 dB throughout the devices storage range.

The ramp rate between the two temperature extremes is set to deliver the most severe thermal shock that the thermal chamber can manage; this does not appear to have an effect on the insertion loss. Dwelling at a low temperature does increase the insertion by approximately 0.5 dB in each case. If the AWG was to be used at the full avionic operational temperature uncooled this would have to be measured with a ruggedized device to check that the insertion loss did not increase to problematic levels.

As previously mentioned, the entire passband of each channel is not used for carrying the signal, only a narrow section is used. This should lead to decreased levels of adjacent channel crosstalk when compared to the spectrum slicing scenario. The adjacent

channel crosstalk of in channels 2, 26 and 38 are plotted in Figure 30 over the storage temperature range of the AWG.



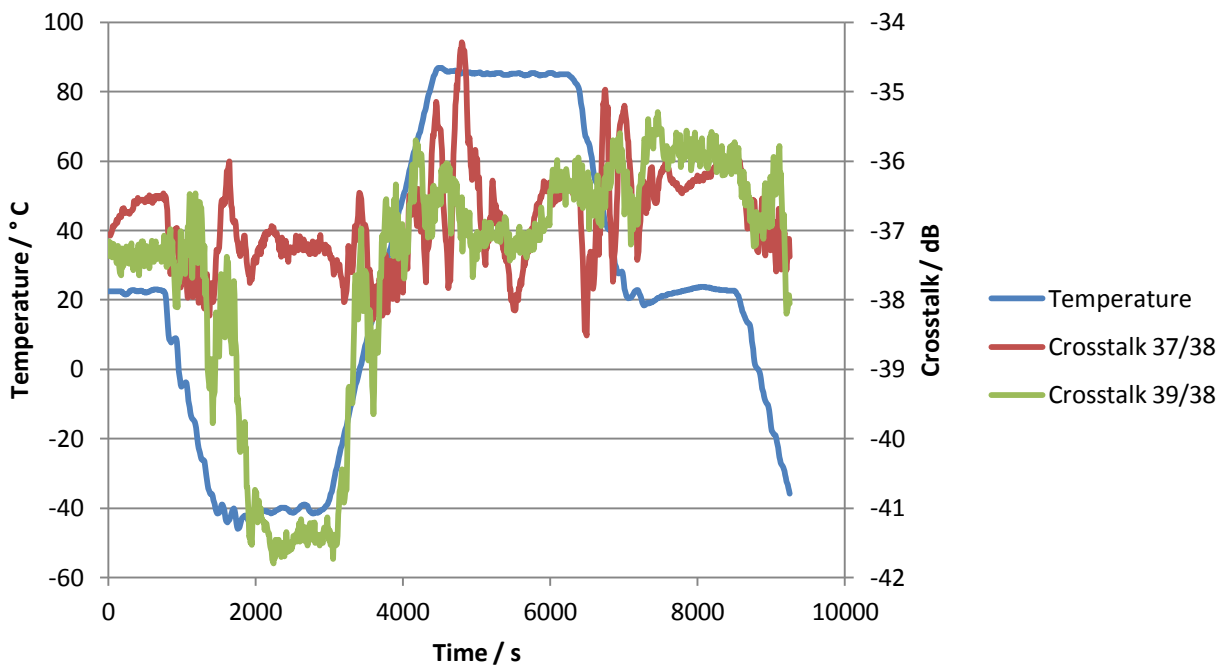


Figure 30: Adjacent channel crosstalk over the AWG operational temperature range

The adjacent channel crosstalk, using a DFB transmitter, is specified as -25 dB. The measured adjacent channel crosstalk in each of the channels is much less than this throughout the storage temperature range. The low levels of crosstalk when using laser transmitters is to be expected as this is what the AWG is designed for and should not impact network performance.

In summary, the AWG seems suitable to be used on aircraft as a multiplexer, although more testing must be done if it is to be deployed throughout the aircraft. If spectrum slicing it may be necessary to use an AWG with 200 GHz channel spacing to avoid high levels of adjacent channel crosstalk, this will operate 'athermally' between 0 °C and 60 °C. In the case of using a laser end node, an AWG can be used with 100 GHz spacing over the device's storage range of -40 °C to +85 °C.

### 3.4.2 Thin Film Filter

A multiplexer based on thin film filters (TFF) is, like the AWG, a passive fibre optic device. The working principle is similar to that of the red/blue coupler described earlier in this chapter. Again there are many differing techniques to build a multiplexer using TFF. One method [69] is to use layers of dielectric film to create Fabry-Perot type filters which will pass



one narrow wavelength band. In the cited literature these filters are fused to the sides of a crystal slab which reflects the signal from filter to filter, either adding or dropping a wavelength at each reflecting depending on whether it operates as a multiplexer or demultiplexer.

The TTF multiplexer tested here was loaned to BAE Systems by the University of Strathclyde, it was supplied by Kamelian and the precise internal structure of the device is unknown. The multiplexer is an 8 channel device with 200 GHz channel spacing.

#### **3.4.2.1 Centre Wavelength**

The centre wavelength was measured in the same way as with the AWG, the filter was interrogated using an unseeded SOA which was thermally regulated using a thermo-electric cooler. The spectral slice at each channel can be measured using an optical spectrum analyser. The spectral power distribution is assumed to be constant across the narrow passband, of approximately 1.2 nm, of each channel. With this assumption the optical spectrum analyser will analyse the spectral slice from any channel and provide the central wavelength automatically, this will ensure continuity in measuring the central wavelength as a function of temperature.

The centre wavelength of three channels has been measured as a function of temperature and is plotted in Figure 31.

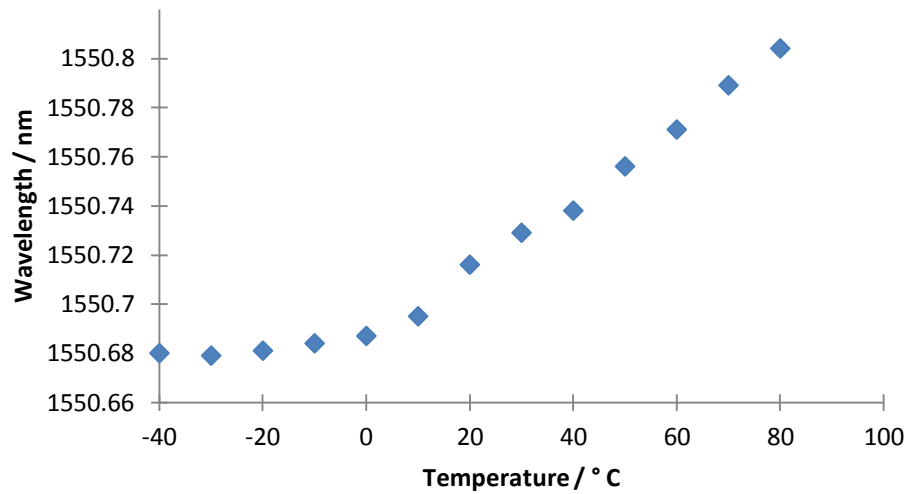
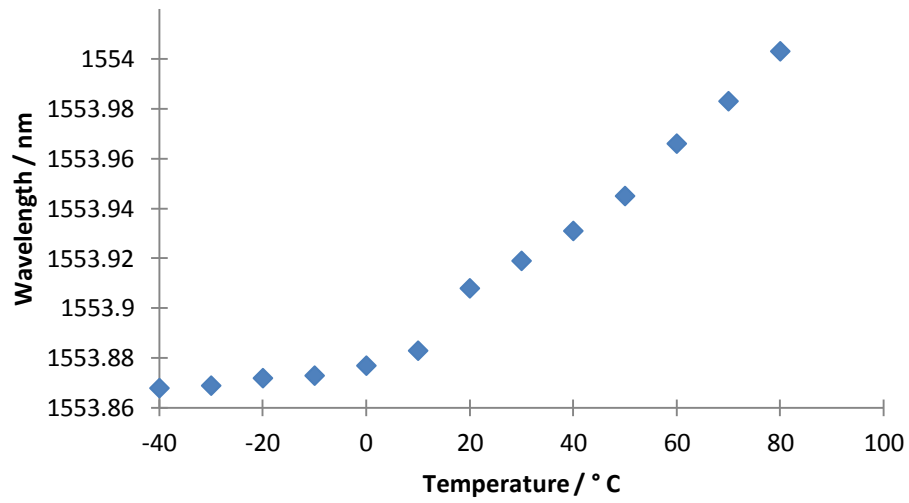
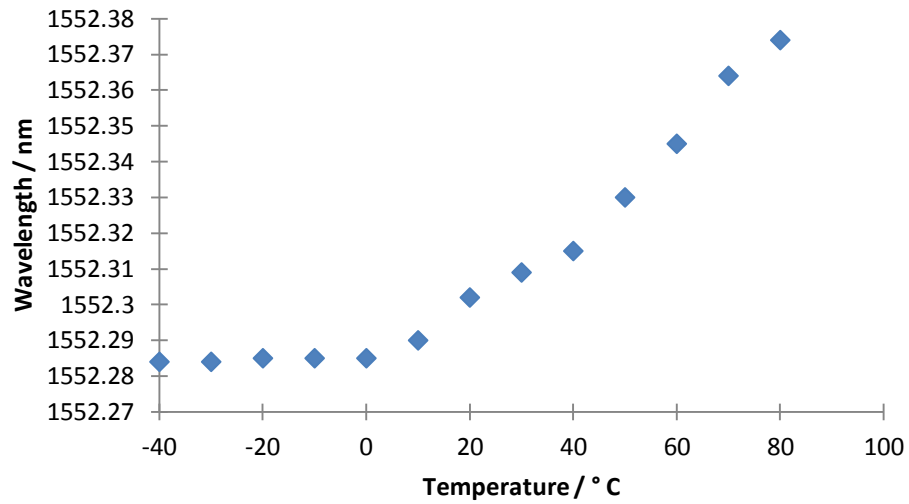


Figure 31: Centre wavelength of thin film multiplexer channels 31, 29 and 33 respectively, as a function of temperature.

No specifications were supplied with this multiplexer and it is not known if it is marketed as an athermal device. It has been assumed that the specified storage temperature meets telecommunications standards so is the same as the previous components. Between the temperature -40 °C and + 80 °C there is a change in wavelength of over 0.1 nm in each channel. This is small in comparison to the 1.6 nm channel spacing but the effects of the wavelength drift must be directly measured before any comparisons can be drawn with the AWG.

### 3.4.2.1.1 Spectral Slicing Case

Spectrum slicing using TFF is the same as with an AWG, an RSOA is seeded with broadband light sliced by the multiplexer. The multiplexer sets the operational wavelength at each channel and the spectral power distribution of each channel is the same as that of the passband. The spacing between the channels is larger than with the AWG but the channel width is also larger so the problem with crosstalk may remain.

The procedure to measure the insertion loss and adjacent channel crosstalk is the same as that used in the AWG experiments. The insertion loss and adjacent channels crosstalk are plotted, in Figure 32, as a function of the difference in the central wavelength in the passband of the multiplexer and demultiplexer channels under test.

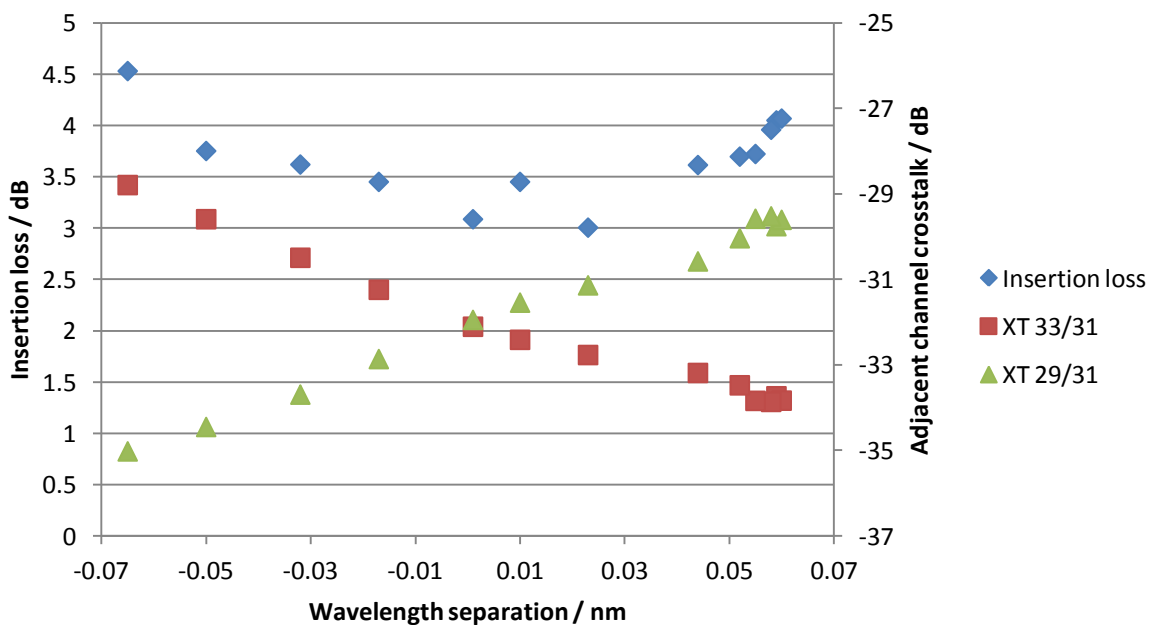


Figure 32: Insertion loss and adjacent channel crosstalk as a function of the difference between the centre wavelengths of mux and demux of TFF multiplexer

The two multiplexers used for these measurements did not sit exactly on the specified ITU wavelengths and each multiplexer did not match precisely. The channels are within range to thermally tune the wavelengths so the multiplexer and demultiplexer can be matched. Again the maximum acceptable insertion loss is 5 dB, across the testable wavelength separation the maximum insertion loss measured is 4.5 dB.

In the AWG case the insertion loss was not problematic but the crosstalk was high. This is not the case with the thin film filter where the crosstalk is less than -28 dB throughout the separation range. The channel spacing in the thin film multiplexer is 200 GHz as opposed to 100 GHz in the AWG although the channel width scales with the channel spacing so it is unlikely that this is the cause of the improved crosstalk. The shape of each passband in the thin film multiplexer is very different to the Gaussian AWG as shown in Figure 33. The thin film filter has more of a top hat shape than the Gaussian with the passband edges having the same gradient as the AWG albeit with a wider channel so they have a steeper relative gradient. In the graphs there is little overlap between the passband in the TFF multiplexer and more in the AWG passbands. This will lead to less crosstalk between adjacent channels in the TFF multiplexer. In Figure 33 the transmission in channel 31 is notably higher than the other two channels; this is due to dirty connectors on the other channels, all fibre connectors were cleaned prior to crosstalk measurements.

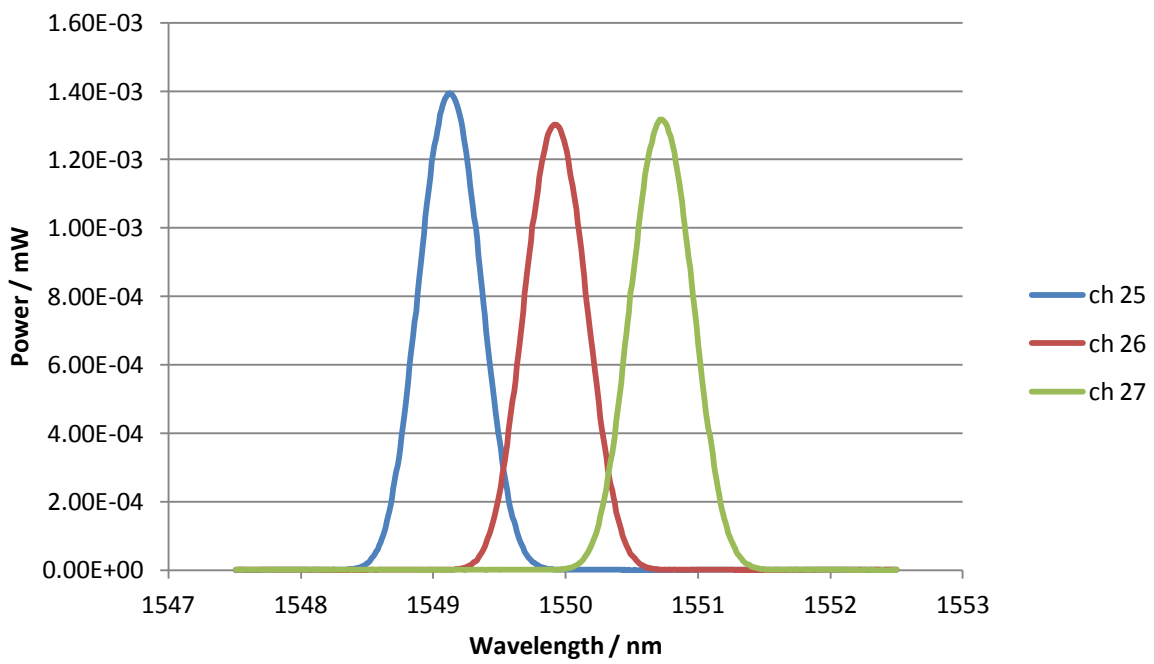
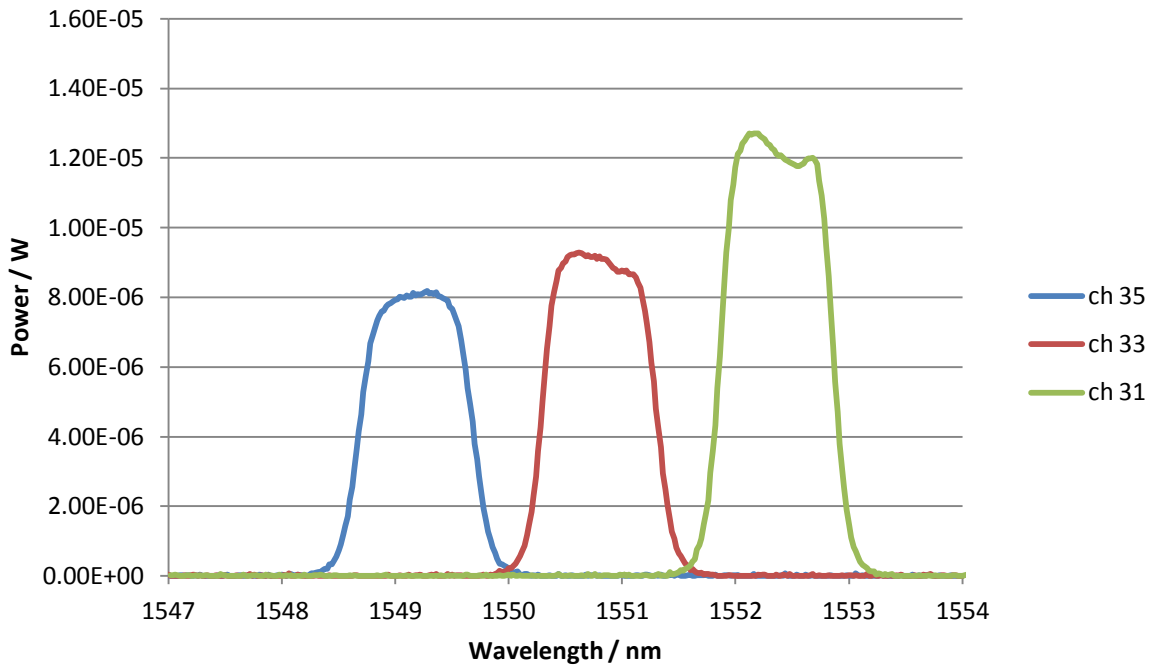


Figure 33: Passband shape of the thin film multiplexer and the AWG respectively

The insertion loss and isolation has also been plotted as a function of demultiplexer temperature with the multiplexer at a constant 23 °C in Figure 34.

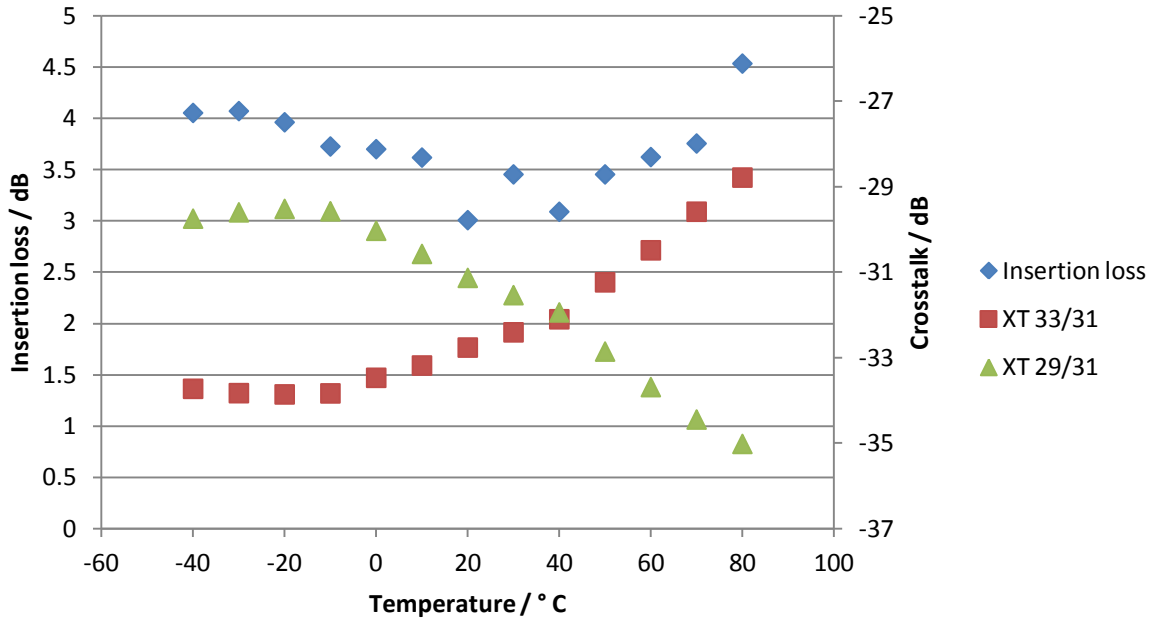


Figure 34: Insertion loss and crosstalk of TFF multiplexer as a function of demultiplexer temperature

From looking at the centre wavelength of channel 33 as a function of temperature, plotted in Figure 31, a period of approximately athermal operation between -40 and 0 °C is noticeable. Over this temperature range the crosstalk is relatively constant, although is not at its minimum value as the channels are not matched. Even without the channels matching the insertion loss and crosstalk are not at problematic levels throughout the storage range. With changes to the internal structure of the device it may be possible to move the athermal temperature range and enable the device to work uncooled over a larger range. This would require input from manufacturers and ruggedized packaging.

#### 3.4.2.1.2 Laser Case

The experiments carried out on the thin film multiplexer with a laser transmitter are the same as those in the AWG section. The wavelength of operation is no longer set by the multiplexer but by the laser, only insertion losses and crosstalk are of interest. The insertion loss and crosstalk are plotted as a function of demultiplexer temperature, with the multiplexer at a constant 23 °C, in Figure 35.

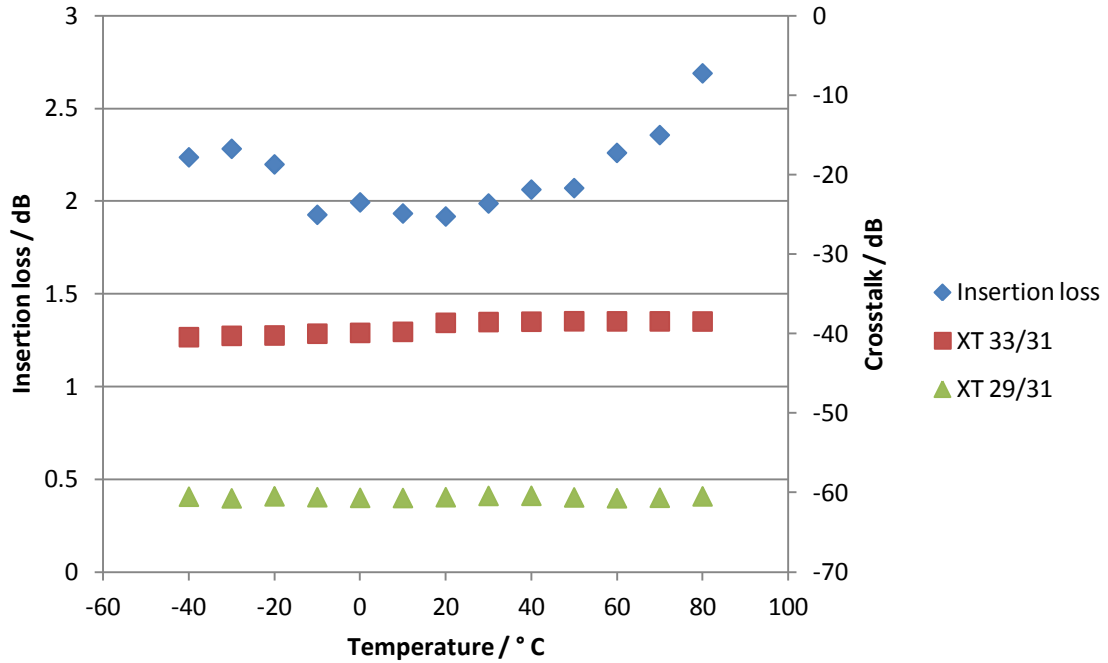


Figure 35: Crosstalk and insertion loss measured for channel 31 on TFF multiplexer with a laser transmitter

In this case the insertion loss is well within the acceptable limit of 5 dB with maximum losses less than 3 dB. The adjacent channel crosstalk is not equal in each adjacent channel, this could be because the laser wavelength is not precisely in the middle of the channel or could be an effect from the device design. Nevertheless the isolation is not within problematic levels with crosstalk from one channel -40 dB and the other -60 dB throughout the storage temperature range.

In comparison to the AWG the TFF multiplexer performs well both in the spectral slicing tests and the laser tests with a larger temperature range suitable for uncooled operation. These two devices have different channel spacing's with the AWG operating with 100 GHz spacing and the TFF 200 GHz spacing. This is significant when comparing the levels of adjacent channel crosstalk in these multiplexer technologies as it could be the case that using an AWG with 200 GHz spacing may reduce crosstalk if the crosstalk at 100 GHz proves to be problematic. The AWG is still the more desirable option because of its cyclic property which potentially makes it possible to operate different wavelength bands in either direction and offer increased network capacity.

### 3.5 Network Demonstrator

In order to demonstrate the technique of spectrum slicing with RSOAs a network demonstrator has been constructed. This was to be used to demonstrate the technique and show that a working network could be constructed which works in line with theory as well as for internal marketing within BAE Systems. The demonstrator was shown to other parts of the company who may have potential interests in this type of communications network. The demonstrator specification was for data rates of 1.25 Gbps to show suitability for gigabit Ethernet traffic in both upstream and downstream directions simultaneously. It should also exhibit 'colourless' operation of the RSOAs, where an RSOA can operate in any channel regardless of the central wavelength. The schematic of the proposed RSOA network is shown below in Figure 36 and the lab layout of the demonstrator is sketched in Figure 37.

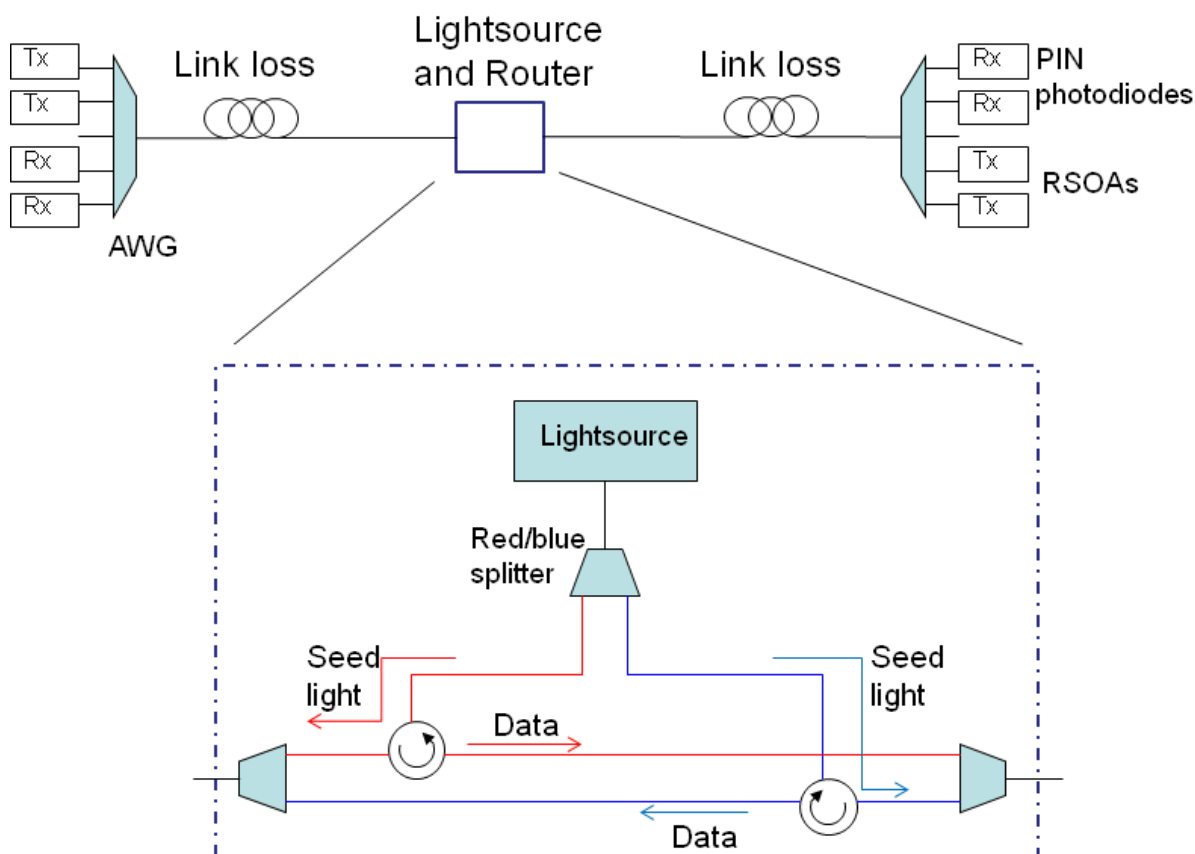


Figure 36: Schematic of the proposed RSOA network

In the proposed network a broadband lightsource was split into the red and blue halves of the AWG spectrum, in this case the C-band. Wavelengths in the range 1525 nm to 1542.54 nm to be used as seed light for upstream transmitters and 1547.3 nm to 1565 nm are



directed to be used at the downstream transmitters. The AWGs slice the broad band light before it is input to the RSOAs where it is amplified and modulated. In the upstream and downstream directions only half of the AWG spectrum is used, opposing halves for up and down stream transmission. Due to the cyclic nature of an AWG it is possible to use the full C-band in one direction and another band, possibly the L-band, in the opposite direction however this relies on the details of the cyclic property of the AWG which was not explored in the current project.

Building a network demonstrator, with a high number of operational channels in both directions, was not considered feasible within the financial constraints of the current project. Within the laboratory at BAE Systems there is only one communications signal analyser capable of gigabit operation and one gigabit Ethernet camera, although this will not give a BER just a picture of whether the signal is of sufficient quality. As a result only one channel upstream and one channel downstream will be used in the demonstration. Supplying data to the RSOA using the communications signal analyser, or bit error rate test equipment (BERT), is straightforward with SMA connections on the device itself. Using the camera is more complicated as this has a typical Ethernet connection. This can be converted to an optical signal using media converters which operate at 850 nm, by using an 850 nm SFP transceiver on an evaluation board a digital electrical signal can be used to encode the optical signal at the RSOA. This is detected at the receiver where it is then converted to an 850 nm to send to the other media converter in order to display the video on a laptop.

A schematic of how the network was set up is sketched in Figure 37 and a photograph of the completed demonstrator is shown in Figure 38. The conversion of the electrical signal from the camera to a signal input to the RSOA via an 850 nm fibre optic link is not important to the concept of the network as a whole. This set-up was what would work using the parts available and working within the financial constraints of the project. The section involving an 850 nm link could be represented as a 'black box' taking signal from the camera and converting it to a format usable by the RSOA driver circuitry.

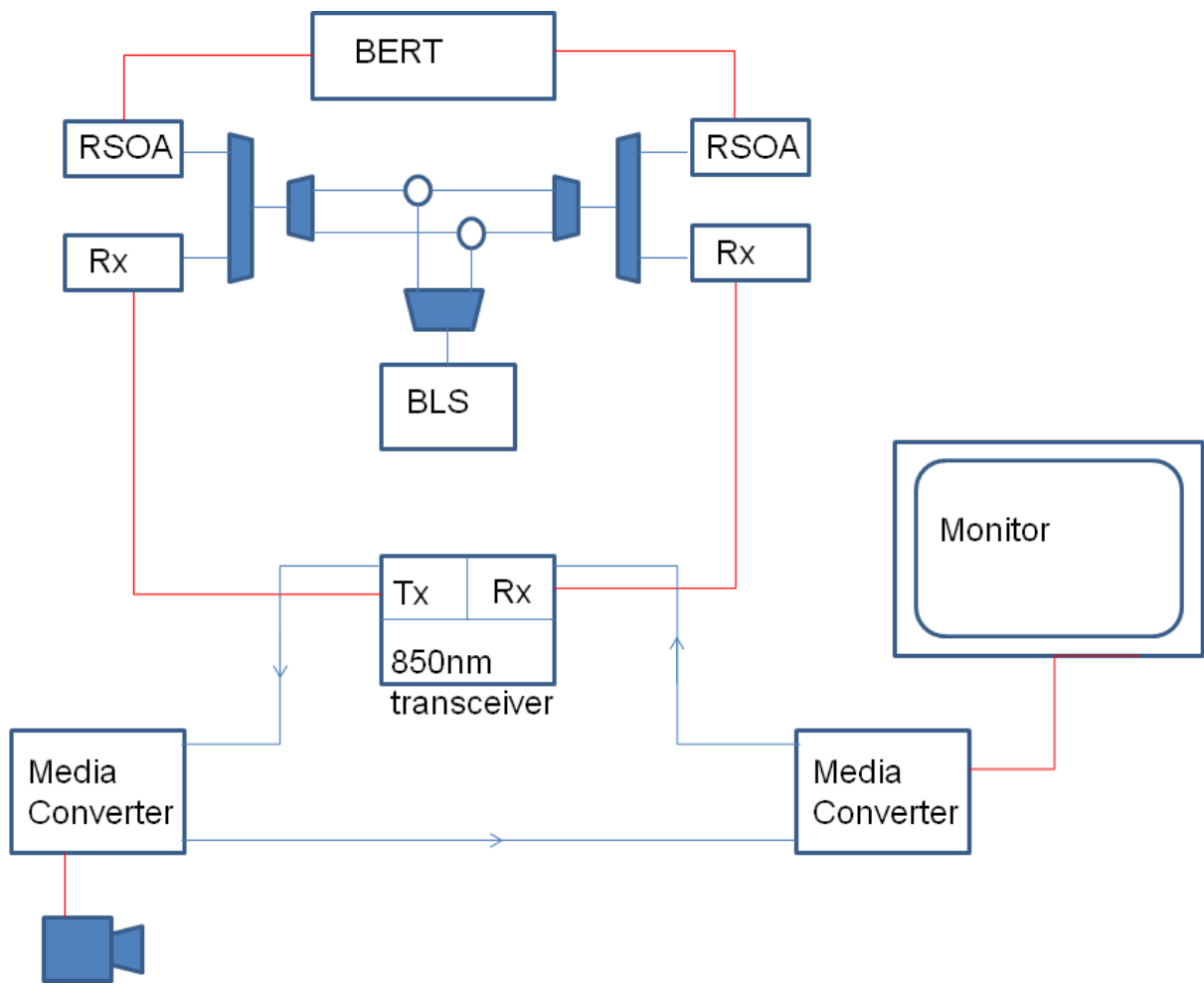


Figure 37: Lab layout of network demonstrator, red lines indicate electrical connections and blue lines indicate optical connections

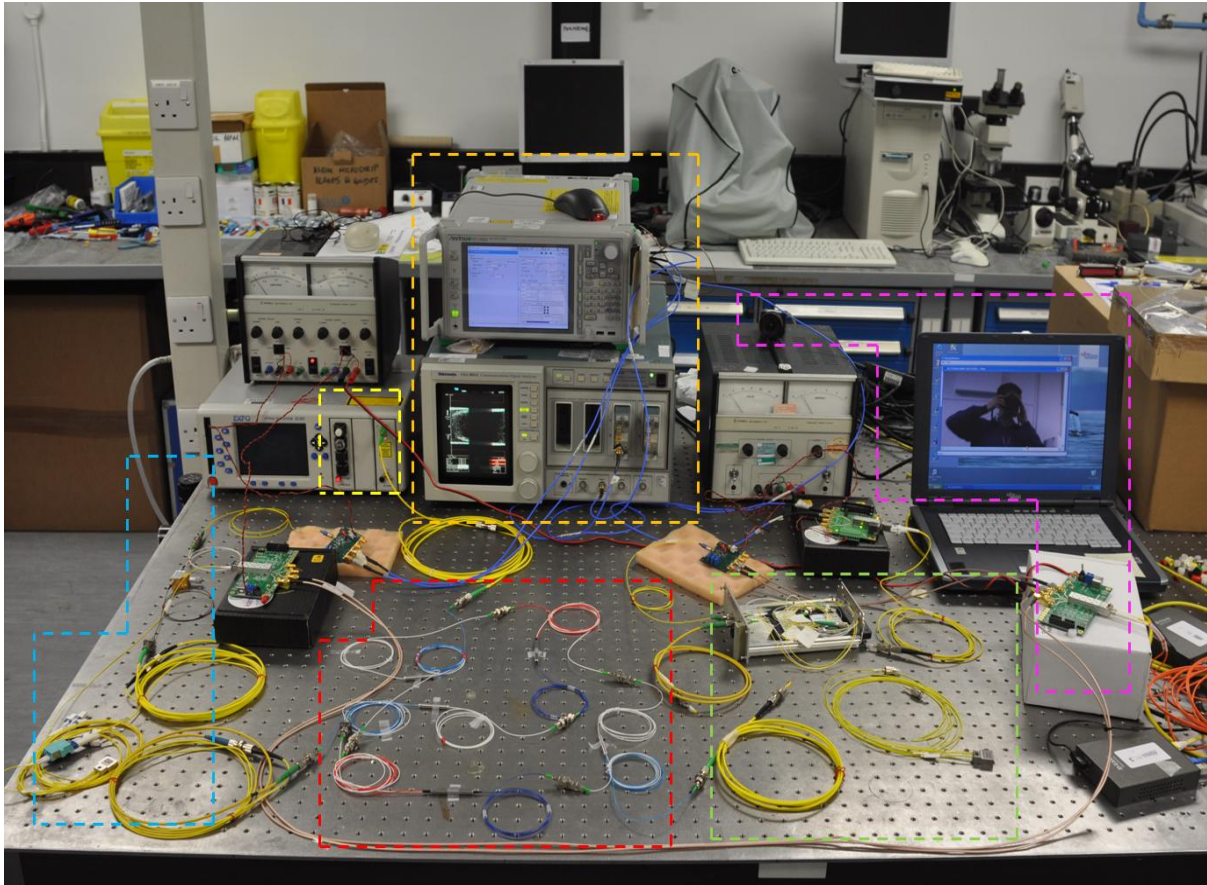


Figure 38: Photograph of working demonstrator in laboratory environment

Sections of the photograph have been highlighted so that they can be easily identified and compared with the schematic in Figure 37. Broadband light is generated using an erbium doped fibre; this is highlighted in the yellow box. This light is split into the red and blue sections of its spectrum and routed to either end of the link using splitters and circulators, these routing components are highlighted in the red box. In principle, all routing components could be packaged with the broadband source if appropriate to minimise any cooling required. One half of the spectrum is routed towards the multiplexer in the blue box. The transition in pass and reflect in the C-band splitters did not occur in the middle of the spectrum of the thin film multiplexer so all available channels were in the pass band and none in the reflect band. A thin film multiplexer for CWDM was used in conjunction with a tuneable filter with a spectral width of 200 GHz to simulate the narrow channels in the proposed DWDM network.

This is then routed to the RSOA and the signal from the opposite end of the link is routed to a photodiode in a SFP transceiver. The signal for the RSOA is provided by an Anritsu MP 1800A signal quality analyser (BERT in Figure 37). A pseudo random binary sequence of  $2^7 - 1$  is generated at the BERT, The length of this sequence accurately

simulates the conditions when using 8b/10b encoding with gigabit Ethernet. The received signal is sent to the BERT to measure a bit error rate and to a Tektronix CSA 803A communications signal analyser where an eye diagram is displayed. Both these are shown in the large orange box in the centre of the photo.

At the other end of the link the DWDM multiplexer is simulated using a CWDM multiplexer to carry out the actual multiplexing and a thin film multiplexer with 200 GHz channel spacing to simulate the narrow channel width. These are highlighted in the green box on the right of the photo. From this multiplexer the signal is routed to a receiver in a SFP transceiver and seed light is input to the RSOA.

The data for this channel is provided by a ProSilica Gigabit Ethernet camera which generates gigabit Ethernet data, although with an electronic output incompatible with the RSOA driver circuitry. This can be converted to an optical output using TP-LINK MC 200 CM media converters, which operate at 850 nm. Using a standard 850 nm transceiver and evaluation board the optical signal can be converted into a signal which can be used for modulation at the RSOA. The same process happens in reverse when the signal is received at the other end of the link. The camera, laptop monitor displaying the video, and the 850 nm transceiver are highlighted in the pink box on the far right of the photo.

The network operated as expected with error free transmission over a period of 12 hours when operating at 1.25 Gbps video transmission was observed during the transmission of the pseudo random binary sequence (PRBS) indicating no problems with bi-directional traffic. As this was purely a functional demonstration no analysis of the loss budget of the network was carried out, this will take place in later chapters.

### 3.6 Conclusions

A summary of the results from this chapter is shown in Table 3.

Component	Test parameter	Result
Circulator	Insertion loss	-0.4 to -1.2 dB
	Isolation	<-50 dB
Red/blue Coupler	Insertion loss	-0.6 to -1.2 dB
	Isolation	-14.4 to -14.8 dB pass band -22.9 to -23.9 dB reflect band
AWG, spectrum slicing. (Reduced temperature range of 0 °C to 60 °C)	Insertion loss	< -5 dB
	Crosstalk	< -18 dB
AWG, laser transmitter	Insertion loss	< -4.5 dB
	Crosstalk	< -28 dB
Thin Film Filter, spectrum slicing	Insertion loss	< -5 dB

	Crosstalk	< -28 dB
Thin Film Filter, laser transmitter	Insertion loss	< -3 dB
	Crosstalk	< -40 dB

Table 3: Results table from thermal testing

Thermal testing of a number of passive fibre optic devices has been carried out in order to assess their compatibility with avionic requirements. Although these components cannot be tested over the full avionic temperature range of -55 to +125 °C due to packaging issues they can be tested over a lesser range of -40 to +85 °C to establish any limitations. The overarching finding of this chapter is that the components tested behave as expected over an extended temperature range out their specified operating ranges.

The first device to be tested was a fibre optic circulator. The insertion losses for a signal being routed from port 1 to port 2 and from port 2 to port 3 were measured using a tuneable laser. Over the devices storage temperature range the losses were measured as 0.8 to 1.2 dB and 0.4 to 0.5 dB respectively. The isolation in both ports was less than -50 dB over all temperatures. Over this limited temperature range the circulator showed a slight increase in insertion loss at higher temperatures although not to a problematic level. The circulator could be used uncooled over the tested range, in order to assess suitability over the full range a ruggedized device would have to be purchased and tested.

The next device to be tested was a C-band red/blue coupler; this will divide light, in the C-band section of the spectrum, into the short and long wavelength halves of the band. This device works by reflecting one half of the spectrum and allowing the other half to pass, in this case the longer, red wavelengths, are reflected and the shorter, blue wavelengths, are passed. The average insertion losses were measured in both pass and reflect bands using light from a broadband source. This interrogates the device with light spanning the C-band so the loss each channel would see on passing through the device is averaged. The average loss in the blue arm is between 0.8 dB and 1.2 dB over the temperature range -40 °C to +85 °C. Over the same temperature range the loss in the red arm varies from 0.6 dB to 0.7 dB. The losses in both pass and reflect bands increase with increasing temperature although they do not increase to problematic levels. The insertion was then measured at various single wavelengths using a tuneable laser to measure the loss for an individual channel. This measurement was taken at 4 wavelengths, the shortest and longest wavelength specified for operation in each of the red and blue arms. The losses measured with the laser were close to the average values measured using the broadband source, this indicates that the loss is likely to be relatively stable across each band without any large changes in insertion loss localised by wavelength.

The wavelength range where the device transitions from pass to reflect and how temperature affects this wavelength range is very important in designing the network. If the channels on the edges of the pass band at low temperatures shift to be in the reflect band at high temperatures for example, there would be failures within the network. Where these band edges are defined will have a clear effect on the isolation between channels. In order to prevent any adverse effects with the band edges drifting a five channel guard band is proposed, these five channels will not be used to carry data. Defining the guard band as between the wavelengths 1541.349 nm and 1546.917 nm gives a guard band spanning 8 channels. The isolation has been measured at the shortest and longest wavelengths in each arm of the coupler over a range of temperatures. In the pass band the isolation is specified as  $< -12$  dB, over the  $-40$  °C to  $+80$  °C temperature range it is measured as a varying from  $-14.4$  dB to  $-14.8$  dB. In the reflect band it is measured as between  $-23.9$  dB and  $-22.9$  dB, although this is specified by the manufacturer as  $< -24$  dB it is not at a problematic level. The isolation values indicate that the guard band is sufficiently large to protect against poor isolation between the arms over the tested temperature range. In order to be sure that this will work over the full avionic range further testing must be undertaken but this would require a ruggedized device to survive the temperature extremes.

Two different types of multiplexer have also been tested, an AWG and a TFF based multiplexer. The AWG is marketed as an athermal device, it is a 40 channel multiplexer with channel spacing of 100 GHz. The centre wavelength of selected channels was measured as a function of temperature, again over the storage range of  $-40$  °C to  $+85$  °C. The device is specified for athermal operation between  $0$  °C and  $+60$  °C, over this range the centre wavelength is stable within 0.02 nm. For the proposed network wavelength stability is the most important aspect. If the central wavelength of one or many channels in one multiplexer changes then there will be losses in the same channel at the demultiplexer and may be high levels of crosstalk, both are detrimental to the network. Instead of looking at the effects of temperature on the insertion loss and crosstalk in the AWG these were measured as a function of the difference in central wavelength of the multiplexer and demultiplexer, this can then be used to evaluate the temperature over which the AWG can be treated as athermal. The insertion loss is less than 5 dB for a wavelength difference,  $\Delta\lambda$ , of  $\pm 0.2$  nm. More problematic is the adjacent channel crosstalk. When  $\Delta\lambda$  is zero, the channels are matched, the adjacent channel crosstalk is approximately equal from each channel. As the wavelength of one channel drifts the crosstalk will be increased from one channel and decrease from another. The increase in adjacent channel crosstalk is greater than the decrease in the other channel so both channels matching is the ideal scenario. The high levels of crosstalk mean that it is recommended that the AWG is operated, when spectrum slicing, in the region

where it exhibits athermal characteristics, 0 to +60 °C. If spectrum slicing is not used, and laser transmitters are used instead then the crosstalk is much improved. In this case the insertion loss over the full storage range of an AWG, with another AWG at a constant temperature, is less than 4.5 dB. This is equivalent to a  $\Delta\lambda$  of  $\pm 0.2$  nm in each channel of the AWG. In this scenario there is also much less crosstalk since the optical carrier is only at the centre wavelength and not filling the passband as in the spectrum slicing case. The adjacent channel crosstalk is less than -34 dB throughout the same range for each channel.

The other multiplexer tested was TFF based, it has 8 channels on ITU specified wavelengths with 200 GHz spacing between each channel. Like with the AWG the centre wavelengths of selected channels were measured as a function of temperature over the specified storage range of the device, -40 °C to +85 °C. In two of the tested channels the centre wavelength drifts over a 0.12 nm range, in one tested channel the drift is measured as 0.09 nm. Although this is a larger drift than that of the athermal region of the AWG the channel spacing is larger so performance may not be affected as greatly in comparison to the AWG case. The insertion loss and adjacent channel crosstalk were measured as a function of demultiplexer temperature with a multiplexer at constant lab temperature. Measurements were taken using both spectrum slicing and a laser. When using spectrum slicing, the insertion loss, over the full storage temperature range, is less than 5 dB in the measured channel. The crosstalk is also low, less than -28 dB throughout the temperature range. The extra channel spacing offers an increase in performance to the level where the multiplexer can be used uncooled throughout the storage range. Similarly with a laser transmitter where the insertion loss is less than 3 dB and the adjacent channel crosstalk is approximately -40 dB from one channel and -60 dB from the other neighbouring channel.

The TFF based multiplexer can operate over a larger temperature range, when uncooled, than the AWG. This is due to greater channel spacing rather than differences in the technologies. A 100 GHz AWG could be used with blank channels left between each data carrying channel to achieve the same result as with the TFF while offering scalability due to the cyclic nature of the device.

# **4. Reflective Semiconductor Optical Amplifiers in a Spectrum Sliced Wavelength Division Multiplexed Passive Optical Network**

## **4.1 Introduction**

In order to meet the growing bandwidth demands on aircraft of a number of sensors and electronic components, a fibre optic network must be used. A WDM-PON will meet the needs of this next generation aircraft delivering capacity, scalability and network security. In order to operate throughout the temperature range on aircraft thermally regulating components is to be avoided. Typically WDM-PON uses DFB transmitters which must be held at precise temperatures. One method to avoid using DFB transmitters is to use a SS-WDM-PON [37], with RSOAs at the end nodes acting as modulators and amplifiers. This involves using 'slices' of spectrum from a broadband and using these to seed an amplifier, as the multiplexer used to separate the spectrum into these slices can be considered athermal, the wavelength of operation in each channel is not temperature sensitive.

Although the operational wavelength in each channel is independent of the temperature at the end node, other aspects of network performance are not. The RSOAs are temperature sensitive devices, most notably the gain of the amplifier and its maximum output power being functions of the RSOA temperature. In this chapter a potential SS-WDM-PON is proposed using RSOA end nodes, the effects of end node temperature on the performance of this network are calculated and limits of operation suggested.

In order to predict network performance a mathematical model of the proposed network is presented and is experimentally validated. By using parameters taken from experiment for RSOA gain and saturation output power, the model can be used to predict network performance at a number of different temperatures and at different wavelengths corresponding to channels in the network. From this a temperature range where the end nodes can operate uncooled, while maintaining acceptable network performance, can be predicted.



## 4.2 Network Architecture

### 4.2.1 DWDM PON

DWDM is a universally adopted strategy for maximizing the usage of fibre bandwidth by carrying hundreds of channels down a single fibre backbone [70], [71]. DWDM systems require transmitters to be locked to a range of established and known wavelengths [70], [71]. Hence, each transmitter has to be manufactured to a high specification and close temperature control is required to eliminate the potential for temperature induced wavelength drift. The combination of these requirements results in transmitters that are expensive, require significant cooling powers and gives systems operators the additional burden of maintaining an inventory of equipment to guard against the possibility of failure of an individual wavelength.

In order to make implementation of DWDM on aircraft feasible the cooling requirements need to be lessened so that the power consumption of the network is not prohibitively large. One potential method of lessening the cooling requirements is to use a RSOA as colourless transmitter at each end node [72]. This is achieved by using spectrum slicing where the RSOA is seeded with a signal wavelength from a broadband source that has been spectrum sliced, usually by an AWG [73]. A schematic of how this technique may be implemented is shown in Figure 39.

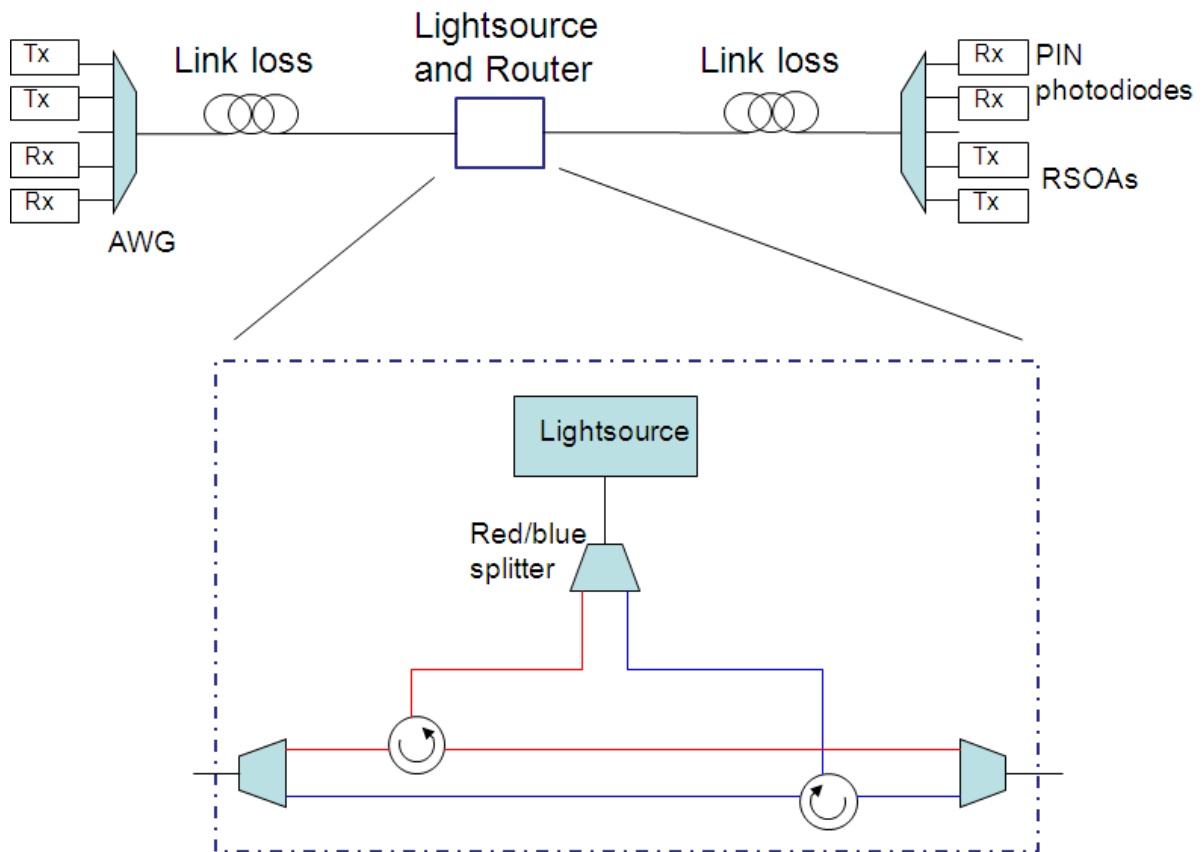


Figure 39: An example of SS WDM-PON using RSOA transmitters

Light from a broadband light source (BLS) is routed onto an athermal AWG where it is spectrum sliced, this involves splitting the light into multiple channels of a narrow band of wavelengths. These channels are then routed onto the RSOA where the input light is amplified and modulated to encode the data. This amplified signal will have the same wavelength of the input light, the wavelength of each channel is defined by the AWG not the transmitters so the transmitters are said to be colourless. As the transmitters are colourless the systems operator no longer needs to hold such a large inventory as each device can be used in any channel. Since the wavelength is defined by the AWG which is athermal its performance is consistent over a large temperature range and the transmitters do not need to be cooled in order to maintain a constant wavelength, although the gain and output power of the RSOA will still be affected by temperature. The signal is reflected by the RSOA and is then multiplexed by the AWG onto a single fibre backbone where it can be routed through the airframe. The signals are then demultiplexed by a matching AWG at the other end of the network where they are received and decoded. In Figure 39 different wavelengths are used for upstream and downstream communications, due to the cyclic nature of an AWG it can simultaneously act as both a multiplexer and demultiplexer to these wavelengths.

Spectrum sliced WDM-PON architectures using RSOAs as colorless transmitters at each end node can potentially meet the demands of an aircraft network [74], [75] in a more cost effective manner. We analyze the performance of such a network using two different RSOAs - firstly using a standard commercially available RSOA [76] and secondly an aluminium containing quaternary based RSOA designed to operate at elevated temperatures. The findings from this analysis are then used to quantify the overall performance of the two cases within an avionics context.

## 4.3 Modelling

### 4.3.1 Bit Error Rate

In a communications network the Bit Error Rate is used as a measure of the systems performance by quantifying the signal quality. The BER is the probability of any one bit of data being detected incorrectly at the receiver and can be estimated as [77]

$$BER = 0.5 \operatorname{erfc} \left( \frac{Q}{\sqrt{2}} \right) \quad (1)$$

here  $\operatorname{erfc}$  is the complementary error function and  $Q$ , the Q factor, can be expressed

$$Q^2 = SNR \quad (2)$$

where  $SNR$  is the signal to noise ratio at the receiver. SNR can be estimated as

$$SNR = \frac{\text{signal power}}{\text{noise power}} = \frac{I_p^2}{\sigma_{TOT}^2} \quad (3)$$

where  $I_p$  is the photocurrent generated at the photodiode and  $\sigma_{TOT}^2$  is the total noise on transmission of both the bit '1' and the bit '0'.

In addition to the SNR the BER is also affected by the extinction ratio,  $r_e$ , which is the ratio between powers in logic levels '1' and '0'. Defining  $r_e$  as

$$r_e = P_1/P_0 \quad (4)$$

where  $P_1$  is the power in logic level '1' and  $P_0$  is the power in logic level '0'. And defining the average power  $P_{AVE}$  as

$$P_{AVE} = (P_1 + P_0)/2 \quad (5)$$

then it is possible to further define

$$P_0 = 2P_{AVE} \left( \frac{1}{1+r_e} \right). \quad (6)$$

As a result the Q factor at the receiver becomes

$$Q = \frac{P_{AVE}}{\sigma_1^2 + \sigma_0^2} \left( \frac{1-r_e}{1+r_e} \right)^2 \quad (7)$$

and a power penalty associated with an imperfect extinction ratio can be quantified.

### 4.3.2 Noise Terms

Noise is the variance of the current fluctuations in the photocurrent from the photodiode. It is equal to the mean square current fluctuation. There are five noise terms that are needed to accurately model an amplified link.

Signal shot noise,  $\sigma_S^2$ , is derived from the fact that the current consists of a stream of electrons which are generated at random times. The shot noise is written as

$$\sigma_S^2 = 2eI_p B_e = 2eRP_{rec} B_e = 2eR\alpha G P_{SIG} B_e \quad (8)$$

where  $e$  is the electron charge,  $R$  the diode responsivity,  $P_{SIG}$  the optical signal power and  $B_e$  the receiver bandwidth. The term  $G$  relates to the amplifier gain and  $\alpha$  is the post amplification loss (the loss between the amplifier and the receiver). The amplifier gain is dependent on the input power as the gain can be limited by the amplifiers maximum output power. This effective gain can be expressed as

$$G = \frac{G_{MAX}}{1 + \frac{G_{MAX} P_{SAT}}{G_{MAX}}} \quad (9)$$

where  $G_{MAX}$  is the maximum amplifier gain, also known as small signal gain and  $P_{SAT}$  is the saturation output power of the amplifier.

Thermal noise,  $\sigma_T^2$ , also known as Johnson noise or Nyquist noise, is derived from the circuitry in the receiver. At a temperature above absolute zero electrons move randomly around a conductor, this motion of electrons in a resistor manifests itself as a fluctuating current. The thermal noise can be written

$$\sigma_T^2 = \frac{4k_B T}{R_L} \Delta f \quad (10)$$

where  $k_B$  is the Boltzmann constant,  $T$  is the temperature at the resistor,  $R_L$  is the load resistance and  $\Delta f$  is the effective noise bandwidth.

The other three noise terms are all dependent on the ASE from the amplifier. This is caused by carriers in the amplifier recombining spontaneously and then being amplified by the process of stimulated emission. The level of ASE in the system can affect the signal to noise ratio and in some cases can be the limiting factor in system performance. The ASE power emitted from an amplifier over an optical frequency bandwidth  $dv$  can be written

$$P_{ASE}^{dv} = \mu[G - 1] \cdot hv \cdot dv = \rho_{ASE} dv \quad (11)$$

where  $\mu$  is the population inversion factor, this is equal to half the amplifier noise factor,  $NF/2$ ,  $h$  is the Planck constant,  $v$  is the optical frequency and  $\rho_{ASE}$  is the ASE spectral power density. From the ASE power it is possible to calculate further noise terms.

The ASE shot noise,  $\sigma_{ASE}^2$ , stems from statistical fluctuations in the ASE causing fluctuations in the photocurrent and can be written

$$\sigma_{ASE}^2 = 2eI_{ASE}B_e = 2eR\alpha P_{ASE}B_e \quad (12)$$

where  $P_{ASE}$  is the ASE power at the receiver.

The ASE propagates in the fibre with the signal and these cannot be separated, as the signal and the ASE propagate they beat. The ASE is randomly generated and its phase components vary randomly in time, this means that the optical power produced by the beat between the signal and the ASE is randomly varying and produces a randomly varying current in the photodiode. This is the basis for the signal-ASE beat noise,  $\sigma_{S-ASE}^2$ , which can be written

$$\sigma_{S-ASE}^2 = 4R^2 G \alpha^2 P_0 \rho_{ASE} B_e = 4R^2 G \alpha^2 P_{SIG} P_{ASE}^{B_e} \quad (13)$$

where  $\rho_{ASE}B_e = P_{ASE}^{B_e}$  is the ASE power falling within the electrical bandwidth.

Similarly to the signal-ASE beat noise there is also a noise term derived from the ASE beating with itself which also gives rise to a randomly fluctuating component in the photocurrent. This is the ASE-ASE beat noise,  $\sigma_{ASE-ASE}^2$ , and can be written

$$\sigma_{ASE-ASE}^2 = 2R^2\alpha^2\rho_{ASE}B_oB_e = 2R^2\alpha^2P_{ASE}^{B_o}P_{ASE}^{B_e} \quad (14)$$

where  $P_{ASE}^{B_o}$  is the ASE power is contained within the optical bandwidth.

In order to calculate the SNR to total noise,  $\sigma_{TOT}^2$ , is needed. This is the noise on transmission of both the bit '1' and the bit '0' where the noise on bit '1',  $\sigma_1^2$ , can be written

$$\sigma_1^2 = \sigma_T^2 + \sigma_S^2 + \sigma_{ASE}^2 + \sigma_{S-ASE}^2 + \sigma_{ASE-ASE}^2 \quad (15)$$

and the noise on bit '0',  $\sigma_0^2$ , can be written

$$\sigma_0^2 = \sigma_T^2. \quad (16)$$

Meaning the total noise can be expressed as

$$\sigma_{TOT}^2 = 2\sigma_T^2 + \sigma_S^2 + \sigma_{ASE}^2 + \sigma_{S-ASE}^2 + \sigma_{ASE-ASE}^2. \quad (17)$$

### 4.3.3 Point to Point Link Model

The network proposed in Section 4.2 can be modelled by reducing the network to a series of point to point links as shown in Figure 40, starting with the broadband source and ending with the signal being received by a photodiode. In order to accurately model the network the following parameters from the components in Figure 40 are needed.

- Broadband lightsource: defines the spectral power density so the optical power into the amplifier can be calculated
- Loss 1: this is mostly routing losses and defines the decrease in power from the BLS
- AWG 1: the channel width of the AWG determines how much of the BLS spectrum, and therefore the optical power level, input to the amplifier. The channel width also has an effect on the noise calculations
- RSOA: the relevant amplifier parameters are gain (G), saturation output power ( $P_{SAT}$ ), and the noise figure (NF). Since in this case the amplifier is also acting as the

modulator it provides the extinction ratio and the modulation rate. In this case the modulation rate defines the data rate.

- Loss 2: more routing losses, defines losses to signal strength
- AWG 2: matches AWG 1 so the channel width is the same and is centred on the same wavelengths, this AWG adds an insertion loss
- PIN photodiode: need the thermal noise, this is not usually given on data sheets so must be calculated from experimental measurements.

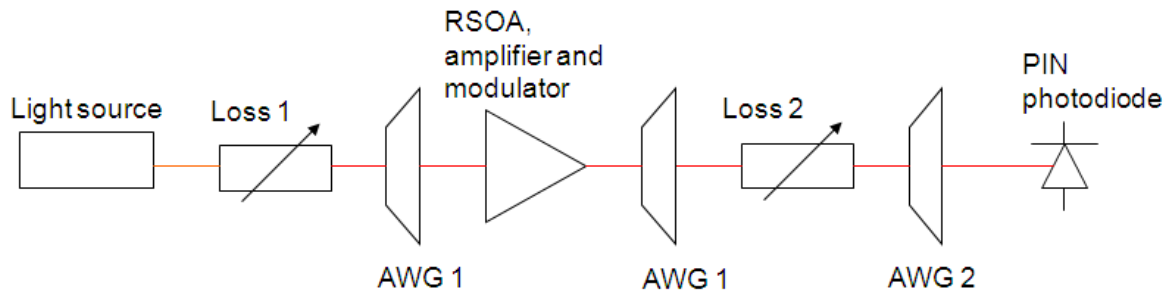


Figure 40: An example of how the network is reduced to a point to point link

The essential operating features of an RSOA are described in the parametric summary graph shown below in Figure 41. In the context of a RSOA acting as a modulator in SS WDM-PON, the two key parameters of interest are the small signal gain, and the saturation power. The noise figure, a measure of the excess noise added to the signal, is also useful for the model. The polarization dependent gain describes the difference in the gain between input light of TE and TM polarizations and gain ripple describes the variation in the gain over small wavelength ranges in the input light. Both PDG and gain ripple will be suppressed as the RSOA is driven into saturation.

Figure 41 shows that the RSOA exhibits a gain of over 20 dB from around 1530 nm through to 1590 nm. Similarly, the  $P_{SAT}$  value, representing the maximum output power that the device can deliver, is in excess of 3 dBm over this range. This means that an RSOA, seeded with a signal power level of -15 dBm will deliver 0 dBm (assuming a 5 dB insertion loss for the AWG) back in to the network. The -15 dBm seed power per wavelength band (corresponding to one slice from the AWG) is readily achievable using a broad band source [78] spectrally sliced to 200 GHz which corresponds to a wavelength spacing of 1.6 nm.

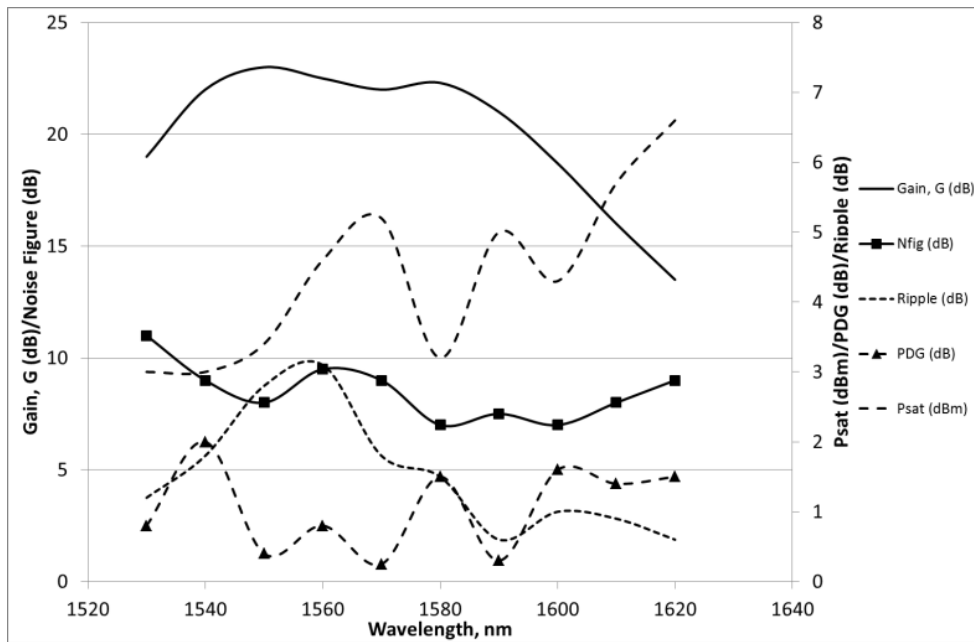


Figure 41: Parametric Performance of Commercial RSOA

The amplified and modulated signal is then transmitted back through the AWG and is routed to the matching AWG via more red/blue splitters and circulators. Here the signals are demultiplexed according to wavelength. Fibre losses and remaining architectural loss (2.5 dB for the lightsource/router and 3 dB for the demux) must be overcome for the system to operate.

Logically, the link can be simplified for analysis purposes by using lumped losses to describe the influence of the multiplexers and circulators. In an avionics environment it is possible that a fibre link can see high bend losses and losses associated with the operational temperatures. With bend insensitive fibres and fibre meeting the temperature specifications these losses are small and can be represented by lumped losses. Optical return loss or the presence of unwanted reflections have not been accounted for. The optical circulator will provide some degree of isolation against the influence of reflections but no attempt has been made to quantify this issue.

The components from Figure 40 show the path taken by the light from broadband source to receiver. The light passes through couplers and circulators (networking components) which are represented by loss 1. It is sliced by AWG 1, amplified, encoded and reflected by the RSOA, the signals are then multiplexed, again by AWG 1. The multiplexed signals pass through more networking components, represented by loss 2, before being demultiplexed at AWG 2 and received at the photodiode. AWG 2 matches AWG 1, the



wavelength and linewidth at each channel at AWG 2 will therefore match that defined at AWG 1. The loss at AWG 2 in addition to Loss 2, architectural loss plus fibre losses will define the total losses between the RSOA and receiver. Knowledge of these losses enables estimating the signal power at the receiver and also noise terms that are calculated using the ASE. The receiver used in the model and subsequent work in this chapter is based on a PIN photodiode.

#### 4.3.4 Results of Model

The following model uses the subsequent parameters which are typical of commercially available components:

- Maximum gain of 23 dB
- Saturation power of 7 dBm
- Responsivity of 0.8 A/W
- Noise Figure of 8.13 dB
- Sensitivity of -23 dBm
- Extinction Ratio of 7.5 dB
- Channel (filter) width of 1.4 nm
- Data Rate of 1.25 Gbps
- Signal wavelength of 1550 nm.

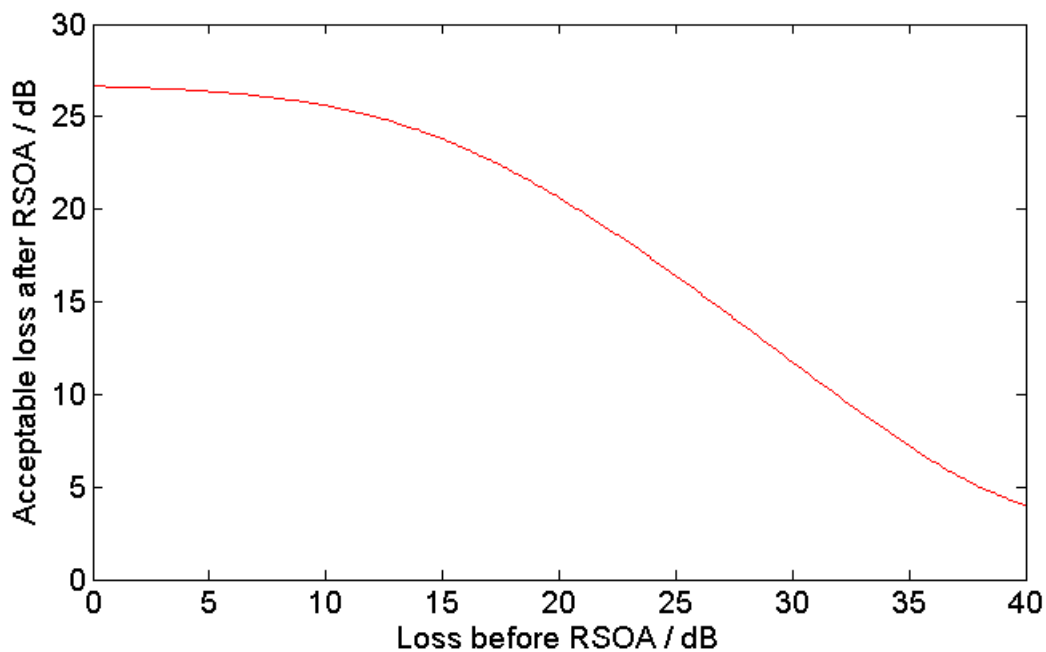


Figure 42: Example of results produced by model

A typical plot from the model is shown in Figure 42. This model calculates the maximum allowable output loss (loss after the amplifier) for a given seed power into the amplifier while maintaining a BER of  $10^{-9}$ . The seed power into the amplifier is dependent on the loss between the BLS and the RSOA so the output loss can be plotted as a function of the input loss. With zero losses before the RSOA, no loss between the broadband lightsource and the amplifier, there is 0 dBm input power. The amplifier has a maximum gain of 23 dB and  $P_{SAT}$  of 7 dBm so this level of input power will lead to high levels of gain compression and saturate the amplifier. At this point the amplifier is operating at its maximum optical output power so at this point the system offers the largest possible loss after the amplifier, 27 dB, before the signal level is insufficient to realise a BER of  $10^{-9}$ . As the loss before the RSOA is decreased so the optical power into the amplifier decreases. For the first 10 dB of loss before the amplifier this has very little effect on the acceptable output loss because the seed power is sufficient to saturate the amplifier.

After 15 dB loss before the amplifier, corresponding to a seed power of -15 dBm, the amplifier is no longer being saturated and is providing high levels of gain. As the input power falls to -20 dBm the gain of the amplifier is approaching the maximum gain. Since the amplifier is no longer being saturated the gain is approximately constant so there is an approximate linear relationship between the loss before the amplifier and the acceptable loss after the amplifier.

There comes a point where the loss before the amplifier is so high, and the seed signal strength is so low, that the RSOA begins to emit broadband ASE. The ASE within the passband of the AWG channel will still be routed through the link and be received as signal at the other end of the link. This ASE will be modulated and will still carry data, if the loss after the RSOA is sufficiently low the link can still operate even with no input signal to the RSOA. In practice this region of operation is to be avoided.

In order to validate the model results from the model have been compared to experimental measurements with a maximum of -3 dBm input power to the RSOA which, when driven with a current of 100 mA, has a G of 23 dB and  $P_{SAT}$  of 9 dBm.

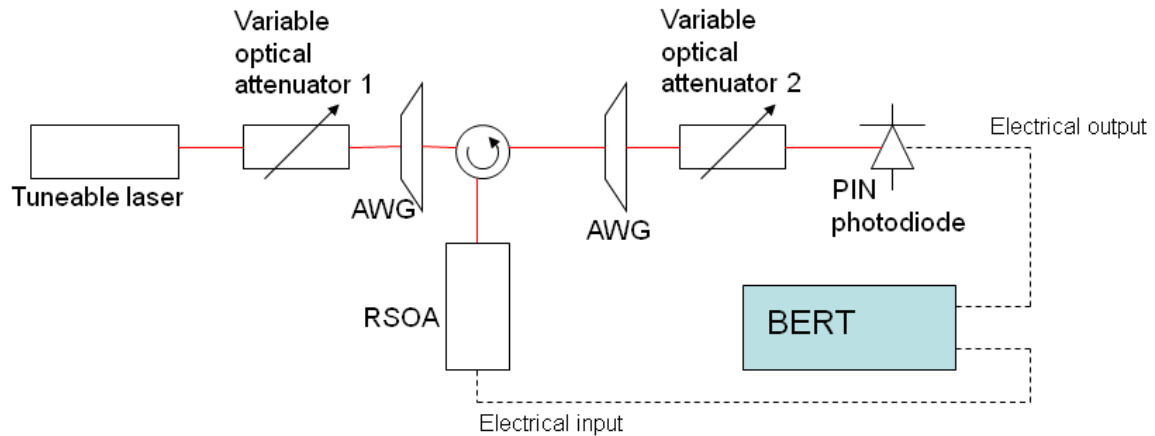


Figure 43: Experimental set up used to validate model

The model is compared to experimental results taken from a setup as shown in Figure 43. A tuneable laser, with the output power controlled with a variable optical attenuator, is filtered by an AWG with 200 GHz channel spacing. This is directed, using a circulator, into the RSOA to be amplified and modulated. The amplified signal is then routed using the same circulator onto another AWG to act as a multiplexer; the signal is then attenuated at another variable optical attenuator before the pin photodiode so the BER can be adjusted to the required level.

Starting with -3 dBm input power to the RSOA the maximum acceptable output loss is measured whilst maintaining a BER of  $10^{-9}$ . The attenuation in variable optical attenuator 1 is increased incrementally, thus decreasing the input power incrementally, and the acceptable output loss measured at each step. This has been done with both laser seed light and spectrum sliced broadband, ASE from an unseeded EDFA. The tuneable laser will be used in experimental work in the following section of this chapter whereas spectrum sliced ASE will be used as seed light in the proposed network. In theory these should both offer the same path loss capability for a given seed power. The results of both experiments and the model for the same case are plotted in Figure 44.

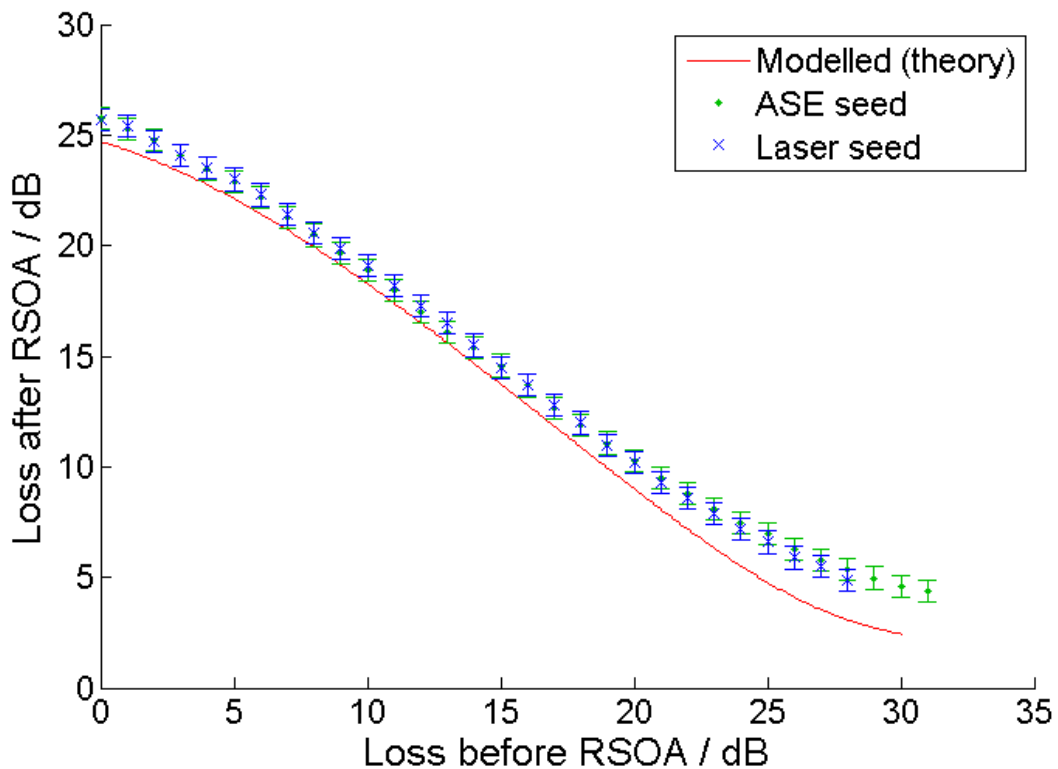


Figure 44: Comparison of predicted path loss capability and experimentally measured path loss capability using both laser seed and ASE seed

Comparing the results from the experiment seeding the amplifier with a laser to that of seeding the amplifier with spectrum sliced ASE shows there is a small difference in the system performance within experimental errors. This shows that the performance of the network using either laser seed or spectrum slicing is comparable and results of experiment using laser seed can be applied to spectrum slicing.

Comparing these results with those produced by the model also shows very little difference. With low loss before the RSOA and higher losses after the RSOA the model predicts the system performance reliably, as these are the conditions the network are designed to operate in the model is valid. At higher losses before the amplifier, meaning there is little input power to the amplifier, the signal does not fall off as in Figure 42. This is because in Figure 42 it is assumed that ASE will not contribute to the signal, this is not the case. If the ASE is within the passband of the AWG for that channel it will be routed to the photodiode and be detected as signal, the amplifier is being modulated so the ASE is being modulated as well. The model does not account for this effect accurately because it takes the average ASE power for each channel as opposed to taking different ASE powers at each wavelength corresponding to the measured ASE profile. As the network is not intended to operate with little or no seed signal this is acceptable.

## 4.4 RSOA Thermal Measurements

As previously mentioned the performance of an RSOA is dependent on temperature. In particular the gain and saturation power can decrease significantly at elevated temperatures meaning a network that performs very well at room temperature will fail at the high temperatures on aircraft. To quantify the operational temperature range of the network as a whole the model validated in the previous section can be used. In order to model the network over an extended temperature range the performance of an RSOA must be characterised over this range so the relevant parameters can be input into the model.

### 4.4.1 Elevated Temperature Operation

Two different RSOAs were characterised over a range of elevated temperatures. The first device was a standard commercially available RSOA in a TO package supplied by Kamelian. The second device was a multiple quantum well (MQW) ridge-waveguide (RWG) RSOA designed to support high temperature operation. This device was fabricated using an AlInGaAs quaternary; the Al<sup>3+</sup> ions contained in the quantum wells facilitate higher temperature operation by deepening the well and hence obstructing carrier leakage at high temperatures. The RWG-RSOA was also supplied by Kamelian although it was supplied as an unpackaged chip on carrier. As the RWG-RSOA was unpackaged it could not be cooled below the lab ambient temperature as this would cause condensation to form on the device which could damage the device. For this reason in this section we look only at elevated temperature operation, this analysis is still valid as it is at elevated temperatures that the gain and  $P_{SAT}$  decrease whereas performance should be better at low temperatures, this will be investigated later.

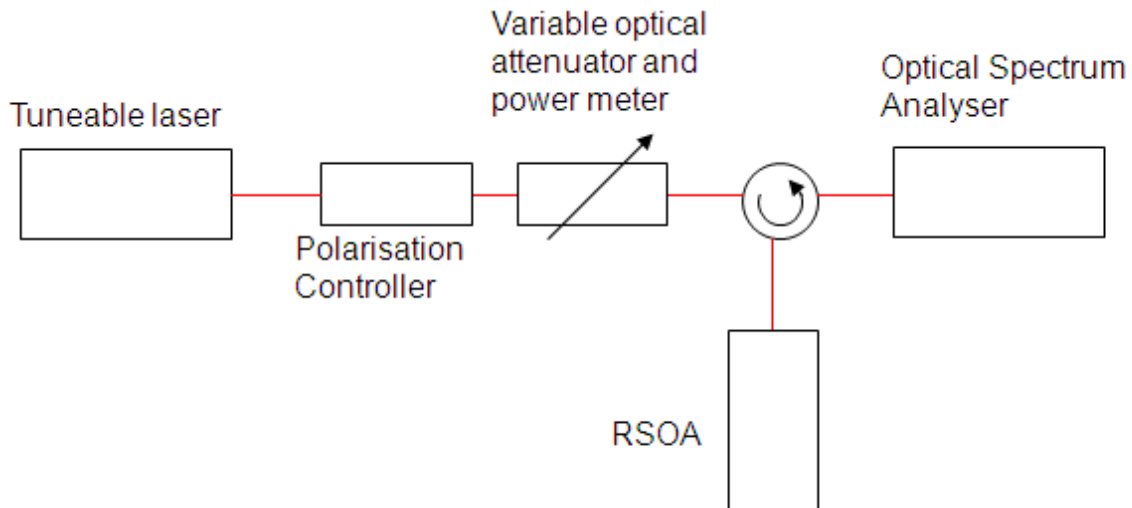


Figure 45: Experimental layout of system used for measurements of Gain and  $P_{SAT}$ .

The  $G$  and  $P_{SAT}$  of both these devices were measured over a range of temperatures using the experimental setup shown in Figure 45. A tuneable laser was used to seed the device under test with light of specified wavelengths; 1528 nm, 1550 nm and 1563 nm. The seed light was passed through a polarization controller to align the polarization of the seed light to polarizations of both the maximum and minimum gain in the device under test. From the polarization controller the seed light passed through a variable optical attenuator with integrated power meter. This allows the input power of seed light to be simultaneously altered and monitored to calculate the RSOA gain. The light was injected into the RSOA which was placed on a thermo-electric cooler to control the devices temperature. At the RSOA the signal wavelength was amplified before being routed via a circulator onto an optical spectrum analyzer to measure the output power. Gain and  $P_{SAT}$  variation is shown for the wavelengths under consideration; 1528 nm, 1550 nm and 1563 nm in over temperatures ranging from 20 to 60 °C. The maximum operating temperature for this device is 60 °C, it is limited by the packaging because the glues in the package will start to soften above this temperature. If it is found that the device may operate above 60 °C it is possible to house the chip in a more rugged package. The  $P_{SAT}$  was measured at a drive current of 100 mA. Gain measurements were carried out with an input power of -25 dBm to ensure small signal gain conditions. The variation of gain and  $P_{SAT}$  with temperature for the standard RSOA is shown in Figure 46.

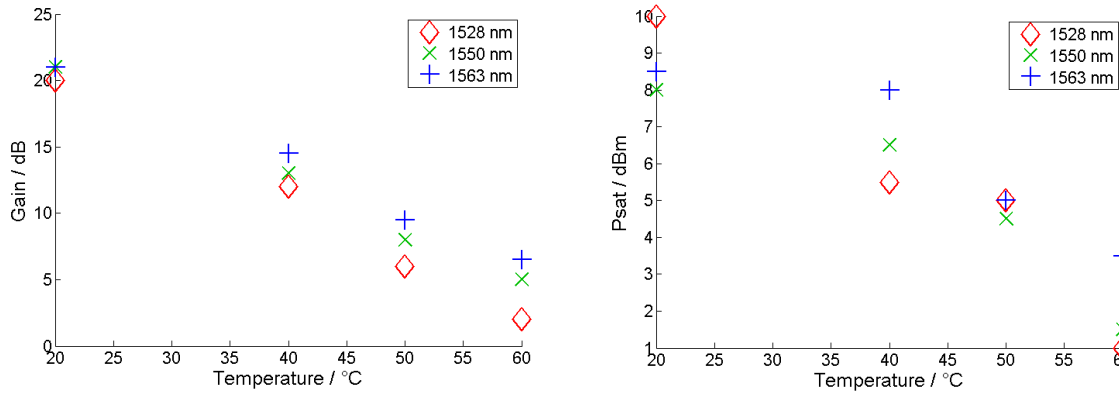


Figure 46: Gain and  $P_{SAT}$  of standard RSOA as a function of Peltier temperature for all tested wavelengths

The experiment was repeated over a greater temperature range with the RWG-RSOA and the results are plotted in Figure 47.

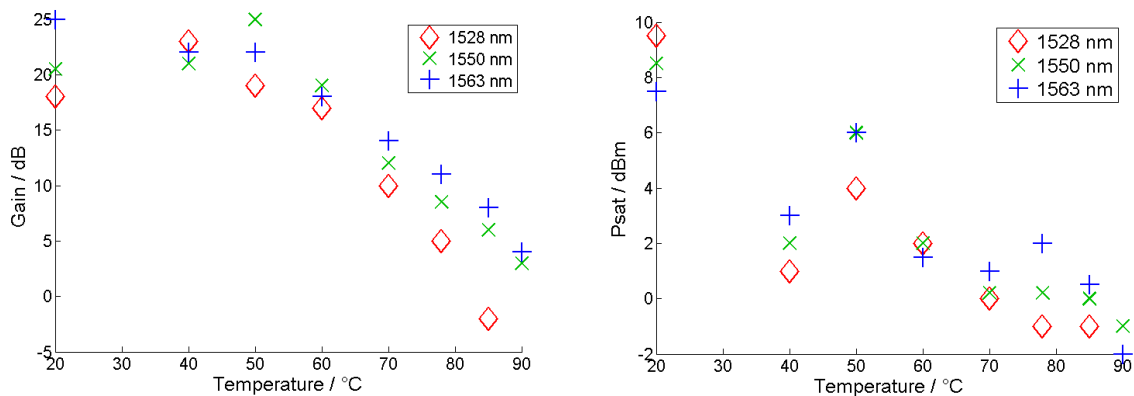


Figure 47: Gain and  $P_{SAT}$  of standard RSOA as a function of Peltier temperature for all tested wavelengths

As expected both the gain and  $P_{SAT}$  decrease with increasing temperatures for both devices. The following sets of experiments were carried out using two different samples packaged in different methods, each with different thermal characteristics. To avoid systematic errors associated with the influence of device packaging on the thermal behaviour, the parametric performance was normalised to chip temperature. In the case of the MQW RSOA, the chip temperature measurement was obtained directly from the temperature of the carrier. In the case of the RSOA can the chip temperature was estimated from a set of calibration curves that were previously established to relate chip temperature to can temperature. These were supplied by Dr. Tony Kelly of Glasgow University.

Figure 47 contains plots of  $G$  and  $P_{SAT}$  as a function of chip temperature for the RWG-RSOA. This device was not supplied in a pigtailed package but was a chip on carrier and single mode fibre had to be aligned to the device before each measurement at a different temperature. Care was taken to optimize the coupling efficiency after fibre alignment however it remained very sensitive to vibrations which would cause misalignments. The second plot in Figure 47 shows  $P_{SAT}$  as a function of temperature, at 40 °C the fibre alignment was optimized as in the other measurements. Across the entire wavelength band, the  $P_{SAT}$  is noticeably lower than would be expected from looking at the trend as a whole. This is because the fibre became misaligned during measurement so the value for  $P_{SAT}$  is incorrect, without repeating the measurement it is not possible to know if the gain value is also incorrect. In the following analysis the 40 °C point has been omitted for the RWG-RSOA.

#### **4.4.2 Performance Comparison**

With a validated model of network performance and the parametric characterization of two different RSOAs over an elevated temperature range it is possible to quantify the upper operating temperature of both types of RSOA in the network and quantify any improvement offered by using the RWG-RSOA. In order to analyse the performance relevant parameters from the network architecture must be defined. Commercially available state of the art broadband lightsources have a spectral power density of 1 mW/nm, the lightsource in the following analysis is assumed to have the same spectral power density. Architectural losses between the lightsource and the amplifier will affect the input power into the RSOA, these are measured for one circulator, one AWG and two red/blue C-band couplers. Architectural losses from transmitter to receiver are also included in the model; the architectural link losses included represent two matched AWGs, two red/blue C band splitters and one circulator. With the seed power and the architectural losses defined the model can be run for both devices at each wavelength measured across the elevated temperature range in which the devices have been characterised. Each time the model is run it calculates the losses which are acceptable over and above the architectural losses whilst maintaining a BER of  $10^{-9}$ ; this can be referred to as the Path Loss Capability (PLC). The PLC is calculated at each temperature and wavelength combination the RSOAs were characterised. The wavelengths 1528nm, 1550nm and 1563nm represent the shortest, longest and central wavelength channels in the C-band. All other channels in the C-band will fall within the range of the calculated PLC, as this range encapsulates the C-band calculating the PLC for each of these wavelengths ensures that all channels in the network are accounted for. For the



case of the RWG-RSOA an additional 3 dB loss preceding the amplifier is assumed. This is because the RWG-RSOA has a much higher PDG than the standard RSOA, the maximum gain has been used in the analysis so the worst case scenario is that only one plane of polarization is amplified, this corresponds to a 3dB loss before the amplifier. As the amplifier is still operating close to saturation this should not have a great effect on the results of this analysis. The results of this comparison are plotted in Figure 48.

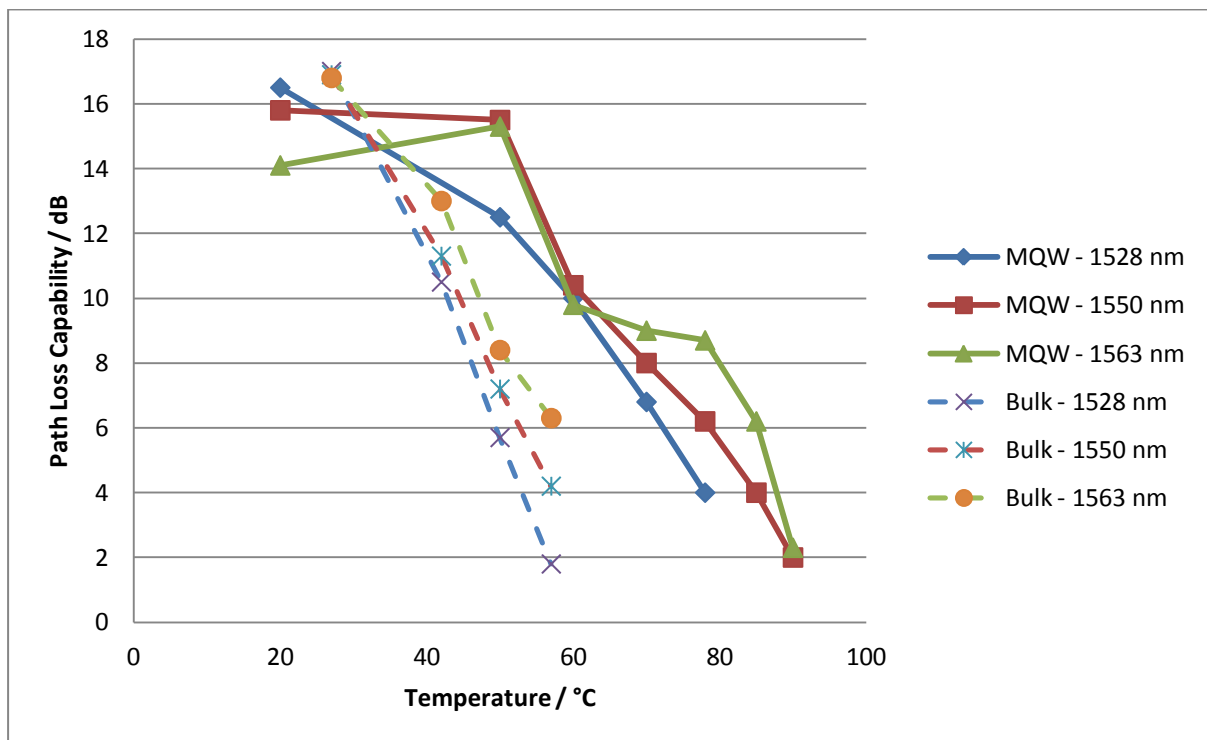


Figure 48: Plot of the maximum loss allowed in the link in order to keep a BER of  $10^{-9}$  as a function of RSOA chip temperature. The thin dashed lines are the standard bulk active region device and the thicker solid lines are the MQW RWG-RSOA.

The effect of calibrating the chip temperature is noticeable in Figure 48 for the standard RSOA in a TO-can, plotted in the lighter lines. The test temperatures have become slightly compressed, at the lower temperatures active heating is the dominant factor and since the packaging acts as an insulator the device sits above the cooler set point. At the higher temperatures the passive heating from the cooler is the dominant heating mechanism, due the poor thermal conductivity of the packaging the chip sits at a temperature slightly below the cooler set point. The RWG-RSOA, plotted in Figure 48 in the heavier lines, is mounted as a chip on carrier and is unpackaged; this means there is a highly thermally conductive path from chip to the Peltier so the chip temperature is very close to the set point of the cooler.

As expected from the response of both devices gain and  $P_{SAT}$  at elevated temperatures the network performance is impaired by increased temperatures and the RWG-RSOA does perform better at elevated temperatures than the standard device. The model has only accommodated architectural losses and no allowances have been made for trunk losses and losses associated with component aging and thermal degradation. As links in aircraft are short, in the order of 100 m, link losses of approximately 0.04 dB can be ignored. If a 3 dB overhead is introduced to account for component and connector aging, as is typical in aircraft links, and a 3 dB overhead is introduced, to account for thermal effects on the passive components and receiver throughout the link, a 6 dB total overhead is needed, this corresponds to a PLC of 6 dB. By looking at the PLC as a function of chip temperature in Figure 48 it is straightforward to read off the maximum operating temperature while maintaining the 6 dB overhead and the required  $10^{-9}$  BER. For the standard RSOA the PLC drops below 6 dB around 50 °C chip temperature for the short wavelength channel and at 58 °C for the longest wavelength channel. This does not mean uncooled operation of the RSOAs is impossible, the RSOAs can be operated uncooled up to this temperature at which point they must be cooled. With the RWG-RSOA the uncooled area of operation is extended with the short channel needing cooling at 70 °C and the longer channels working to almost 85 °C.

In theory the longer wavelengths could be used in locations throughout the aircraft with higher ambient temperatures in order to utilise their increased performance but for this analysis we are going to use the lower performance short wavelengths so all channels throughout the network can be treated in the same way and complexity is reduced. In this case the RWG-RSOA offers a 20 °C increase in the maximum operating temperature across all channels. Although this does not allow uncooled operation throughout the aircraft it allows uncooled operation in more areas throughout the aircraft and reduces the power consumption of any cooling due to relaxed requirements. This analysis has also shown that the same amplifier can be used a transmitter across the entire C-band eliminating any inventory issues that would be present in other transmitters such as DFBs.

#### **4.4.3 Low Temperature Operation**

The previous analysis has calculated the operational constraints at elevated temperature. It has previously been mentioned that at the lower end of the temperature regime the gain and  $P_{SAT}$  will, in theory, increase. However, the gain spectrum will gradually move to shorter wavelengths as the temperature decreases. It is possible that this will lead to decreased gain and  $P_{SAT}$  values at low temperatures, particularly at the longer wavelengths in the C band.

So, even though the gain and  $P_{SAT}$  are generally increasing with the decreasing temperature, there could still be link failure at low temperature due to decreasing gain and  $P_{SAT}$  at a particular wavelength. Therefore the gain and  $P_{SAT}$  must be measured at low temperatures and used in the model to predict the operational temperature range as in the previous section. These measurements cannot be made for the RWG-RSOA as this device is an unpackaged chip on carrier, when the temperature at the chip surface is below the ambient temperature condensation will form on the chip and will lead to damage of the device. Only a standard, packaged device was tested using the experimental set-up shown in Figure 49.

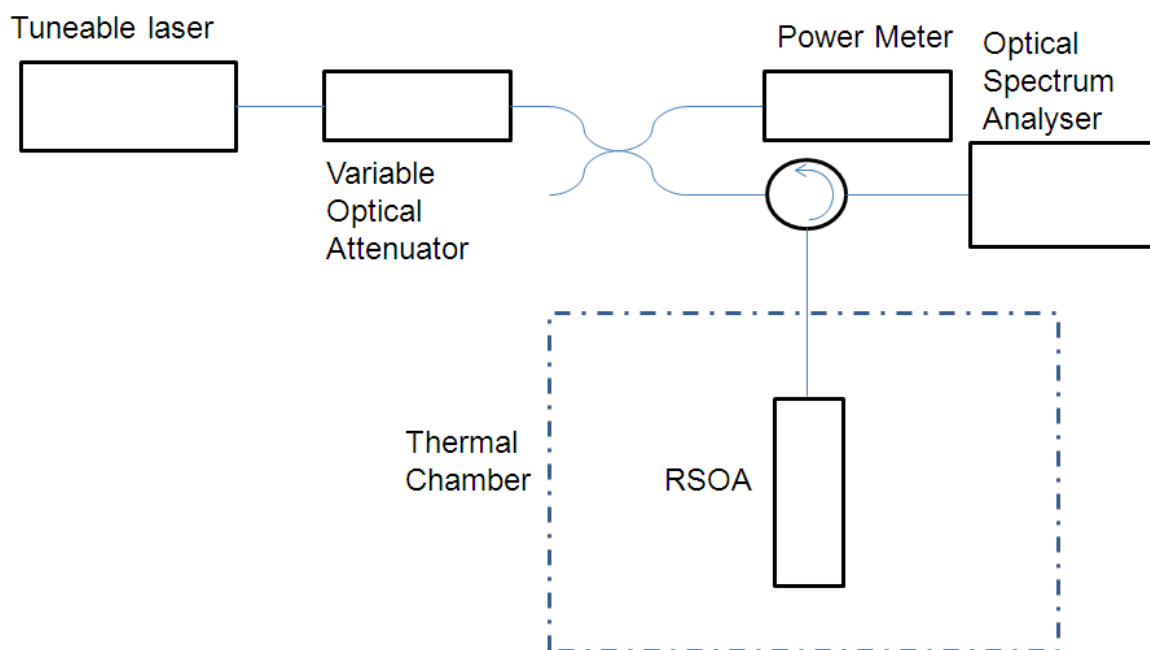


Figure 49: Schematic of experimental set-up to measure RSOA parameters at low temperature

The RSOA used in the high temperature measurements was not available for this experiment but a similar device from the same manufacturer with the same specifications was used for all measurements. The apparatus used in the previous experiment was also unavailable so the same experiment was carried out using a slightly different set-up, this will not affect the reliability of the results. A tuneable laser was used as the lightsource to supply the signal for amplification, this seed light was passed through a variable optical attenuator, VOA, to control the input power supplied to the RSOA. From the VOA the signal was routed to a 50:50 coupler, this splits the signal equally down two separate fibres. One fibre was input to an optical power meter, with knowledge of the exact splitting ratio and the insertion loss of a circulator this is used to monitor the power into the RSOA. The other fibre is

directed, via a circulator, to the RSOA in the thermal chamber where the temperature can be controlled. The amplified signal was then routed by the circulator to an optical spectrum analyser where the optical power of the amplified signal can be measured.  $G$  and  $P_{SAT}$  were measured at 1528 nm, 1550 nm, and 1563 nm at 20 degree intervals from 20 °C to -60 °C. The results of these measurements are plotted in Figure 50.

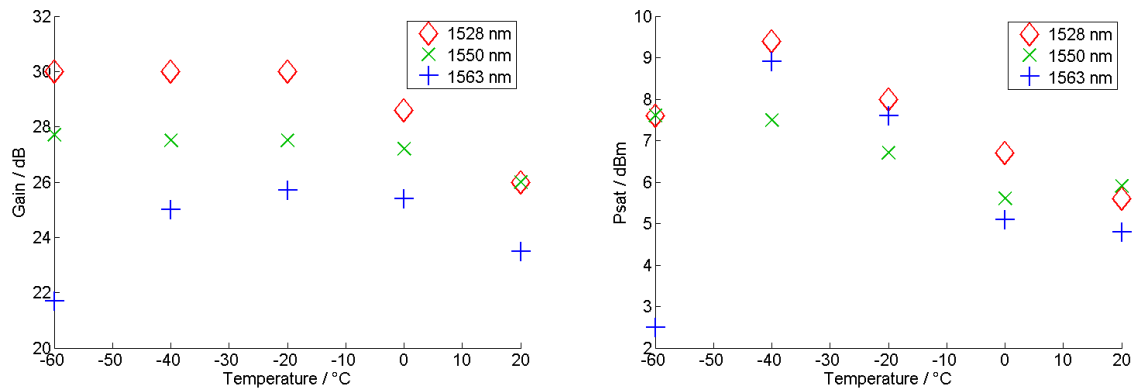


Figure 50: Plots of Gain and  $P_{SAT}$  at low temperatures

These plots display a similar trend to those in Figure 46 in that both  $G$  and  $P_{SAT}$  generally increase with decreasing temperature as expected. Unlike Figure 46 these temperatures are not the chip temperature but are the ambient temperature in the thermal chamber. In this case the ambient temperature measurement is applicable and not the chip temperature as used beforehand. At the lower temperatures it is not expected that the RSOA will require additional heating so the chip temperature is of less concern. What is of more concern is the ambient temperature as this is what is specified in the operational requirements. These plots alone are not sufficient to assess the suitability of the RSOA to operate in the proposed network at low temperatures so this data has been used in the model to predict the path loss capability as a function of temperature. This is plotted in Figure 51.

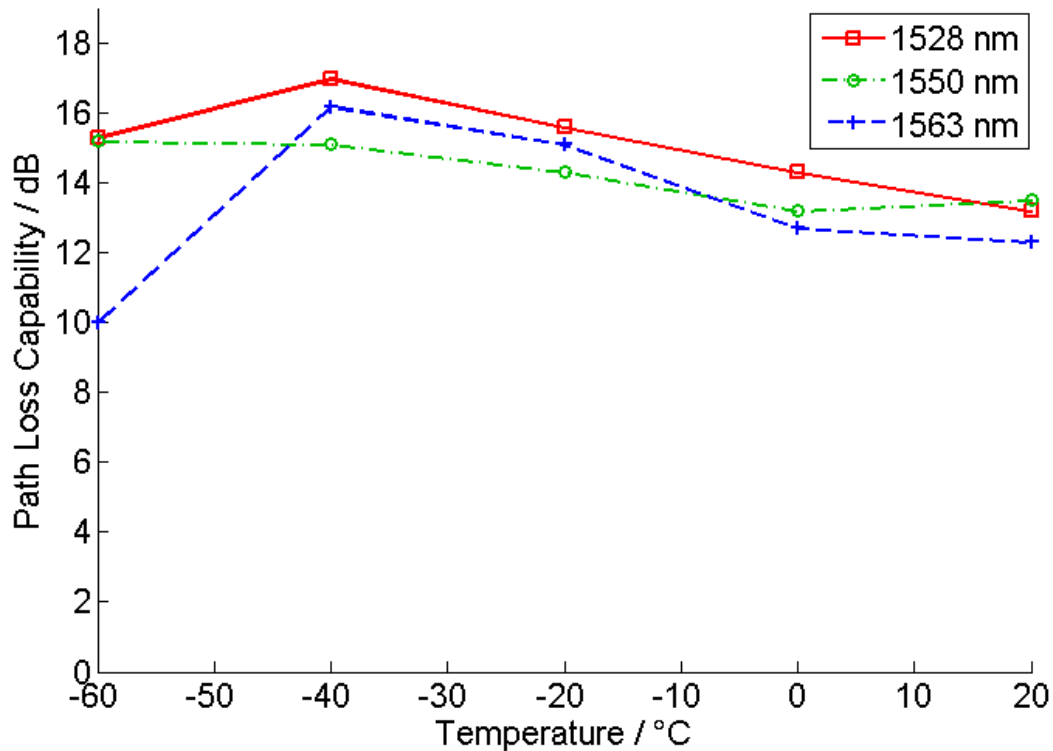


Figure 51: Maximum acceptable loss in link while maintaining a BER of  $10^{-9}$  as a function of temperature

Again all architectural losses incurred throughout the network have been accounted for and it is assumed that a 6 dB overhead is required. At -60 °C the path loss capability is at its lowest for the 1563 nm channel at 10 dB. This is above the 6 dB overhead that is required to say the device can operate uncooled. This is not the RWG-RSOA, which can operate uncooled up to 70 °C, and although the performance of the standard device and the RWG-RSOA are different at high temperatures it is not expected that they be different at low temperatures. The difference in performance at high temperatures stems from deep quantum wells due to the Al contained in the active region of the RWG-RSOA, this means that carriers need more energy to leak from the quantum wells which means that gain and  $P_{SAT}$  are more stable at elevated temperatures. At room temperature the RWG-RSOA and standard bulk RSOA have similar values for gain and  $P_{SAT}$ . At lower temperatures, such as those in the previous analysis, the gain and  $P_{SAT}$  of both devices are likely to remain similar. Since the standard RSOA can operate at the lowest temperatures in the avionic specification the RWG-RSOA should also be capable of uncooled operation at these temperatures.

## 4.5 Conclusions

This chapter considers the implementation of a SS WDM-PON for aircraft using COTS components and a single, centralized lightsource to minimize size, weight and power requirements. The idea of using a seeded RSOA as a modulator has been introduced and the mathematical framework to model the performance of this situation detailed. A mathematical model has been created for an idealized link which can be used to represent each channel in the network using a lumped losses approach. Results from this model have been compared with experimental results and display good agreement.

Two different designs of RSOA were evaluated for use in the SS WDM-PON, a standard bulk heterostructure device and a single polarization ridge-waveguide device designed to have an extended operating temperature range. The performance of these devices was characterised over an elevated temperature and relevant parameters from this characterization used in the network model. The model was used to calculate the upper operational temperature of the network using each device while maintaining a 6 dB overhead in the path loss capability and a BER of  $10^{-9}$ . It has been predicted, that with these requirements, the standard RSOA can be used at any DWDM wavelength channel in the C-band up to 50 °C without additional cooling. The RWG-RSOA is designed to have increased performance at high temperatures and is predicted to operate in the defined network uncooled up to 70 °C. This extension in operating temperature will reduce the power consumption of any additional cooling and may open up the possibility of using limited passive cooling as will be discussed in later chapters.

At low temperatures only one device could be tested, the standard bulk heterostructure RSOA. The performance of this device was characterised over the low temperature range specified for avionic operation. Again results from this characterization were used in the model to predict network performance. It is anticipated that the RSOA can operate as an amplifier and modulator in the proposed network at the lowest temperature required for avionic operation without additional heating. It is also expected that this result will also apply to the RWG-RSOA meaning that this device can operate uncooled from -55 °C to +70 °C and only requires cooling at the upper range of the avionic temperature specification.

# 5. Thermoelectric Cooler Power Consumption and Passive Phase Change Cooling

## 5.1 Introduction

In the previous chapter it has been predicted that the end nodes of the proposed network may operate uncooled up to +70 °C if using a RSOA as an amplifier and modulator. At temperatures beyond this point the RSOA must be held at 70 °C in order to ensure acceptable network performance. The industry standard approach to cooling over a 55 degree range would be to use a TEC. In the aerospace industry this is usually avoided due to the additional power consumption associated with the use of a TEC, particularly with a high temperature difference when the ambient temperature would be +125 °C.

Typically, modern military aircraft have short flight durations, although this does not always apply to UAVs. Assuming that this will also apply to some future manned aircraft the present work will attempt to determine whether or not an alternative cooling method with no power consumption may be suitable. The idea behind this 'passive' cooling is to blunt extreme temperature excursions over a short period of time. One such technique could be the use of phase change materials where the phase change is engineered to occur at a useful temperature for cooling. At this point the material will melt and, due to the latent heat, will absorb large amounts of energy in the form of heat. In this chapter a mathematical model of one potential cooling package using a phase change material is presented. From the output of this model the suitability of using passive cooling with respect to performance, practicality and cost is presented. This is then compared to the performance and cost of using a TEC in the same environment.

The work in this chapter was intended as preliminary study into the concept of phase change cooling. The purpose of this work is to assess the relative efficiency of phase change cooling with respect to conventional methods before purchasing software such as ANSYS for a more detailed design stage.

## 5.2 Thermo-Electric Cooling

A thermo-electric cooler is a refrigeration device which uses electricity to pump heat from a cold area to a hotter area. A TEC has no moving parts and uses no bulk fluids such as chlorofluorocarbons (CFCs). Most refrigeration failures stem from mechanical failures and (potentially environmentally harmful) coolant leakages. As the TEC will not suffer from these issues it is much less prone to failure. A TEC is small, lightweight and is a very mature and reliable technology [79,80]. A TEC can also be used to generate electricity directly from heat.

### 5.2.1 Theory

TECs work by using the Peltier effect which was discovered by Jean Peltier in 1834. When electric current is passed across the junction of two dissimilar conductors, a thermocouple, there is a heating effect that cannot be explained by Joule heating. Joule heating being the heat which accompanies an electrical current. In addition to the heating there is a cooling effect when the direction of the current is reversed. A schematic of a TEC is shown in Figure 52.

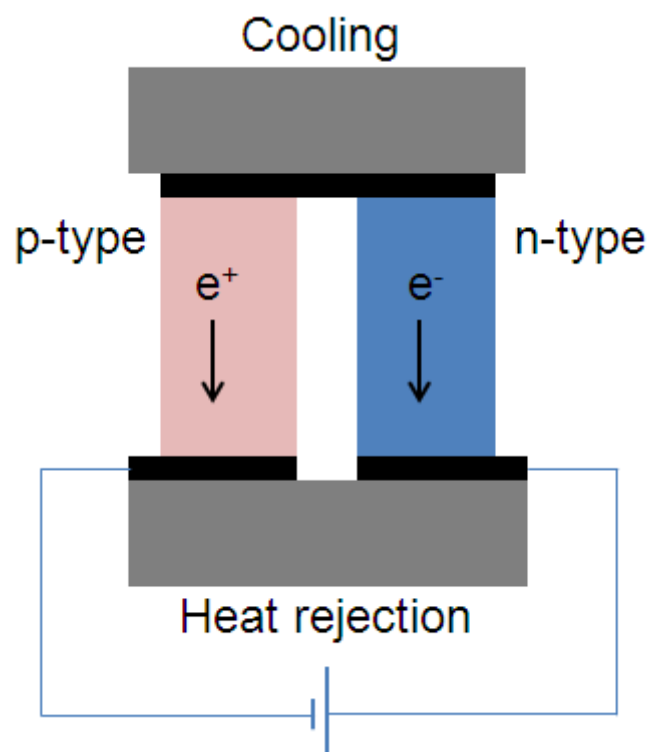


Figure 52: Schematic of a thermoelectric cooler



Devices are currently made by joining one **p** doped semiconductor material to an **n** doped semiconductor material. These two different semiconductors have a different Fermi level, when they are put into contact electrons will flow from the semiconductor with the higher Fermi level in an attempt to restore equilibrium and bring the two Fermi levels to the same value. A schematic of a TEC is shown in Figure 52; it is composed of two semiconductors forming one thermocouple. These two materials are joined at the top of the diagram by a (black in Figure 52) conducting bar to form a semiconductor junction. When a current flows, as shown in the diagram, electrons flow away from the junction in the n-type semiconductor towards the bottom of the couple. The positively charged holes in the p-type semiconductor also flow away from the junction towards the bottom of the diagram. Both carriers conduct heat away from the junction through the Peltier effect, so the junction becomes cold.

If the heat flow into the junction, for example from the surrounding environment, is less than the heat flow out of the junction the junction will become cold. If the materials are well chosen a temperature drop of 50 K to 70 K is possible. In order to maintain this temperature difference between the two sides of the TEC the hot side must be placed in good thermal contact with a heatsink so the temperature does not increase too greatly. In addition to the cooling effect there are other heating effects that must be considered, mostly Joule heating. Driving a current through the device causes Joule heating, this is proportional to the square of the drive current. Additionally, since the junction will be colder than the base there will be a heatflow back towards the junction, although by choosing materials with a low thermal conductivity this effect can be minimised. The two dominant effects are the Peltier effect cooling the junction, which is proportional to the current, and the Joule heating which is proportional to the current squared. The maximum decrease in junction temperature will therefore be realised at an optimum current.

The TEC can also be used to generate electrical power. If the junction is heated and the opposite side of the TEC is not, then heat will flow through the device towards the junction in the opposite direction to the heat flow when cooling. This heat is partly carried by carriers in the opposite of the Peltier effect so a voltage is generated. This effect is known as the Seebeck effect.

### **5.2.2 Power Consumption**

On an aircraft one of the most important aspects of a devices performance is the power consumption. The power consumption of the cooling tends to be particularly high over the full avionic temperature specification. The power consumption of a TEC is dependent on two

variables: the temperature difference between the hot and cold side of the TEC,  $\Delta T$ , and the heat that must be pumped through the TEC, this includes any heat generated by the drive current. The power consumption of a small TEC in a butterfly package cooling an SOA has already been measured by others within BAE Systems [81] with an SOA drive current of 150 mA over a wide temperature range, this has been repeated over a range of TEC set points and is shown in Figure 53.

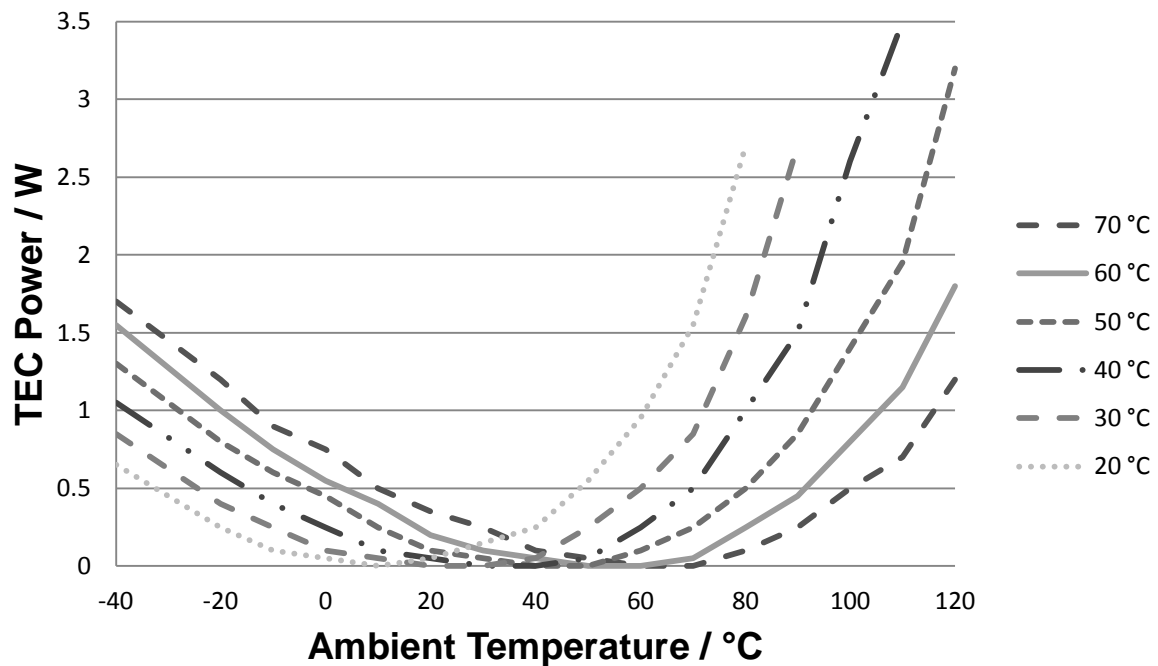


Figure 53: Power consumption of a TEC in a butterfly package cooling an SOA with a 100 mA drive current over a range of set points as a function of ambient temperature [81].

It is reasonable to assume that an RSOA could be packaged in a single ended butterfly package with a TEC. SOAs are widely available packaged with a TEC in a butterfly package. Due to the similarity of this device and an RSOA the TEC power consumption, plotted in Figure 53, should be same for both devices. This power consumption is dependent on the heatsink arrangement; this will depend on the size and weight tolerances of the aircraft and not the device itself.

Considering a TEC in the context of cooling an RSOA end node as discussed in the previous chapter Figure 53 can provide valuable details on the predicted power consumption. From the analysis of the RWG-RSOA it was found that particular device could operate uncooled up to 70 °C. If the RWG-RSOA were to be packaged with a TEC and exposed to temperatures of 120 °C the approximate power consumption of the TEC to cool

the device to its maximum operational temperature would be 1.2 W. The maximum specified operational temperature on aircraft is 125 °C so the power consumption for the TEC when cooling the RWG-RSOA end node at the maximum temperature would be higher than this. Using the data from the other set points it is possible to extrapolate the power consumption at 125 °C. At 110 °C ambient temperature the power consumption decreases by a factor of approximately 0.6 for every 10 °C increase in TEC set point, this trend also holds at 120 °C. Considering that the two factors affecting TEC power consumption are the temperature difference between the two sides and the amount of heat being pumped through the device, an increase of 5 °C in ambient temperature has the same impact on power consumption as a 5 °C decrease in set point. In this case the power consumption will be decreased by a factor of 0.77 (half of the temperature interval therefore the factor will be the square root of 0.6). The approximate power consumption of a TEC cooling a RWG-RSOA driven at 100 mA at the aircraft's maximum temperature is therefore 1.4 W. This value may change depending on heatsink specification. At present we are only concerned with producing a comparative measure of performance so different cooling strategies can be assessed.

## **5.3 Passive Cooling using Phase Change Materials**

Passive cooling refers to any type of thermal management which has no direct power consumption. In this case a Phase Change Material, PCM, is used to absorb heat above a certain temperature. PCMs are widely used in many different industries from insulation used in the NASA space program [82] to heat retainers in coffee cups [83].

### **5.3.1 Theory**

PCMs can be used for short term heat storage and can be seen analogous to a capacitor in electronics. As the PCM is heated it will absorb heat according to its specific heat, sometimes this is referred to as normal heating. As the temperature of the PCM (in its solid phase) meets the melting point the PCM starts to melt. Since the latent heat, the energy required for the phase change, is much higher than the normal heat capacity the material requires much more energy to raise its temperature. This means that it will absorb more heat at this temperature until it has completely melted. When a material with a high latent heat is chosen the temperature can be clamped near the materials melting point until the material is entirely melted because the specific heat of the PCM during the melting process can be increased by a factor of 100. It is from this effect that PCMs can be used for short term cooling although it may also be thought of as temperature selective insulation.

The theory and mathematics behind PCMs are well understood and well explained in the literature [84]. The simplest way of describing the process mathematically is by presenting the specific heat as a function of temperature. If the ambient temperature is less than the melting point of the PCM the specific heat can be expressed as;

$$(\rho C)_{PCM} = (\rho C)_{solid} \quad (18)$$

where  $\rho$  is the density in units of  $\text{kg/m}^3$  and  $C$  is the specific heat in  $\text{kJ/kg } ^\circ\text{C}$ . When the ambient temperature is above the melting temperature of the PCM the specific heat becomes;

$$(\rho C)_{PCM} = \frac{(\rho C)_{solid} + (\rho C)_{liquid}}{2} + \frac{\rho_{solid} + \rho_{liquid}}{2} \left( \frac{\lambda}{\Delta T} \right) \quad (19)$$

where  $\lambda$  is the latent heat of melting in units of  $\text{kJ/kg}$  and  $\Delta T$  is the phase change transition temperature in  $^\circ\text{C}$  ( in this case this equals  $1^\circ\text{C}$  <sup>85</sup>). When the PCM is entirely melted, or when the ambient temperature exceeds the maximum operational temperature of the PCM as given in its specifications, the specific heat can be expressed;

$$(\rho C)_{PCM} = (\rho C)_{liquid}. \quad (20)$$

Throughout the preceding equations subscripts refer to the parameters in either the solid or liquid phase, or the parameters of the PCM as a whole.

### 5.3.2 Package Design and Modelling

Considering that the types of military aircraft which the proposed network may be aimed at typically have short flight durations it may be possible to use a PCM to blunt the temperature at the RSOA for short flights. When a conducting container is filled with a suitable PCM, with a high latent heat and melting point just below the maximum operational temperature, is placed in good thermal contact with a RSOA it can be used as a passive cooling system. If this is encapsulated in an insulating package any excess heat will be absorbed by the PCM during the melting process. When above the PCM melting temperature this will clamp the temperature in the package close to the melting temperature and should keep the RSOA below its maximum operational temperature until the PCM is completely melted. Here we are considering whether or not such a method can be used to accommodate short (e.g. 1 hour) periods where the device is operated above the maximum temperature we have previously

defined. The basic design of this system is shown in Figure 54 as well as the components of heat flow involved.

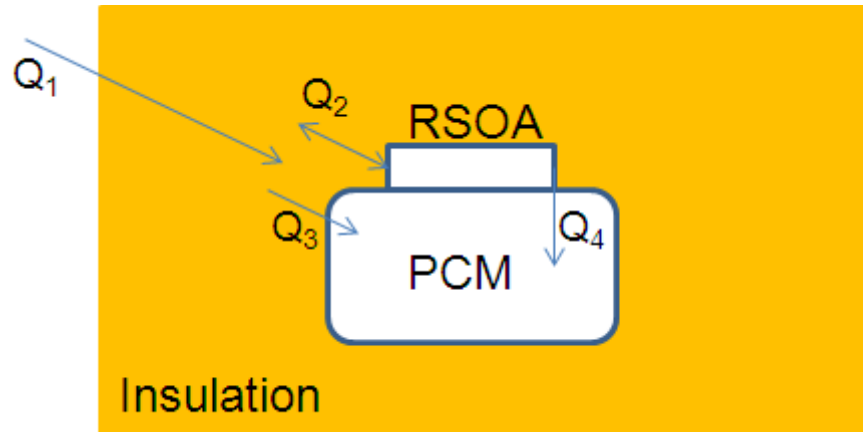


Figure 54: Schematic of passive cooling package including heat flows

From Fourier's law of Thermodynamics [86] the heat flow,  $\vec{Q}$ , can be expressed as

$$\vec{Q} = -k\Delta T. \quad (21)$$

Where  $k$  is the thermal conductivity in  $W/(m \cdot K)$  and  $\Delta T$  is the temperature gradient in  $K/m$ . The temperatures of the separate bodies in Figure 54 are related by the equations;

$$C_{ins} + \dot{\theta}_{ins} = Q_1 + Q_2 + Q_3 \quad (22)$$

$$C_{PCM} + \dot{\theta}_{PCM} = Q_3 + Q_4 \quad (23)$$

$$C_{RSOA} + \dot{\theta}_{RSOA} = -Q_2 - Q_4 + \text{Active Load}. \quad (24)$$

Where  $C_{ins}$ ,  $C_{PCM}$  and  $C_{RSOA}$  are the heat capacity of the insulation, the PCM and the RSOA respectively;  $\dot{\theta}_{ins}$ ,  $\dot{\theta}_{PCM}$  and  $\dot{\theta}_{RSOA}$  are the derivatives of the insulation, PCM and RSOA temperatures with respect to time and Active Load is the heat generated by the RSOA.  $Q_1$  is the heat flow into the insulation from the surroundings,  $Q_2$  is the net heat flow between the RSOA and the insulation,  $Q_3$  is the heat flow from the insulation into the PCM and  $Q_4$  is the heat flow from the RSOA into the PCM.

Using these equations along with the previously discussed equations describing the effects of latent heat it is possible to model how the temperature of the RSOA will change

over time for different insulating materials given a certain PCM. Selecting a PCM is relatively straightforward, there are numerous companies offering PCMs made from wax. These are very cheap and are also inert so pose no risk to the aircraft. They have a high latent heat of melting and can be manufactured at a range of melting points. For the following work a PCM consisting of wax RT 62 offered by Rubitherm, this melts at 62 °C and has a latent heat of 146 kJ/kg. Although this cooling technique has no direct power consumption it does add weight to the aircraft which will lead to an increased fuel burn, for this reason the weight of any associated insulation must be kept to a minimum. This design may be considered at an end node in a remote location such as a wing tip, the overall size and shape of the package will need to be altered to fit into small spaces. With both of these requirements in mind insulation must be chosen in accordance with its thermal conductivity and density. The three materials considered are aerogel, fibre blanket, polyimide foam, and an aerogel blanket. The relevant parameters are listed in Table 4.

<b>Material</b>	<b>Density / kg m<sup>-3</sup></b>	<b>Thermal Conductivity / W(m.K)<sup>-1</sup></b>
Aerogel	2	0.02
Polyimide foam	5	0.05
Fibre blanket	50	0.04
Aerogel Blanket	1.3	0.015

Table 4 : Parameters of insulation

Of the materials listed the aerogel blanket was chosen for detailed investigation because it has the lowest density and the lowest thermal conductivity. This material is commercially available from Aspen Aerogels and sold as Cryogel Z. It is a flexible silica aerogel blanket strengthened with internal, reinforcing fibres [87]. Using these values and those previously mentioned for the PCM it is possible to solve the above equations for temperature for a given ambient temperature. The temperature can be plotted as a function of time to show the temperature limiting effects of the melting PCM and also gives an indication of how long the cooling is useful. This is plotted in Figure 55 for an RSOA with an active load of 0.3 W, 0.26 kg of PCM and 10 g of insulation. The total volume of the package is one litre.

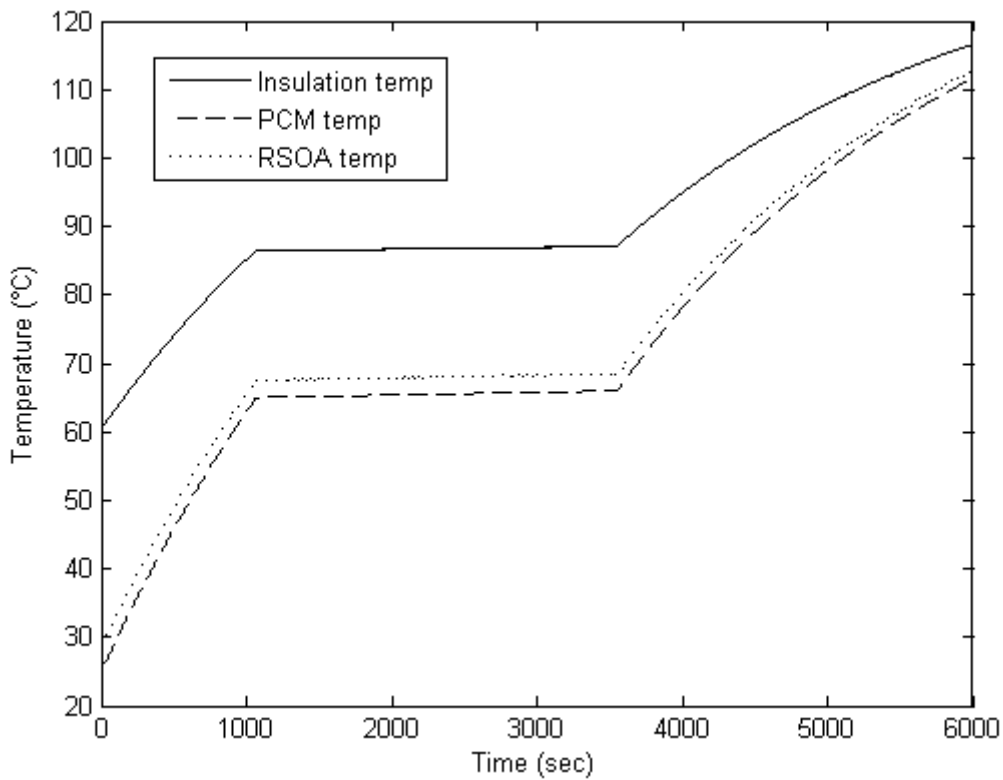


Figure 55: Graph showing the temperature as a function of time for an RSOA with an active load of 0.3 W.

The plot in Figure 55 shows the average temperature across the three bodies in the proposed design. In producing this model a number of assumptions have been made. From looking at graph a clear melting point is visible, similarly the point where the PCM is fully melted is also visible. In reality these points may not be as well defined as they are in this plot. The melting point would typically spread over a few degrees due to different lengths in the wax molecules [88]. The PCM heat capacity does not change instantly when the PCM is entirely melted as assumed in the model, there is a more gradual change. Nevertheless these assumptions should not have too much of an impact in the final assumptions drawn from as their effects will be slight. It has also been assumed that the PCM is packaged in a thin walled metal box to contain the wax when melted. A model with the effects of this box has also been made and the results are almost identical. Including the box in the model significantly slows the processing of the calculation to around 20 hours, therefore the model without the box has been used as this gives a reasonable approximation. It has also been assumed that this box would have a mechanism to ensure there is efficient heat transfer to

the wax. This could be a thin wire mesh inside the box to spread the heat through the wax and ensure melting throughout the wax.

### 5.3.3 Cooling Performance of PCM

There are two processes heating the RSOA; active heating, where the heat is generated from driving the RSOA, and passive heating, where the heat comes from the surroundings. With these considered there are a number of different parameters affecting the model such as; volume of PCM, thickness of insulation, ambient temperature and the heat generated by the RSOA. The cooling will have to operate in a range of different environments so the effects of changing each parameter must be investigated. Figure 56 shows a plot of the melt time, which is the amount of time the PCM will limit the temperature of the RSOA, as a function of PCM mass for a fixed package size of one litre. In order to maintain a constant volume as the PCM volume is increased the thickness of the insulation must decrease. This means there is an optimum point, at which the effective cooling time is maximised, for each given overall package volume.

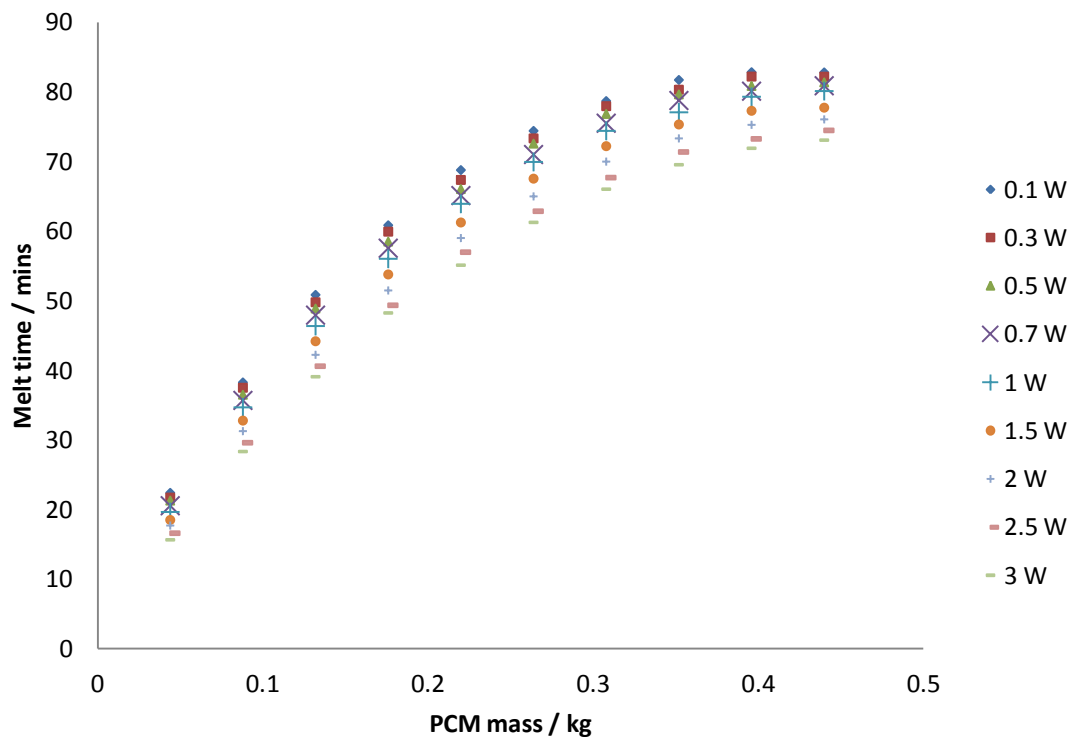


Figure 56: Melt time (effective cooling duration) as a function of PCM mass for a range of active loads with an ambient temperature of 85 °C



The optimum point may not occur at the same value when another parameter is changed, in Figure 56 the melt time is calculated at each value of PCM mass over a range of different active loads. As the active load is increased, the melt time will decrease. However, the decrease in melt time is not directly proportional to the increase in active load, this is because of the effect of the passive load which is the dominant heating mechanism in this case. The graph in Figure 56 shows an optimum PCM mass to maximise melt time. Without knowledge of exact parameters from the aircraft such as the size of the area the cooling is to be placed and the maximum specified temperature proposing a fixed design maximised for cooling duration is not sensible.

Figure 55 and Figure 56 show that the PCM cooling can operate for the required lengths of time, in practice it will be the size and weight of the cooling that will determine whether or not this method will be of interest to aircraft manufacturers. These are defined by the volume of PCM and thickness of the insulation. In some cases it may be more desirable to minimise size and weight for a given melt time as opposed to maximising melt time for a given weight. Figure 57 shows the size and total mass of the cooling package as a function of PCM mass.

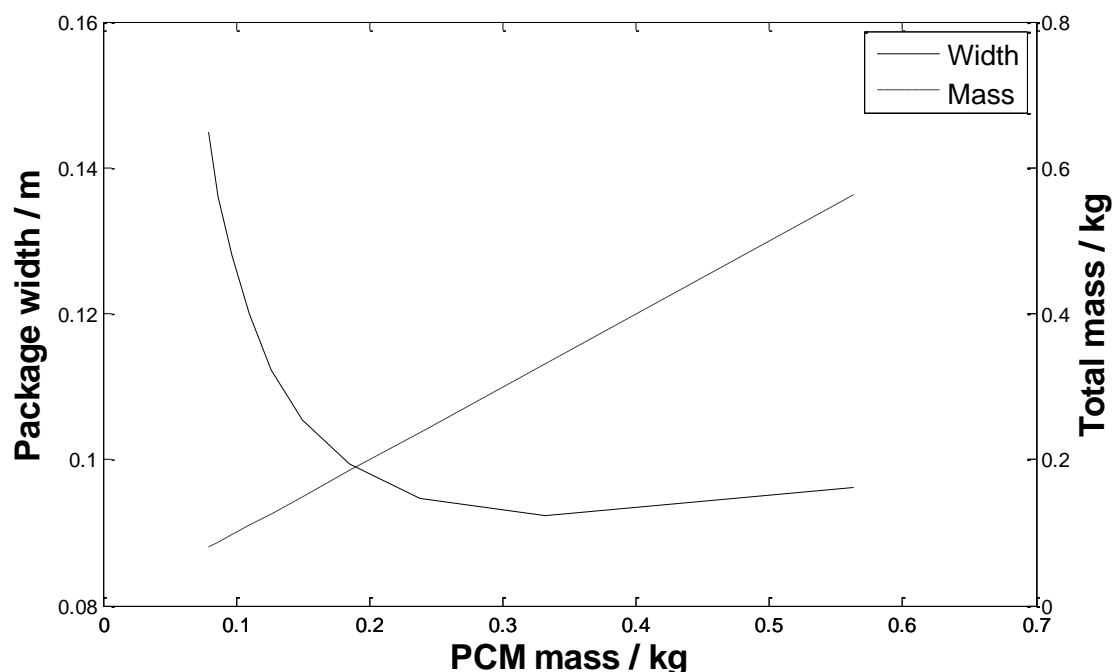


Figure 57: Size and weight of cooling package required to cool RSOA with 0.3 W active load in a 85 °C ambient temperature

There is a minimum in the possible volume of the cooling package in this case. This occurs with a total mass of approximately 0.33 kg, there is no benefit in adding more PCM beyond

this point. There is a trade-off between small package size and minimising the additional weight added to the aircraft. If the amount of PCM is increased the amount of heat that can be absorbed will increase. If the same duration of cooling is to be maintained with the increased PCM, the amount of insulation used can be decreased. The density of the PCM is much higher than that of the insulation, the size of the package is dominated by the size of the insulation and the weight of the package is dominated by the weight of the PCM. Adding a little PCM will slightly increase the size of the package but will have a significant effect on the total weight. Similarly decreasing the amount of insulation will have an effect on the package size but will have little effect on total weight. This explains why the trade-off between size and weight is unavoidable; both size and weight cannot be minimised simultaneously. Figure 57 shows the scenario at 85 °C, this is a useful temperature to use for the modelling as some areas of the aircraft have a maximum operational temperature of 85 °C but if passive cooling is to be used throughout the aircraft it must be operational at 125 °C. This is plotted in Figure 58. Both Figure 57 and Figure 58 show the trade-off between size and weight which complicates how the efficiency of the PCM cooling can be measured and expressed. It is not possible to propose a common cooling solution using the PCM, the cooling would have to be designed based on the active load, the ambient temperature and how much space is available on the aircraft. With these parameters defined it would then be possible to optimise the design for minimum weight. Knowledge of these parameters and a well-defined cooling design are beyond the reach of this thesis.

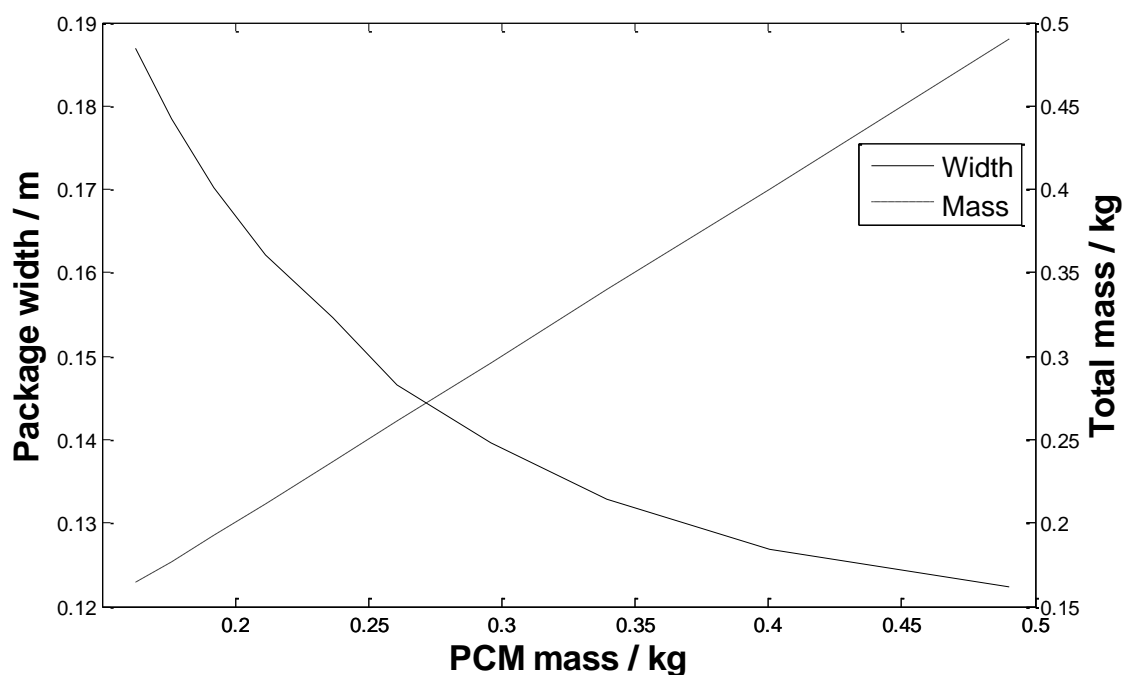


Figure 58: Size and weight of cooling package in a 125 °C ambient temperature

## 5.4 TEC PCM Comparison

As previously discussed it is not possible at this stage to fully define the cooling design, nevertheless an approximate evaluation of alternative cooling techniques can be made. Two possible cooling techniques have been examined; a TEC, which will have a power consumption and adds negligible weight to the aircraft, and a PCM insulating package, which has no direct power consumption but does add weight to the aircraft. Since the PCM method adds weight to the aircraft it will increase fuel burn while the aircraft is in flight, this is the indirect power consumption of the PCM. In order to assess which method of cooling is more efficient the power consumption of the TEC must be compared to that of the PCM.

### 5.4.1 Impact on Fuel Burn

One method of directly comparing the efficiency of each cooling method is to compare the effect each has on the fuel burn. With the PCM cooling the increase in fuel burn is derived from the increased weight. Although this work is concerned with small military aircraft it is not possible to source the data on how the increased weight will increase the fuel burn and data from civil aircraft must be used. The Boeing 737-800 is a short to medium range, narrow body jet airliner used throughout the world. Because of this aircraft's popularity among many different airlines data on fuel burn is available, it has been found that a reduction of 1 kg in weight saves 100 EUR a year in fuel costs on this aircraft [89]. Considering cooling for a short (1 hour) flight with the transmitter exposed to the full temperature specification the range of weights the package may take, depending on space constraints, is between 0.2 and 0.5 kg as shown in Figure 58. This equates to an additional 20 to 50 EUR per transmitter per year.

In the TEC case the current used to drive the cooler can be generated by the engines, this takes energy out of the engines and can be expressed as an increase in fuel burn. In order to make the comparison with the PCM, which expresses the additional cost from fuel burn as a cost per year, the yearly flight duration must be defined. It has been assumed that each flight takes one hour. The Boeing 737-800 aircraft is used for short routes so may fly eight times a day. Assuming time for maintenance the aircraft may be in service 300 days a year. With these assumptions the aircraft will fly for 8.6 Mseconds per year. The energy used in the TEC comes from burning jet fuel, the energy released in burning 1 kg of jet fuel is 43370 kJ [90]. This can be converted to electrical energy with a conversion efficiency of approximately 20% [91], thus burning 1 kg of fuel will deliver 8 MJ of

electrical energy. In this scenario the worst case in terms of temperature exposure is assumed, as discussed earlier the TEC will require 1.4 W which over a year of flying means that 12 MJ are needed. This means that the additional fuel required per transmitter per year is 1.5 kg which has a cost of approximately 1 EUR. This cost may rise slightly when the weight of the TEC and additional circuitry is included but it is still clear that the TEC is much more efficient in this case.

The previous analysis has assumed that all the RSOA transmitters are in remote locations throughout the aircraft. However, if the RSOAs are co-located it is possible that they may share a PCM cooling package. This is not possible with a TEC and each RSOA would have to use its own dedicated TEC. As the additional fuel burn introduced when using PCM would be shared among multiple RSOA transmitters there may come a point where the PCM method is more efficient.

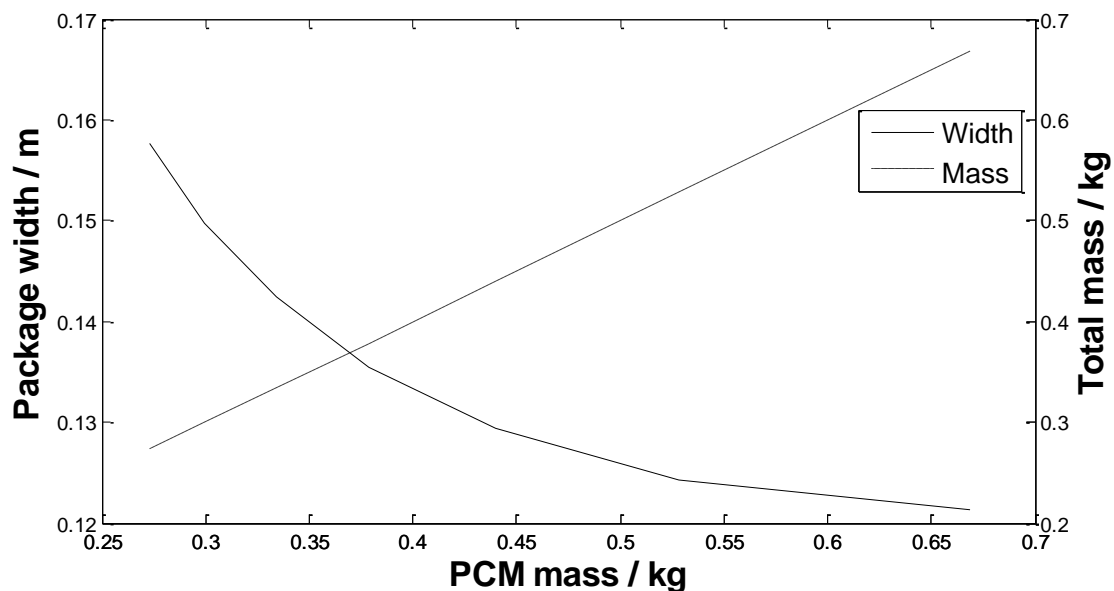


Figure 59: Size and weight for a PCM cooling package with a 125 °C ambient temperature cooling to 70 °C with an active load representative of 20 RSOAs

Repeating the calculations performed in the previous section with an active load of 3 W which is representative to that of 10 RSOAs yields the plot in Figure 59. Assuming that the design can be optimised for weight and a large volume is available the total mass of the PCM cooling package can be less than 0.3 kg which will cost less than 30 EUR per year in additional fuel. Using a TEC to cool the RSOAs individually would mean that 20 separate TECs are needed; the additional fuel to power these TECs would have a cost of 20 EUR per year. In order to get precise costs to assess at what number of grouped RSOAs the PCM cooling becomes more efficient the model would have to be refined and parameters for

multiple aircraft types researched. This is beyond the scope of this thesis but nevertheless the previous analysis does show that if a large number of the RSOAs can be grouped and cooled with one PCM package the efficiency will approach that of using separate TECs. This does not consider the cost of buying the TEC or the reliability of the devices.

## 5.5 Conclusions

This chapter introduces two different techniques of cooling an RSOA end node at the upper end of the avionic operational range. The first method involves the use of a TEC packaged with the RSOA inside a butterfly package. This is a solid state heat pump and is a very mature and reliable technology. It has been shown that a TEC packaged inside a butterfly package can cool an SOA, which is a very similar device to an RSOA, in the required environment and has a power consumption of 1.4 W.

The second method considers that typical flight durations of military aircraft are short so cooling does not have to work continuously. A PCM type cooling has been investigated to blunt exposure to high temperatures. The PCM would be placed inside an insulating package with the RSOA, when the temperature inside the package reaches the PCM melting point the PCM will begin to melt. The energy required for this phase change is much greater than the energy required for normal heating; the PCM will absorb energy inside the package in the form of heat. This means the temperature inside the package will remain around the PCM melting point as the PCM melts. A mathematical model of the PCM cooling package has been made in order to evaluate the size and mass required to cool in certain temperatures for fixed durations. The results of this model have been presented and discussed with particular attention paid to a trade-off between size and weight of the cooling package.

The efficiency of both these solutions has been compared via a power consumption comparison with the TEC consuming power directly and the additional mass from the PCM leading to an increase in fuel burn. This comparison has been made using data for fuel burn from a Boeing 737-800 as the relevant information for military platforms is not available, nevertheless the comparison will still show the relative efficiencies of both techniques. From this comparison it has been shown that the TEC would be a more favourable option for single isolated transmitters. If the transmitters are situated in the same location it could be possible that they share the same PCM cooling package whereas individual TECs would be used in the same circumstance. As the main heat source is from the surroundings rather than the heat generated by the devices the cost of counteracting this heating in the PCM

would be shared among many RSOAs which would increase the cooling efficiency per transmitter. With large numbers of RSOAs in the same PCM cooling package the efficiency does approach that of the TEC although this would have to be studied in more detail with data for the specific platform before one design could definitively be said to be more efficient.

## 6. Energy Savings in DWDM-PON

### 6.1 Introduction

Fibre optic communications networks, particularly those based on DWDM, are known to provide a robust future proof path for communications systems. Previous chapters have examined the performance of SS DWDM with respect to meeting this goal within the context of avionics networks. The WDM-PON is also being considered as the next step towards a future proofed network [23,92]. To date extensive research has been undertaken on long reach WDM-PON [93], low cost light sources [94], fault localization [95] and increasing data rates [56] among many other topics. Although these problems do apply to aircraft networks they are not considered as pressing as the power consumption of the network. Recent analysis in [96] has analysed the power consumption of critical network components within an optical transmission system. The analysis considered different data rates and many different transmitter/receiver designs. In general it was established that while there are small savings that can be obtained by optimizing the receiver electronics design, a major consideration within the overall power budget of the network was identified as being the power required to drive the optical transmitters. Recent research focusing on energy reduction in PONs has considered doze and sleep modes of operation in the ONUs [97,98]. The ITU defines the doze mode as “powering off or reducing power to non-essential functions and services while maintaining a fully functional optical link” and the sleep mode as “both the ONU receiver and transmitter are switched off for substantial periods of time” [99]. In practice this means that the transmitter of the ONU is turned off when it is not required to transmit upstream traffic. In the applications on aircraft which this thesis is concerned with, this may not be applicable or acceptable. Some end nodes on the aircraft will be required throughout the flight so dozing will not useable as a power saving technique. The turn on time of the transmitter may limit the use of dozing for flight critical systems on the aircraft again meaning that this technique is unusable. With the generic network currently considered in this thesis it would be prudent to assume that dozing will not be useful for aircraft networks. Similarly sleep modes will also be unusable, this introduces the same two problems as dozing but the effects are more pronounced. This chapter presents a theoretical assessment of a technique using optical amplification to minimize the overall power consumption of optical components in a WDM-PON in environments representative of those found on aircraft.

## 6.2 Amplified WDM-PON

The proposed network in this chapter is very different to that proposed in earlier chapters, it does not use RSOA modulators and instead uses directly modulated distributed feedback lasers. The previous chapter showed the feasibility of using a thermo-electric cooler in certain scenarios; this will be investigated in this chapter with the use of DFB transmitters instead of RSOAs. One possible layout of the proposed network is shown in Figure 60.

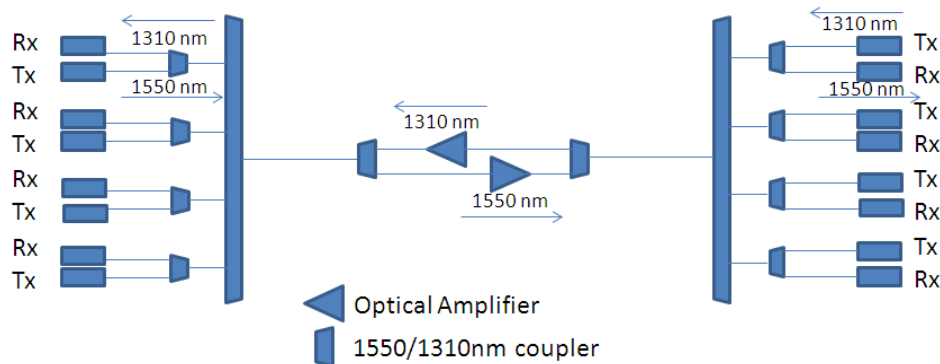


Figure 60: Schematic of amplified WDM-PON.

The proposed network will allow bi-directional communication with different wavelength bands used in either direction, for example wavelengths around 1310 nm operating in one direction down the main fibre backbone and signals carried on the 1550 nm band in the opposite direction. Typically a WDM-PON consists of laser transmitters at a number of ITU specified wavelengths on a 100 GHz grid. These signals are multiplexed by an AWG and carried on a single fibre to a de-multiplexer at the other end of the link. By introducing wavelength selective splitters the transmission and amplification of both signals can be accommodated. A key consideration when using an amplifier is where the amplifier is positioned. It can be used as a pre-amplifier immediately before detection, a mid-span amplifier, or a booster amplifier to increase the signal power before transmission. In Figure 60 the amplifiers are co-located so could both be used as mid-span amplifiers, there is no reason why the amplifiers must be co-located and either amplifier can be used as pre-amps, mid-span amplifiers or boosters. Although there is no need for an aircraft network to be ITU compatible it will be, as components manufactured for the mass telecommunications market are inexpensive and will be used where possible over bespoke non ITU specified components.

All components in the network may be exposed to the full avionic temperature range. This presents a particular problem with respect to the DFBs. As the temperature of the DFB changes so does the operational wavelength, this will lead to network failure as the



wavelength drifts out of the passband of its AWG channel. This means the DFBs must be temperature controlled.

### **6.2.1 Problem Formulation**

Recent analysis of the power consumption of network components has shown that a significant component of optical networks power consumption comes from the optical transmitters. The greatest savings in power consumption can therefore be achieved by reducing the power consumption of the transmitters. As required data rates increase, DFBs become the most realistic transmitter option. DFBs are relatively power hungry transmitters requiring a drive current of 10 mA to 20 mA per mW of optical output power. Typically, when designing a network, the goal is to maximize the optical power budget and the energy budget may be overlooked. The energy budget could conceivably be significantly reduced while maintaining the required BER.

The simplest method to design the network while concentrating on the energy power budget is to reduce the transmitter output power until the minimum acceptable SNR is achieved at the receiver, this is a straightforward solution and if applicable would save power. In this chapter an analysis is made where optical amplifiers are used as power boosters. The contention being that, by reducing the optical power at the transmitter and recovering the power at an amplifier shared by all channels in the network, significant savings in power consumption can be made since the additional power used by the amplifier is shared among many channels. The power saving expected by using this approach must be calculated while maintaining adequate system performance, quantified by the BER. Using established design processes, an optical system is considered from the perspective of optimising the Signal to Noise Ratio and thus minimising the BER. This drives the solution towards high transmit powers. By changing the emphasis of the design towards optimising energy consumption, transmitter power levels will in general be lower, even more so if mid span booster amplifiers are used to recover optical signal strength. The following analysis presents the power consumption of the network as a function of channel count and shows that significant savings can be made by including amplifier technologies into the network.

## **6.3 Power Consumption of Cooling**

The use of DFBs in the proposed network necessitates the use of cooling. As the temperature of the DFB changes the emitted wavelength will drift approximately 0.1 nm per

degree, the DFBs must be thermally regulated to avoid this drift. The wavelength of emission of each transmitter must match the wavelength on each channel of the AWG over the full range of temperatures the aircraft may be exposed to. As in previous chapters the ideal device for this application is a thermo-electric cooler, a small semiconductor device which can be used as a heat pump.

This chapter is concerned with reducing the power consumption of a WDM-PON by reducing the drive current to the laser transmitters. This has the additional effect of reducing the heat generated by the transmitters which will, potentially, further reduce the power needed to cool the lasers. Power consumption of a TEC as a function of temperature cooling a semiconductor optical amplifier (SOA) with a drive current of 100 mA has been presented in a previous chapter. The power required to thermally regulate a DFB in a butterfly package with a TEC should be the same as the power required if it were an SOA in the same type of package, assuming both have the same drive current. In this case, however, the idea is to reduce the drive current to the DFB, so the power consumption of the TEC will have to be measured again with a range of SOA drive currents below 100 mA.

### **6.3.1 TEC Measurements**

The experimental setup for the TEC measurements is shown in Figure 61. The SOA is provided by Kamelian and is packaged with a TEC in a standard 14 pin butterfly package; this was then mounted on a 14 K/W heat sink. The SOA and TEC were controlled separately, the SOA with an ILX Lightwave LDX-3207B laser diode driver to control the drive current and the TEC set point was controlled with an ILX Lightwave LDT-5910B temperature controller.

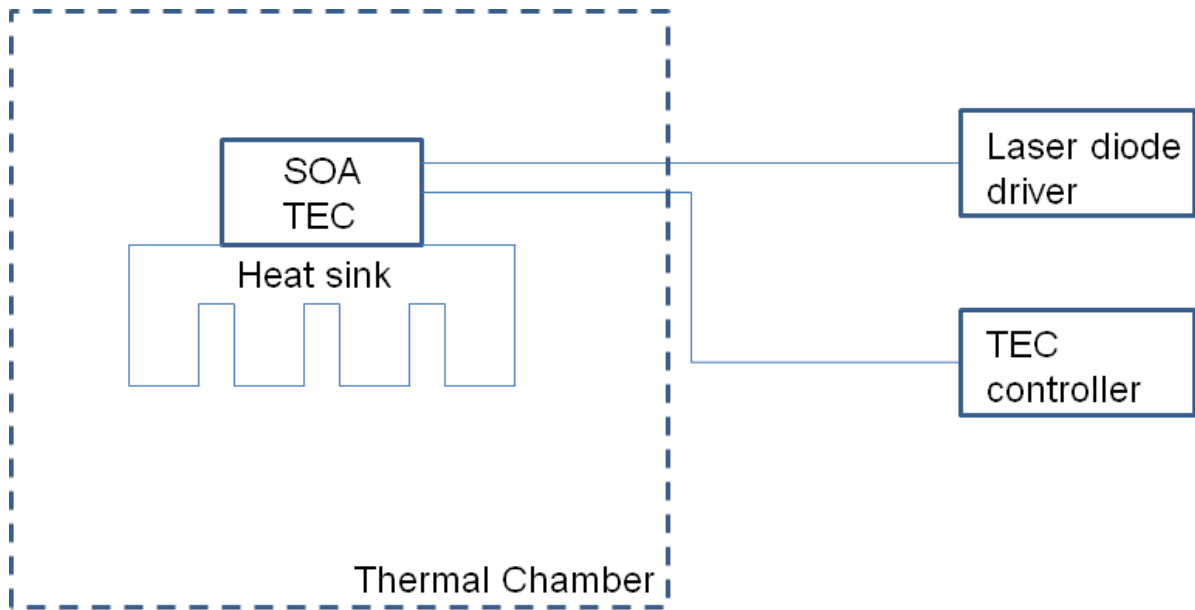


Figure 61: Schematic of the experimental set up to measure the TEC power consumption as a function of temperature over a range of SOA drive currents

The butterfly package was placed inside a thermal chamber with connections to the controllers passing through ports at the side of the chamber. The fibres from the SOA were unconnected and remained inside the chamber. Outside the chamber two separate Fluke multimeters were used to measure the current supplied to the TEC and the voltage, from these readings the TEC power consumption was calculated. The temperature in the thermal chamber was increased incrementally from  $-65\text{ }^{\circ}\text{C}$  until the TEC could no longer hold the SOA at the set point. This was repeated at various SOA drive currents, the different drive currents will result in different amounts of heat being generated by the SOA placing different active loads on the TEC. A plot of the TEC power consumption as a function of temperature for a range of SOA drive currents with a cooler set point of  $25\text{ }^{\circ}\text{C}$  is shown in Figure 62. The set point of  $25\text{ }^{\circ}\text{C}$  was chosen to correspond to the manufacturer's guidelines.

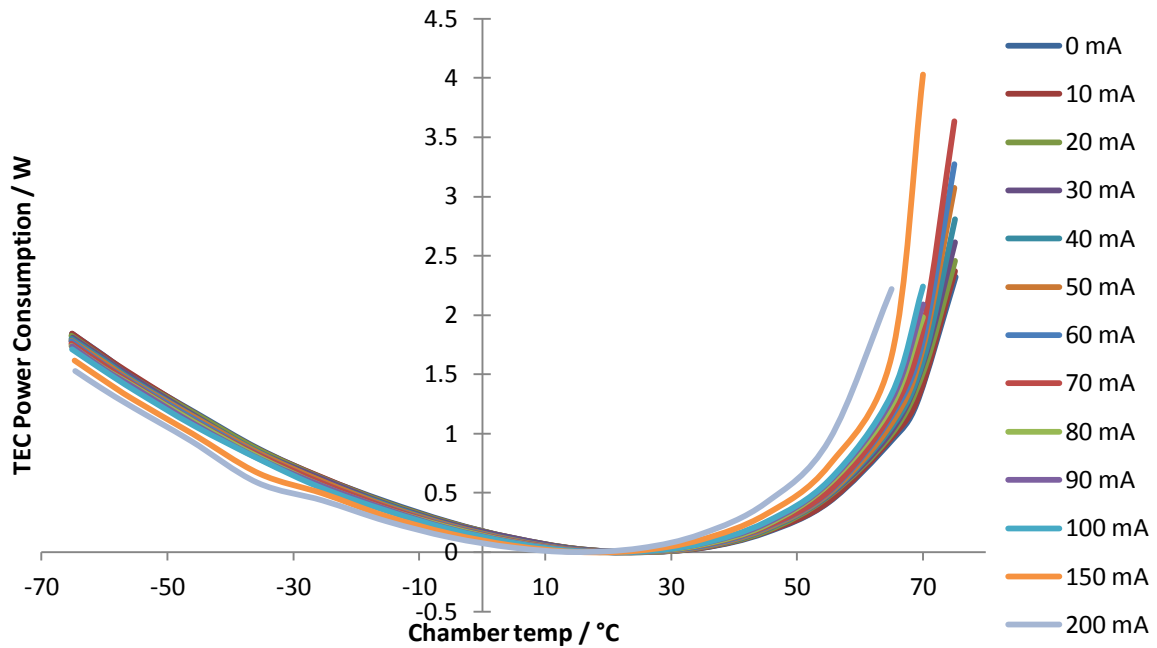


Figure 62: Plot of TEC power consumption with 25 °C set point with a different SOA drive current for each curve

The low temperature regime, where the TEC is used as a heater for the SOA, has a lesser power consumption than the point with the corresponding temperature difference in the high temperature regime. This is because of the Joule heating in both the TEC and the SOA, the drive current to both these devices results in heat generation which is helpful when the TEC is used as a heater but must be removed when the TEC is used as a cooler. This also explains why the TEC can maintain the set point at a larger temperature difference in the low temperature regime than the high temperature regime. With the high temperatures the current to the TEC is increased with increasing temperatures in order to remove more heat from the hot side of the device. This will lead to more Joule heating and further increase the heat which be pumped through the TEC, at the point where the TEC cannot hold the SOA at the set point the TEC controller will increase the drive current to the TEC in order to pump more heat through the TEC. This will lead to increasing the TEC temperature and thermal runaway will occur with the temperature and TEC drive current both increasing. At this point the TEC has failed; the exact point of failure has not been identified in Figure 62.

With this data it is possible to include the cooling power consumption in addition to that of the transmitters and amplifiers in order to get a full picture of the overall effects of introducing an amplifier into the proposed WDM-PON.

## 6.4 Modelling the Amplified Link

In order to quantify the level of the potential power savings by reducing transmitter output power and introducing an amplifier, the amplified and unamplified links must be fully modelled. A functional schematic of the amplified link is sketched in Figure 63.

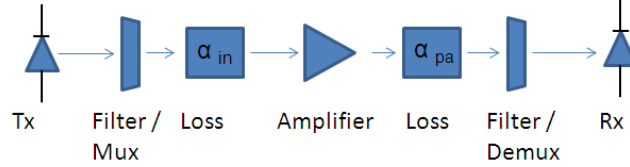


Figure 63: Functional schematic of WDM-PON

The parameters associated with the schematic which are relevant to the analysis are as follows:

- The transmitter parameters – output power and extinction ratio;
- Filter/multiplexer parameters – channel count and filter width;
- Loss before the amplifier – component insertion losses and trunk losses;
- Amplifier parameters – gain, saturation power and noise figure;
- Post amplification filter/multiplexer – channel count and filter width, both match earlier multiplexer parameters;
- Post amplification losses – insertion losses and trunk losses;
- Receiver parameters.

In order to accurately model the networks performance the receiver parameters must be known, most notably the thermal noise must be quantified. In general, this is not easy to find, as manufacturers tend to quote performance figures to demonstrate compatibility with relevant ITU standards so the performance can be understated. It is therefore necessary to make measurements in order to estimate the receiver thermal noise as discussed previously in this thesis.

The modelling, like that in in section 4.3.1 Bit Error Rate, follows the methods detailed in the literature [77]. Unlike the previous model of an amplified link the current driving the amplifier is not being modulated, this alters the noise calculations and means that the calculations are the same as those given in the literature:

$$\sigma_1^2 = \sigma_T^2 + \sigma_S^2 + \sigma_{ASE}^2 + \sigma_{S-ASE}^2 + \sigma_{ASE-ASE}^2 \quad (25)$$

$$\sigma_0^2 = \sigma_T^2 + \sigma_{ASE}^2 + \sigma_{ASE-ASE}^2 \quad (26)$$

where  $\sigma_1^2$ , the noise variance of a '1', is the summation of  $\sigma_T^2$ , the thermal noise,  $\sigma_S^2$  the signal induced shot noise,  $\sigma_{ASE}^2$ , the shot noise derived from the ASE power,  $\sigma_{S-ASE}^2$ , the noise resulting from the beat between the signal and ASE power and  $\sigma_{ASE-ASE}^2$  the beat noise derived from components of the ASE. Similarly  $\sigma_0^2$ , is the noise variance of a '0', and includes  $\sigma_T^2$ ,  $\sigma_{ASE}^2$  and  $\sigma_{ASE-ASE}^2$ . Each of these individual noise components can be calculated as in the previous chapter.

### 6.4.1 Model Results

Using this methodology the performance of an amplified WDM network can be characterised. An analysis of the dynamic range of an amplified WDM-PON for various channel counts is shown in Figure 64, which shows the losses which can be tolerated before and after the amplifier while maintaining the required BER. This model has used an amplifier with a gain of 18 dB,  $P_{SAT}$  of 13 dBm and an 8 dB NF across the entire C-band. These parameters are in line with those of an SOA. Also included in Figure 64 is a plot of the dynamic range of the link without amplification, this assumes link losses of 26 dB.

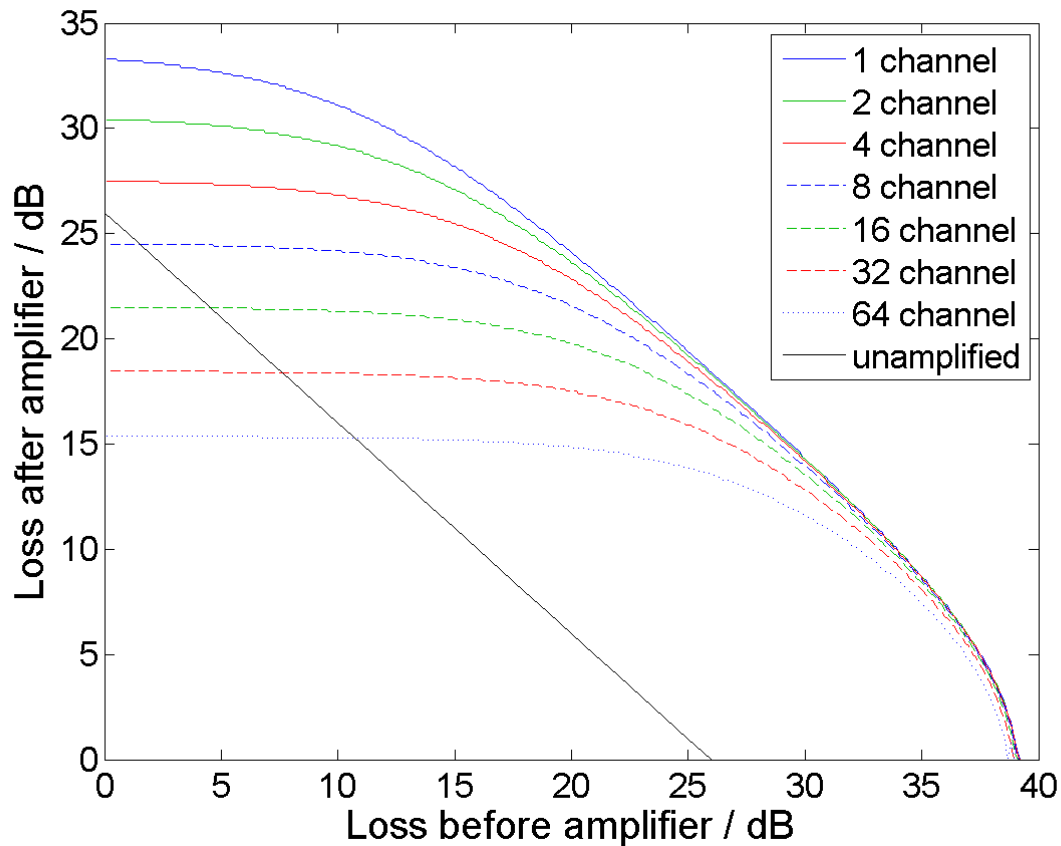


Figure 64: Dynamic range of an amplified WDM-PON link showing reach extension

WDM-PON does not yet have an official standard like other PON technologies such as GPON and XG-PON. This means that no official requirements for link loss are available. In addition the loss requirements on next generation aircraft are not yet known. Insertion losses from the components in the architecture in Figure 60 add up to approximately 13 dB; 2 AWGs with a 5 dB insertion loss and 3 splitters with a 1 dB insertion loss. In practice the link losses will be much higher than this with additional losses like connection losses and losses from optical rotary joints for example. For the remainder of this chapter it is assumed that the loss requirement will be 26 dB. Typical commercial off the shelf transmitters provide output powers of between 0 dBm and 5 dBm [100,101], here 3 dBm has been taken as an illustrative example. This means that the receiver must be able to deliver a BER of  $10^{-12}$  with a received power of -23 dBm; this sensitivity can be achieved with a pin photodiode at the receiver. While the exact details of the receiver design will influence the detail of any analysis that is based upon the receiver, this is less important from the perspective of the present analysis since it is the relative performance of the amplified and unamplified networks that are of interest. Hence, modelling the system performance with a receiver that is slightly better than the minimum required by the standard is perfectly valid.

In light of these assumptions a transmitter, without amplification, has a system path loss capability of 26 dB per channel regardless of the number of channels in the link. Amplifying the signal at the transmitter, or with little loss preceding the transmitter, will offer little benefit over the unamplified link at low channel counts and will be detrimental to the system at higher channel counts. The transmitter power needs little amplification before the amplifier is saturated so the gain from the amplifier will be much less than the stated maximum gain of 18 dB. For example, if there are eight transmit wavelengths operating with a 3 dBm transmitter power using an AWG with a 5 dB insertion loss the total input power to the amplifier would be 7 dBm.

Power per wavelength = 3dBm;

8 wavelengths is equivalent to an additional 9 dB (of total power);

Multiplexer loss = 5 dB giving a total input power of 7 dBm.

This is marginally less than the stated 13 dBm saturation output power of the amplifier, therefore the amplifier could only deliver 6 dB of gain before it is driven to saturation and its performance becomes non-linear. With increased channel counts the total power could exceed that of the amplifiers saturation power. In this case amplification is not feasible, particularly in the case of a SOA where non-linear processes would dominate the

performance and significantly increase the BER.

If the amplifier is positioned some way into the network, the losses preceding the amplifier will be high due to fibre and connector losses and the signal will be attenuated before reaching the amplifier. In this scenario the amplifier can be used to boost the signal strength and increase the system path loss capability. If the amplifier is a long way from reaching saturation the signal will see the maximum gain of the amplifier, in this situation an additional loss preceding the amplifier will lead to an equal decrease in the acceptable loss following the amplifier. The linear section on Figure 64 shows this effect. Eventually, if the signal is highly attenuated in a high loss link prior to amplification, the SNR degrades to the point that it cannot be recovered using amplification alone. This drop off in performance is due to rapidly increasing noise resulting from ASE in the amplifier, determined by the amplifier noise figure. This area would be avoided when designing a network, the area where the amplifier delivers the greatest benefit will be examined more closely.

The previous analysis covers WDM networks of a range of channel counts, in order to future proof the network to the demands on next generation aircraft a 32 channel 40 Gbps link is being proposed in this thesis. The dynamic range of a 32 channel amplified and unamplified link is shown in Figure 65 with a plot of the enhancement in dynamic range achieved with the inclusion of an amplifier. All parameters are the same as for the previous analysis.



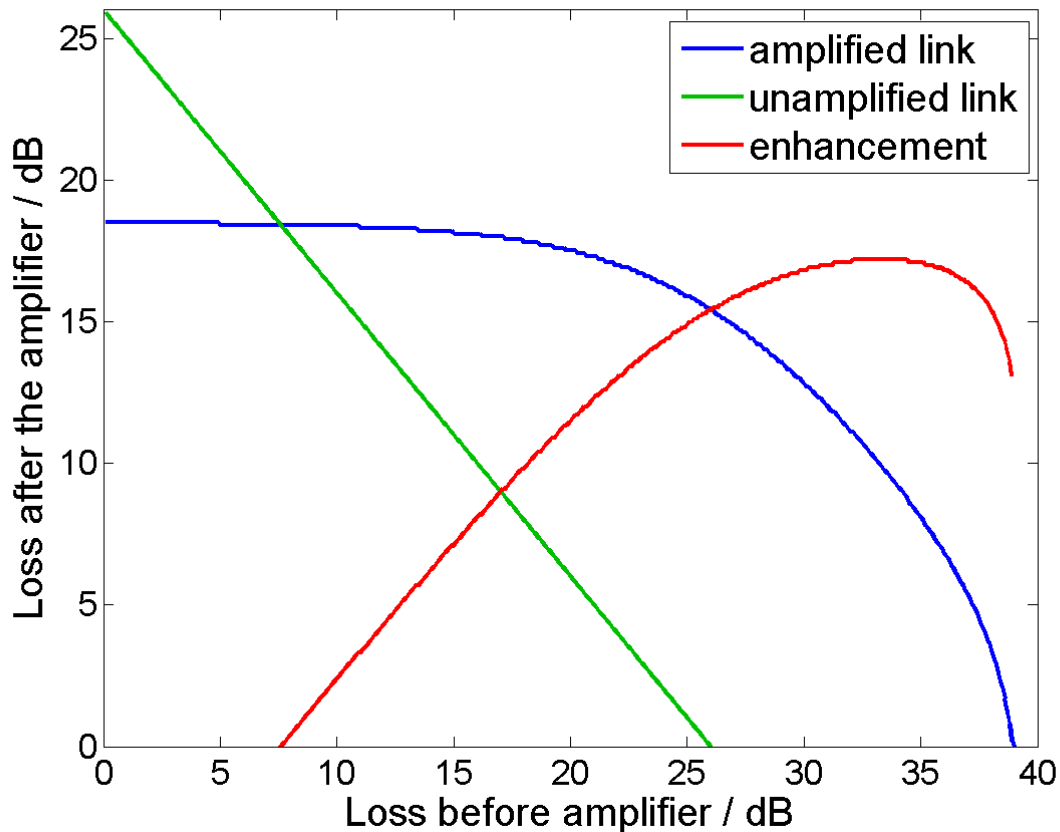


Figure 65: Dynamic ranges of 32 channel link both with and without amplification and a plot of the enhancement delivered with the use of an amplifier.

In the case of the link with 32 channels, if the amplifier is positioned directly after multiplexing, which is the closest possible location to the transmitters, there will be a decrease in the path loss capability when compared with the unamplified case. In the present model this is entirely due to gain compression as previously discussed. Other than compressing the gain in response to a strong input signal the present model does not allow for the effects of gain dependent non-linearity in an SOA which would decrease the dynamic range further. In practice an amplifier would not be used in this scenario so this region of operation is not relevant to the analysis.

As the attenuation before the amplifier is increased the system does start to get some benefit from the amplifier in the form of additional dynamic range or link reach. If the amplifier is positioned in the network where there are significant losses between the transmitter and amplifier, e.g. 30 dB, the enhancement in the dynamic range with respect to the unamplified case is at a maximum. The maximum enhancement in dynamic range possible with the use of an amplifier is approximately equal to the gain of the amplifier, which in this case is 18 dB. The high loss before the amplifier is analogous to reducing the transmitter power in a low

loss network. In the context of reducing network power consumption with the use of an amplifier this is an important point. It means that transmitter power may be reduced, in an attempt to decrease power consumption of the network as a whole, while still maintain an adequate SNR if an amplifier is introduced and shared amongst the transmitters. Reducing the transmitter power means less heat will be generated by the transmitters so the power required to maintain the operational wavelength stability needed for a WDM transmitter is also reduced.

## **6.5 Power Savings**

In the previous section it was shown how the inclusion of an amplifier in a WDM-PON could enhance the dynamic range of the network. In the present context a more pressing concern in the power efficiency of the optical components within the network. The enhancement in dynamic range allows the optical output power of the transmitters to be decreased; this means the drive current to the transmitters is reduced resulting in lower power consumption of the transmitters. This saving must be set against the inclusion of an amplifier and the extra power requirements this introduces. As the network is designed to be deployed on aircraft, which presents a particularly harsh environment with respect to temperature, particular attention must be paid to the cooling requirements and the power usage that this introduces will form a significant part of the overall power requirement. The different power requirements both with and without amplification will be analysed for varying channel counts in three different temperature profiles. Firstly in an idealized environment with constant room temperature before the analysis is extended to cater for two temperature ranges characteristic of aircraft.

### **6.5.1 Idealized Environment**

Typically the threshold current of a DFB is in the region of 10 mA and the output power rises by 0.1 mW per mA. Reducing the output power of a DFB from 2 mW to 0.5 mW, a 6 dB reduction will decrease the current requirement by 15 mA. Reducing the drive current in this manner will also reduce the extinction ratio (ER) that can be achieved which will mean that more power is required at the receiver to maintain a give BER. In the following analysis a power penalty corresponding to an extinction ratio of 7 dB is included in the calculations for the low current transmitter in the amplified network. A 20 dB extinction ratio is assumed for the unamplified scenario where the transmitter is operating at its recommended optical output power level. This represents a near ideal condition with a very small power penalty. In

practice it may be lower, nearer 10 dB; however, the near ideal case is a useful benchmark to use in the comparison. The reduced ER in the case with low output power is more problematic; it is assumed in the low drive current regime that 7 dB is achievable, which may not be the case. None the less the analysis is still important because the alternative transmitters which have low power consumption with low output power but have a high ER may be substituted for DFB.

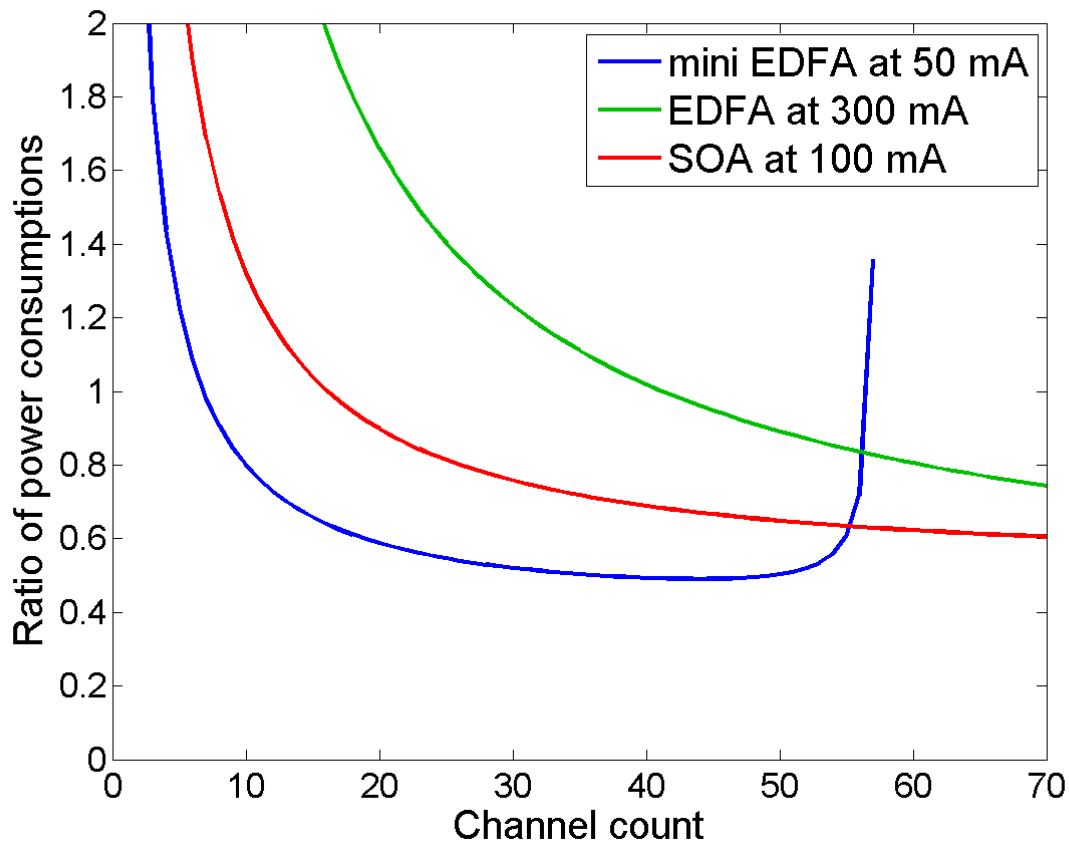


Figure 66: Relative power consumption of amplified WDM-PON to unamplified WDM-PON as a function of channel count for three amplifier technologies

Figure 66 presents the power consumption of an amplified network, relative to that of the unamplified network, for three different amplifiers of varying levels of power consumption. The amplifier is used as a pre-amplifier, positioned just before demultiplexing, so the signal encounters the highest levels of loss possible before amplification in order to maximise the power saving potential. The ambient temperature throughout the link is assumed to be 25 °C. The three different types of amplifier modelled are shown below in Table 5. The first case is a miniature EDFA, this is an amplifier which delivers a high gain but a low  $P_{SAT}$  [102]. This has low current requirements and does not require cooling between the temperatures 0 °C and +70 °C. This amplifier should enhance network performance when it has small input

powers and does not need large output powers, this corresponds to low channel count networks. The second amplifier is a conventional, high power, EDFA [103]. This amplifier has high current requirements and high cooling requirements due to the amount of heat it generates. However, it does have high gain and offers a high  $P_{SAT}$ . This should offer improvements in high power high channel count links where a large output power is required to share among the many channels using the amplifier. Finally an SOA is considered, relative to the other amplifiers this has moderate current and cooling requirements. It gives relatively low gain and has a moderate  $P_{SAT}$ . This should offer benefits in medium channel count links, with channel numbers between those improved by the two types of EDFA.

Amplifier	Drive Current	Gain (dB)	Psat (dBm)	NF (dB)
Mini EDFA	50 mA	29	9	4
EDFA	300 mA	20	16	4.3
SOA	100 mA	10	11	7

Table 5: Amplifier parameters

The analysis presented in Figure 66 finds that each channel requires 3 dBm of transmitter output power; each transmitter therefore requires approximately 30 mA of drive current. With the inclusion of an amplifier the current requirement is reduced in accordance with the transmit power. As previously discussed, and as Figure 65 shows, the amplifier is most useful when used as a pre-amplifier with the largest amount of loss possible between transmitter and amplifier. In this case, where the network losses are assumed to be 26 dB, the amplifier is positioned with a 20 dB loss from transmitter and amplifier and a 6 dB loss from the amplifier to the receiver. At low channel counts the inclusion of an amplifier is not effective. The additional power required to drive and cool the amplifier adds significantly to the total network power consumption. As the number of channels in the network is increased the power used in amplification is shared between a greater number of channels and a reduction in power consumption per channel is realized. If the network is viewed as a whole, the power requirements of the amplifier make up an increasingly small proportion of total network power consumption as channel count increases. The relative power saving from the transmitters increases as more transmitters are added to the network, eventually becoming greater than the power required by the amplifier so a power saving in the network as a whole is realized.

In order to compare the same conditions across three amplifiers in a scenario that is useful to aircraft networks a 32 channel link is again used for comparison. The greatest reduction, of 49%, is achieved by using the mini EDFA. The low current requirements of the amplifier and no cooling requirement mean that even at relatively low channel counts the mini EDFA is offer some benefit in this idealized temperature range. However, with increased channel counts the amplifier will begin to saturate before the others due to its  $P_{SAT}$  being lower. As the amplifier approaches saturation its gain becomes compressed and the gain it can give is much less than the maximum gain in the stated parameters, initially this can be overcome with higher transmitter powers which lead to an increase in power consumption. As the channel count increases so too does the optical input power to the amplifier, and the output must be divided between more channels, eventually not enough power will be provided per channel and the link will fail. This failure mechanism explains the bathtub shape of the curve in Figure 66.

The enhancement is also plotted for a high power EDFA. This amplifier has much higher current requirements than the mini EDFA and also requires cooling, because of these power requirements the savings associated with the use of an EDFA are not as high as those with the mini EDFA and no saving is realized when used in a 32 channel link. Although, due to the high  $P_{SAT}$  of this amplifier it will be useful in links with high channel counts and power savings are realized with higher channel counts. Finally the case where an SOA was used is plotted, the particular SOA used in the model is not the usual choice for an SOA pre-amplifier which typically has high gain and a low  $P_{SAT}$ . In this case it is important to have a high  $P_{SAT}$  in order to accommodate more channels and offer scalability beyond a 32 channel link, a booster amplifier has been chosen to use in the model although it is still deployed as a pre-amplifier. With an SOA a reduction in power consumption of 27% is predicted. The SOA can be seen as a compromise between the two fibre amplifiers and this is reflected in its performance: it will work at higher channel counts than the mini EDFA, due the increased  $P_{SAT}$ , but offers a better saving at low channel counts than the high power EDFA. The overarching result from this analysis is that the inclusion of an amplifier in a WDM-PON, in an ideal environment with no passive heating meaning minimal cooling is required; the power requirements of the network can be significantly reduced.

### **6.5.2 LRU Cooling**

A Line Replaceable Unit (LRU), in an avionic system, is a modular component of an aircraft designed to be replaced quickly at an operating location. In this context it can be a box in the avionics bay containing components of the mission control network. It is likely that future

LRUs will require high bandwidth links to other LRUs and other areas throughout the aircraft. The temperature in an LRU on a civil passenger jet has been measured as part of a previous project within BAE Systems; the temperature history is shown in Figure 67.

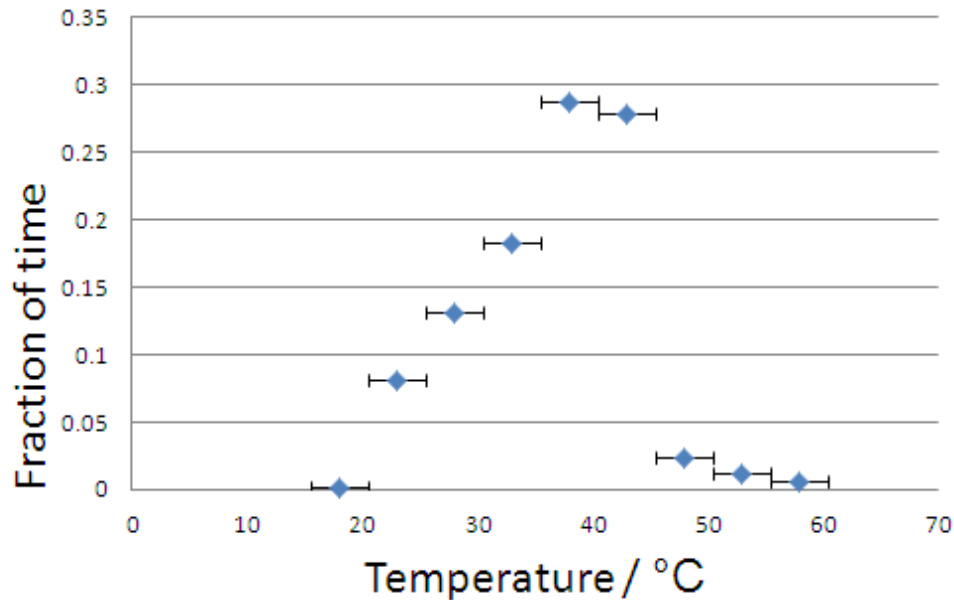


Figure 67: Measured temperatures in an LRU on a commercial jet

In order to repeat the previous analysis and establish the power usage over this temperature profile, the temperature regulation of the transmitters must be accounted for. In the previous case the temperature regulation was included but there was no heating from the surroundings and the ambient temperature was constant. In this case the TECs will have a significant passive load from the surroundings as well as the active load from the transmitters. From the previous experiment measuring the power consumption of a TEC cooling an SOA, both contained in a butterfly package, a weighted average for the power consumption of the cooling can be calculated for various SOA drive currents. The voltage across a DFB is less than that across an SOA, this means that the power delivered to the SOA per unit current is higher so the thermal load per unit current is higher. The drive current corresponding must be scaled down for the DFB using a scaling factor which will be the ratio between the two voltages across the SOA and the DFB. Other than this scaling the cooling requirements of the SOA and DFB should be very similar and the data, plotted in Figure 62, is representative of the power consumption of the expected cooling for a DFB. The power consumptions of the amplified and unamplified networks have been compared considering the requirements of the cooling in this environment and the results are plotted in Figure 68.

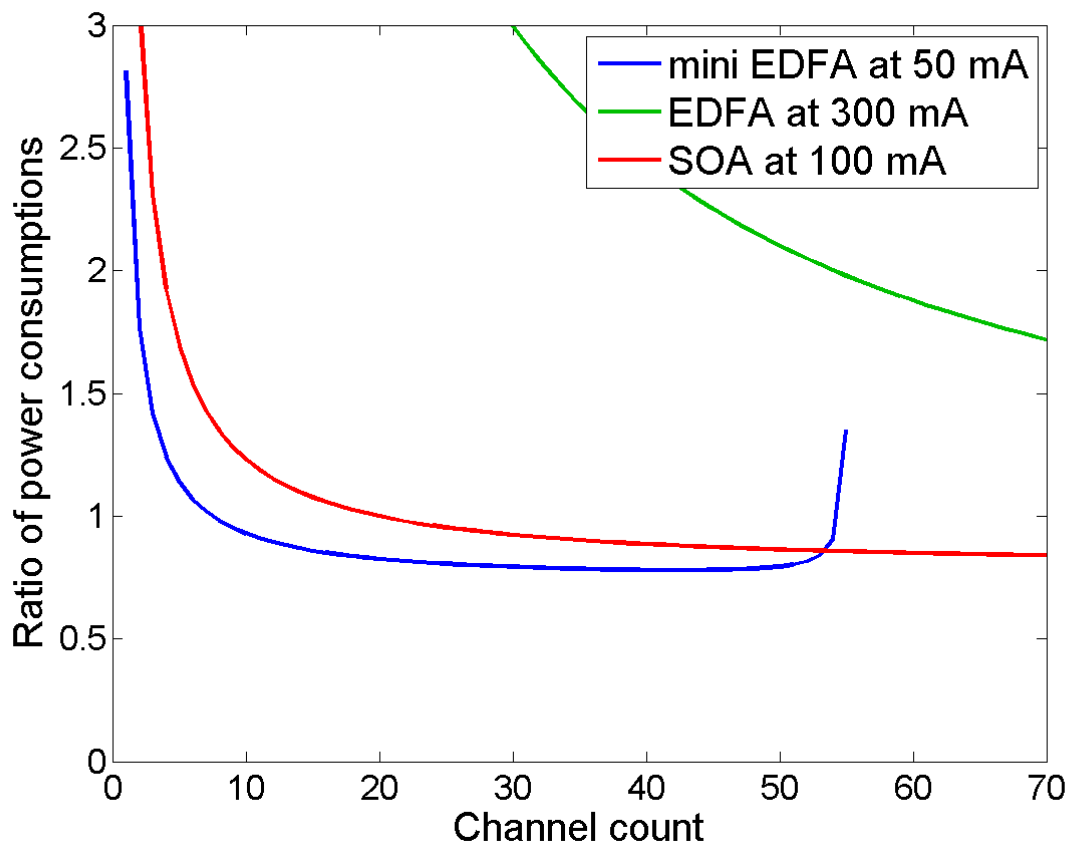


Figure 68: Relative power consumption of amplified network to unamplified network in an environment found on a commercial jet

The weighted average for the cooling power consumption in the specified temperature profile is 40 mW. The majority of heat which must be removed is from the passive heating by the surroundings, this is not dependent on the transmitter drive current so cannot be reduced with an optical amplifier. As a result the relative savings seen previously are eroded by this extra power consumption. Even with this erosion however, savings are realized using both the mini EDFA and the SOA. The mini EDFA offers a reduction of 21 % and the SOA offers a 10 % saving, both for a 32 channel link. It could also be argued that the additional power consumption for the cooling is still sufficiently low so as to make the implementation of WDM realistic.

The current network has a capacity of 40 Gbps, this bandwidth could easily be doubled with the use of a 2.5 Gbps transmitter. Beyond 80 Gbps there may not be any immediate uses if the capacity was scaled further, however, should the need for increased capacity arise the SOA does allow for significant power savings if the network is scaled by increasing the channel count. At 64 channels the inclusion of an SOA offers a reduction in power consumption of 15 % and the gain is compressed by 0.5 dB so there would be no gain

dependent non-linear effects in the SOA. This is assuming that the SOA can function over this wider section of spectrum which may not be the case, this may be avoided by using narrower channel spacing although more modelling would need to be undertaken as moving to a 50 GHz spacing may affect the noise conditions.

### **6.5.3 Full Temperature Specification**

In order for a component to be specified for operation throughout an aircraft it must be able to operate in the temperature range  $-55\text{ }^{\circ}\text{C}$  to  $+125\text{ }^{\circ}\text{C}$  [52]. As shown in the LRU case the time spent at each temperature is not distributed evenly across the entire range. There is a lack of information on how long the components are expected to spend at each temperature throughout the operational range but it is probable that the distribution would be similar to that measured and plotted in Figure 67 with the majority of time spent at a median temperature and significantly less spent at the extremes. In the following analysis it is assumed that the temperature profile will be a Gaussian distribution with the mean temperature at  $+35\text{ }^{\circ}\text{C}$  and the extremes of the operating range three standard deviations from the mean. Although a TEC cannot operate at the high end of this temperature range the power consumption of such a cooler has been extrapolated into this range to illustrate the power consumption over the full avionic temperature range. Again a weighted average for the power consumption in this range has been calculated and included in the comparison; the resulting plot is shown in Figure 69.



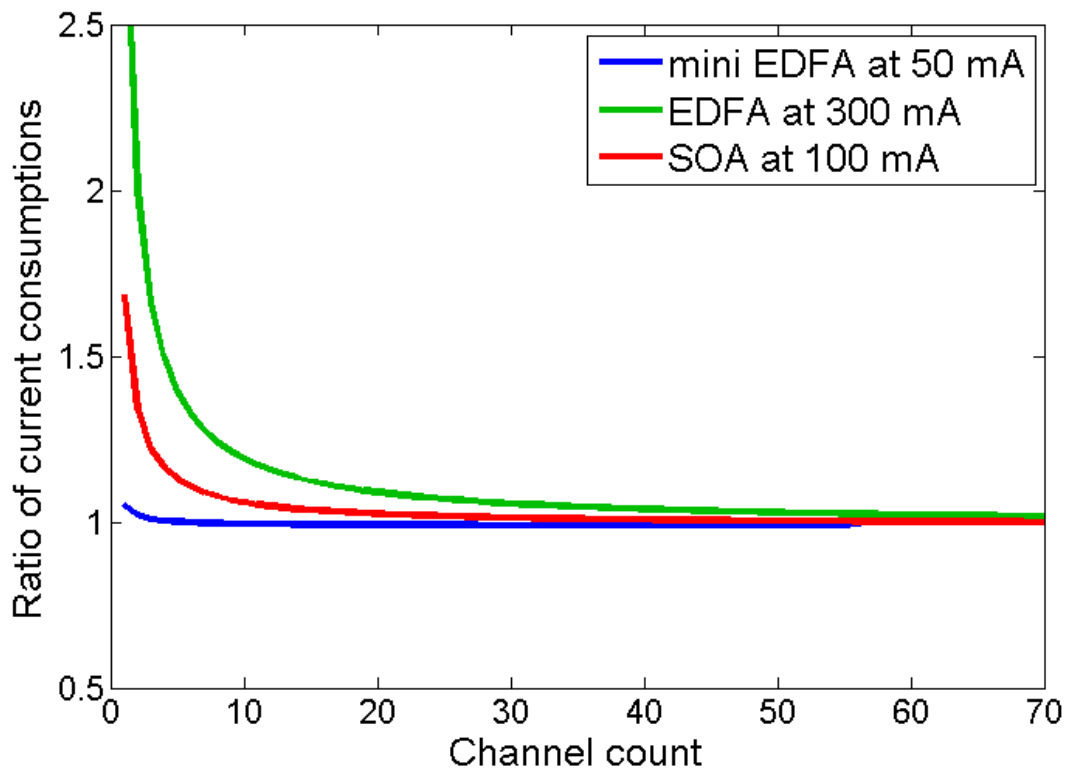


Figure 69: Relative power consumption of amplified WDM-PON with respect to an unamplified network in a temperature range specified for operation throughout aircraft

The weighted average for the power consumption of the TEC in this environment exceeds 1 W per transmitter in both amplified and unamplified cases. When considered in comparison with the cooling requirements in the LRU case, which significantly eroded the savings; and considering the transmitters require power in the order of tens of mW, it is clear that this level of power consumption will be the dominant requirement throughout the network and is unfeasible for full aircraft operation. This idea is reinforced by the plot in Figure 69 which shows that the savings from reduced transmitter output power have been completely eroded by the TEC. This analysis shows that, even with the power saving associated with the introduction of an amplifier, WDM-PON on aircraft is not feasible if the transmitters are expected to be deployed in any area of the aircraft due to excessive cooling requirements which stem from passive heating. Significant reductions, by at one order of magnitude, must be made in the cooling power consumption before this can be considered. However, it has also been shown, with data taken from aircraft, that the power savings can be significant if the transmitters are used in selected areas of the aircraft. These selected areas are not exposed to the same harsh temperatures and it is likely that these will be the locations throughout the aircraft where high bandwidth links will be useful in the future.

## 6.6 Comparison with RSOA Modulators

As has been previously discussed the use of DFBs as the transmitters necessitates the use of additional cooling. As main idea behind using the DFB, with mid span amplification, is to reduce the overall power consumption of the network, it is necessary to compare the power consumption of the uncooled spectrum sliced WDM-PON using RSOAs as amplifiers and modulators to the current WDM network with DFB transmitters.

### 6.6.1 SS-WDM-PON

The use of SS-WDM-PON has been fully explained in chapter 4, and the implementation of an RSOA designed for operation at elevated temperatures has been evaluated. As such only a brief description is included in this chapter.

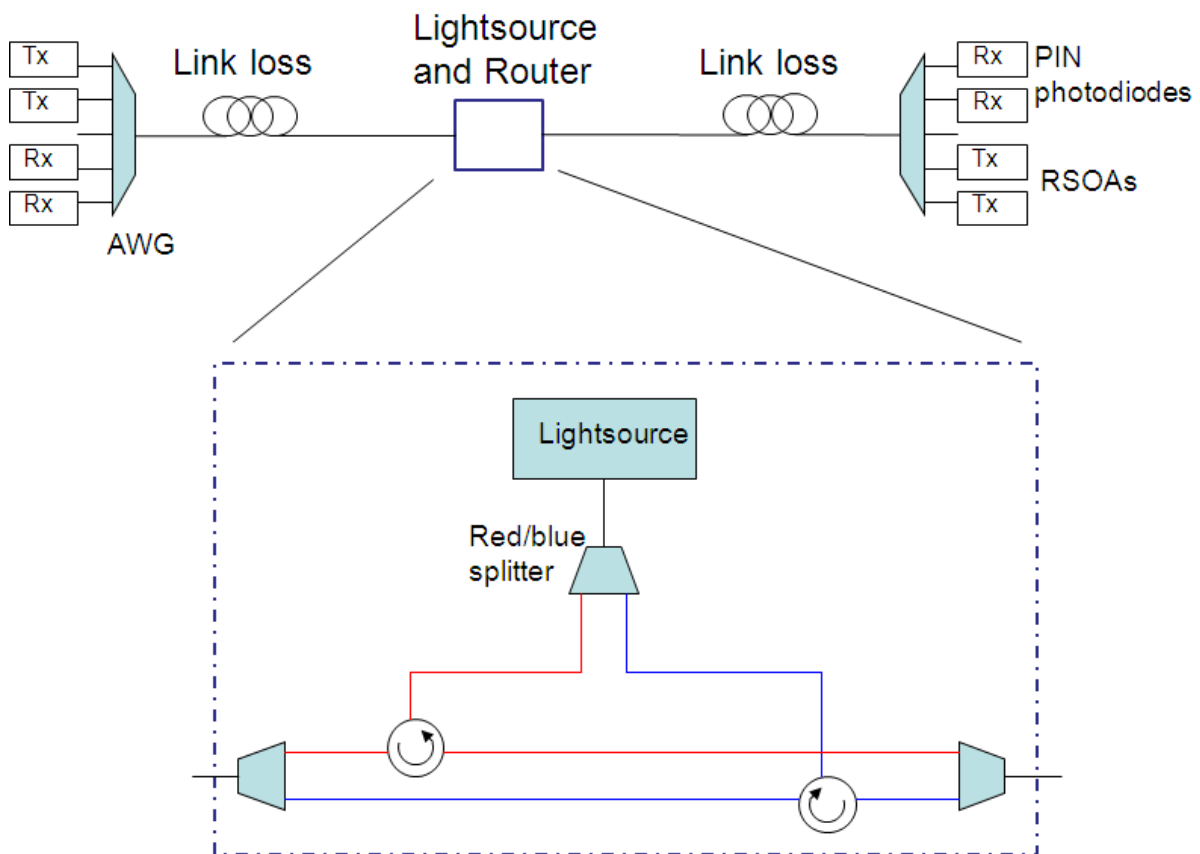


Figure 70: Schematic of WDM-PON network using RSOA modulators seeded with a spectrum sliced broadband lightsource.

A schematic of the proposed WDM-PON with RSOA modulators used in modelling in the remainder of this chapter is shown in Figure 70. The output from a broadband lightsource is divided, into the long and short halves of its spectrum, by a red/blue C-band splitter. Each

half is routed to either end of the link where it is spectrum sliced into narrow channels, spaced at 100 GHz, by an AWG. Each of these channels are used to seed an RSOA, the drive current to the RSOA is modulated which then modulates the optical power output from the RSOA. The AWG is athermal over the range -5 to +65 °C, beyond this range the AWGs can still be used uncooled as long as both AWGs are exposed to the same temperature, meaning the drift in wavelength will be the same at each multiplexer; this could be achieved by co-locating the AWGs. The wavelength used as a carrier by each channel is not chosen by the RSOA but by the AWG, this means that the RSOA, unlike the DFBs in the alternative network design, does not require cooling to stop any wavelength drift with temperature.

It has been previously shown that by using a multiple quantum well ridge-waveguide RSOA, designed to support high temperature operation, that the RSOA can operate in this network, uncooled, up to +70 °C. This assumes network link losses of 12 dB, which accounts for the insertion losses of the components in Figure 70, and a 6 dB overhead to allow for network degradation arising from both time and harsh environment. This gives a total network loss of 18 dB.

The gain and saturation power of the RSOA is affected by temperature so reducing the drive current to the RSOA when a large signal to noise ratio is achieved at the receiver is not possible. The RSOA must operate across the temperature -55 to +70 °C, and the gain and  $P_{SAT}$  vary across this range. A temperature sensor would need to be included with the RSOA to monitor how much the drive current could be decreased. This would add to system complexity and could turn out to be counter-productive in terms of power consumption as the additional sensors and current controllers would also require power. When comparing the power consumption of the RSOA network to that of the DFB network the calculations are very similar to those in the previous section, although in order to compare like for like it has been assumed that the total loss in the DFB network is also 18 dB. The DFB output power can be reduced and the signal recovered with a shared amplifier in order to maintain SNR whereas in the other case the drive current must remain constant. Where this differs is with the current requirements of the RSOA, which are higher than those of a DFB, and the cooling requirements, which are less.

### **6.6.2 LRU Case**

The temperature history found on an LRU on a commercial aircraft has been plotted in Figure 67. As has been discussed, using a DFB transmitter in this environment means each transmitter must have an individual cooler which will have an associated power consumption.

This power consumption has been measured previously and a weighted average of the required power to hold a DFB at a steady temperature in this environment has been calculated.

In the case of the RSOA modulators used in a SS WDM-PON, no cooling is required in the LRU environment as the RSOA can be used uncooled from -55 to +70 °C as has been shown previously. The power consumption in this case comes from the broadband source, used for spectrum slicing, and the power requirements of the RSOAs. These requirements are higher than the respective power consumptions in the DWDM-PON with DFBs. The comparison of the power consumptions of these networks is a way to quantify the possible power savings realized using a modulator with a higher power requirement but lower cooling requirements. The comparison is shown in Figure 71.

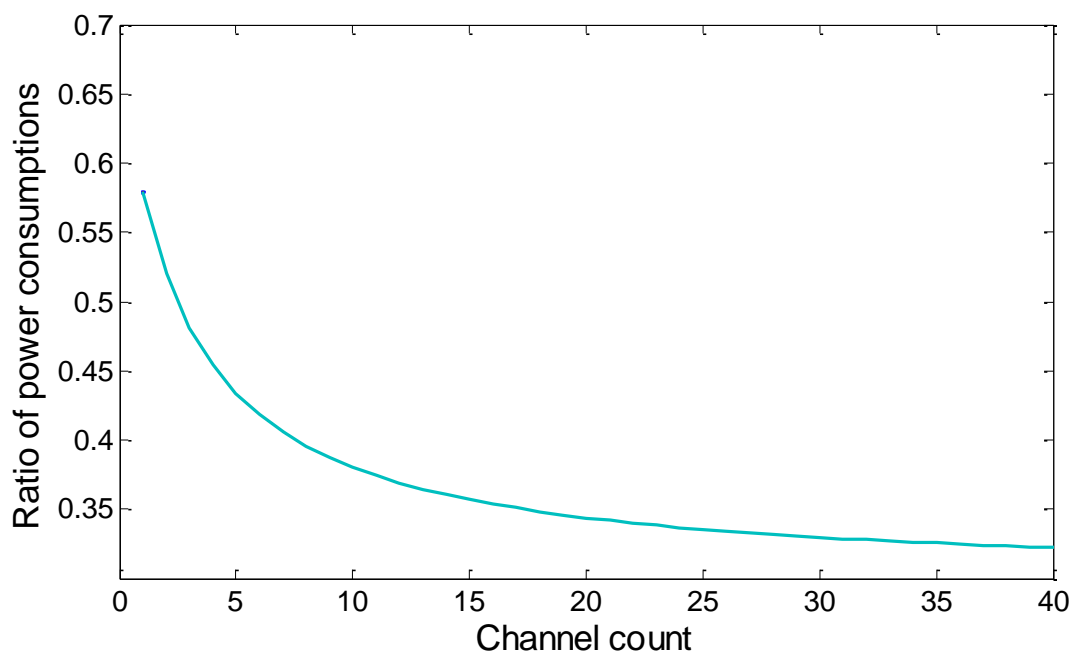


Figure 71: Ratio of the power consumptions of the DFB network to the RSOA network in a temperature range found on a civil aircraft.

The plot in Figure 71 predicts that the power consumption of the DFB network will be 33% of the network using RSOAs for a 32 channel link. This assumes each transmitter operating 1.25 Gbps with 100 GHz channel spacing and a total network loss of 18 dB. The amplifier used in the DFB network is the same as the SOA used in the previous analysis. A breakdown of the power consumptions of each network is shown in Table 6.

DFB	RSOA
TX: 15 mW	TX: 180 mW

Amplifier: 300 mW	Broadband Light Source: 500 mW
Cooling: 40 mW	Cooling: 0 mW

Table 6: Breakdown of power consumptions for both networks

Of the parameters listed in Table 6 both the transmitter power and the cooling power are required for each transmitter whereas only one broadband source or amplifier are required for the network as whole.

Considering the idea behind the use of the RSOA network is that a high drive current to the RSOA will mean that no cooling is required to hold the emitted wavelength at that specified for each channel. With the cooling requirements being only 0.04 W in this environment, there is no benefit to be gained in using the RSOA. In addition the power requirements of the RSOA the broadband source required for spectrum slicing has a higher power consumption that the amplifier used in the network with DFB transmitters. At low channel counts the power consumption of both networks is dominated by the amplifier/broadband source. The difference between these two powers is not as great as the difference in the powers associated with the transmitters, so at lower channel counts the ratio is around 0.57. As the channel count increases the power requirements associated with each transmitter make up an increasingly large proportion of the total power consumption meaning that the ratio decreases, to 0.33 at 32 channels.

The overarching finding in this comparison is that in the LRU environment it is more efficient to use the DFB transmitters. This has additional advantages that the DFBs can be easily scaled to 2.5 Gbps or 10 Gbps should the need arise. The network is more complicated however, a different DFB is required for each channel, unlike the RSOAs which are colourless and will work in any channel. This means the network is more complicated to build and maintain, and a large inventory of spare DFBs must be held.

### 6.6.3 Full Temperature Specification

The full temperature range specified for aircraft, excluding engine areas, is -55 °C to +125 °C. In the case of the WDM network with DFB transmitters, a TEC could not hold the transmitter at a fixed temperature throughout this range. In the previous sections analysis at the full temperature range the power consumption of the TEC was extrapolated from experimental data. This allowed calculation of a weighted average of the cooling power consumption with the assumption that the time spent at each temperature would form a Gaussian distribution with a +35 °C mean and the extremes of the range three standard deviations away from the mean.

In the case of the SS WDM-PON with RSOA modulators the cooling requirements are significantly reduced in comparison. The RSOAs require cooling only when the chip temperature is above 70 °C. Again, assuming the temperature profile with time is Gaussian, a weighted average of the power consumption can be calculated. The power consumptions of the two network designs have again been compared and the result plotted in Figure 72.

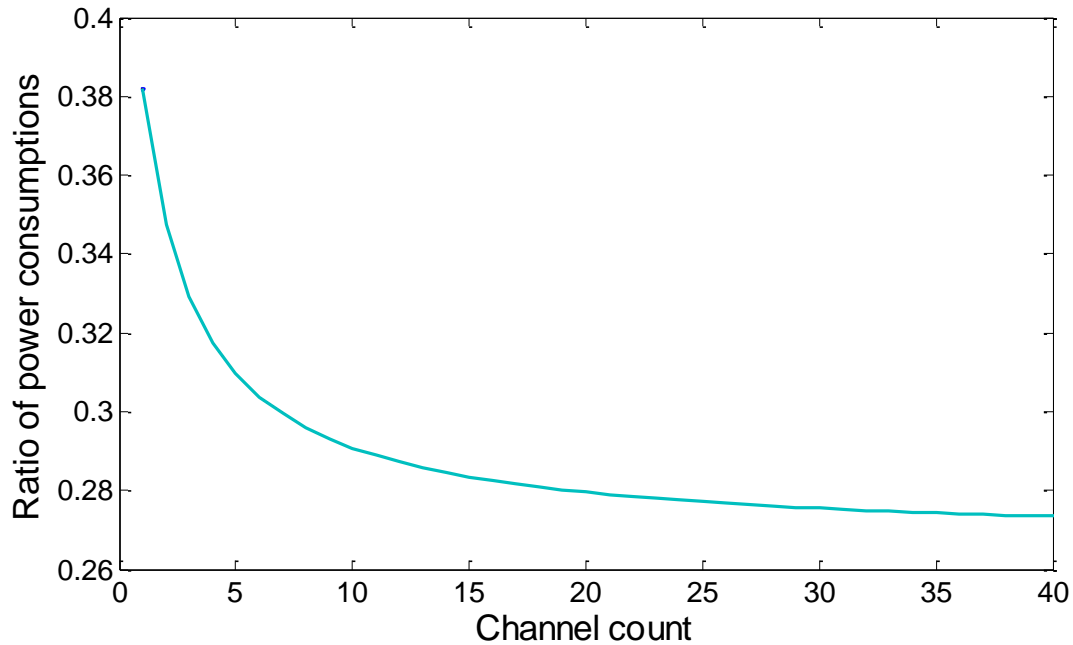


Figure 72: Ratio of the power consumptions of the DFB network to the RSOA network in the full temperature range specified for aircraft.

In this case the fraction presented is the reciprocal of that in the LRU case; it is the ratio of the RSOA network power consumption to that of the DFB network. For a 32 channel link this ratio is 0.28. The breakdown of power requirements throughout each network is listed in Table 7.

<b>DFB</b>	<b>RSOA</b>
TX: 15 mW	TX: 180 mW
Amplifier: 300 mW	Broadband Light Source: 500 mW
Cooling: 770 mW	Cooling: 30 mW

Table 7: Power requirements of each network

The only change in the power requirements from the LRU case are in the cooling. The DFB must be cooled throughout the full 180 degree range whereas the RSOA only needs cooling above 70 degrees; this is reflected in the relative power consumptions. The extrapolated cooling in the DFB case, where the device is held at +35 °C throughout the range, is by far the largest contributing factor to the total power consumption of the DFB network with 770

mW per transmitter. For even a small number of transmitters this becomes the dominant power requirement, far above that of the transmitters and the amplifier. In this case the increased drive current to the RSOA, which allows higher temperature operation and lessens cooling requirements, leads to significant savings. At 180 mW the power consumption of the RSOA is much higher than the 15 mW required by the DFB but this means cooling must only be used above 70 °C and that the device only be held at this temperature. The effects of this are two-fold, as a Gaussian distribution of temperature has been assumed there is only a fraction of time where the RSOA must be cooled whereas the DFB must be cooled continuously. Also, at the elevated temperatures where the RSOA does require cooling the temperature difference between the environment and the TEC set point is not as large as the corresponding case with the DFB transmitters, this means the DFB cannot function at these temperatures. If it could the extrapolated power consumption of the cooling is very high in comparison to that in the RSOA case.

In the LRU case the principal finding of the analysis was that the extra uncooled operational range offered with increased drive current to the RSOA was too high to see a power saving in that particular environment. In this the opposite is true; the capability to operate uncooled, even at the cost of increased drive current, is predicted to open up new temperature regimes to operation and realise large power savings.

To illustrate the comparative performance of the two networks the key parameters are listed in Table 9.

	<b>RSOA</b>	<b>DFB</b>
<b>Data Rate (Gbps)</b>	1.25	1.25
<b>Scalable (data rate)</b>	Not currently scalable with COTS components	10 Gbps with COTS components
<b>Scalable (maximum channel count)</b>	40	80+
<b>Inventory</b>	One device covers C-band	One device needed per wavelength channel

Table 9: Performance metrics of RSOA and DFB based networks

## 6.7 Conclusions

In this chapter a novel technique for reducing the power consumption of the optical

transmitters in DWDM-PON has been introduced. As the transmitters provide a significant contribution to the total network power consumption any reduction in their power requirements will have a significant impact on the overall power consumption. The idea is to reduce the output power at the transmitter and recover this power using a shared amplifier in order to achieve the required signal to noise ratio at the receivers. This leads to a reduction in power consumption of the transmitters but also reduces the heat generated by the transmitters which reduces the drive currents of the associated cooling. The power consumption of a TEC with different active loads over a wide temperature range has been measured experimentally and is used in a calculation of power consumptions alongside a mathematical model of an amplified WDM link. The model calculates the output power required from a DFB in a network of given path loss and amplifiers with given parameters for a number of channels in the link operating at 1.25 Gbps. From the output power of the DFB and the specifications of the amplifier the power consumption per channel is calculated. This is compared to the power consumption per channel in the unamplified case.

This calculation includes the effects of cooling each DFB which is dependent on the ambient temperature. This means the comparative power consumptions are also dependant on the ambient temperature at the DFBs so the calculations have been carried out in a selection of environments. Firstly the calculations were carried out in an 'idealised' environment where the ambient temperature is a constant 25 °C for three different amplifiers, a mini EDFA, a SOA and a high power EDFA. In this environment the mini EDFA is predicted to provide a 49 % power saving and the SOA a reduction of 28 % in comparison to the unamplified network when operating with 32 channels. The high power EDFA does not give a reduction in power consumption. It is unlikely that the DFBs will be exposed to such a constant temperature range, data from an LRU on a civil aircraft shows the temperature range between 17 °C and 62 °C with significantly more time spent at temperatures in the centre of this range. The comparative reductions in power consumptions in this range, including the increased power consumption of cooling, are 27 % and 10% for the mini EDFA and the SOA respectively. Although the SOA offers a scalable network, if the channel spacing was to be halved to 50 GHz and the channel number increased to 64 the SOA would offer a 15 % reduction in the power consumption of the transmitters in comparison to the unamplified network. The calculations were repeated using values for cooling power consumption over the full avionic temperature range, it was assumed that the histogram of this temperature range will be Gaussian, with the extremes three standard deviations away from the mean at 35 °C. A TEC cannot operate throughout this range so the power consumption was extrapolated from experimental measurements. The high power requirements of the TEC over the full avionic temperature range erode any power savings,



using a DFB based network over this range is not possible and if cooler were identified to work in this range it is likely that the power consumption would be prohibitively large.

Finally the power consumption of the amplified DWDM-PON is compared to that of the SS-WDM-PON from previous chapters. This was calculated in the LRU environment and the full avionic temperature range. In the LRU environment the DFB based network has a transmitter power consumption of 33 % of the RSOA based network. An LRU to LRU link could be a high bandwidth link between flight computers; in this case the scalability offered by the DFBs may be useful and offset the problems in maintenance and high inventory. In the full avionic environment the RSOA network has a transmitter power consumption of 28 % of the DFB network. With the 70 °C set point required by the RSOA only when the ambient temperature is above 70 C, the TEC can operate throughout the full temperature range. In the full temperature range the links are likely to service isolated points throughout the aircraft such as high bandwidth sensors and cameras. The components are more likely to degrade in this harsher environment so reduced inventory and simplicity of maintenance is important in this scenario, this is a further argument in favour of the RSOA in this case. What this final set of calculations shows is that there is no 'silver bullet' for an avionic network but the amplified DWDM PON and SS-WDM-PON are both applicable to be deployed in different areas of the aircraft. Both should be considered when assessing different options of fibre optic links for aircraft.

## 7. Conclusions

Advances in the technologies being deployed on aircraft such as high bandwidth sensors and real time high definition video capture have stimulated a need for a high data capacity avionic communications network. The data rates required to be carried by this network are not feasible over copper links, the next obvious solution is to use a fibre optic network. In addition to fibre having an inherently higher bandwidth than a copper link, there are advantages with respect to weight reduction leading to lower operating costs, a natural resistance to electromagnetic interference and a reduced spark hazard to name a few.

The point to point links currently in use on aircraft are not suitable for the next generation aircraft which requires high numbers of interconnected nodes operating at 1.25 Gbps. Wavelength division multiplexing, WDM, fulfils these requirements very well with multiple channels being carried on a single fibre by different wavelengths. The main problem with using WDM on aircraft is the operational temperature range of -55 to +125 °C. WDM is usually implemented with distributed feedback, DFB, laser transmitters, as the temperature of a DFB changes so does its operational wavelength. In WDM each channel is assigned a different wavelength, changes in the wavelength will lead to network failure so the DFBs must be thermally regulated. The power consumption of holding a DFB at a constant temperature throughout the avionic temperature range would be prohibitively high and adding extra weight through coolers and heatsinking is to be avoided as it would negate the weight savings in using fibre.

One possible technique to reduce the temperature tolerance of the transmitters and potentially realise uncooled operation is to use the spectrum slicing technique. This involves routing light from a broadband source onto a multiplexer where it is 'sliced' into the wavelength channels of that multiplexer. These channels can be used to seed a reflective semiconductor amplifier which amplify and modulate the input wavelength. The wavelength of operation of each channel is set by the multiplexer and not the RSOA, if the multiplexer is temperature insensitive then so is the wavelength in each channel. This technique lends itself to use of a passive optical network, PON, type architecture. In a PON all the routing components in the network are passive, i.e. have no power requirements, this lends itself to many different configurations and possible architectures which is ideal for a network aiming to be deployed on future aircraft which may not yet be designed.

In order to show that a PON can be deployed on an aircraft it is necessary to show that the passive optical components used on a PON can operate in the avionic temperature

range (chapter 3). Unfortunately COTS components are not specified to operate in the avionic temperature range and exposure to the extremes of the avionic range would damage the devices. It is assumed that this is an issue with the packaging of the devices and if the packaging were ruggedized, with different glues used for example, then the components could operate beyond the telecommunications temperature ranges. To measure the physical effects of temperature on the components and not the packaging tests have only been carried out in the specified storage range of components, for telecoms parts this is usually -40 to +85 °C.

The first component tested was a fibre optic circulator, across the storage temperature range the insertion loss and isolation in each port of the device is not problematic. Red/blue C band couplers were tested over the same temperature range. The insertion in both arms of this device was acceptable throughout the tested range although does increase with increasing temperature, if the losses increase at the same rate with respect to temperature then at the extreme of the avionic range the insertion loss will be acceptable for this component. The crosstalk between the two bands in the coupler is acceptable throughout the testable range as long as an 8 channel guard band is used between the pass and reflect wavelengths of the coupler. It cannot be said definitively from these measurements if the coupler could function throughout the full avionic temperature range, the test would have to be repeated with a ruggedized coupler to be certain that insertion loss and crosstalk were still at acceptable levels.

Two different types of multiplexer have been tested, one is an arrayed waveguide grating, AWG, and the other is made from thin film filters, TFF. Again, both these multiplexers were tested over the -40 to +85 °C temperature range. The AWG is specified as 'athermal' from 0 to 60 °C, over this range the central wavelength in three channels is constant  $\pm 0.02$  nm; outside this range the shift in wavelength is much greater. The insertion loss and adjacent channel crosstalk were measured as a function of the wavelength difference in the two channels in each multiplexer, this simulates a multiplexer and demultiplexer at different temperatures. The insertion loss and crosstalk of a multiplexer may be different when using spectrum slicing or laser transmitters since spectrum slicing uses the entire passband whereas a laser will not. When spectrum slicing with an AWG it was found the insertion loss of the device is not problematic, even at the maximum separation in centre wavelength between multiplexer and demultiplexer, the limiting factor will be the crosstalk. The crosstalk when both channels are matched is different in each channel measured but it is at level where it may be problematic depending on the final system design, if one or both multiplexers have a drift in central wavelength the crosstalk increases to unacceptable levels. The AWG can only be used in its specified athermal range of 0 to 60 °C, if the crosstalk in

this region is too high or a greater temperature range is required it may be possible to skip channels and use the AWG with channel spacing of 200 GHz. When using a laser as opposed to spectrum slicing the insertion loss and adjacent channel crosstalk is within acceptable levels for the maximum possible channel separation in the storage temperature range.

The TFF multiplexer tested had a channel spacing of 200 GHz, twice that of the AWG. This device is not designed to have an athermal operating range, over its -40 to + 80 °C storage range the centre wavelength shifts by approximately 0.1 nm in each channel. Due to limits in the lab it is only possible to thermally tune one multiplexer while the other remains at lab temperature so the maximum achievable difference in central wavelengths was 0.065 nm. Over this separation the insertion loss and crosstalk were within acceptable limits in both the spectrum slicing and laser transmitter cases. This increased temperature tolerance in comparison to the AWG is because of the increased channel spacing and not because of a different multiplexer technology.

Using spectrum slicing with RSOAs it is possible to create 'colourless' end nodes for WDM, i.e. the wavelength is not set at the node and one type of RSOA can function in many different nodes. This has significant advantages from an operational perspective because requirements to keep an inventory of the wavelength associated with a transmitter at locations throughout the aircraft is eliminated, as is the need to maintain a wide range of transmitter wavelengths as replacement stock. A possible network architecture using this method has been proposed in chapter 4. This network uses half the C band upstream and half downstream, this is an energy saving measure as it is expected that this network will meet bandwidth demands in the near term and in the longer term it is easily scalable. In order to assess the suitability of this network for use in aircraft network performance has been modelled as a function of temperature at the RSOAs. The measure of network performance used is the path loss capability, this is the maximum loss the network can tolerate while still maintaining a BER of  $10^{-9}$ . Although the RSOA does not define the wavelength of operation in each channel, the saturation power and gain of the RSOA will affect the path loss capability of the network. Both the saturation power and gain are dependent on temperature meaning network performance will also be temperature dependant. In order to evaluate the implications of this temperature dependency on the operational temperature range of the proposed network two different RSOAs were characterised over a range of temperatures. One of these RSOAs was a standard bulk active region device, the other was a multiple quantum well device designed for high temperature operation. The saturation power and gain from the tests were then used in the network model to calculate the path loss capability as a function of temperature for the scenarios

where either device was used as the modulator. It is predicted that over the entire operating range the standard RSOA will not function satisfactorily over 50 °C and with the MQW device the network will work up to 70 °C. These are significant findings as this predicts that the SS WDM PON concept is feasible in the avionic environment. It is not feasible, given size, weight and power constraints, to hold a laser transmitter at 25 °C with an ambient temperature of 125 °C, however holding an RSOA at 70 °C in an ambient temperature of 125 °C is feasible. It is also predicted that a slight change in the internal structure of the RSOA, which will not alter how the device is packaged, will extend the operational temperature range by 20 °C. This offers significant savings in power requirements of cooling, particularly at high temperatures.

If, by using the MQW RSOA, the end node need only be cooled above 70 °C, and considering that typical flight durations for military aircraft are relatively short, there may be an opportunity to take advantage of passive cooling using phase change materials, PCMs. This is investigated in chapter 5. The idea behind PCM is that a material, usually a type of wax, with a melting point that at the required cooling set point, is used as a 'heat reservoir'. As the wax heats up it absorbs heat in accordance with its specific heat, sometimes known as normal heating. As the solid wax meets its melting point it begins to soften and change phase. The latent heat, the energy required for the phase change, is much higher than the normal heat capacity, so while melting the wax requires more energy to raise its temperature. In practice this means that the wax temperature is clamped close to its melting point during the phase change due to an increase in specific heat of a factor of roughly 100. A mathematical model to quantify the size and weight of an insulating package, containing an RSOA and PCM, required to effectively cool the RSOA for one hour has been made. The model predicts that there is a trade-off between the size and weight of the package, a small package can be made with less insulation but more wax for example. Although the PCM has no power requirements it does add to the weight of the aircraft so does increase the fuel burned per flight, because of the increased fuel burn the PCM may not be any more efficient than a TEC which does require power but is much lighter. The power consumption of a TEC has been measured for various set points as a function of temperature; this can be translated into a monetary cost associated with the increase in fuel requirements. Similarly the additional weight added with the PCM package can also be translated into a fuel cost. For cooling an RSOA to 70 °C in an ambient temperature of 125 °C for 1 hour the TEC cost is between 20 and 50 times less than the PCM depending on how much space is available for the PCM. The PCM may become a viable alternative if many transmitters are grouped in the same space, in this scenario the PCM can be shared among the RSOAs whereas individual TECs for each RSOA would have to be used. Modelling indicates that 20 RSOAs would be

required to match the increases in fuel burn of both TEC and PCM. In both these comparisons it is assumed that when in-flight the RSOAs throughout the aircraft are in an ambient temperature of +125 C. If this is not the case the TEC will have a lower power consumption and cost less fuel whereas the PCM must always be carried.

Previous chapters have shown that although using RSOAs in a SS WDM-PON will increase the temperature tolerance of the network it will not allow uncooled operation throughout the entire avionic temperature range. One of the reasons for discounting a network using DFB transmitters was that this would require cooling, in light of the previous conclusions it is worth reconsidering a DFB based network. Chapter 6 introduces such a network and reports on a potential method for reductions in power consumption of this network. In a PON it has been reported that the dominant contribution to the power consumption comes from the optical transmitters, if the power consumption of these can be decreased this will have a large effect on the power consumption of the entire network. Typically, when designing a network, the signal quality is optimised. However, with an aircraft network, the overall power consumption will be of more importance than the signal quality, provided that a specified BER can be maintained. It may therefore be possible to design the network with reduced power from the optical transmitters to attain the minimum acceptable signal to noise ratio at the receiver. This idea can be extended to say that if the optical output power of each transmitter is reduced beyond acceptable levels, the power can be recovered at a shared amplifier, as this amplifier is shared between many channels this may also see a reduction in the total power requirement of the network. This has been modelled in two different temperature histograms.

The first temperature range has been measured in a line replaceable unit on a civil aircraft, this is a conditioned area of the aircraft densely populated with electronic systems, and the temperatures measured here could be close to those in a flight computer in military aircraft. In this temperature range the relative power consumption of an amplified network compared to an unamplified network has been calculated for three different amplifiers as a function of the numbers of channels in the network. The first amplifier is a mini EDFA, this offers a reduction of 20% with a 32 channel link, the second amplifier, a semiconductor optical amplifier, SOA, offers a 10% reduction in power consumption. A third amplifier, a high power EDFA, was also included in the calculations, this does not offer any power saving due to the high power consumption of this amplifier and its cooling. The calculations were repeated allowing for cooling throughout the full temperature range, assuming that the temperature histogram is Gaussian with the extremes 3 standard deviations away from a mean at 35 °C. In this case the power consumption of a TEC had to be extrapolated from experimental data. There is no power saving in this case as the power consumption of the

cooling is the dominant source of the power requirements.

This technique is predicted to provide savings in power consumption in certain, realistic, conditions on aircraft but what matters is how the power requirements compare to those of the RSOA network. The power consumptions of both the RSOA network and DFB network have been calculated for the same network path loss in the same temperature profiles operating at 1.25 Gbps per channel for a 32 channel link. In the LRU environment the DFB network has 33% of the power requirements of the RSOA network, this is because the cooling requirements of the DFB are relatively low and the drive current to the RSOA is high. Over the full avionic temperature range the TEC power consumption is extrapolated in the DFB case again as the TEC will not function over this range, in the RSOA case the TEC will function however. In the RSOA case the power consumption is 28% of the DFB network. In terms of optimising network design for power consumption there is no 'silver bullet', it must be considered on a case by case basis with particular attention paid to the operational environment as this has a large effect on the cooling.

In summary, the main findings and contributions of this thesis are:

1. Identification of the operational temperature ranges of standard telecoms fibre optic components. In particular multiplexing components, a 100 GHz spaced athermal AWG can be used from 0 °C to 60 °C when spectrum slicing and a 200 GHz spaced, thin film filter multiplexer from -40 °C to +85 °C.
2. A SS WDM-PON demonstrating bi-directional 1.25 Gbps traffic using RSOAs as amplifiers and modulators has been demonstrated.
3. A numerical model has been made to predict the path loss capability of a WDM-PON using RSOAs has been made and its output has been validated experimentally
4. RSOA parameters taken from experimental work have been used in the model to predict that use of a novel RSOA can operate in a SS WDM-PON as a modulator, uncooled, from -55 °C to +70 °C. This is an improvement on standard devices which are predicted to operate up to +50 °C before the signal quality becomes unsatisfactory.
5. Passive cooling in the form of phase change materials have been investigated and shown to be less efficient than thermo-electric cooling when deployed on a Boeing 737-800.
6. A novel power saving technique for WDM-PON networks on aircraft has been proposed and is predicted to offer savings of 20% in power consumption of the

optical transmitters in a realistic environment.

7. Power consumptions of the RSOA network and DFB based networks have been compared. In conditioned areas of the aircraft the DFB is more efficient whereas operating over the full avionic temperature range the RSOA network is more efficient.

## 7.1 Future Work

In order to deploy a fibre optic network on aircraft further work is needed. The temperature performance of the SS-WDM-PON network using RSOAs presented in chapter 4 considered the effects of temperature on the gain and saturation power of the amplifier, the modulation characteristics were not considered. Decreasing of the modulation bandwidth has been reported with increasing temperature due to carrier leakage leading to an increased carrier lifetime [104]. In the cited work the modulation bandwidth can be recovered at high temperatures by increasing the RSOA drive current. The proposed ridge waveguide RSOAs are more stable at higher temperature due to reduced carrier leakage from quantum wells so, in theory, degradation in modulation bandwidth should be less severe than in the cited work. Nevertheless, the effects of temperature on the modulation bandwidth and extinction ratio should be studied in future work. If the bandwidth or extinction ratio are degraded at high temperatures a simple bias control system, where the drive current is increased at high temperature, as in the cited work, may be a potential solution.

Although the SS-WDM-PON in chapter 4 offers data rates beyond those currently required on aircraft there will come a point where the data rate on this network must be increased. In order to future proof the network increasing the modulation bandwidth of the RSOA could be researched. This has been worked on extensively but not in the harsh conditions found on aircraft within the usual avionic constraints [56, 57]. The use of FEC would allow increased modulation speeds but at the expense of additional system complexity. Recently published work has modelled the modulation bandwidth of RSOAs of varying lengths and increased bandwidths are predicted [105]. This has assumed the RSOA will be thermally regulated and it may be of interest to characterise these devices over an extended temperature range.

The work contained in this thesis is aimed at aircraft but it may also be relevant to large ships or submarines. The use of WDM is particularly useful in these scenarios as use of a single fibre to carry multiple channels will greatly reduce the number of hull penetrations needed for a communications system. The use of the SS-WDM-PON is attractive because of the minimised inventory and ease of upkeep associated with colourless end nodes. It may be



useful to BAE Systems to explore the use of this network on other platforms.

# References

- [1] D. E. Anderson, M.W. Beranek '777 Optical LAN technology review', Electronic Components and Technology Conference 1998, pp 386-390
- [2] Eurofighter Typhoon technical guide, page 28, from [www.eurofighter.com/downloads/TecGuide.pdf](http://www.eurofighter.com/downloads/TecGuide.pdf) retrieved 27/8/14
- [3] G. P. Agrawal, "Fibre Optic Communication Systems" pp 375-381, John Wiley and Sons, Third edition, 2002
- [4] Nguyen-Cac Tran et al. "A 10 Gb/s Passive-Components-base WDM-TDM Reconfigurable Optical Access Network Architecture" OFC 2011, OThT1
- [5] S. Ihara et al. "Experimental Demonstration of C-band Burst-mode Transmission for High Power Budget (64-split with 40km distance) TWDM-PON Systems", ECOC 2013, Mo.4.F.2
- [6] N. Chand et al. "An Approach To Reducing SWAP and Cost for Avionics High-Speed Optical Data Networks" MILCOM 2008, pp 1-7
- [7] P. Winzer, "Spatial Multiplexing: The Next Frontier in Network Capacity Scaling", ECOC 2013, We.1.D.1
- [8] H. Takara, "1.01- Pb/s (12 SDM/222 WDM/456 Gb/s) crosstalk-managed transmission with 91.4-b/s/Hz aggregate spectral efficiency", ECOC 2012, Th.3.C.1
- [9] I.H. White, R.V. Penty, J. Hankey, K.A. Williams, G.F. Roberts, "Optical Local Area Networking Using CWDM," Cambridge University Engineering Department White Paper
- [10] Fu-Tai An et al. "Evolution, Challenges and Enabling Technologies for Future WDM-Based Optical Access Networks," Proc. JCIS 2003, Research Triangle Park, NC, Sept. 2003, pp. 1449 – 1453.
- [11] A. Shirley, "Improved Materials for Low-Water Peak Fiber Manufacture", NFOEC 2005, Poster session II JWA61
- [12] A. H. Gnauck et al., "25.6-Tb/s C+L-Band Transmission of Polarization-Multiplexed RZ-DQPSK Signals", Journal of Lightwave Technology, Vol. 26, pp 79-84, 2008.
- [13] D. Horwitz, "C.O.T.S. Fiber Optic Interconnect Solutions For Mobile Platforms", Electronic Components and Technology Conference 1998, pp 395-403.
- [14] G. P. Agrawal, "Fibre Optic Communication Systems" pp 185-188, John Wiley and Sons, Third edition, 2002
- [15] J.M. Simmons, "Survivable Passive Optical Networks Based on Arrayed-Waveguide-Grating Architectures", Journal of Lightwave Technology, Vol. 25, pp 3658-3668, 2007.
- [16] In-Sung Joe, O. Solgaard, "Scalable optical switch fabric for avionic networks", AVFOP 2005, pp 19-20
- [17] D. W. Charlton et al, "An avionic gigabit ethernet network", AVFOP 2013, pp 17-18
- [18] D. E. Anderson, M.W. Beranek, "777 Optical LAN technology review", Electronic Components and Technology Conference 1998, pp 386-390
- [19] R. Wang, R. J. Black, B. Moslehi, A. R. Behbahani, B. Mukherjee, "Optical Control Network for Avionics Applications Using a WDM Packet Ring", IEEE Transactions on Aerospace and Electronic Systems, Vol. 50, pp 637-648, January 2014
- [20] F. Brajou, P. Ricco, "The Airbus A380 - an AFDX-based flight test computer concept", AUTOTESTCON 2004, pp 460-463
- [21] A. J. McLaughlin et al., "Design and development of a Multi-Gigabit WDM Network for use in the Aerospace Environment", Aerospace Conference 2000, pp 115-124

- [22] D. Wang, J. Y. McNair, "A Torus-Based 4-Way Fault-Tolerant Backbone Network Architecture for Avionic WDM LANs" *Journal of Optical Communications and Networking*, Vol. 3, pp 335-346, 2011
- [23] A. Banerjee et al., "Wavelength-division-multiplexed passive optical network (WDM-PON) technologies for broadband access: a review [Invited]", *Journal of Optical Networking*, Vol. 4, pp 737-758, 2005
- [24] SAE International WDM-LAN Standards AIR6004, AIR6005, AIR6006, AS5659/0
- [25] S. Habiby, J. Mazurowski, "SAE standards for WDM LAN: Optical network architecture, access, control and physical layer", AVFOP 2012, pp 1-2
- [26] D. Richards, S. Habiby, J. Mazurowski, L. Cashdollar, "Optical network element simulation results for avionic WDM LANs", AVFOP 2013, pp 15-16
- [27] [http://www.avionics-networking.com/av\\_protocols\\_en.html](http://www.avionics-networking.com/av_protocols_en.html) retrieved 27/8/14
- [28] <http://standards.ieee.org/findstds/standard/802.3-2012.html> retrieved 2/6/14
- [29] B. W. Harris, B. J. Tran, "Fiber Optic AFDX for Flight Control Systems", AVFOP 2012, pp 15-17
- [30] J. Wilson and J.F.B. Hawkes, 'Optoelectronics: An Introduction', pg 208-212, Prentice Hall, 1983
- [31] G. P. Agrawal, "Fibre Optic Communication Systems" pp 100-102, John Wiley and Sons, Third edition, 2002
- [32] Orazio Svelto, "Principles of Lasers", pp 411-413, Springer, Fourth edition, 1998
- [33] K. S. Ly et al., "Bidirectional link Mock-Up For Avionics Applications", AVFOP 2008, pp 13-14
- [34] T. Mukaihara et al., "Highly Reliable 40-mW 25-GHz x 20-ch Thermally Tunable DFB Laser Module, Integrated with Wavelength Monitor", ECOC 2002, P2.7
- [35] D. de Felipe et al., "40 nm Tuneable Source for Colourless ONUs based on Dual Hybridly Integrated Polymer Waveguide Grating Lasers", ECOC 2013, Tu.1.B.5
- [36] J. S. Lee, Y. C. Chung, D. J. DiGiovanni, "Spectrum Sliced Fiber Light Source for Multichannel WDM Applications", *Photonics Technology Letters*, Vol. 5, pp 1458-1461, 1993
- [37] M. S. Leeson, S. Sun, "Spectrum Slicing for Low Cost Wavelength Division Multiplexing", ICTON-MW 2008, Sa2.2
- [38] G. P. Agrawal, "Fibre Optic Communication Systems" pp 136-148, John Wiley and Sons, Third edition, 2002
- [39] J. Wilson and J.F.B. Hawkes, 'Optoelectronics: An Introduction', pg 318-323, Prentice Hall, 1983
- [40] H. Uetsuka, "AWG Technologies for Dense WDM Applications", *Selected Topics in Quantum Electronics*, Vol. 10, pp 393-402, 2004
- [41] Y. Inoue et al., "Athermal silica-based arrayed-waveguide grating (AWG) multiplexer", *Integrated Optics and Optical Fibre Communications*, Vol. 5, pp 33- 36, 1997
- [42] B. Chassagne et al., "Passive Athermal Free Space Flat-Top- Mux/Demux", ECOC 2002, Micro Optics & Thin Film Devices 11.3.4
- [43] [http://www.rp-photonics.com/upper\\_state\\_lifetime.html](http://www.rp-photonics.com/upper_state_lifetime.html) retrieved 27/8/14
- [44] [http://www.rp-photonics.com/erbium\\_doped\\_gain\\_media.html](http://www.rp-photonics.com/erbium_doped_gain_media.html) retrieved 27/8/14
- [45] A. E. Kelly et al. "High Performance Polarisation Independent Reflective Semiconductor Optical Amplifiers in the S, C, and L Bands", *Selected Areas in Communications*, Vol. 28, pp 943-948, 2010
- [46] C. Michie et al. "Polarization-Insensitive SOAs Using Strained Bulk Active Regions", *Journal of Lightwave Technology*, Vol. 24, pp 3920-3927, 2006

- [47] K. E. Stubkjaer, "Semiconductor Optical Amplifier-Based All-Optical Gates for High-Speed Optical Processing", Selected topics in Quantum Electronics, Vol. 6, pp 1428-1435, 2000
- [48] M. J. Conelly, L. Q. Guo, "A novel approach to all-optical wavelength conversion by utilizing a reflective semiconductor optical amplifier in a co-propagation scheme", Optics Communications, Vol. 281, pp 4470-4473, 2008
- [49] F. Payoux, P. Chanclou, N. Genay, "WDM-PON with colorless ONUs", OFC 2007, OTuG5
- [50] H. S. Kim et al., "10.7 Gb/s reflective electroabsorption modulator monolithically integrated with semiconductor optical amplifier for colorless WDM-PON", Optics Express, Vol. 18, pp 23324-23330, 2010
- [51] C. P. Lai et al., "Multi-Channel 11.3-Gb/s Integrated Reflective Transmitter for WDM-PON", ECOC 2013, Tu.1.B.2
- [52] R. D. Gardner et al. "PHONAV – A Photonic WDM Network Architecture for Next Generation Avionics Systems", Aerospace Conference 1999, pp 451-466
- [53] M. Gross, A. Husain, "Rugged Optical Data Distribution Network for Avionics", AVFOP 2010, pp 15-16
- [54] H. H. Lee et al., "First Commercial Service of a Colorless Gigabit WDM/TDM Hybrid PON System", OFC 2009, PDPD9
- [55] K. Y. Cho, A. Agata, Y. Takushima, Y. C. Chung, "FEC Optimization for 10-Gb/s WDM PON Implemented by using Bandwidth-limited RSOA", OFC 2009, OMN5
- [56] K. Y. Cho, Y. Takushima, Y. C. Chung, "10-Gb/s operation of RSOA for WDM PON", Photonics Technology Letters, Vol. 20, pp 1533-1535, 2008
- [57] Y. Takushima, K. Y. Cho, Y. C. Chung, "Design Issues in RSOA-based WDM PON", IPGC 2008, pp 1-4
- [58] E. Wong, K. L. Lee, T. B. Anderson, "Directly Modulated Self-Seeding Reflective Semiconductor Optical Amplifiers as Colorless Transmitters in Wavelength Division Multiplexed Passive Optical Networks", Journal of Lightwave Technology, Vol. 25, pp 67-74, 2007
- [59] Q. Deniel, F. Saliou, P. Chanclou, D. Erasme, "Self-Seeded RSOA based WDM-PON Transmission Capabilities", OFC 2013, OW4D.3
- [60] D. de Philipe et al., "Hybrid InP/Polymer Optical Line Terminals for 40-Channel 100 GHz spectrum-sliced WDM-PON", ECOC 2013, Tu.1.F.1
- [61] K. Taguchi et al., "100-ns  $\lambda$ -selective Burst-Mode Transceiver for 40-km Reach Symmetric 40-Gbit/s WDM/TDM-PON", ECOC 2013, Mo.4.F.5
- [62] D. J. Blumental, "Terabit Optical Ethernet for Avionics", AVFOP 2011, pp 61-62
- [63] J. Ahadian, K. Kusumoto, R. Hagan, C. Kuznia, "Mil-Avionic Octal DWDM Transmitter", AVFOP 2013, pp 71-72
- [64] Qi Li et al., "Scaling star-coupler-based optical networks for avionics applications", Journal of Optical Communications and Networking, Vol. 5, pp945-956, 2013
- [65] M. Gross, A. Hussain, "Rugged Optical Data Distribution Network for Avionics", AVFOP 2010, pp 15-16
- [66] IBM white paper "Understanding Optical Communications" , <http://www.redbooks.ibm.com/redbooks/pdfs/sg245230.pdf> pg 20, retrieved 28/8/14
- [67] S. D. Dods, T.B. Anderson, "Calculation of bit-error rates and power penalties due to incoherent crosstalk in optical networks using Taylor series expansions", Journal of Lightwave Technology, Vol. 23, pp.1828-1837, 2005

- [68] M.R. Jimenez, R. Passy, M.A. Grivet, J.P. Von der Weid, "Computation of power penalties due to intraband crosstalk in optical systems", *Photonics Technology Letters*, Vol. 15, pp.156-158, 2003
- [69] IBM white paper "Understanding Optical Communications" , <http://www.redbooks.ibm.com/redbooks/pdfs/sg245230.pdf> pg 237, retrieved 28/8/14
- [70] J. X. Cai et al., "A DWDM demonstration of 3.73 Tb/s over 11,000 km using 373 RZ-DPSK channels at 10 Gb/s", *OFC 2003*, PD22- P1-3
- [71] W. M. Hendrix, "Thermal Design of a DWDM Optical Network System", *IMECE 2005*, pp 349-370
- [72] A. Borghesani, I. F. Lealman, A. Poustie, D.W. Smith, R. Wyatt, "High Temperature, Colourless Operation of a Reflective Semiconductor Optical Amplifier for 2.5Gbit/s upstream transmission in a WDM-PON", *ECOC 2007*, Paper 06.4.1
- [73] K. Grobe, J. P. Elbers, "PON in adolescence: from TDMA to WDM-PON", *IEEE Communications Magazine*, Vol. 46, pp 26-34, 2008
- [74] F. Payoux, P. Chanclou, R. Brenot, "WDM PON with a single SLED seeding colorless RSOA-based OLT and ONUs," *ECOC 2006*, Tu4.5.1
- [75] H. S. Shin et al., "16 x 1.25 Gbit/s WDM-PON based on ASE-injected R-SOAs in 60 °C temperature range," *OFC 2006*, pp.3-5
- [76] <http://www.kamelian.com/products.html> retrieved 31/05/12
- [77] C. Michie, A. E. Kelly, J. McGeough, S. Karagiannopoulos, I. Andonovic, "Optically amplified passive optical networks: a power budget analysis", *Journal of Optical Networking*, Vol. 8, pp 370-382, 2009
- [78] D. D. Sampson, W. T. Holloway, "100 mW Spectrally-Uniform Broadband ASE Source for Spectrum-Sliced WDM Systems," *Electronics Letters*, Vol. 30, pp 1611-1612, 1994
- [79] X. C. Xuan, "Analyses of the performance and polar characteristics of two-stage thermoelectric coolers", *Semiconductor Science and Technology*, Vol. 17, pp 414-420, 2002
- [80] F. J. DiSalvo, "Thermoelectric Cooling and Power Generation", *Science*, Vol. 285, pp 703-706, 1999
- [81] A. Proudfoot, C. Michie, W. Johnstone, H. White, "Power Requirements and Operation of Amplified Optical Networks for Future Aerospace Applications", *AVFOP 2010*, pp 17-18
- [82] [http://www.nasa.gov/centers/johnson/engineering/life\\_support\\_systems/crew\\_payload/index.html](http://www.nasa.gov/centers/johnson/engineering/life_support_systems/crew_payload/index.html) retrieved 28/8/14
- [83] <http://www.gizmag.com/phase-change-temperfect-coffee-mug/30109/> retrieved 28/8/14
- [84] E. M. Alawadhi, "Thermal analysis of a building brick containing phase change material", *Energy and Buildings*, Vol. 40, pp 352-357, 2008
- [85] H. Li, C. Hsieh, D. Goswami, "Conjugate heat transfer analysis of fluid flow in a phase change energy storage unit", *International Journal of Numerical Methods for Heat and Fluid Flow*, Vol. 6, pp 77-90, 1996
- [86] M. W. Zemansky, R. H. Dittmam, "Heat and Thermodynamics", page 86, Sixth Edition, McGraw Hill International, 1981
- [87] [http://www.aerogel.com/resources/common/userfiles/file/Data%20Sheets/Cryogel\\_Z\\_D\\_S.pdf](http://www.aerogel.com/resources/common/userfiles/file/Data%20Sheets/Cryogel_Z_D_S.pdf) retrieved 28/8/14
- [88] Conversation with Nick Chandler of BAE Systems Advanced Technology Centre
- [89] Tobias Berglund, Bachelor Thesis, "Evaluation of fuel saving for an airline," Dept. Mathematics and Physics, Mälardalen University, Västerås and Eskilstuna, Sweden, 2008

- [90] Air BP product handbook, <http://www.bp.com/sectiongenericarticle.do?categoryId=4503759&contentId=57765> retrieved 31/05/12
- [91] A. Gomez, J. J. Berry, S. Roychoudhury, B. Coriton, J. Huth, "From jet fuel to electric power using a mesoscale, efficient Stirling cycle", Proceedings of the Combustion Institute, Vol. 31, pp. 3251-3259, 2007
- [92] "Full service access network", Next Generation PON Task Group (NGPON) [Online]. Available: <http://www.fsan.org>
- [93] S. P. Jung, Y. Takushima, and Y. C. Chung, "Generation of 5-Gbps QPSK Signal using Directly Modulated RSOA for 100-km Coherent WDM PON," OFC 2011, OTuB3
- [94] S. G. Mun, S-G., H-S Cho, C-H Lee, "A Cost-Effective WDM-PON Using a Multiple Section Fabry-Pérot Laser Diode", Photonics Technology Letters, Vol. 23, pp 3-5, 2011
- [95] J-H Park, J-S Baik, C-H Lee, "Fault-localization in WDM-PONs", NFOEC 2006, JThB79
- [96] K. Lee, B. Sedighi, R. S. Tucker, H. Chow, P. Vetter, "Energy efficiency of optical transceivers in fiber access networks", Journal of Optical Communications and Networking, Vol. 4, pp A59-A68, 2012
- [97] R. Kubo et al., "Study and Demonstration of Sleep and Adaptive Link Rate Control Mechanisms for Energy Efficient 10G-EPON", Journal of Optical Communications and Networking, Vol. 2, pp 716-729, 2010
- [98] J. Kani, "Power Saving Techniques and Mechanisms for Optical Access Networks Systems", Journal of Lightwave Technology, Vol. 31, pp 563-570, 2013
- [99] "GPON power conservation" ITU-T REC. G. Sup 45, 2009
- [100] <http://www.sanspot.com/v/vspfiles/downloadables/FTGN3025Q1TAx.pdf> retrieved 15/11/13
- [101] <http://www.liverage.com.tw/UploadFile/Download/2011621537015T37U0SC.pdf> retrieved 15/11/13
- [102] [http://www.3spgroup.com/3SPG/ProductsFlas.php?locale=en&Line\\_no=22&sub\\_category\\_id=5400&cat\\_category\\_id=400](http://www.3spgroup.com/3SPG/ProductsFlas.php?locale=en&Line_no=22&sub_category_id=5400&cat_category_id=400) retrieved 9/01/14
- [103] <http://www.finisar.com/products/optical-amplifiers/EDFA-and-Raman-Modules> retrieved 28/8/14
- [104] K. Y. Cho, Y. Takushima, Y. C. Chung, "Enhanced Operating Range of WDM PON Implemented by Using Uncooled RSOAs", Photonics Technology Letters, Vol. 20, pp. 1536-1538, 2008
- [105] E. Udvary, "Investigation of Semiconductor Optical Amplifier Direct Modulation Speed", ICTON 2014, Mo.C2.5